


Università degli Studi di Cagliari

PhD DEGREE

Earth and Environmental Sciences and Technologies (ICAR/03)

Cycle XXXIII

TITLE OF THE PhD THESIS

APPLICATION OF MICROBIAL ELECTROCHEMICAL SYSTEMS FOR VALORISATION OF CHEESE WHEY IN BIOREFINERY FRAMEWORK

PhD Student:	Marco Isipato
Coordinator of the PhD Programme	Giorgio Ghiglieri
Supervisor	Giorgia De Gioannis
Co-supervisors	Aldo Muntoni
	Michele Mascia
	Daniela Spiga

Final exam. Academic Year 2019 – 2020

Thesis defence: July 2021 Session

Abstract

In the last decades, the current unsustainable fossil-based economic model has been worldwide disputed by policies and public opinion. As consequence, the exploitation of biomasses has arisen as pivotal towards a green and circular economy.

In this context, waste biorefineries would represent the optimal technical solution. Firstly, the integration of feasible bioprocess can generate a mix of biofuels and bioproducts, according to the cascade principle, thus making possible to hit the market with products characterised by either significant market size or high market value, guaranteeing economic sustainability. In addition, the use of organic wastes as alternative to dedicated biomasses would significantly tackle costs of waste management and related environmental impacts. Due to their qualitative homogeneity and volumes of production, agro-industrial residues are currently pointed out as suitable for multi-step valorisation in biorefinery. However, their valorisation is currently aimed to few products, like biogas and compost, characterised by low market value. Therefore, the full achievement of waste biorefineries potential has to be achieved yet, since it would greatly impact the economic and environmental resilience of the whole agro-industrial sector, in particular for smaller supply chains. Sheep milk supply chain is a notable example in this respect: even though it represents a small portion of European milk market, it is a fundamental source of income in few southern regions like Sardinia, and it cyclically experiences economic difficulties.

This research aims to evaluate the integration of Microbial Electrochemical Systems (MESs) in a biorefinery framework for the valorisation of cheese whey, as the main by-product of dairy industry. It started by assessing the state of art of available bioprocesses for feedstock valorisation. The literature review highlighted the current weakness of MESs treating this substrate, but also found how their integration as downstream process of Dark Fermentation (DF) can significantly enhance the power output generation in comparison to standalone processes. Consequently, a general overview on DF and MESs was provided, to also stress out how MESs can also expand material outputs generated during DF. The experimental work focused then on the application of Electro fermentation of lactate rich effluents from DF to propionate and acetate, which are seldom reported as main metabolites in DF broths. Then, a novel Microbial Fuel Cell for electricity generation is presented and characterised by mathematical modelling, aiming to a deeper understanding of reactor design to favour future systems scale up. Last experimental work gives a proof of concept of hydrogen production by Microbial Electrochemical Cells, underlining the further energy recovery and carbon removal achievable by their implementation. Finally, two biorefinery schemes are presented and analysed, pointing out their novelty and potential benefits to cheese making plants.

Acknowledgements

Marco Isipato gratefully acknowledges Sardinian Regional Government for the financial support of his PhD scholarship (P.O.R. Sardegna F.S.E. - Operational Programme of the Autonomous Region of Sardinia, European Social Fund 2014-2020 - Axis III Education and training, Thematic goal 10, Investment Priority 10ii), Specific goal 10.5.

List of acronyms

AEF Anodic Electrofermentation

BES Bioelectrochemical synthesis

CE Coulombic efficiency

CEF Cathodic Electrofermentation

COD Chemical Oxygen Demand

CV Cyclic Voltammetry

CW Cheese whey

DEET Direct External Electro Transfer

DF Dark Fermentation

EB Electron Balance

EF Electrofermentation

FW Food Waste

HPB Hydrogen Producing Bacteria

HPR Hydrogen Production Rate

HPY Hydrogen Production Yield

HRT Hydraulic Retention Time

LAB Lactic Acid Bacteria

MCA Membrane Cathode Assembly

MEC Microbial Electroysis Cell

MEET Mediated External Electro Transfer

MES Microbial Electrochemical Systems

MFC Microbial Fuel Cell

OCP Open Circuit Potential

SCFA Short Chain Fatty Acids

SCW Sheep Cheese Whey

SEM Scanning Electron Microscopy

SMSC Sheep Milk Supply Chain

TCD Thermal Conductivity Detector

TOC Total Organic Carbon

VFA Volatile Fatty Acids

Contents

Chapter 1

Introduction, framework, main objectives and structure

In the last decade, European Commission has been integrating the concept of bioeconomy in its policies as a tool for sustainable development and environmental protection. A circular bioeconomy model promotes the conversion of renewable biological resources – biowastes included – into food, feed, bio-based products and biofuels by a range of technologies (European Commission, 2012). The Bioeconomy Strategy has been subject to revision in 2018 with the purpose of accelerating its implementation, since it was recognised as a key factor towards 2030 agenda goals achievement, along with EU industrial and energy policies.

Valorisation of organic waste is currently pursued mostly in the form of a few products, e.g. biogas and compost, characterized by a relatively low economic value (Clarke, 2018; Alibardi et al., 2020). The new context requires a shift aimed at implementing the circular economy principles (Vrancken et al., 2017; Sarc et al., 2019; Walmsley et al., 2019; Alibardi et al., 2020); in this respect, organic residues may represent a readily available, widely distributed and renewable source for the recovery of a plurality of products characterized by high economic value (Ma et al., 2018; Papież et al., 2018; Alibardi et al., 2020).

The full achievement of such a goal requires the integration of multiple processes and correlating the availability of different residues as well as different environmental and economic needs (Asunis et al., 2020; Longati et al., 2020; Flórez-Fernández et al., 2021).

The waste biorefinery concept is suited to the task; it is an evolution of the biorefinery concept to include waste as an alternative to dedicated biomass and to enhance the recovery of value from organic waste. The feasibility of the concept greatly benefits in the case of application to agro-industrial residues characterized by a qualitative homogeneity close to that of dedicated crops (Akhlaghi et al., 2017).

Waste biorefineries, thus, would represent the optimal technical solution from several points of view: promoting a shift from a linear fossil-based economy to a circular bio-based one; tackling CO_2 emissions from waste management; guaranteeing an efficient recovery of materials and energy from biowastes; cutting costs for waste disposal or mere treatment which is disconnected from recovery and valorisation, conversely pursuing the recovery of high value resources.

Several processes can be flexibly integrated into a biorefinery scheme according to the cascade recovery principle, resulting in an output composed by products with either significant market size (*direct cascade*) or high market value (*inverse cascade*).

The sheep milk supply chain (SMSC) provides a small contribution to the European annual production of milk is, however it is recognised as a crucial sector in areas where is fully developed.

Nevertheless, SMSC is experiencing peculiar economic difficulties, which are induced by a multitude of factors: price volatility on the global market; the small size of the dairy farm, low generational turnover, low remuneration of raw material. Sardinian SMSC is a notable example: in 2017, regional sheep milk production reached 330000 tonnes, corresponding to 71% of Italian production and 16% of European one; in the same year, 47000 tonnes of cheese were produced, mainly constituted by "Pecorino Romano", in large part sold in the US as grating cheese type. Milk is produced in small size dairy farmers (<300 sheep per herd) and processed in 41 plants (of which only 5 process 45% of the milk).

The management of the main cheese making bioproduct, called cheese whey (CW), while on one hand is characterized by strong uncertainties about its effectiveness in terms of percentage intercepted with respect to the actual production volumes, on the other, it can represent a significant increase in production costs and, in disadvantaged contexts such as the Sardinian one, a sort of coup de grace for a sector already in difficulty. Conversely, a management approach based on the criteria of enhanced valorisation mentioned above would contribute to improve SMSC's resilience.

Cheese whey (CW) represents the most important residue of dairy industries (0.8-0.9 L produced per L of processed milk) and it is considered of great concern due to produced amounts, high organic load, presence of salts and low alkalinity.

Cheese whey, and sheep cheese whey (SCW) in particular, has a high TOC (32 g L^{-1}), mainly constituted by soluble carbohydrates in form of lactose (46 g L^{-1}) (Asunis et al., 2019), while average protein and fat content is 5.5 and 5.9 g/100g respectively (Balthazar et al., 2017).

Although SCW can eventually be used to produce ricotta cheese, generating a biowaste know as secondary CW, "traditional" management approaches are not environmentally sustainable and forbidden by EU and national regulations. Land spreading causes alteration of physio-chemical characteristics of soils, while nitrogen compounds could contaminate groundwaters (Ahmad et al., 2019). If disposed in aquatic environment, the high organic content may cause depletion of oxygen, eutrophication and be toxic for aquatic fauna (Ahmad et al., 2019).

Even animal feeding is not encouraged anymore, being lactose harmful to farm animals, and acidification may occur if the dairy farm is not in proximity of the processing plant.

Aerobic treatments have been extensively applied to treat CW in general, but they allow a mere reduction of organic content without further valorisation. Nonetheless, they heavily

impact on process costs due to aeration, and the high organic content may favour the growth of filamentous bacteria.

Anaerobic digestion, while much more consistent with the aim of resource recovery, have proved to be often affected by CW characteristics, the tendency to acidification in particular (Carvalho et al., 2013)

CW has a significant nutritional value, in particular in terms of proteins content, and membrane separation methods, most of all ultrafiltration, are currently acknowledged as the most viable methods for recovery. However, CW pre-treatments are necessary to increase the shelf life of whey and reduce membrane fouling, the use of cascades and bio-activated membranes is deemed necessary for enhancing separation efficiencies as well as post-processing of whey proteins (spray and freeze drying) for effective utilization as valuable (Ganju and Gogate, 2017). The energy demanding use of combined heat and ultrasonic pre-treatment can significantly enhance the membrane separation efficacy both in terms of enhanced flux and allowing reuse of the cleaned membranes. Finally, protein recovery may negatively affect the availability of nutrients for subsequent biological processes.

Looking to a future in which enhanced valorisation is a priority objective, the single process approach cannot represent the ultimate solution, since often the energy/chemicals production rates are too small for an effective economically sustainable scale-up. The implementation of integrated processes according to the waste biorefinery approach is instead the key for a cost effective and efficient valorisation.

In this framework, Microbial Electrochemical Systems (MESs) can be implemented to recover energy, either in the form of electricity or H_2, or soluble metabolites from carbon-rich substrates as CW (Liu et al., 2009; Montpart et al., 2015; Shanthi Sravan et al., 2018).

MESs operation relies on specific microorganisms, namely electroactive, able to use solid electrodes in electrochemical cells as terminal electron acceptor or electron donor (Logan et al., 2019).

Microbial Fuel Cells (MFCs) represent an interesting approach for bioelectricity generation. In such devices, exoelectrogenic microorganisms oxidise organic substrates generating electrons, protons and metabolic end products. Electrons are transferred to the anode by the biomass and flow through an external circuit connected to the cathode, on which surface are combined with protons to reduce oxygen to water, thus generating net electrical energy (Logan et al., 2006). Application of MFCs is currently limited to few pilot scale reactors, and their implementation at full scale is limited by power outputs in the order of mW, while a capacity of kW or MW is required in conventional power plants. In literature, several parameters were

addressed to influence MESs performances, but contact time between microbial cells and substrate is recognized as critical in terms of power production and organics removal. However, contrasting results on hydraulic retention time (HRT) effects are reported in the literature. Thus, mathematical modelling can help in the identification of the most influential parameters towards scaling up.

Microbial Electrolysis Cells (MECs) are conceptually similar to MFCs. However, in this case the cathode is operated in anaerobic conditions. The protons resulting from substrate oxidation are the final electron acceptors to generate H_2, if enough energy is provided as input current to drive the reaction (Escapa et al., 2016). Even though these systems represent a valid alternative to the fossil-based production of H_2, their use is currently limited to bench scale reactors and have only few examples on the exploitation of real substrates are reported in the literature.

Electro-fermentation (EF), in which a solid electrode acts as a source of oxidizing (anodic EF) or reducing (cathodic EF) power, is one the most novel concepts among MESs. The application of anodic and/or cathodic currents can properly address metabolic pathways, fostering otherwise energetically unfavourable reactions or balancing electrons in redox reactions, overcoming thermodynamic limitations typical of Dark Fermentation (DF) and expanding the range of soluble metabolites attainable. In this respect, cathodic EF can synthesize products not commonly obtained in dark fermentation and proton consumption/OH generation at the cathode provide for direct pH buffering, which is generally provided with acid/base addition during DF. Finally, CO_2 produced from fermentation can potentially be recycled into carboxylic acids via microbial electrosynthesis.

MESs system have their main strength in the wide range of biochemical reactions, which makes them extremely flexible and therefore useful in a treatment philosophy that wants to dynamically relate to the needs of the market.

However, MESs are complex systems still under development and require a huge number of studies to deepen aspects ranging from microbiology, to materials technology, to electrochemistry, to reactor fluid dynamics. MESs are also difficult to upscale and, with regard to energy production, can hardly compete with technologies such as solar energy and wind power at a large scale. Moreover, due to the high cost and the typically low power density and H_2 yield achievable through MFC and MEC, respectively, their use for treatment of high strength effluents such as raw CW does not appear feasible.

Therefore, the possibilities offered by MESs systems can be enhanced by being applied downstream of other processes, such as dark fermentation which is capable of hydrolysing and

simplifying the complex organic substance present in substrates such as raw CW. Nevertheless, even CW fermentate, characterised by high carboxylic acid concentration, needs to be diluted.

Unfortunately, compared to the initial PhD thesis objectives, the COVID-19 pandemic emergency that affected the last year of activity has prevented us from deepening the experimental activity, in particular by drastically limiting the tests performed on a real fermented cheese whey.

During the 3 years of PhD, the activities focused on the aspects that are summarized below and deepened in the specific chapters.

1. Conversion of the lactate attainable through DF of SCW into propionate and acetate through electro-fermentation, as such a conversion is hardly achievable through DF, evaluating the carbon recovery efficiency, production yields and microbiological dynamics;
2. Development and modelling of a novel MFC configuration for electrical energy recovery from a VFA-containing substrate which can be produced from a preliminary dark fermentation step, evaluating in particular the influence of flow condition and initial concentration on power output and substrate degradation;
3. Enhanced hydrogen production from SCW by coupling DF and MEC, which serving as downstream process for fermenters effluents would also allow further organics oxidation, thus reducing final treatment cost prior to disposal.

The experimental work conducted led to the drafting of papers published and submitted to international journals which, in accordance with the board of the PhD course, are reported as an integral part of the thesis and interspersed and accompanied by chapters.

The structure of the thesis is as follows: in addition to the present introductory chapter (Chapter 1) in **Chapter 2**, a review on CW valorisation options in a waste biorefinery framework is presented (Asunis et al., 2020). As for the paragraph focusing on MESs, it will emerge that they were only applied for energy recovery (as electrical energy or hydrogen) and their performances may be limited by the use of raw CW as feedstock.

In **Chapter 3**, DF is introduced as a potential pivot process in cheese whey biorefineries, due to the reasons provided above.

In **Chapter 4**, a literature review on MESs is presented, with a focus on critical aspects of system scale up and previous experiences of their use with substrates different from CW.

The following three chapters are dedicated to the core of the experimental activity. **Chapter 5** focuses on the electro-fermentation driven process of propionate and acetate production from lactate; lactate is the first soluble metabolite to be produced to significant extent during CW fermentation. Experimental work was performed during the exchange period at National university of Ireland Galway. In **Chapter 6** provides the results related to a newly designed flow through MFC, in which the use of a 3D anode maximise the active area of the electrode, boosting power production and carbon removal. The prototype of novel reactors was developed at University of Bath. **Chapter 7** gives a proof of concept of MECs as downstream process for DF of SCW, highlighting the benefits deriving from the integration of the two processes for hydrogen production and showing how MFC configuration proposed in Chapter 6 could act as power source for MECs in a CW biorefinery.

In **Chapter 8**, the analysis of two hypothetical biorefinery schemes involving the proposed technologies and having dark fermentation as pivotal process will be presented, highlighting strengths and weaknesses.

Finally, **Chapter 9** is dedicated to the final conclusions and perspectives.

References

Ahmad, T., Aadil, R. M., Ahmed, H., Rahman, U. ur, Soares, B. C. V., Souza, S. L. Q., et al. (2019). Treatment and utilization of dairy industrial waste: A review. *Trends Food Sci. Technol.* 88, 361–372. doi:10.1016/j.tifs.2019.04.003.

Akhlaghi, M., Boni, M. R., De Gioannis, G., Muntoni, A., Polettini, A., Pomi, R., et al. (2017). A parametric response surface study of fermentative hydrogen production from cheese whey. *Bioresour. Technol.* 244, 473–483. doi:10.1016/j.biortech.2017.07.158.

Alibardi, L., Astrup, T. F., Asunis, F., Clarke, W. P., De Gioannis, G., Dessì, P., et al. (2020). Organic waste biorefineries: Looking towards implementation. *Waste Manag.* 114, 274–286. doi:10.1016/j.wasman.2020.07.010.

Asunis, F., De Gioannis, G., Dessì, P., Isipato, M., Lens, P. N. L., Muntoni, A., et al. (2020). The dairy biorefinery: Integrating treatment processes for cheese whey valorisation. *J. Environ. Manage.* 276. doi:10.1016/j.jenvman.2020.111240.

Asunis, F., De Gioannis, G., Isipato, M., Muntoni, A., Polettini, A., Pomi, R., et al. (2019). Control of fermentation duration and pH to orient biochemicals and biofuels production from cheese whey. *Bioresour. Technol.* 289. doi:10.1016/j.biortech.2019.121722.

Carvalho, F., Prazeres, A. R., and Rivas, J. (2013). Cheese whey wastewater: Characterization and treatment. *Sci. Total Environ.* 445–446, 385–396. doi:10.1016/j.scitotenv.2012.12.038.

Clarke, W. P. (2018). The uptake of anaerobic digestion for the organic fraction of municipal solid waste – Push versus pull factors. *Bioresour. Technol.* 249, 1040–1043. doi:10.1016/j.biortech.2017.10.086.

European Commission (2012). *Innovating for Sustainable Growth: A Bioeconomy for Europe*. doi:10.1089/ind.2012.1508.

Flórez-Fernández, N., Illera, M., Sánchez, M., Lodeiro, P., Torres, M. D., López-Mosquera, M. E., et al. (2021). Integrated valorization of Sargassum muticum in biorefineries. *Chem. Eng. J.* 404, 125635. doi:10.1016/j.cej.2020.125635.

Ganju, S., and Gogate, P. R. (2017). A review on approaches for efficient recovery of whey proteins from dairy industry effluents. *J. Food Eng.* 215, 84–96. doi:10.1016/j.jfoodeng.2017.07.021.

Liu, Z., Liu, J., Zhang, S., and Su, Z. (2009). Study of operational performance and electrical response on mediator-less microbial fuel cells fed with carbon- and protein-rich substrates. *Biochem. Eng. J.* 45, 185–191. doi:10.1016/j.bej.2009.03.011.

Logan, B. E., Hamelers, B., Rozendal, R., Schröder, U., Keller, J., Freguia, S., et al. (2006). Microbial fuel cells: Methodology and technology. *Environ. Sci. Technol.* 40, 5181–5192. doi:10.1021/es0605016.

Logan, B. E., Rossi, R., Ragab, A., and Saikaly, P. E. (2019). Electroactive microorganisms in bioelectrochemical systems. *Nat. Rev. Microbiol.* 17, 307–319. doi:10.1038/s41579-019-0173-x.

Longati, A. A., Batista, G., and Cruz, A. J. G. (2020). Brazilian integrated sugarcane-soybean biorefinery: Trends and opportunities. *Curr. Opin. Green Sustain. Chem.* 26, 100400. doi:10.1016/j.cogsc.2020.100400.

Ma, H., Guo, Y., Qin, Y., and Li, Y. Y. (2018). Nutrient recovery technologies integrated with energy recovery by waste biomass anaerobic digestion. *Bioresour. Technol.* 269, 520–531. doi:10.1016/j.biortech.2018.08.114.

Montpart, N., Rago, L., Baeza, J. A., and Guisasola, A. (2015). Hydrogen production in single chamber microbial electrolysis cells with different complex substrates. *Water Res.* 68, 601–615. doi:10.1016/j.watres.2014.10.026.

Papież, M., Śmiech, S., and Frodyma, K. (2018). Determinants of renewable energy development in the EU countries. A 20-year perspective. *Renew. Sustain. Energy Rev.* 91, 918–934. doi:10.1016/j.rser.2018.04.075.

Sarc, R., Curtis, A., Kandlbauer, L., Khodier, K., Lorber, K. E., and Pomberger, R. (2019). Digitalisation and intelligent robotics in value chain of circular economy oriented waste

management – A review. *Waste Manag.* 95, 476–492. doi:10.1016/j.wasman.2019.06.035.
Shanthi Sravan, J., Butti, S. K., Sarkar, O., Vamshi Krishna, K., and Venkata Mohan, S. (2018). Electrofermentation of food waste – Regulating acidogenesis towards enhanced volatile fatty acids production. *Chem. Eng. J.* 334, 1709–1718. doi:10.1016/j.cej.2017.11.005.
Vrancken, C., Longhurst, P. J., and Wagland, S. T. (2017). Critical review of real-time methods for solid waste characterisation: Informing material recovery and fuel production. *Waste Manag.* 61, 40–57. doi:10.1016/j.wasman.2017.01.019.
Walmsley, T. G., Ong, B. H. Y., Klemeš, J. J., Tan, R. R., and Varbanov, P. S. (2019). Circular Integration of processes, industries, and economies. *Renew. Sustain. Energy Rev.* 107, 507–515. doi:10.1016/j.rser.2019.03.039.

Chapter 2

The dairy biorefinery: Integrating treatment processes for cheese whey valorisation

(Article published on Journal of Environmental Management)

Journal of Environmental Management 276 (2020) 111240

Contents lists available at ScienceDirect

Journal of Environmental Management

journal homepage: http://www.elsevier.com/locate/jenvman

Review

The dairy biorefinery: Integrating treatment processes for cheese whey valorisation

Fabiano Asunis [a,b], Giorgia De Gioannis [a,c], Paolo Dessì [b,*], Marco Isipato [a,b], Piet N.L. Lens [b], Aldo Muntoni [a,c], Alessandra Polettini [d], Raffaella Pomi [d], Andreina Rossi [d], Daniela Spiga [a]

[a] DICAAR - Department of Civil and Environmental Engineering and Architecture, University of Cagliari, Piazza D'Armi 1, 09123, Cagliari, Italy
[b] Microbiology, School of Natural Sciences and Ryan Institute, National University of Ireland Galway, University Road, Galway, H91 TK33, Ireland
[c] IGAG-CNR, Environmental Geology and Geoengineering Institute of the National Research Council - Piazza D'Armi 1, 09123, Cagliari, Italy
[d] Department of Civil and Environmental Engineering, University of Rome "La Sapienza", Via Eudossiana 18, 00184, Rome, Italy

ARTICLE INFO

Keywords:
Anaerobic digestion
Bioplastic
Circular economy
Dairy industry
Fermentation
Microbial electrochemical technology

ABSTRACT

With an estimated worldwide production of 190 billion kg per year, and due to its high organic load, cheese whey represents a huge opportunity for bioenergy and biochemicals production. Several physical, chemical and biological processes have been proposed to valorise cheese whey by producing biofuels (methane, hydrogen, and ethanol), electric energy, and/or chemical commodities (carboxylic acids, proteins, and biopolymers). A biorefinery concept, in which several value-added products are obtained from cheese whey through a cascade of biotechnological processes, is an opportunity for increasing the product spectrum of dairy industries while allowing for sustainable management of the residual streams and reducing disposal costs for the final residues. This review critically analyses the different treatment options available for energy and materials recovery from cheese whey, their combinations and perspectives for implementation. Thus, instead of focusing on a specific valorisation platform, in the present review the most relevant aspects of each strategy are analysed to support the integration of different routes, in order to identify the most appropriate treatment train.

1. Introduction

Fossil fuels, which include coal, oil and natural gas, supply about 80% of the world total energy (International Energy Agency, 2017). These non-renewable sources provide electricity, heat, and transportation fuels, as well as supply raw materials and platform chemicals for the manufacturing of a wide range of products. Fossil fuels and industrial processes, on the other hand, account for 65% of the global greenhouse emissions to the atmosphere (IPCC, 2014). In 2015, the increased awareness of climate change issues led to the Paris agreement, in which 195 countries committed themselves to reducing their greenhouse gases emissions by 40% by 2030. Achieving such an ambitious target requires a shift from fossil fuels to renewable sources for energy and chemicals production. Among renewable resources, biodegradable waste streams are a promising source of green energy and (bio)-chemicals.

Recently, the awareness of the unexploited potential of waste has increasingly driven the industrial sector to implement integrated systems, the so-called biorefineries, to produce not only biofuels, but also a wide spectrum of bio-based chemicals from organic by-products and waste streams (Cherubini, 2010; Mohan et al., 2016; Moscoviz et al., 2018). Such a transition is fully in line with the efforts the EU is making towards a circular bioeconomy (European Commission, 2018) as well as its commitment to becoming the first climate-neutral area in the world by 2050 (European Commission, 2020).

Among the business areas producing waste and wastewater potentially suitable for biorefineries, the dairy sector plays a significant role in the EU economy and many dairy companies are making tremendous efforts to meet the European environmental protection measures and targets (European Dairy Association, 2019). In the EU, a total of 170 billion kg of milk was produced in 2017, 93% of which was converted into dairy products including cheese (37%), butter (30%), cream (13%), fresh milk (11%), acidified milk (4%), milk powder (2%), and other minor products (Eurostat, 2018). Dairy industries produce an average of 2.5 L of wastewater per L of processed milk, as well as about 9–10 L of cheese whey (CW) per kg of cheese produced, resulting in approximately 400 billion L of wastewater per year (Eurostat, 2018). Dairy effluents, and CW in particular, are characterised by a high organic load representing, at the same time, a severe hazard for the environment and a

* Corresponding author.
E-mail addresses: paolo.dessi@nuigalway.ie, paolo_dessi89@yahoo.it (P. Dessì).

https://doi.org/10.1016/j.jenvman.2020.111240
Received 10 June 2020; Received in revised form 13 August 2020; Accepted 15 August 2020
Available online 28 August 2020

Abbreviations

AD	Anaerobic digestion
AFBR	Anaerobic fluidized bed reactors
AS	Activated sludge
ASTBR	Anaerobic structured-bed reactor
BMP	Biomethane potential
BOD	Biological oxygen demand
CE	Coulombic efficiency
COD	Chemical oxygen demand
CSTR	Continuous stirred tank reactor
CW	Cheese whey
DF	Dark fermentation
FBR	Fluidized bed reactor
GDL	Gas diffusion layer
HAc	Acetic acid
HBu	Butyric acid
HCa	Caproic acid
HPr	Propionic acid
HRT	Hydraulic retention time
MEC	Microbial electrolysis cell
MET	Microbial electrochemical technology
MFC	Microbial fuel cell
OLR	Organic loading rate
PABR	Periodic anaerobic baffled reactor
PBR	Packed bed reactor
PEM	Proton exchange membrane
PHA	Polyhydroxyalkanoates
PHB	Polyhydroxybutyrate
PHV	Polyhydroxyvalerate
PLA	Polylactic acid
PTFE	Polytetrafluoroethylene
SBR	Sequence batch reactor
TOC	Total organic carbon
TRL	Technology readiness level
UASB	Upflow anaerobic sludge blanket
UFAF	Up-flow anaerobic filter
VFAs	Volatile fatty acids
VS	Volatile solids
VSS	Volatile suspended solids

huge opportunity for bioenergy and biochemicals production (Ahmad et al., 2019).

Currently, a large share of dairy effluents, including about 50% of the CW produced worldwide, is discharged into the environment without any treatment (Bosco et al., 2018; Slavov, 2017). Among the available treatment options, traditional activated sludge processing is economically not sustainable due to the high organic load of dairy effluents, and the consequent huge quantities of both oxygen required for aeration and excess sludge produced. Activated sludge treatment consumes an average of 900 $kWh_{(el)}$ d^{-1}, including 100 $kWh_{(el)}$ d^{-1} for dewatering (using a filter press) and 800 $kWh_{(el)}$ d^{-1} for aerobic stabilization, accounting for 30% of the total energy required for aerobic treatment of dairy effluents (Dąbrowski et al., 2017). Thermo-catalytic treatment has also been proposed for CW valorisation (Remón et al., 2016), but the high temperature required (450-600 °C) and the production of solids make such a process expensive.

Bioprocesses such as anaerobic digestion or fermentation, as well as biological production of polymers and bioelectrochemical systems, have the advantage of coupling the treatment of dairy effluents with the production of bioenergy and/or biochemical commodities at mild temperature conditions, typically within the range 20–55 °C. Though promising, none of the mentioned options alone represents the ultimate solution for CW treatment, since the energy/chemicals production rates are too small for an economically sustainable scale-up. The implementation of an integrated process, including a combination of physical, chemical and biological processes, is therefore the key for a cost-effective and efficient valorisation of dairy effluents. The aim of this review is to summarize and critically discuss the progress made towards the implementation of biorefineries for energy and chemicals recovery in dairy industries, with a specific focus on CW. This review provides an insight into the most promising biorefinery models for resource recovery from CW, based on critical considerations on the potentials, prospects and limitations of the available options, to support the creation of an innovative and scalable industrial chain.

2. Cheese whey characterisation

Cheese production usually generates three different waste streams, including CW and secondary CW (from cheese and ricotta/cottage cheese production, respectively), and dairy wastewater (from washing of tanks and equipment) (Fig. 1).

CW is a green-yellow by-product of cheese and casein powder production, with an estimated worldwide production of about 190 billion kg $year^{-1}$. Due to its high organic and volumetric load, CW is considered the main polluting waste stream in dairy industries (Ryan and Walsh, 2016; Slavov, 2017). The CW composition depends on the cheese production process, on the milk source (sheep, goat, cow or buffalo), as well as on the quantity of water, detergents and sanitizing agents used (Demirel et al., 2005; Shete and Shinkar, 2013). In general, CW accounts for 85–95% of the milk volume, retains 55% of milk nutrients (vitamins and minerals) and 20% of milk proteins, and is characterised by COD and BOD concentrations of 50–102 and 27–60 g L^{-1}, respectively, more than 90% of which is made up of lactose (Carvalho et al., 2013; Ryan and Walsh, 2016). CW also contains sodium, potassium and calcium salts (0.46–10%), and has a pH of 3.8–6.5 depending on the whey type (acidic or sweet), and a low alkalinity (Prazeres et al., 2012). More details can be found in the comprehensive review by Carvalho et al. (2013).

CW can be processed to obtain cottage, curd, or ricotta cheese, generating secondary CW as a by-product. Secondary CW retains about 60% of the dry matter contained in CW, and is characterised by a lower protein concentration and a higher salinity because of the second flocculation step and addition of salts in the manufacturing process (Carvalho et al., 2013). Dairy wastewater contains similar compounds as CW, but at lower concentrations. Another waste stream, whey permeate,

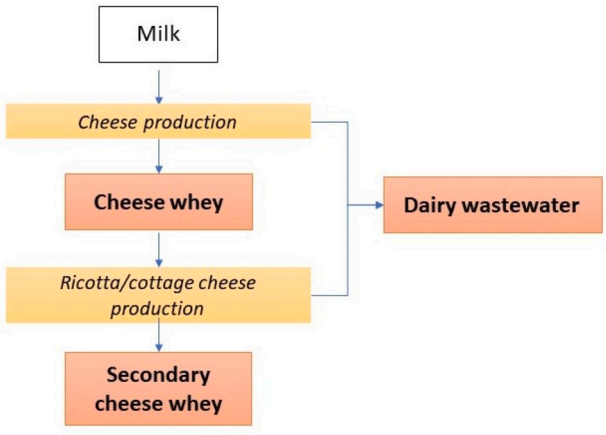

Fig. 1. Cheese production process and effluents generated.

can be obtained as a by-product of protein recovery from CW by ultrafiltration. CW permeate retains about 80% of the lactose contained in the original CW, has a high salinity and low concentration of proteins and fats, depending on the efficiency of the ultrafiltration process (Bosco et al., 2018).

3. Biotechnologies for bioenergy and biochemicals production from cheese whey

3.1. Anaerobic digestion

Anaerobic digestion (AD) is a well-established process to exploit the energy content of CW (De Gioannis et al., 2017; Traversi et al., 2013). However, due to the high organic load and low alkalinity of CW, AD may result in the accumulation of volatile fatty acids (VFAs). This leads to acidification and inhibition of the methanogenic activity, adversely affecting the CH_4 yield and process stability (De Gioannis et al., 2014; Escalante-Hernández et al., 2017; Hagen et al., 2014; Prazeres et al., 2012; Traversi et al., 2013). As a consequence, relatively low biomethane potentials (BMPs) ranging from 270 to 600 L CH_4 kg^{-1} VS have been reported for AD of CW under mesophilic conditions (35–37 °C) (Escalante et al., 2018; Labatut et al., 2011; Vivekanand et al., 2018), implying that HRT values >5 days are required in continuously operated AD systems to prevent process instability (Table 1).

In AD, alkali addition or dilution is generally required to mitigate acidification, but both strategies increase the operational costs, and/or the volumes to be treated. A more economic option is co-digesting CW with substrates characterised by a high buffering capacity, such as sewage sludge (Carrieri et al., 1993), dairy manure (Kavacik and Topaloglu, 2010; Rico et al., 2015; Vivekanand et al., 2018), poultry manure (Gelegenis et al., 2007), cattle slurry (Comino et al., 2012), or fish ensilage (Vivekanand et al., 2018), although literature results are controversial. Furthermore, when digesting CW in combination with pathogenic waste streams, health and safety issues may hamper the use of the digestate as a fertilizer. Labatut et al. (2011) reported that co-digestion of CW with dairy manure, at 10:90 or 25:75 ratios, resulted in a lower CH_4 yield (238–252 L kg^{-1} VS) than with raw CW (424 L kg^{-1} VS). Vivekanand et al. (2018) also reported a decreased CH_4 yield when blending CW with cattle manure, fish ensilage, or both. On the other hand, Comino et al. (2012) obtained the highest CH_4 yield of 343 L CH_4 kg^{-1} VS co-digesting 50% CW and 50% cattle slurry at 35 °C and 42 d HRT. Hublin and Zelić (2013) reported a maximum CH_4 yield of 288 L kg^{-1} VS by co-digestion of CW and cow manure at 55 °C, with an optimum mixing ratio of 10:90, and addition of 5 g $NaHCO_3$ L^{-1} for alkalinity control.

In co-digestion, not only the maximum CH_4 yield, but also the process stability, may be affected by the mixing ratio of substrates. When co-digesting CW and diluted poultry manure in a continuous-flow stirred tank reactor (CSTR), Gelegenis et al. (2007) reported an increasing CH_4 yield for mixtures with CW concentrations up to 35%, but the process became unstable when the CW fraction exceeded 50% (based on VS). In contrast, when co-digesting CW and the screened liquid fraction of dairy manure, Rico et al. (2015) reported an increase in the CH_4 yield from 161 to 187 L CH_4 kg^{-1} COD when increasing the CW proportion from 15 to 85% at 35 °C and 15.6 d HRT, with no instability concerns.

A two-stage process, where hydrolysis-acetogenesis and methanogenesis are carried out in two separate reactors, is another strategy to avoid process instability (Fernández et al., 2015) and enhance COD removal and CH_4 production (Bertin et al., 2013; Yazar et al., 2016), although with increased capital and operational costs. Another advantage of two-stage AD is the possibility of operating the methanogenic reactor at lower HRTs (<5 d) compared to the single-stage process. More innovative systems involve a two-stage process in which H_2 is recovered in the acidogenic reactor (see Section 3.2), which can be used as a fuel, either alone or in combination with CH_4 (hythane). Yilmazer and Yenigün (1999) and Saddoud et al. (2007) reported a biogas yield of 550 and 300 L kg^{-1} $COD_{removed}$, respectively, with COD removal efficiencies above 90%, in a two-stage AD process with 4 d HRT in the methanogenic reactor. With a HRT of 4.4 d, Antonopoulou et al. (2008) obtained a CH_4 yield of 75.6 L CH_4 d^{-1} (or 383 L CH_4 kg^{-1} COD_{feed}), notably higher than that obtained by Venetsaneas et al. (2009) with a CSTR at 20 d HRT (1 L CH_4 d^{-1} or 134 L CH_4 kg^{-1} COD_{feed}). Fernández et al. (2015) compared single- and two-stage AD of CW under thermophilic conditions (55 °C), reporting for the former a maximum yield of 349 L CH_4 kg^{-1} COD_{feed} at 8.3 d HRT, whereas for the latter an inhibition effect at a HRT < 12.5 d. This suggests that two-stage processes may not be optimal for thermophilic AD.

Table 1
Continuous methane production from CW, either as the sole substrate or in co-digestion, in single-stage or two-stage (acidogenesis and methanogenesis in separate reactors) AD processes.

Process	Substrate	Inoculum	Reactor[a]	T (°C)	pH	HRT (d)	Methane production	COD removal (%)	Reference
One-stage	50% CW 50% cattle slurry (v/v)	None	CSTR	35	6.9–8.7	42	187 L CH_4 kg^{-1} COD_{feed}	82	Comino et al. (2012)
	CW	Granular anaerobic cultures	UASB	35	n.a.[c]	2–4.95	424 L CH_4 kg^{-1} COD_{feed}	95–97	Erguder et al. (2001)
	2 L CW + 1 kg Dairy manure + 1 L water	None	CSTR	34	6.5–7.5	5	0.9 L CH_4 L^{-1} d^{-1}	n.a.[c]	Kavacik and Topaloglu (2010)
	85% CW 15% liquid fraction of dairy manure (v/v)	None	CSTR	35	6.4–7.1	15.6	392 L CH_4 kg^{-1} VS_{feed}	n.a.[c]	Rico et al. (2015)
Two-stage	CW	None	PABR	35	8.0	4.4	383 L CH_4 kg^{-1} $COD_{removed}$[b]	94	Antonopoulou et al. (2008)
	CW	None	SBR	55	n.a.[c]	25	349 L CH_4 kg^{-1} COD_{feed}[b]	n.a.[c]	Fernández et al. (2015)
	Diluted CW	Anaerobic sludge	CSTR	37	7.3–8.5	4	300 L biogas kg^{-1} $COD_{removed}$[b]	99	Saddoud et al. (2007)
	CW	Anaerobic sludge	CSTR	35	7.7	20	134 L CH_4 kg^{-1} COD_{feed}[b]	95	Venetsaneas et al. (2009)
	CW	Anaerobic sludge	UFAF	n.a.[c]	n.a.[c]	4	550 L biogas kg^{-1} $COD_{removed}$[b]	90	Yilmazer and Yenigün (1999)

[a] CSTR, continuously stirred tank reactor; PABR, periodic anaerobic baffled reactor; SBR, sequencing batch reactor; UASB, upflow anaerobic sludge blanket; UFAF, up-flow anaerobic filter.
[b] For two-stage processes, it refers to the COD of the acidogenic effluent rather than the initial substrate.
[c] Not available.

3.2. Fermentative processes

3.2.1. Dark fermentation

Dark fermentation (DF) is a promising option for CW valorisation due to its high carbohydrate content, which can be converted to biohydrogen and VFAs (Akhlaghi et al., 2019; Asunis et al., 2019; De Gioannis et al., 2014). In the absence of CW pre-treatments and external inoculum, DF of CW mainly involves three steps, including (i) lactose hydrolysis into glucose and galactose, (ii) conversion of monomeric sugars into lactate by homolactic microorganisms, such as *Lactobacilllus*, and (iii) conversion of lactate into H_2 and VFAs by fermentative microorganisms, such as *Clostridium* (Fig. 2).

A theoretical maximum yield of 8 mol H_2 mol^{-1} lactose can be obtained by DF, if acetate is the only soluble reaction product. However, DF is sensitive to substrate composition, organic loading rate, inoculum type and pre-treatment, reactor type and operation regime, temperature, pH, hydraulic and cell residence time (Akhlaghi et al., 2017). This results in actual H_2 yields between 1 and 4 mol H_2 mol^{-1} lactose, accompanied by the production of a mixture of VFAs, mainly acetic, propionic, and butyric acid (Table 2).

Inocula of different origin, including pure cultures, anaerobic sludge, activated sludge, and compost, with or without pre-treatment, have been used in DF of CW (Table 2). However, some studies relied exclusively on the indigenous biomass of CW (Akhlaghi et al., 2017; Antonopoulou et al., 2008; De Gioannis et al., 2014; Montecchio et al., 2018; Venetsaneas et al., 2009), reporting as high H_2 yields as those obtained using external inocula. De Gioannis et al. (2014) compared batch DF of CW with pre-treated activated sludge and without an external inoculum, obtaining similar yields of 160–170 L H_2 kg^{-1} TOC at pH 6–6.5. To achieve faster start-up, pre-fermented CW can be used as the inoculum in large-scale plants in place of methanogenic inocula that require chemical or thermal pre-treatment to inhibit methanogenesis. However, Perna et al. (2013) obtained a yield of only 0.7 mol H_2 mol^{-1} lactose (40 L H_2 kg^{-1} $COD_{lactose}$) when using fermented CW as the inoculum in a packed bed reactor (PBR), with a relatively high production of acetate (10 g L^{-1}), which suggests the onset of H_2-consuming homoacetogenic pathways. Among pure cultures, both *Clostridium saccharoperbutyacetonicum* (Ferchichi et al., 2005) and *Escherichia coli* (Rosales-Colunga et al., 2010) yielded 2.7 mol H_2 mol^{-1} lactose (158 L H_2 kg^{-1} $COD_{lactose}$) from diluted CW and CW powder, respectively, therefore of the same order of magnitude as mixed cultures. The use of pure cultures, which increases operational costs, does not seem a cost-effective approach for CW fermentation when H_2 is the desired end product.

Various CW-based substrates have been used for DF. Raw CW is easily degraded by indigenous bacteria, even at 4 °C, making storage difficult (Tribst et al., 2019). Thus, many studies used re-hydrated CW powder (Table 2), adjusting the water content to restore the original content of raw CW. Addition of bicarbonate was proposed to prevent acidification (Perna et al., 2013), although co-digestion with an alkaline substrate such as manure can also be done (Ghimire et al., 2017). Dilution of CW can prevent acidification of the fermentation broth, thus increasing the H_2 yields, but also drastically increasing the already huge amount of wastewater to be treated. Furthermore, dilution of CW would reduce the concentration of micro and macro nutrients available to the microorganisms. Yields above 3 mol H_2 mol^{-1} lactose, and acetate and isobutyrate concentrations above 5 g L^{-1} were obtained by supplementing CW with micronutrients such as calcium (Azbar et al., 2009a), whereas yields below 2 mol H_2 mol^{-1} lactose (117 L H_2 kg^{-1} $COD_{lactose}$), as well as low VFA concentrations were obtained from deproteinizedor ultrafiltered CW (Fernández et al., 2015; Montecchio et al., 2018). Since this was likely due to the lack of nitrogen to support microbial growth, excessive dilution or inclusion of a protein recovery step before DF of CW are not recommended.

Bioreactors with high biomass retention, such as fluidized bed reactors (FBR) (Ferreira Rosa et al., 2014a, 2014b; Ottaviano et al., 2017), or sequencing batch reactors (SBR) (Fernández et al., 2015) can be advantageous for DF of CW, compared to CSTRs, as much lower HRTs can be applied (Table 2). However, too short HRTs, below 4 h, may decrease the H_2 yield (Ferreira Rosa et al., 2014a). Among the operating parameters, pH has the strongest impact on both H_2 yield and VFA production. An optimum pH between 5.5 and 6.5 for H_2 production from CW under mesophilic conditions was identified in several studies (Asunis et al., 2019; Azbar et al., 2009b; Davila-Vazquez et al., 2008; De Gioannis et al., 2014; Ferchichi et al., 2005). However, an optimum pH of 4.5 was reported under thermophilic conditions by Azbar et al. (2009b). Ottaviano et al. (2017) obtained a remarkable yield of 3.67 mol H_2 mol^{-1} lactose (214 L H_2 kg^{-1} $COD_{lactose}$) from diluted CW in a thermophilic (55 °C) FBR operated at pH 4–4.5 and HRT of 4 h.

Besides H_2 production, the pH affects the yield and spectrum of VFAs, so that the operating conditions of DF reactors can be adjusted to target specific VFAs (or a mixture of them), in combination with or as an

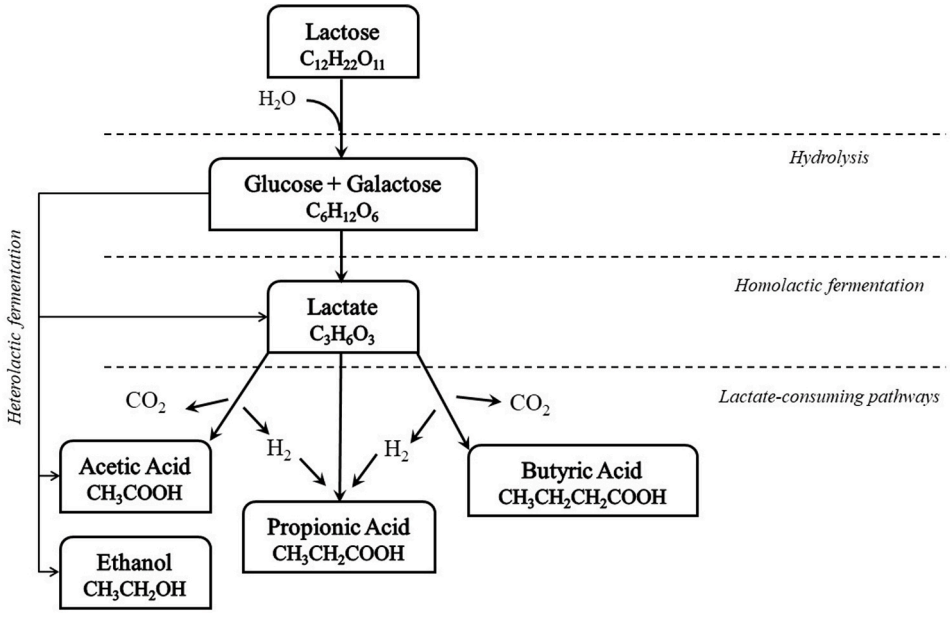

Fig. 2. Most common lactose fermentation pathways from CW indigenous microorganisms.

Table 2
Continuous hydrogen and VFA production from CW-based substrates.

Substrate	Inoculum	Reactor[a]	T (°C)	pH	OLR	HRT (h)	H_2 yield	VFA[b] production	Reference
Cheese whey	None	CSTR	35	5.2 (at steady state)	n.a.[c]	24	41 L H_2 kg^{-1} COD	HAc: 9.4 g L^{-1} HBu 7.2 g L^{-1}	Antonopoulou et al. (2008)
Cheese whey powder	Pre-fermented cheese whey	ASTBR	25	5.1 (average)	24 g_{COD} L^{-1} d^{-1}	24	82 L H_2 kg^{-1} $COD_{lactose}$	HAc: 5.0 g L^{-1} HBu: 3.0 g L^{-1}	Blanco et al. (2019)
Cheese whey	Acidogenic sludge	UASB	30	5.0 (average)	10–20 g_{COD} L^{-1} d^{-1}	24–12	122 mL H_2 L^{-1} d^{-1}	n.a.[c]	Castelló et al. (2009)
Cheese whey	Kitchen waste compost	CSTR	30	5.5 (controlled)	29 g_{COD} L^{-1} d^{-1}	24	52 L H_2 kg^{-1} $COD_{lactose}$	HAc: 3.0 g L^{-1} HBu: 1.6 g L^{-1}	Castelló et al. (2018)
Cheese whey powder	Pretreated anaerobic granular sludge	CSTR	37	5.9 (controlled)	92.4–184.4 $g_{lactose}$ L^{-1} d^{-1}	4–10	163 L H_2 kg^{-1} $COD_{lactose}$	HAc: 4.5 g L^{-1} HPr: 6.2 g L^{-1} HBu: 10.6 g L^{-1}	Davila-Vazquez et al. (2009)
Cheese whey	Pretreated digested sludge	UASB	35	5.0 (controlled)	20-80 g_{COD} L^{-1} d^{-1}	24	40 L H_2 kg^{-1} COD	HAc: 9.1 g L^{-1} HBu: 13.5 g L^{-1}	Dessì et al. (2020)
Deproteinized cheese whey	None	SBR	35	4.5–5.5 (pulse controlled)[d]	12.7–25.3 g_{COD} L^{-1} d^{-1}	1.5–3.0	12 L H_2 kg^{-1} COD	HAc: 2.3–3.4 g L^{-1} HPr: 1.0 g L^{-1} HBu: 0.5 g L^{-1}	Fernández et al. (2015)
Cheese whey powder supplemented with medium	Pretreated anaerobic granular sludge	AFBR	30	4.0–4.5 (controlled)	30–120 g_{COD} L^{-1} d^{-1}	1–4	77 L H_2 kg^{-1} $COD_{lactose}$	HAc: 0.2 mol mol^{-1} lactose HBu: 0.4 mol mol^{-1} lactose HPr: 0.4 mol mol^{-1} lactose	Ferreira Rosa et al. (2014a)
Cheese whey powder supplemented with medium	Pretreated anaerobic granular sludge	AFBR	30	4.0–4.5 (controlled)	n.a.[c]	6	74 L H_2 kg^{-1} $COD_{lactose}$	n.a.[c]	Ferreira Rosa et al. (2014b)
Cheese whey + buffalo manure	Pretreated anaerobic sludge	CSTR	55	4.8–5.0 (at steady state)	0.7–2.6 g_{VS} L^{-1} d^{-1}	192–288	131.8 L H_2 kg^{-1} VS	HAc: 4.2 mmol g^{-1} VS HBu: 14.1 mmol g^{-1} VS HPr: 0.5 mmol g^{-1} VS	Ghimire et al. (2017)
CW powder	Acclimated anaerobic sludge	CSTR	30	4.5–7.0 (controlled)	15 g_{COD} L^{-1} d^{-1}	1	n.a.[c]	HAc: 3.5–12 g L^{-1} HBu: 2–3 g L^{-1} HPr: 2–3 g L^{-1}	Gouveia et al. (2017)
Ultrafiltered cheese whey	None	CSTR	36	5.5 (controlled)	n.a.[c]	6–12	78–107 L H_2 kg^{-1} $COD_{lactose}$	n.a.[c]	Montecchio et al. (2018)
CW powder solution	Pretreated anaerobic granular sludge	AFBR	55	4.0–4.5 (controlled)	235.2 $g_{lactose}$ L^{-1} d^{-1}	4	214 L H_2 kg^{-1} $COD_{lactose}$	HAc: 0.5 g L^{-1} HBu: 0.7 g L^{-1}	Ottaviano et al. (2017)
Cheese whey powder supplemented with sodium bicarbonate	Pre-fermented cheese whey	PBR	30	5.6 (controlled)	22–37 g_{COD} L^{-1} d^{-1}	24	39 L H_2 kg^{-1} $COD_{lactose}$	HAc: 10 g L^{-1} HBu: 2 g L^{-1}	Perna et al. (2013)
Cheese whey	None	CSTR	35	5.0–6.0 (controlled)	60 g_{COD} L^{-1} d^{-1}	24	48 L H_2 kg^{-1} $COD_{consumed}$	HAc: 9.2 g L^{-1} HBu: 14.5 g L^{-1}	Venetsaneas et al. (2009)
Dry whey permeate powder	Anaerobic sludge	CSTR	35	Uncontrolled condition	14 g_{COD} L^{-1} d^{-1}	24	52 L H_2 kg^{-1} COD	HAc: 2.1 g L^{-1} HPr: 0.1 g L^{-1} HBu: 0.8 g L^{-1} HCa: 1.2 g L^{-1}	Yang et al. (2007)

[a] AFBR, anaerobic fluidized bed reactor; ASTBR, anaerobic structured-bed reactor; CSTR, continuously stirred tank reactor; PBR, packed bed reactor; SBR, sequence batch reactor; UASB, upflow anaerobic sludge blanket reactor.
[b] HAc, acetic acid; HBu, butyric acid; HCa, caproic acid; HPr, propionic acid.
[c] Not available.
[d] pH adjusted to 5.5 whenever it dropped to 4.5.

alternative to H_2. The production of butyrate and acetate from CW occurs at pH 5–6 (Table 2), whereas propionate production prevails over the butyrate pathway at pH 7–7.5 (Asunis et al., 2019). Generally, a total of 0.5–0.6 g VFA g^{-1} CW is obtained in the pH range 5–7 (Asunis et al., 2019; Colombo et al., 2016; Duque et al., 2014; Gouveia et al., 2017). CW fermentation at pH < 5 can promote the accumulation of lactic acid (Asunis et al., 2019; Gouveia et al., 2017). Interestingly, in continuous reactors, the type and concentration of VFAs produced at a given pH appear to be the same irrespective of the starting conditions (Gouveia et al., 2017). This suggests that the fermentation pH may be adjusted during continuous operation to target specific metabolic products. In-line VFA extraction can be implemented during DF of CW to improve process stability and allow a continuous recovery of VFAs (Dessì et al., 2020).

3.2.2. *Lactate fermentation*

Lactic acid is characterised by an increasing global demand from 0.7 Mt in 2013 to 1.9 Mt in 2020 (grandviewresearch.com), mainly as the building block for polylactic acid (PLA) production, but also for application in food, pharmaceutical and chemical industries. Most commercial lactic acid is currently produced by bacterial fermentation of corn, sugarcane, molasses and other crops. CW has been proposed as an

alternative feedstock to avoid competition with food production.

Lactic acid is mainly produced by bacteria belonging to the genera *Lactobacillus*, *Lactococcus*, *Streptococcus*, *Bacillus*, and *Enterococcus* (Miller et al., 2011; Ryan and Walsh, 2016). Lactose is hydrolysed by enzymes such as β-galactosidase, produced by lactic acid bacteria, into glucose and galactose, and then converted into lactic acid *via* homolactic fermentation (Fig. 2), resulting in a yield of 4 mol lactate mol^{-1} lactose. However, ethanol or acetate can be produced along with lactate *via* heterolactic fermentation (Castillo Martinez et al., 2013; Sikora et al., 2013), halving the lactate yield. The type of fermentation pathway and the specific lactate isomer (L- or D-) produced depend on the lactic acid bacteria involved and the operating conditions, in particular pH (Mazzoli et al., 2014; Miller et al., 2011; Xu et al., 2018).

Since lactic acid bacteria have limited potential to biosynthesize amino-acids, the presence of a nitrogen source is crucial for their growth (Mazzoli et al., 2014; Prazeres et al., 2012). Due to its high protein content, raw CW can be used for lactate production, although enzymatic hydrolysis of lactose might be necessary. Xu et al. (2018) reported a D-lactic acid productivity of 2.4 g L^{-1} d^{-1} from hydrolysed CW powder by *Lactobacillus bulgaricus* in non-sterile conditions and without the addition of extra nutrients, which was further enhanced by the addition of 9 g L^{-1} yeast extract. The yield can be further improved by continuous extraction of the lactic acid produced, since its accumulation inhibits the biomass activity. Taleghani et al. (2018) reported a lactic acid production rate of 6.1 g L^{-1} h^{-1} in a fermentative reactor with an integrated membrane extraction system, as opposed to 3.4 g L^{-1} h^{-1} obtained in the control reactor without membrane extraction.

3.2.3. Ethanol fermentation

Bioethanol is considered one of the most promising candidates for replacing fossil fuels, and thus its global demand is constantly increasing (marketsandmarkets.com). CW fermentation into ethanol is currently hardly competitive with the established processes that use sugarcane, corn starch or lignocellulosic biomass as raw materials (Guimarães et al., 2010). Solventogenesis from CW has been attempted with yeasts such as *Saccharomyces cerevisiae* (Staniszewski et al., 2007), but low ethanol yields were obtained due to the low lactose conversion and product inhibition. Conversely, the *Kluyveromyces marxianus* yeast was shown to hydrolyse lactose, form a biofilm and tolerate ethanol, and is thus a potential candidate for CW conversion into bioethanol (Joshi et al., 2011; Lane and Morrissey, 2010). Continuous fermentation is potentially superior to batch processes, as it results in higher ethanol production while reducing the fermentation time (Gabardo et al., 2014). Several strategies have been proposed to retain the microorganisms into the bioreactor, including cell immobilization (Dahiya and Vij, 2012), cell recycle (Santos et al., 2016) and membrane retention (Wei et al., 2014). Christensen et al. (2011) obtained continuous ethanol production from CW, with a rate of 2.5–4.5 g L^{-1} h^{-1}, using a pure culture of *K. marxianus* immobilized in Ca-alginate.

The ethanol yield strictly depends on the operating parameters such as substrate concentration, pH and temperature (Table 3). Using a continuous FBR with Ca-alginate immobilized-cells, Gabardo et al. (2014) obtained the highest ethanol productivity of 6.0 g L^{-1} h^{-1} from CW permeate at a concentration of 150 g L^{-1} although the highest ethanol yield was obtained at 90 g L^{-1}. Dragone et al. (2011) reported that a lactose concentration of 200 g L^{-1} and a temperature of 35 °C were optimal for ethanol production (81 g L^{-1} in 44 h) from CW powder by *K. fragilis*. Using the response surface methodology, Diniz et al. (2014) reported that temperatures between 33.3 and 38.5 °C, pH between 4.7 and 5.7, lactose concentrations between 50 and 108 g L^{-1} and biomass concentrations between 2.4 and 3.3 (optical density at 600 nm) are optimal for ethanol production from CW by *K. marxianus*, with yields above 90% of the theoretical value.

3.3. Biopolymers

CW fermentation products, mainly VFAs, can be used as building blocks for biopolymer production (Colombo et al., 2016; Duque et al., 2014; Gouveia et al., 2017; Ryan and Walsh, 2016). Biopolymers such as polylactic acid (PLA) and polyhydroxyalkanoates (PHA) are a bio-based, biodegradable alternative to petroleum-based plastics, and their market size is expected to increase from 2.11 Mt in 2018 to 2.63 Mt in 2023 (European European Bioplastics, 2018).

3.3.1. PLA

PLA is a versatile biopolymer used in a wide range of industrial sectors, such as food packaging, textile, agriculture, electronics, transportation as well as in the biomedical field. PLA is currently the largest compostable synthetic plastic produced worldwide and its production is projected to increase up to 0.6 Mtons $year^{-1}$ in 2025 (IEA Bioenergy Task42, 2012). However, the high costs of the building block used for PLA production, mostly lactic acid from microbial corn starch fermentation, hinders full exploitation of its potential. This may be fostered by optimized lactate production from residual organic materials (including CW), as outlined in section 3.2.2.

3.3.2. PHA

PHAs are polyesters produced from organic substrates by various microorganisms, which accumulate them inside the cell for energy storage purposes. PHA production from CW has been reported from microorganisms able to synthesize polymers from lactose, such as *Thermus thermophilus* (Pantazaki et al., 2009), *Pseudomonas hydrogenovora* (Koller et al., 2008), and *Bacillus megaterium* (Das et al., 2018) or engineered *Cupriavidus necator* (Povolo et al., 2010). Although higher PHA accumulation can be attained with pure cultures, mixed microbial communities can produce PHAs from complex and cheaper substrates, such as dairy biowaste, and do not require sterilisation. PHA-producing microorganisms are selected and enriched by alternating short feast (presence of carbon) and long famine (absence of carbon) regimes (Reis et al., 2003). Despite nutrient addition being commonly reported in the literature for selecting high-capacity PHA-storing microbial communities (Oliveira et al., 2018), the high N and P contained in CW might

Table 3
Batch and continuous bioethanol fermentation from CW-based substrates using *Kluyveromyces marxianus*.

Substrate	Substrate concentration (g lactose L^{-1})	Reactor	T (°C)	Operating conditions	Ethanol production	Reference
Cheese whey	46.8	Continuous fluidized-bed bioreactor (alginate-immobilized cells)	32	Dilution rate: 0.2 h^{-1}	4.5 g L^{-1} h^{-1}	Christensen et al. (2011)
Cheese whey powder	150	Batch reactor	35	pH: 4.5	43.7 g L^{-1}	Das et al. (2016)
Cheese whey permeate	150	Continuous fluidized-bed bioreactor (alginate-immobilized cells)	30	Dilution rate: 0.3 h^{-1}	6.0 g L^{-1} h^{-1}	Gabardo et al. (2014)
Cheese whey	48	Fed-batch reactor	30	Uncontrolled condition	8.0 g L^{-1}	Hadiyanto et al. (2014)
Cheese whey	43.6	Batch reactor	28	Uncontrolled condition	17 g L^{-1}	Zoppellari and Bardi (2013)

reduce, or even eliminate, the need for an external nutrient supply (Colombo et al., 2016).

PHA production from fermented CW by mixed cultures resulted in storage yields of 0.7–0.8 mol PHA mol^{-1} VFA, with a PHA content of 65–75% (Table 4). The PHA composition (polyhydroxybutyrate, PHB, or polyhydroxyvalerate, PHV) depends on the carboxylic acid present in the CW fermentate: the higher the concentration of acetate and butyrate, the higher the PHB fraction, whereas high concentrations of propionate result in PHV accumulation. PHV fractions up to 40% have been reported from fermented CW (Table 4). Recently, fermented CW has also been used as the substrate for PHA production by phototrophic mixed cultures, using light intensities comparable with those typical of sunny regions, yielding 0.6 g COD_{PHA} g^{-1} COD_{VFA} and PHA contents of 20–25% (Fradinho et al., 2019).

3.4. Bioelectrochemical systems

Microbial electrochemical technologies (METs) can be implemented to recover the energy contained in CW as electricity in microbial fuel cells (MFCs) (Table 5) or as H_2 in microbial electrolysis cells (MECs) (Table 6). In MFCs, specific microorganisms, namely exoelectrogens, oxidise the organic substrate and transfer the electrons to an anode electrode. Electrons then flow to a cathode electrode through an external circuit, producing electric power, and combine with an electron acceptor, such as oxygen, closing the circuit (Logan et al., 2006). In MECs, the protons resulting from substrate oxidation are the final electron acceptors, producing H_2, if enough energy is provided as input current to drive the reaction (Rago et al., 2016).

Antonopoulou et al. (2010) were the first to test CW, diluted to 0.73 g COD L^{-1} and amended with nutrients, as the substrate for MFC, yielding a maximum power density of 18.4 mW m^{-2} and a coulombic efficiency (CE) of only 1.9%, due to the presence of undesired microorganisms in CW. To address this issue, Stamatelatou et al. (2011) filter-sterilised CW prior to dilution, obtaining power densities up to 40 mW m^{-2}. The effect of COD concentration (0.35–6.7 g L^{-1}) was investigated by Tremouli et al. (2013), who reported the highest power production (46 mW m^{-2}) and CE (11.3%) from diluted CW at 6.7 g COD L^{-1}, with a 95% COD removal efficiency. Ghasemi et al. (2017) compared CW (50 g lactose L^{-1}) and concentrated CW (100 g lactose L^{-1}) as the substrate in a two-chamber MFC, reporting a higher power density from raw CW (288 mW m^{-2}) than from concentrated CW (188 mW m^{-2}).

Since carboxylic acids are favourable substrates for exoelectrogenic microorganisms, Wenzel et al. (2017) proposed fermented CW as the substrate for a single-chamber MFC, obtaining a dramatically higher power production (439 mW m^{-2}) than a control reactor fed with raw CW (0.34 mW m^{-2}). Indeed, exoelectrogenic microorganisms were enriched in the MFC fed with fermented CW, due to the high concentration of VFAs, whereas the high lactose and lactate concentrations of the raw CW resulted in a prevalence of fermentative microorganisms.

Both CW and fermented CW, as well as digestate from AD of CW, have been used as the substrates for H_2 production in MEC (Table 6). Diluted CW (2 g COD L^{-1}), amended with a phosphate buffer solution, was resulted in a production of 0.8 L H_2 L^{-1} d^{-1}, with energy recoveries up to 71% (Rago et al., 2016). Moreno et al. (2015) combined DF and MEC for two-stage H_2 production from CW, obtaining 0.5 L H_2 L^{-1} d^{-1} from filtered, eight-times diluted CW fermentate, supplemented with acetate, in a MEC. However, a rapid decrease in the MEC performance occurred, probably due to the lack of nutrients in the diluted substrate. Rivera et al. (2017) compared raw, fermented and digested CW for H_2 production in a single-chamber MEC. H_2 production yields of 61 and 48 mL H_2 g^{-1} $COD_{removed}$ were obtained from digested and fermented CW, with a CE of 93 and 32%, respectively, whereas a negligible H_2 production (CE 1%) was obtained from raw CW.. However, besides their composition, the different initial organic load (19.9, 1.6 and 4.0 g L^{-1} COD for raw, fermented and digested CW, respectively) may have affected the results. Fermented CW, rather than raw CW, should thus be used as the substrate for energy recovery in METs. METs can also be seen as a final polishing stage after the AD process. Filtration and dilution should be avoided, since they may result in a lack of nutrients which can hinder the electrogenic activity.

3.5. Integrated processes

A combination of treatment processes to produce an array of valuable products is required for the implementation of a zero-waste-approaching dairy biorefinery (Morais and Bogel-Lukasik, 2013). Combinations of physical, chemical and biological processes (Table 7; Fig. 3) can be implemented. Protein recovery, e.g. by isoelectric or thermocalcic precipitation or nano- or ultrafiltration, may be applied prior to the biological treatment (Bosco et al., 2018; Chen et al., 2016), although negatively affecting the availability of nutrients for the subsequent biological processes.

DF was applied as the first step in most of the studies combining biological treatments for CW valorisation (Table 7), standing as the core of the biorefinery. Several biological downstream processes can be then applied for further valorisation of the DF effluent. Among these, AD is the most applied process on fermented dairy effluent (Table 7). Combination of DF and AD typically leads to high COD removal efficiencies

Table 4
PHA production from CW derived fermentates using mixed microbial communities.

Substrate	Fermentation yield (g COD g^{-1} COD)	Fermentation products (PHA precursors) HLa/HAc/HBu/HPr/HVa/HCa/EtOH[a] (% Organic Acid as COD)	Max PHA content (g PHA kg^{-1} VSS)	PHA storage yield (g COD_{PHA} g^{-1} COD)	Productivity (g PHA L^{-1} d^{-1})	Polymer composition (% HB:%HV)[b]	Reference
Cheese whey	0.4	58/16/26/0/0/0/0	659 ± 46	0.6 ± 0.0	10.9 ± 0.8	100:0	Colombo et al. (2016)
Sterilised cheese whey	0.6 ± 0.1	6/58/13/19/4/0/0	814 ± 57	0.7 ± 0.1	28.2 ± 2.0	60:40	Colombo et al. (2016)
Cheese whey	0.7 ± 0.2	1/58/22/6/4/0/9	650	0.7 ± 0.1	13.4	81:19	Duque et al. (2014)
Cheese whey	0.6–0.7	16/45/23/14/6/0/5	300	0.6	n.a.[c]	88:12	Fradinho et al. (2019)
Sweet cheese whey powder	0.64 ± 0.05	0/46/44/4/5/0/0	430	0.85 ± 0.12	0.20	89:11	Oliveira et al. (2018)
Filtered whey permeate	0.5	0/44/50/2/1/3/0	530–630	0.41–0.63	n.a.[c]	85:15	Valentino et al. (2015)

[a] HLa, Lactic acid; HAc, Acetic acid; HBu, Butyric acid; HPr, Propionic acid; HVa, Valeric acid; HCa, Caproic acid; EtOH, Ethanol.
[b] HB, hydroxybutyrate; HV, hydroxyvalerate.
[c] Not available.

Table 5
Electricity production from dairy wastewater or CW-based substrates in MFCs.

Substrate	Inoculum	Reactor characteristics[a]	T (°C)	HRT (h)	Maximum power production	CE (%)	Reference
Cheese whey	Anaerobic sludge	H-type (310 mL) Anode: Teflon treated carbon filter paper Cathode: Carbon cloth with Pt Membrane: PEM	35.5	Batch	18.4 mW m^{-2}	1.9	Antonopoulou et al. (2010)
Cheese whey powder	Anaerobic sludge	Single chamber (125 mL) Anode: Carbon cloth Cathode: Carbon cloth with GDL Membrane: None	35	Batch	n.a.[b]	0.8–2.0	Colombo et al. (2017)
Synthetic dairy wastewater	Municipal wastewater	Dual chamber (480 mL) Anode: Untreated carbon paper Cathode: Untreated carbon paper Membrane: PEM	22	8.4	90 mW m^{-2}	10.5 ± 10	Faria et al. (2017)
Whey	Anaerobic sludge	Cube-shaped dual chamber (420 mL) Anode: Carbon paper Cathode: Carbon paper with Pt Membrane: PEM	30	Batch	188.8 mW m^{-2}	26	Ghasemi et al. (2017)
Concentrated whey	Anaerobic sludge	Cube-shaped dual chamber (420 mL) Anode: Carbon paper Cathode: Carbon paper with Pt Membrane: PEM	30	Batch	288.1 mW m^{-2}	15	Ghasemi et al. (2017)
Cheese whey (diluted 10 times)	Digested sludge	Tubular dual chamber (500 mL) Anode: Carbon fibre brush Cathode: Carbon cloth and activated carbon powder Membrane: PEM	21	Batch	0.4 W m^{-3}	3.9 ± 1.7 (based on total COD)	Kelly and He (2014)
Cheese whey	MFC enriched community	Single chamber (28 mL) Anode: Graphite fibre brush Cathode: Graphite fibre cloth with PTFE and Pt Membrane: None	n.a.[b]	Batch	3.46 mW m^{-2}	49 ± 8	Rago et al. (2016)
Cheese whey	Anaerobic sludge	Dual chamber (310 mL) Anode: Carbon paper Cathode: Carbon cloth Membrane: PEM	30	Batch	46 mW m^{-2}	5.5–11.3	Tremouli et al. (2013)
Dairy wastewater	Anaerobic mixed consortia	Single chamber (550 mL) Anode: Graphite plate Cathode: Graphite plate Membrane: PEM	29	Batch	6.71 mW m^{-2}	4.3–14.2	Venkata Mohan et al. (2010)
Cheese whey	Planktonic MFC community	Single chamber air cathode (25 mL) Anode: Graphite felt Cathode: Carbon cloth with Nafion and Pt Membrane: PEM	30	Batch	0.34 mW m^{-2}	14	Wenzel et al. (2017)
Fermented cheese whey	Planktonic MFC community	Single chamber air cathode (25 mL) Anode: Graphite felt Cathode: Carbon cloth with Nafion and Pt Membrane: PEM	30	Batch	439 mW m^{-2}	24	Wenzel et al. (2017)

[a] GDL, gas diffusion layer; PEM, proton exchange membrane; PTFE, polytetrafluoroethylene.
[b] Not available.

(>80%), due to the final conversion of VFAs to methane. However, considering the higher pH and HRT required for AD than for DF, pH buffering and high reactor volumes are commonly required for the AD step. Furthermore, the high concentrations (up to 20–30 g L^{-1}) of VFAs produced in DF, as well as the low buffering capacity of CW, may inhibit the AD process (Bertin et al., 2013).

The DF effluent can also be used for further H_2 production, although an external source of energy e.g. in the form of light (photofermentation) or electricity (MEC) is required to overcome the thermodynamic constraints. Rai et al. (2012) combined dark and photofermentation of diluted CW (10 g L^{-1} lactose) using immobilized pure cultures, obtaining a yield of 199 L H_2 kg^{-1} COD, although the COD removal efficiency was low (36%). The application of METs to fermented CW could be favoured by the low ohmic resistance associated to the typically high salinity of CW. A remarkably high yield of over 800 L H_2 g^{-1} COD was obtained from deproteinized ricotta CW, diluted to 3 g COD L^{-1}, by combining DF and MEC, with 63% COD removal efficiency (Marone et al., 2017).

Since DF effluents are rich in VFAs, DF can also be coupled to PHA production. Colombo et al. (2019) proposed an integrated two-stage bioprocess aimed at simultaneously recovery of H_2 (2.4–5.1 L H_2 L^{-1} d^{-1}) and PHB (274–268 g kg^{-1} COD_{feed}) from deproteinized CW. In order to produce PHAs at high concentrations, a VFA extraction and concentration step, e.g. *via* electrodialysis, can be included in the integrated process. Domingos et al. (2018) applied electrodialysis to fermented CW obtaining a concentrated VFA stream (up to 63 g L^{-1} from the original concentration of 13 g L^{-1}), from which a PHA yield of 0.60 g PHA g^{-1} VFA was obtained, comparable to the yields reported from

Table 6
Hydrogen production from dairy wastewater or CW-based substrates in MECs.

Substrate	Inoculum	Reactor characteristics[a]	T (°C)	HRT (h)	Maximum hydrogen production	CE (%)	Reference
Ricotta cheese production wastewater (scotta)	Anaerobic sediments	Cylindrical two-chamber (400 mL) Anode: Carbon felt Cathode: Pt–Ir (90%:10%) mesh Membrane: AEM	37	Batch	0.023 L H_2 L^{-1} d^{-1}	75 (estimated)	Marone et al. (2017)
Fermented cheese whey (diluted)	Planktonic MEC community	Continuous flow membrane-less (50 mL) Anode: Carbon felt Cathode: GDL with Ni nanoparticles Membrane: None	25	10	MEC failure	n.a.[b]	Moreno et al. (2015)
Fermented cheese whey and acetate	Planktonic MEC community	Continuous flow membrane-less (50 mL) Anode: Carbon felt Cathode: GDL with Ni nanoparticles Membrane: None	25	10	MEC failure	n.a.[b]	Moreno et al. (2015)
Fermented cheese whey and salts	Planktonic MEC community	Continuous flow membrane-less (50 mL) Anode: Carbon felt Cathode: GDL with Ni nanoparticles Membrane: None	25	10	0.5 L H_2 L^{-1} d^{-1}	n.a.[b]	Moreno et al. (2015)
Fermented cheese whey, salts and acetate	Planktonic MEC community	Continuous flow membrane-less (50 mL) Anode: Carbon felt Cathode: GDL with Ni nanoparticles Membrane: None	25	10	0.5 L H_2 L^{-1} d^{-1}	n.a.[b]	Moreno et al. (2015)
Cheese whey	MFC enriched community	Single chamber (28 mL) Anode: Graphite fibre brush Cathode: Graphite fibre cloth with PTFE and Pt Membrane: None	n.a.[b]	Batch	0.8 L H_2 L^{-1} d^{-1}	120[c]	Rago et al. (2016)
Cheese whey	Anaerobic sludge	Single chamber (300 mL) Anode: Graphite felt Cathode: Stainless steel mesh Membrane: None	32	Batch	MEC failure	1	Rivera et al. (2017)
Cheese whey digestate	Anaerobic sludge	Single chamber (300 mL) Anode: Graphite felt Cathode: Stainless steel mesh Membrane: None	32	Batch	0.16 L H_2 L^{-1} d^{-1}	31.8	Rivera et al. (2017)
Fermented cheese whey	Anaerobic sludge	Single chamber (300 mL) Anode: Graphite felt Cathode: Stainless steel mesh Membrane: None	32	Batch	0.06 L H_2 L^{-1} d^{-1}	92.7	Rivera et al. (2017)

[a] AEM, anion exchange membrane; GDL, gas diffusion layer; PEM, proton exchange membrane; PTFE, polytetrafluoroethylene.
[b] Not available.
[c] Due to H_2 recycling by homoacetogenic bacteria.

VFA-containing synthetic solutions.

4. Full-scale applications

Despite the potential for CW valorisation, the implementation of integrated, multiple treatment schemes is still limited. Existing full-scale plants are mostly AD plants producing biogas to cover part of the dairy industry energy needs. To be economically viable, more complex processing sequences would require a plant size that often exceeds the potential of small-to medium-size dairy industries.

Among the full-scale applications, the company Valbio provides AD systems to dairy industries through its patented technology Valbio Methcore®, based on UASB technology. Valbio has commissioned more than 10 full-scale plants for dairy companies mostly located in France, Canada and Bulgaria, treating 0.3–10.5 million L of CW $year^{-1}$ with an energy production of 0.3–3.5 MWh $year^{-1}$ and COD removal efficiency higher than 90% (Valbio.com). Dairygold Co-Operative Society Limited recently installed the world's largest above ground anaerobic digester (ADI/BVF®, Evoqua) in Ireland. The Dairygold low-rate anaerobic digester was designed to treat 5500 m^3 d^{-1} wastewater containing powdered milk, cheese waste and CW (Evoqua.com), meeting the discharge limits and contributing to satisfy the dairy industry energy needs. First Milk's Lake District creamery (Cumbria, UK) was the first dairy industry to feed upgraded biomethane generated from cheese process residues to the national gas grid in 2016 (Clearfleau.com). The CSTR was designed to treat 1650 m^3 d^{-1} of dairy wastewater and whey producing 5.4 MWh of bioenergy (Clearfleau.com).

Industrial-scale bioethanol plants are in operation in Ireland, New Zealand, USA, Denmark and Germany. The Carbery Group factory, the largest single cheese-producing facility in Ireland, started the operation of an industrial-scale whey-to-ethanol plant in 1978 (Carbery, 2018). In addition to cheese, the company produces high-quality ethanol, accounting for 50% of Ireland's industrial ethanol needs for beverage, pharmaceutical and food industries (Carbery, 2018). Since 2005, the company has also been supplying ethanol to petrol companies in Ireland. Anchor Ethanol operates three whey-to-ethanol plants in New Zealand, using deproteinated whey, concentrated from 4 to 8% lactose and fermented for 24 h by *Kluyveromyces* sp., as feedstock attaining an ethanol

Table 7
Combination of at least two chemical or biological processes for energy or resource recovery from CW-based substrates.

Process[a]	Substrate	Inoculum	Temperature (°C)	HRT	Output	COD removal (%)	Reference
Dark fermentation (CSTR, 3 L) + methanogenesis (PABR, 15 L)	Cheese whey (61 g COD L^{-1})	Indigenous microflora	35 (both processes)	1 day (dark fermentation); 4.4 days (methanogenesis)	Hydrogen: 41 L kg^{-1} COD; Methane: 383 L kg^{-1} COD	94	Antonopoulou et al. (2008)
Acidogenesis + methanogenesis (two-stage concentric reactor, 190 mL for acidogenic reactor, 790 mL for methanogenic reactor)	Cheese whey + cattle manure (1:1; 35.2 g COD L^{-1})	Methanogenic sludge (both processes)	35 (both processes)	5 days (acidogenesis); 20 days (methanogenesis)	Methane: 258 kg^{-1} VS	83	Bertin et al. (2013)
Thermocalcic precipitation, ultrafiltration + PHA production	Cheese whey (50 g COD L^{-1})	Dairy plant activated sludge enriched on acetate (PHA production)	45–55 (thermocalcic precipitation) Not reported for PHA production	24–48 h (PHA production)	Proteins: 80 g L^{-1}, PHA: 0.75–0.90 g L^{-1}	n.a.[b]	Bosco et al. (2018)
Isoelectric precipitation, nanofiltration + dark fermentation (UASB, 7.4 L)	Milk powder (3.0 g COD L^{-1})	Sewage sludge	25 (precipitation and nanofiltration) 37 (dark fermentation)	12 h (dark fermentation)	Proteins: 192 g kg^{-1} COD; Reusable water; Hydrogen (not quantified); VFAs: 2.2 g L^{-1}	n.a.[b]	Chen et al. (2016)
Enzymatic hydrolysis step with β-galactosidase + Dark fermentation (CSTR, 4 L) + PHA production (SBR, 1 L; Fed-batch assay, 0.5 L)	Secondary cheese whey and concentrated cheese whey permeate(OLR: 8, 11, 15 g sugars L^{-1} d^{-1} for dark fermentation; 1.5 mg_{COD} L^{-1} d^{-1} for PHA production)	Thermally pretreated anaerobic digested sludge (dark fermentation); Activated sludge (PHA production)	55 (dark fermentation) 25 (PHA production)	2 days (dark fermentation) 1 day (PHA production)	Hydrogen: 163–233 L kg^{-1} COD; PHA: 268–274 g kg^{-1} COD	n.a.[b]	Colombo et al. (2019)
Dark fermentation (CSTR, 3 L) + methanogenesis (UASB, 1 L)	Cheese whey powder (45.5 g COD L^{-1})	Anaerobic granular sludge	37 (dark fermentation) 25–30 (methanogenesis)	6 h (both processes)	Hydrogen: 137 L kg^{-1} COD; Methane: 250 L kg^{-1} COD	92	Cota-Navarro et al. (2011)
Dark fermentation (anaerobic column biofilm packed reactor, 1 L) + electrodialysis + PHA production (3 L)	Cheese whey powder (28 g COD L^{-1})	Acidogenic sludge (dark fermentation); *Cupravidus necator* (PHA production)	37 (dark fermentation) 30 (PHA production)	6 h (dark fermentation); 52 h (PHA production, batch mode)	VFAs: 13 g L^{-1} (60 g L^{-1} after electrodialysis); PHA: 500 g kg^{-1} COD	n.a.[b]	Domingos et al. (2018)
Dark fermentation (batch, 2 L) + methanogenesis (batch, 2 L)	Dairy wastewater (11.2 g COD L^{-1})	*Enterobacter aerogens* (dark fermentation); Digested cow dung slurry (methanogenesis)	30 (dark fermentation) 35 (methanogenesis)	13 h (dark fermentation); 7 days (methanogenesis)	Hydrogen: 105 L kg^{-1} COD; Methane: 190 L kg^{-1} COD	64	Kothari et al. (2017)
Dark fermentation (batch, 500 mL) + biocatalyzed electrolysis (MEC, 400 mL)	Deproteinized ricotta cheese whey (57.8 g COD L^{-1}) diluted to 3 g_{COD} L^{-1}	Anaerobic digested sludge (dark fermentation)	37 (both processes)	48 h (dark fermentation); 14 days (MEC)	Hydrogen: 95.1 + 714.7 L kg^{-1} COD; Electric current: 7.46 A m^{-2}	63	Marone et al. (2017)
Dark fermentation (batch, 250 mL) + biocatalyzed electrolysis (MEC, 50 mL)	Cheese whey (fermentation; 122 g COD L^{-1}); Fermented cheese whey (MEC; diluted 8 times and amended with acetate and nutrients)	Digested sludge (dark fermentation); Domestic wastewater-fed MEC effluent (MEC)	35 (dark fermentation) 25 (MEC)	Not reported for dark fermentation; 10 h (MEC)	Hydrogen: 94.2 L kg^{-1} VS; Electric current: 10 mA	82	Moreno et al. (2015)
Dark fermentation (batch, 100 mL) + photofermentation (batch, 100 mL)	Diluted cheese whey (10 g lactose L^{-1})	*Enterobacter aerogens* (dark fermentation); *Rhodopseudomonas* (photofermentation)	30 (dark fermentation) 34 (photofermentation)	84 h (both processes)	Hydrogen: 199 L kg^{-1} COD	36	Rai et al. (2012)
Dark fermentation (CSTR, 0.5 L) + methanogenesis (CSTR, 3 L)	Cheese whey (60.5 g COD L^{-1})	Indigenous microflora	35 (both processes)	1 day (dark fermentation); 20 days (methanogenesis)	Hydrogen: 48 L kg^{-1} COD; Methane: 31 L kg^{-1} COD	95	Venetsaneas et al. (2009)

[a] CSTR, continuously stirred tank reactor; MEC, microbial electrolysis cell; PABR, periodic anaerobic baffled reactor; UASB, upflow anaerobic sludge blanket.
[b] Not available.

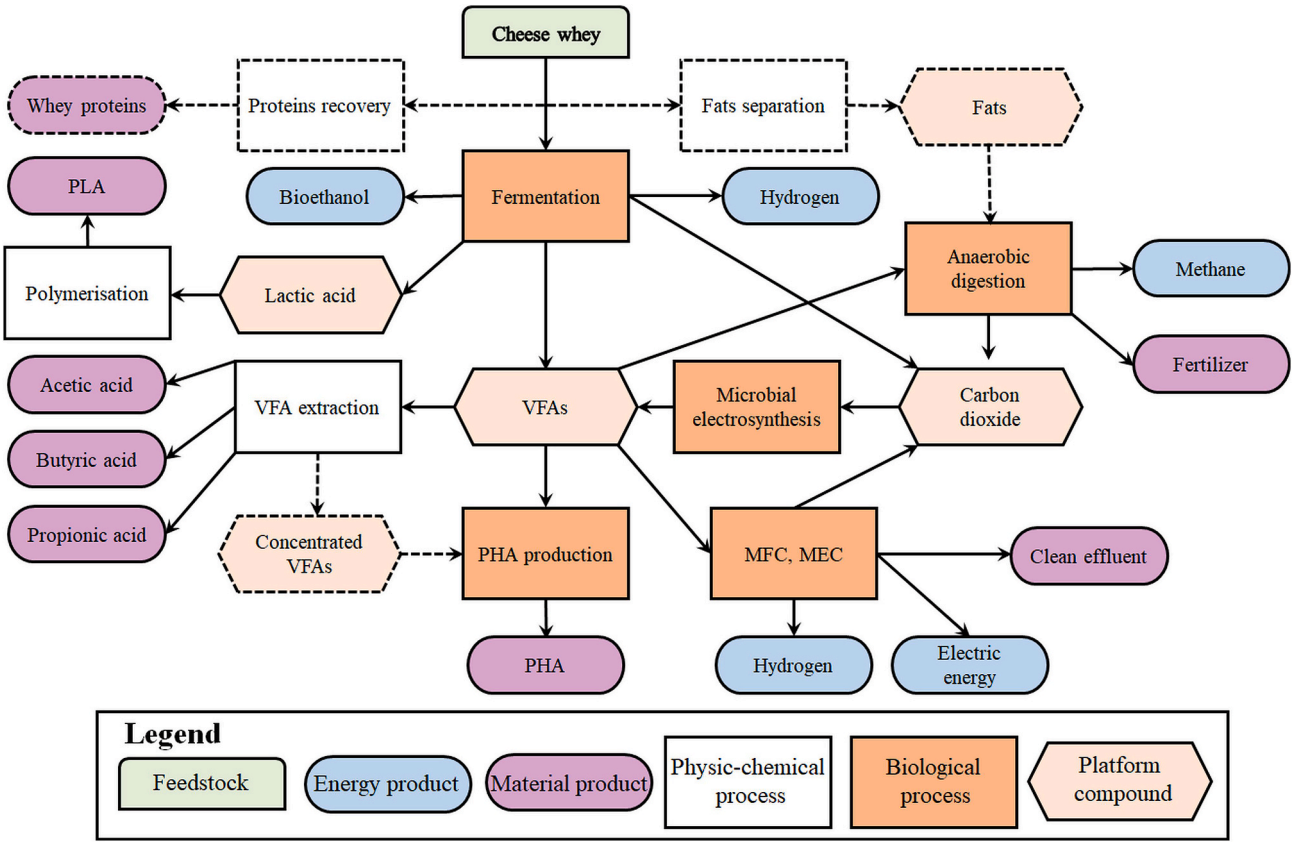

Fig. 3. Integrated treatment processes for cheese whey valorisation according to the circular economy principle. Symbols and colours are represented according to Cherubini et al. (2009). The dashed parts represent optional processes, not essential for the following treatment steps. (For interpretation of the references to colour in this figure legend, the reader is referred to the Web version of this article.)

titre of 4%, successively concentrated to various ethanol grades by distillation (Guimarães et al., 2010).

5. Future perspectives

CW is an abundant substrate, easily available and at low cost, but at the same time needs proper management. Many of the processes applicable for biotechnological valorisation of CW are currently at a medium/high TRL and some integration schemes between these processes are promising. However, some critical aspects need further investigation in order to make the application of the biorefinery concept to the dairy supply chain fully feasible.

CW displays very variable characteristics depending on both the livestock originating the milk, and the geographical context. The milk and the resulting CW production is characterised by a strong seasonal variability in terms of quantity and composition, that follows the lactation period. The seasonal variation could be managed by freezing CW during peak production, and subsequently thawing on demand. A better solution could be based on assessing the availability of CW in the area under concern, and promoting consortia to ensure an even CW supply throughout the year (Ubando et al., 2020).

The optimal combination of the biotechnological processes strictly depends on CW availability and characteristics, as well as legislation and market demand. Pre-treatment of CW might simplify downstream valorisation. For example, a protein extraction stage, already well developed at the industrial scale (TRL 9), could be integrated into the process chain, fostered by the relatively high value of whey proteins (6–22 € kg^{-1}) (Table 8), but addition of nutrients may be required for the subsequent biological treatment stages. Similarly, the need for post-treatments aimed at removing undesired impurities or extracting the compounds of interest must be carefully evaluated, being an important cost item in the entire process scheme.

Among the soluble products of CW fermentation, acetic acid and ethanol are currently characterised by low economic values, but relatively big market sizes, whereas butyric and lactic acid have smaller, but rapidly growing (15–19% compound annual growth rate, CAGR) markets (Table 8). It should be noted, however, that obtaining individual marketable products from the mixture of carboxylic acids typically obtained from CW fermentate would require highly selective and efficient extraction systems, currently available at TRL 2–3.

As an alternative, the carboxylic acids mixture can be used as a feedstock for biopolymer production, and in particular for PHA production. The technology for PHA production from biowaste is still in the development stage (TRL 3–5). However, the high value of PHAs (2.8–3.2 € kg^{-1}), and the rapidly increasing bioplastics market (16.5% CAGR) could make biological PHA production profitable in the near future. Specific tailored solutions can be investigated within the same dairy industry supply chain, e.g. using the PHA produced from CW as a sustainable packaging for dairy products.

METs are still under development (TRL 3–4). Due to the high cost, and the typically low power density and H_2 yield achievable through MFC and MEC, respectively, their use for treatment of undiluted CW fermentate, characterised by high carboxylic acid concentration, does not appear profitable. In particular, MFCs can hardly compete with technologies such as solar energy and wind power for electricity production at a large scale, unless many cells are stacked together (Gajda et al., 2018). However, due to the high COD removal efficiencies, both MFCs and MECs can be seen as a polishing stage prior to effluent disposal. Among the bioelectrochemical systems, microbial electrosynthesis (MES) can be a key player in limiting the carbon emissions by recycling the CO_2 produced by other bioprocesses, and from the dairy industry itself, and converting it to carboxylic acids for downstream

Table 8
Treatment processes applicable in a biorefinery concept (Fig. 3), including their technological readiness level (TRL), and market value and market size (converted into € from original data in USD) of the main products obtained.

Process	TRL[a]	Products	Indicative price (€ kg^{-1})	Global market size (€)	Global market forecast (€)	CAGR[b] (%)	References
Protein recovery	9	Functional proteins	6.4–22.0	3.9×10^9 (2017)	5.3×10^9 (2022)	6.3	Marketsandmarkets.com
Dark fermentation	4–5	Hydrogen	0.9–7.3	124.4×10^9 (2018)	183.4×10^9 (2025)	8.0	Marketsandmarkets.com
VFA extraction from fermentation broth	2–3	Acetic acid	0.4–0.7	8.8×10^9 (2015)	12.2×10^9 (2022)	4.8	Grandviewresearch.com
		Butyric acid	1.4–1.6	114.8×10^6 (2014)	218.1×10^6 (2020)	15.1	Marketsandmarkets.com
		Propionic acid	1.8–2.3	1.2×10^9 (2014)	1.4×10^9 (2020)	2.8	Grandviewresearch.com
Lactic acid fermentation	8	Lactic acid	0.9	1.9×10^9 (2015)	3.5×10^9 (2020)	18.6	Marketsandmarkets.com
Alcohol fermentation	9	Bioethanol	0.6–1.4	48.5×10^9 (2016)	63.5×10^9 (2022)	5.3	Marketsandmarkets.com
Polymerisation	9	PLA	2.0	5.5×10^9 (2017)	13.8×10^9 (2023)	16.5	Marketsandmarkets.com
Biological biopolymer production	3–5	PHA	2.8–3.2				
Microbial fuel cell	3–4	Renewable electric power	48.9[c]	5×10^3 TWh (2018)	7×10^3 TWh (2023)	13.1	International Energy Agency, IEA
Microbial electrolysis cell	3–4	Hydrogen	0.9–7.3	124.7×10^9 (2018)	183.3×10^9 (2025)	5.7	Marketsandmarkets.com
Anaerobic digestion	9	Biomethane	0.4–0.7	1.4×10^9 (2017)	2.4×10^9 (2025)	7.1	Transparencymarketresearch.com
		Fertilizer	0–6[d]	5.6×10^9 (2019)[e]	8.5×10^9 (2024)	6.8	Globenewswire.com
Microbial electrosynthesis	3-4	Acetic acid	0.4–0.7	8.8×10^9 (2015)	12.2×10^9 (2022)	4.8	Grandviewresearch.com
		Butyric acid	1.4–1.6	114.8×10^6 (2014)	218.1×10^6 (2020)	15.1	Marketsandmarkets.com
		Caproic acid	1.5	9.2×10^6 (2018)	11.5×10^6 (2024)	3.2	Marketwatch.com

[a] Technology readiness level.
[b] Compound annual growth rate.
[c] €/MWh, average price in EU.
[d] €/m^3; data from compost global market.

applications (Batlle-Vilanova et al., 2016; Vassilev et al., 2018). This would close the loop in the carbon recovery chain towards a zero-waste-approaching biorefinery.

6. Conclusions

Cheese whey is an outstanding resource for production of green energy and platform chemical compounds, but currently its potential is not fully exploited. In this review, the most promising biotechnologies for cheese whey valorisation were compared, and the strong and weak points of each one were critically analysed. Due to its simple and efficient application on raw CW, the current and potential huge market size of its products (H_2 and VFAs), and the more and more stringent regulations on carbon emissions, fermentation is likely to gradually replace anaerobic digestion as the core of dairy biorefinery. H_2 is indeed a key player towards the decarbonisation of the energy production system, whereas VFAs have several industrial applications, and may also be regarded as precursors for bioplastic production, the market size of which is expected to increase in response to the policies to reduce the use of traditional plastics. Due to the high organic load of CW, inhibitory for electrogenic microorganisms, MFC and MEC can only find application as the final polishing stage of the dairy biorefinery. MES is a promising technology to recycle the CO_2 generated in the other biological treatment processes and in the energy production plants, providing heat and electricity to the dairy industry, such as boilers and co-generation heat and power (CHP) plants, closing the carbon loop.

Web references

http://www.valbio.com/en/VALBIO-Projects/VALBIO-projects/id_1024
https://clearfleau.com/portfolio/lake-district-biogas-green-gas-from-cheese-residues/
https://www.evoqua.com/en/brands/adi-systems/Pages/bvf-worlds-largest-above-ground-digester-installed-in-ireland.aspx
https://www.globenewswire.com/news-release/2019/10/08/1926776/0/en/The-global-compost-market-is-expected-to-reach-an-estimated-9-2-billion-by-2024-with-a-CAGR-of-6-8-from-2019-to-2024.html
https://www.grandviewresearch.com/industry-analysis/acetic-acid-market
https://www.grandviewresearch.com/industry-analysis/lactic-acid-and-poly-lactic-acid-market
https://www.grandviewresearch.com/industry-analysis/propionic-acid-market
https://www.iea.org/reports/world-energy-outlook-2019/electricity#abstract
https://www.marketsandmarkets.com/Market-Reports/bioethanol-market-131222570.html
https://www.marketsandmarkets.com/Market-Reports/biopolymers-bioplastics-market-88795240.html
https://www.marketsandmarkets.com/Market-Reports/butyric-acid-market-76962011.html
https://www.marketsandmarkets.com/Market-Reports/dairy-ingredients-market-974.html
https://www.marketsandmarkets.com/Market-Reports/hydrogen-generation-market-494.html
https://www.marketsandmarkets.com/Market-Reports/polylacticacid-387.html
https://www.marketwatch.com/press-release/at-29-cagr-hexano

ic-acid-market-size-poised-to-touch-usd-45-million-by-2024-2020-01-14

https://www.transparencymarketresearch.com/bio-methane-market-2018-2026.html

Declaration of competing interest

The authors declare that they have no known competing financial interests or personal relationships that could have appeared to influence the work reported in this paper.

Acknowledgements

This work was supported by the Science Foundation of Ireland (SFI) Research Professorship Programme on *Innovative Energy Technologies for Bioenergy, Biofuels and a Sustainable Irish Bioeconomy* (IETSBIO^3, award 15/RP/2763). It was conducted on the framework of the "Waste Biorefinery" task group of the International Waste Working Group (IWWG). Fabiano Asunis and Marco Isipato gratefully acknowledges Sardinian Regional Government for the financial support of their PhD scholarship (P.O.R. Sardegna F.S.E. - Operational Programme of the Autonomous Region of Sardinia, European Social Fund 2014–2020 - Axis III Education and training, Thematic goal 10, Investment Priority 10ii, Specific goal 10.5).

References

Ahmad, T., Aadil, R.M., Ahmed, H., ur Rahman, U., Soares, B.C.V., Souza, S.L.Q., Pimentel, T.C., Scudino, H., Guimarães, J.T., Esmerino, E.A., Freitas, M.Q., Almada, R.B., Vendramel, S.M.R., Silva, M.C., Cruz, A.G., 2019. Treatment and utilization of dairy industrial waste: a review. Trends Food Sci. Technol. 88, 361–372. https://doi.org/10.1016/j.tifs.2019.04.003.

Akhlaghi, M., Boni, M.R., De Gioannis, G., Muntoni, A., Polettini, A., Pomi, R., Rossi, A., Spiga, D., 2017. A parametric response surface study of fermentative hydrogen production from cheese whey. Bioresour. Technol. 244, 473–483. https://doi.org/10.1016/j.biortech.2017.07.158.

Akhlaghi, M., Boni, M.R., Polettini, A., Pomi, R., Rossi, A., De Gioannis, G., Muntoni, A., Spiga, D., 2019. Fermentative H_2 production from food waste: parametric analysis of factor effects. Bioresour. Technol. 276, 349–360. https://doi.org/10.1016/j.biortech.2019.01.012.

Antonopoulou, G., Stamatelatou, K., Venetsaneas, N., Kornaros, M., Lyberatos, G., 2008. Biohydrogen and methane production from cheese whey in a two-stage anaerobic process. Ind. Eng. Chem. Res. 47, 5227–5233. https://doi.org/10.1021/ie071622x.

Antonopoulou, G., Stamatelatou, K., Bebelis, S., Lyberatos, G., 2010. Electricity generation from synthetic substrates and cheese whey using a two chamber microbial fuel cell. Biochem. Eng. J. 50, 10–15. https://doi.org/10.1016/j.bej.2010.02.008.

Asunis, F., De Gioannis, G., Isipato, M., Muntoni, A., Polettini, A., Pomi, R., Rossi, A., Spiga, D., 2019. Control of fermentation duration and pH to orient biochemicals and biofuels production from cheese whey. Bioresour. Technol. 289, 121722. https://doi.org/10.1016/j.biortech.2019.121722.

Azbar, N., Dokgöz, F.T., Keskin, T., Eltem, R., Korkmaz, K.S., Gezgin, Y., Akbal, Z., Öncel, S., Dalay, M.C., Gönen, Ç., Tutuk, F., 2009a. Comparative evaluation of biohydrogen production from cheese whey wastewater under thermophilic and mesophilic anaerobic conditions. Int. J. Green Energy 6, 192–200. https://doi.org/10.1080/15435070902785027.

Azbar, N., Tuba Çetinkaya Dokgöz, F., Keskin, T., Korkmaz, K.S., Syed, H.M., 2009b. Continuous fermentative hydrogen production from cheese whey wastewater under thermophilic anaerobic conditions. Int. J. Hydrogen Energy 34, 7441–7447. https://doi.org/10.1016/j.ijhydene.2009.04.032.

Batlle-Vilanova, P., Puig, S., Gonzalez-Olmos, R., Balaguer, M.D., Colprim, J., 2016. Continuous acetate production through microbial electrosynthesis from CO_2 with microbial mixed culture. J. Chem. Technol. Biotechnol. 91, 921–927. https://doi.org/10.1002/jctb.4657.

Bertin, L., Grilli, S., Spagni, A., Fava, F., 2013. Innovative two-stage anaerobic process for effective codigestion of cheese whey and cattle manure. Bioresour. Technol. 128, 779–783. https://doi.org/10.1016/j.biortech.2012.10.118.

Blanco, V.M.C., Oliveira, G.H.D., Zaiat, M., 2019. Dark fermentative biohydrogen production from synthetic cheese whey in an anaerobic structured-bed reactor: performance evaluation and kinetic modeling. Renew. Energy 139, 1310–1319. https://doi.org/10.1016/j.renene.2019.03.029.

Bosco, F., Carletto, R.A., Marmo, L., 2018. An integrated cheese whey valorization process. Chem. Eng. Trans. 64, 379–384. https://doi.org/10.3303/CET1864064.

Carbery, 2018. A New Horizon, Our Journey of Sustainable Progress. https://www.carbery.com/wp-content/uploads/Carbery-Sustainability-Report-2018.pdf.

Carrieri, C., Di Pinto, A.C., Rozzi, A., Santori, M., 1993. Anaerobic co-digestion of sewage sludge and concentrated soluble wastewaters. Water Sci. Technol. 28, 187–197. https://doi.org/10.2166/wst.1993.0102.

Carvalho, F., Prazeres, A.R., Rivas, J., 2013. Cheese whey wastewater: characterization and treatment. Sci. Total Environ. 445–446, 385–396. https://doi.org/10.1016/j.scitotenv.2012.12.038.

Castelló, E., García y Santos, C., Iglesias, T., Paolino, G., Wenzel, J., Borzacconi, L., Etchebehere, C., 2009. Feasibility of biohydrogen production from cheese whey using a UASB reactor: links between microbial community and reactor performance. Int. J. Hydrogen Energy 34, 5674–5682. https://doi.org/10.1016/j.ijhydene.2009.05.060.

Castelló, E., Braga, L., Fuentes, L., Etchebehere, C., 2018. Possible causes for the instability in the H_2 production from cheese whey in a CSTR. Int. J. Hydrogen Energy 43, 2654–2665. https://doi.org/10.1016/j.ijhydene.2017.12.104.

Castillo Martinez, F.A., Balciunas, E.M., Salgado, J.M., Domínguez González, J.M., Converti, A., Oliveira, R.P. de S., 2013. Lactic acid properties, applications and production: a review. Trends Food Sci. Technol. 30, 70–83. https://doi.org/10.1016/j.tifs.2012.11.007.

Chen, Z., Luo, J., Chen, X., Hang, X., Shen, F., Wan, Y., 2016. Fully recycling dairy wastewater by an integrated isoelectric precipitation – nanofiltration – anaerobic fermentation process. Chem. Eng. J. 283, 476–485. https://doi.org/10.1016/j.cej.2015.07.086.

Cherubini, F., 2010. The biorefinery concept: using biomass instead of oil for producing energy and chemicals. Energy Convers. Manag. 51, 1412–1421. https://doi.org/10.1016/j.enconman.2010.01.015.

Cherubini, F., Jungmeier, G., Wellisch, M., Willke, T., Skiadas, I., Van Ree, R., De Jong, E., 2009. Toward a common classification approach for biorefinery systems. Biofuels, Bioprod. Biorefining 3, 534–546. https://doi.org/10.1002/bbb.

Christensen, A.D., Kádár, Z., Oleskowicz-Popiel, P., Thomsen, M.H., 2011. Production of bioethanol from organic whey using *Kluyveromyces marxianus*. J. Ind. Microbiol. Biotechnol. 38, 283–289. https://doi.org/10.1007/s10295-010-0771-0.

Colombo, B., Sciarria, T.P., Reis, M., Scaglia, B., Adani, F., 2016. Polyhydroxyalkanoates (PHAs) production from fermented cheese whey by using a mixed microbial culture. Bioresour. Technol. 218, 692–699. https://doi.org/10.1016/j.biortech.2016.07.024.

Colombo, A., Schievano, A., Trasatti, S.P., Morrone, R., D'Antona, N., Cristiani, P., 2017. Signal trends of microbial fuel cells fed with different food-industry residues. Int. J. Hydrogen Energy 42, 1841–1852. https://doi.org/10.1016/j.ijhydene.2016.09.069.

Colombo, B., Villegas Calvo, M., Sciarria, T.P., Scaglia, B., Savio Kizito, S., D'Imporzano, G., Adani, F., 2019. Biohydrogen and polyhydroxyalkanoates (PHA) as products of a two-steps bioprocess from deproteinized dairy wastes. Waste Manag. 95, 22–31. https://doi.org/10.1016/j.wasman.2019.05.052.

Comino, E., Riggio, V.A., Rosso, M., 2012. Biogas production by anaerobic co-digestion of cattle slurry and cheese whey. Bioresour. Technol. 114, 46–53. https://doi.org/10.1016/J.BIORTECH.2012.02.090.

Cota-Navarro, C.B., Carrillo-Reyes, J., Davila-Vazquez, G., Alatriste-Mondragón, F., Razo-Flores, E., 2011. Continuous hydrogen and methane production in a two-stage cheese whey fermentation system. Water Sci. Technol. 64, 367–374. https://doi.org/10.2166/wst.2011.631.

Dahiya, M., Vij, S., 2012. Comparative analysis of bioethanol production from whey by different strains of immobilized thermotolerant yeast. Int. J. Sci. Res. Publ. 2, 3.

Das, B., Sarkar, S., Maiti, S., Bhattacharjee, S., 2016. Studies on production of ethanol from cheese whey using *Kluyveromyces marxianus*. In: Materials Today: Proceedings, pp. 3253–3257. https://doi.org/10.1016/j.matpr.2016.10.006.

Das, S., Majumder, A., Shukla, V., Suhazsini, P., Radha, P., 2018. Biosynthesis of Poly(3-hydroxybutyrate) from cheese whey by *Bacillus megaterium* NCIM 5472. J. Polym. Environ. 26, 4176–4187. https://doi.org/10.1007/s10924-018-1288-2.

Davila-Vazquez, G., Alatriste-Mondragón, F., de León-Rodríguez, A., Razo-Flores, E., 2008. Fermentative hydrogen production in batch experiments using lactose, cheese whey and glucose: influence of initial substrate concentration and pH. Int. J. Hydrogen Energy 33, 4989–4997. https://doi.org/10.1016/j.ijhydene.2008.06.065.

Davila-Vazquez, G., Cota-Navarro, C.B., Rosales-Colunga, L.M., de León-Rodríguez, A., Razo-Flores, E., 2009. Continuous biohydrogen production using cheese whey: improving the hydrogen production rate. Int. J. Hydrogen Energy 34, 4296–4304. https://doi.org/10.1016/j.ijhydene.2009.02.063.

De Gioannis, G., Friargiu, M., Massi, E., Muntoni, A., Polettini, A., Pomi, R., Spiga, D., 2014. Biohydrogen production from dark fermentation of cheese whey: influence of pH. Int. J. Hydrogen Energy 39, 20930–20941. https://doi.org/10.1016/j.ijhydene.2014.10.046.

De Gioannis, G., Muntoni, A., Polettini, A., Pomi, R., Spiga, D., 2017. Energy recovery from one- and two-stage anaerobic digestion of food waste. Waste Manag. 68, 595–602. https://doi.org/10.1016/j.wasman.2017.06.013.

Demirel, B., Yenigun, O., Onay, T.T., 2005. Anaerobic treatment of dairy wastewaters: a review. Process Biochem. 40, 2583–2595. https://doi.org/10.1016/j.procbio.2004.12.015.

Dessì, P., Asunis, F., Ravishankar, H., Cocco, F.G., De Gioannis, G., Muntoni, A., Lens, P. N.L., 2020. Fermentative hydrogen production from cheese whey with in-line, concentration gradient-driven butyric acid extraction. Int. J. Hydrogen Energy. https://doi.org/10.1016/j.ijhydene.2020.06.081.

Diniz, R.H.S., Rodrigues, M.Q.R.B., Fietto, L.G., Passos, F.M.L., Silveira, W.B., 2014. Optimizing and validating the production of ethanol from cheese whey permeate by *Kluyveromyces marxianus* UFV-3. Biocatal. Agric. Biotechnol. 3, 111–117. https://doi.org/10.1016/j.bcab.2013.09.002.

Domingos, J.M.B., Puccio, S., Martinez, G.A., Amaral, N., Reis, M.A.M., Bandini, S., Fava, F., Bertin, L., 2018. Cheese whey integrated valorisation: production, concentration and exploitation of carboxylic acids for the production of polyhydroxyalkanoates by a fed-batch culture. Chem. Eng. J. 336, 47–53. https://doi.org/10.1016/j.cej.2017.11.024.

Dragone, G., Mussatto, S.I., Almeida e Silva, J.B., Teixeira, J.A., 2011. Optimal fermentation conditions for maximizing the ethanol production by *Kluyveromyces*

fragilis from cheese whey powder. Biomass Bioenergy 35, 1977–1982. https://doi.org/10.1016/j.biombioe.2011.01.045.
Duque, A.F., Oliveira, C.S.S., Carmo, I.T.D., Gouveia, A.R., Pardelha, F., Ramos, A.M., Reis, M.A.M., 2014. Response of a three-stage process for PHA production by mixed microbial cultures to feedstock shift: impact on polymer composition. N. Biotech. 31, 276–288. https://doi.org/10.1016/j.nbt.2013.10.010.
Dąbrowski, W., Żyłka, R., Malinowski, P., 2017. Evaluation of energy consumption during aerobic sewage sludge treatment in dairy wastewater treatment plant. Environ. Res. 153, 135–139. https://doi.org/10.1016/j.envres.2016.12.001.
Erguder, T.H., Tezel, U., Guven, E., Demirer, G.N., 2001. Anaerobic biotransformation and methane generation potential of cheese whey in batch and UASB reactors. Waste Manag. 21, 643–650. https://doi.org/10.1016/j.jbiotec.2005.05.017.
Escalante, H., Castro, L., Amaya, M.P., Jaimes, L., Jaimes-Estévez, J., 2018. Anaerobic digestion of cheese whey: energetic and nutritional potential for the dairy sector in developing countries. Waste Manag. 71, 711–718. https://doi.org/10.1016/j.wasman.2017.09.026.
Escalante-Hernández, H., Besson, V., Casro-Molano, L., Jaimes-Estévez, J., 2017. Feasibility of the anaerobic digestion of cheese whey in a plug flow reactor (PFR) under local conditions. Ing. Investig. y Technol. 18, 265–277.
European Bioplastics, 2018. Global Production Capacities of Bioplastics 2018-2023. https://www.european-bioplastics.org/wp-content/uploads/2016/02/Report_Bioplastics-Market-Data_2018.pdf.
European Commission, 2018. A Sustainable Bioeconomy for Europe: Strengthening the Connection between Economy, Society and the Environment Updated Bioeconomy Strategy. https://doi.org/10.2777/478385.
European Commission, 2020. Financing the Green Transition: the European Green Deal Investment Plan and Just Transition Mechanism. https://ec.europa.eu/commission/presscorner/detail/en/ip_20_17.
European Dairy Association, 2019. The Dairy Sector & the Green Deal. https://doi.org/10.1787/9789264015906-en.
Eurostat, 2018. Agriculture, Forestry and Fishery Statistics, 2018 Edition.
Faria, A., Gonçalves, L., Peixoto, J.M., Peixoto, L., Brito, A.G., Martins, G., 2017. Resources recovery in the dairy industry: bioelectricity production using a continuous microbial fuel cell. J. Clean. Prod. 140, 971–976. https://doi.org/10.1016/j.jclepro.2016.04.027.
Ferchichi, M., Crabbe, E., Gil, G.H., Hintz, W., Almadidy, A., 2005. Influence of initial pH on hydrogen production from cheese whey. J. Biotechnol. 120, 402–409. https://doi.org/10.1016/j.jbiotec.2005.05.017.
Fernández, C., Cuetos, M.J., Martínez, E.J., Gómez, X., 2015. Thermophilic anaerobic digestion of cheese whey: coupling H_2 and CH_4 production. Biomass Bioenergy 81, 55–62. https://doi.org/10.1016/j.biombioe.2015.05.024.
Ferreira Rosa, P.R., Santos, S.C., Sakamoto, I.K., Varesche, M.B.A., Silva, E.L., 2014a. Hydrogen production from cheese whey with ethanol-type fermentation: effect of hydraulic retention time on the microbial community composition. Bioresour. Technol. 161, 10–19. https://doi.org/10.1016/j.biortech.2014.03.020.
Ferreira Rosa, P.R., Santos, S.C., Silva, E.L., 2014b. Different ratios of carbon sources in the fermentation of cheese whey and glucose as substrates for hydrogen and ethanol production in continuous reactors. Int. J. Hydrogen Energy 39, 1288–1296. https://doi.org/10.1016/j.ijhydene.2013.11.011.
Fradinho, J.C., Oehmen, A., Reis, M.A.M., 2019. Improving polyhydroxyalkanoates production in phototrophic mixed cultures by optimizing accumulator reactor operating conditions. Int. J. Biol. Macromol. 126, 1085–1092. https://doi.org/10.1016/j.ijbiomac.2018.12.270.
Gabardo, S., Rech, R., Rosa, C.A., Ayub, M.A.Z., 2014. Dynamics of ethanol production from whey and whey permeate by immobilized strains of *Kluyveromyces marxianus* in batch and continuous bioreactors. Renew. Energy 69, 89–96. https://doi.org/10.1016/J.RENENE.2014.03.023.
Gajda, I., Greenman, J., Ieropoulos, I.A., 2018. Recent advancements in real-world microbial fuel cell applications. Curr. Opin. Electrochem. 11, 78–83. https://doi.org/10.1016/j.coelec.2018.09.006.
Gelegenis, J., Georgakakis, D., Angelidaki, I., Mavris, V., 2007. Optimization of biogas production by co-digesting whey with diluted poultry manure. Renew. Energy 32, 2147–2160. https://doi.org/10.1016/j.renene.2006.11.015.
Ghasemi, M., Ahmad, A., Jafary, T., Azad, A.K., Kakooei, S., Wan Daud, W.R., Sedighi, M., 2017. Assessment of immobilized cell reactor and microbial fuel cell for simultaneous cheese whey treatment and lactic acid/electricity production. Int. J. Hydrogen Energy 42, 9107–9115. https://doi.org/10.1016/j.ijhydene.2016.04.136.
Ghimire, A., Luongo, V., Frunzo, L., Pirozzi, F., Lens, P.N.L., Esposito, G., 2017. Continuous biohydrogen production by thermophilic dark fermentation of cheese whey: use of buffalo manure as buffering agent. Int. J. Hydrogen Energy 42, 4861–4869. https://doi.org/10.1016/J.IJHYDENE.2016.11.185.
Gouveia, A.R., Freitas, E.B., Galinha, C.F., Carvalho, G., Duque, A.F., Reis, M.A.M., 2017. Dynamic change of pH in acidogenic fermentation of cheese whey towards polyhydroxyalkanoates production: impact on performance and microbial population. N. Biotech. 37, 108–116. https://doi.org/10.1016/j.nbt.2016.07.001.
Guimarães, P.M.R., Teixeira, J.A., Domingues, L., 2010. Fermentation of lactose to bio-ethanol by yeasts as part of integrated solutions for the valorisation of cheese whey. Biotechnol. Adv. 28, 375–384. https://doi.org/10.1016/j.biotechadv.2010.02.002.
Hadiyanto, Ariyanti, D., Aini, A.P., Pinundi, D.S., 2014. Optimization of ethanol production from whey through fed-batch fermentation using *Kluyveromyces marxianus*. Energy Procedia 47, 108–112. https://doi.org/10.1016/j.egypro.2014.01.203.
Hagen, L.H., Vivekanand, V., Linjordet, R., Pope, P.B., Eijsink, V.G.H., Horn, S.J., 2014. Microbial community structure and dynamics during co-digestion of whey permeate and cow manure in continuous stirred tank reactor systems. Bioresour. Technol. 171, 350–359. https://doi.org/10.1016/j.biortech.2014.08.095.
Hublin, A., Zelić, B., 2013. Modelling of the whey and cow manure co-digestion process. Waste Management and Research, pp. 353–360. https://doi.org/10.1177/0734242X12455088.
IEA Bioenergy Task42, 2012. Bio-based Chemicals - Value Added Products from Biorefineries. https://doi.org/10.1007/978-3-319-07593-8_30.
International Energy Agency, 2017. Energy Statistics. https://doi.org/10.1017/CBO9781107415324.004.
IPCC, 2014. Climate Change 2014: Mitigation of Climate Change, Working Group III Contribution to the Fifth Assessment Report of the Intergovernmental Panel on Climate Change. https://doi.org/10.1017/CBO9781107415416.
Joshi, Y., Senatore, B., Poletto, M., 2011. *Kluyveromyces marxianus* biofilm in cheese wheey fermentation for bioethanol production. Chem. Eng. Trans. 24, 493–498. https://doi.org/10.3303/CET1124083.
Kavacik, B., Topaloglu, B., 2010. Biogas production from co-digestion of a mixture of cheese whey and dairy manure. Biomass Bioenergy 34, 1321–1329. https://doi.org/10.1016/j.biombioe.2010.04.006.
Kelly, P.T., He, Z., 2014. Understanding the application niche of microbial fuel cells in a cheese wastewater treatment process. Bioresour. Technol. 157, 154–160. https://doi.org/10.1016/j.biortech.2014.01.085.
Koller, M., Bona, R., Chiellini, E., Fernandes, E.G., Horvat, P., Kutschera, C., Hesse, P., Braunegg, G., 2008. Polyhydroxyalkanoate production from whey by *Pseudomonas hydrogenovora*. Bioresour. Technol. 99, 4854–4863. https://doi.org/10.1016/j.biortech.2007.09.049.
Kothari, R., Kumar, V., Pathak, V.V., Tyagi, V.V., 2017. Sequential hydrogen and methane production with simultaneous treatment of dairy industry wastewater: bioenergy profit approach. Int. J. Hydrogen Energy 42, 4870–4879. https://doi.org/10.1016/j.ijhydene.2016.11.163.
Labatut, R.A., Angenent, L.T., Scott, N.R., 2011. Biochemical methane potential and biodegradability of complex organic substrates. Bioresour. Technol. 102, 2255–2264. https://doi.org/10.1016/j.biortech.2010.10.035.
Lane, M.M., Morrissey, J.P., 2010. *Kluyveromyces marxianus*: a yeast emerging from its sister's shadow. Fungal Biol. Rev. 24, 17–26. https://doi.org/10.1016/j.fbr.2010.01.001.
Logan, B.E., Hamelers, B., Rozendal, R., Schröder, U., Keller, J., Freguia, S., Aelterman, P., Verstraete, W., Rabaey, K., 2006. Microbial fuel cells: methodology and technology. Environ. Sci. Technol. 40, 5181–5192. https://doi.org/10.1021/es0605016.
Marone, A., Ayala-Campos, O.R., Trably, E., Carmona-Martínez, A.A., Moscoviz, R., Latrille, E., Steyer, J.-P., Alcaraz-Gonzalez, V., Bernet, N., 2017. Coupling dark fermentation and microbial electrolysis to enhance bio-hydrogen production from agro-industrial wastewaters and by-products in a bio-refinery framework. Int. J. Hydrogen Energy 42, 1609–1621. https://doi.org/10.1016/j.ijhydene.2016.09.166.
Mazzoli, R., Bosco, F., Mizrahi, I., Bayer, E.A., Pessione, E., 2014. Towards lactic acid bacteria-based biorefineries. Biotechnol. Adv. 32, 1216–1236. https://doi.org/10.1016/j.biotechadv.2014.07.005.
Miller, C., Fosmer, A., Rush, B., McMullin, T., Beacom, D., Suominen, P., 2011. Industrial production of lactic acid. Compr. Biotechnol. 3, 179–188. https://doi.org/10.1016/B978-0-08-088504-9.00177-X.
Mohan, S.V., Butti, S.K., Amulya, K., Dahiya, S., Modestra, J.A., 2016. Waste Biorefinery: a new paradigm for a sustainable bioelectro economy. Trends Biotechnol. 34, 852–855. https://doi.org/10.1016/j.tibtech.2016.06.006.
Montecchio, D., Yuan, Y., Malpei, F., 2018. Hydrogen production dynamic during cheese whey dark fermentation: new insights from modelization. Int. J. Hydrogen Energy 43, 17588–17601. https://doi.org/10.1016/j.ijhydene.2018.07.146.
Morais, A.R., Bogel-Lukasik, R., 2013. Green chemistry and the biorefinery concept. Sustain. Chem. Process. 1, 18. https://doi.org/10.1186/2043-7129-1-18.
Moreno, R., Escapa, A., Cara, J., Carracedo, B., Gómez, X., 2015. A two-stage process for hydrogen production from cheese whey: integration of dark fermentation and biocatalyzed electrolysis. Int. J. Hydrogen Energy 40, 168–175. https://doi.org/10.1016/j.ijhydene.2014.10.120.
Moscoviz, R., Trably, E., Bernet, N., Carrère, H., 2018. The environmental biorefinery: state-of-the-art on the production of hydrogen and value-added biomolecules in mixed-culture fermentation. Green Chem. 20, 3159–3179. https://doi.org/10.1039/c8gc00572a.
Oliveira, C.S.S., Silva, M.O.D., Silva, C.E., Carvalho, G., Reis, M.A.M., 2018. Assessment of protein-rich cheese whey waste stream as a nutrients source for low-cost mixed microbial PHA production. Appl. Sci. 8, 1817. https://doi.org/10.3390/app8101817.
Ottaviano, L.M., Ramos, L.R., Botta, L.S., Amâncio Varesche, M.B., Silva, E.L., 2017. Continuous thermophilic hydrogen production from cheese whey powder solution in an anaerobic fluidized bed reactor: effect of hydraulic retention time and initial substrate concentration. Int. J. Hydrogen Energy 42, 4848–4860. https://doi.org/10.1016/j.ijhydene.2016.11.168.
Pantazaki, A.A., Papaneophytou, C.P., Pritsa, A.G., Liakopoulou-Kyriakides, M., Kyriakidis, D.A., 2009. Production of polyhydroxyalkanoates from whey by *Thermus thermophilus* HB8. Process Biochem. 44, 847–853. https://doi.org/10.1016/j.procbio.2009.04.002.
Perna, V., Castelló, E., Wenzel, J., Zampol, C., Fontes Lima, D.M., Borzacconi, L., Varesche, M.B., Zaiat, M., Etchebehere, C., 2013. Hydrogen production in an upflow anaerobic packed bed reactor used to treat cheese whey. Int. J. Hydrogen Energy 38, 54–62. https://doi.org/10.1016/j.ijhydene.2012.10.022.
Povolo, S., Toffano, P., Basaglia, M., Casella, S., 2010. Polyhydroxyalkanoates production by engineered *Cupriavidus necator* from waste material containing lactose. Bioresour. Technol. 101, 7902–7907. https://doi.org/10.1016/J.BIORTECH.2010.05.029.

Prazeres, A.R., Carvalho, F., Rivas, J., 2012. Cheese whey management: a review. J. Environ. Manag. 110, 48–68. https://doi.org/10.1016/j.jenvman.2012.05.018.
Rago, L., Baeza, J.A., Guisasola, A., 2016. Bioelectrochemical hydrogen production with cheese whey as sole substrate. J. Chem. Technol. Biotechnol. 92, 173–179. https://doi.org/10.1002/jctb.4987.
Rai, P.K., Singh, S.P., Asthana, R.K., 2012. Biohydrogen production from cheese whey wastewater in a two-step anaerobic process. Appl. Biochem. Biotechnol. 167, 1540–1549. https://doi.org/10.1007/s12010-011-9488-4.
Reis, M.A.M., Serafim, L.S., Lemos, P.C., Ramos, A.M., Aguiar, F.R., Van Loosdrecht, M.C. M., 2003. Production of polyhydroxyalkanoates by mixed microbial cultures. Bioproc. Biosyst. Eng. 25, 377–385. https://doi.org/10.1007/s00449-003-0322-4.
Remón, J., García, L., Arauzo, J., 2016. Cheese whey management by catalytic steam reforming and aqueous phase reforming. Fuel Process. Technol. 154, 66–81. https://doi.org/10.1016/j.fuproc.2016.08.012.
Rico, C., Muñoz, N., Rico, J.L., 2015. Anaerobic co-digestion of cheese whey and the screened liquid fraction of dairy manure in a single continuously stirred tank reactor process: limits in co-substrate ratios and organic loading rate. Bioresour. Technol. 189, 327–333. https://doi.org/10.1016/j.biortech.2015.04.032.
Rivera, I., Bakonyi, P., Cuautle-Marín, M.A., Buitrón, G., 2017. Evaluation of various cheese whey treatment scenarios in single-chamber microbial electrolysis cells for improved biohydrogen production. Chemosphere 174, 253–259. https://doi.org/10.1016/j.chemosphere.2017.01.128.
Rosales-Colunga, L.M., Razo-Flores, E., Ordoñez, L.G., Alatriste-Mondragón, F., De León-Rodríguez, A., 2010. Hydrogen production by *Escherichia coli* ΔhycA ΔlacI using cheese whey as substrate. Int. J. Hydrogen Energy 35, 491–499. https://doi.org/10.1016/j.ijhydene.2009.10.097.
Ryan, M.P., Walsh, G., 2016. The biotechnological potential of whey. Rev. Environ. Sci. Biotechnol. 15, 479–498. https://doi.org/10.1007/s11157-016-9402-1.
Saddoud, A., Hassaïri, I., Sayadi, S., 2007. Anaerobic membrane reactor with phase separation for the treatment of cheese whey. Bioresour. Technol. 98, 2102–2108. https://doi.org/10.1016/J.BIORTECH.2006.08.013.
Santos, S.C., de Sousa, A.S., Dionísio, S.R., Tramontina, R., Ruller, R., Squina, F.M., Vaz Rossell, C.E., da Costa, A.C., Ienczak, J.L., 2016. Bioethanol production by recycled *Scheffersomyces stipitis* in sequential batch fermentations with high cell density using xylose and glucose mixture. Bioresour. Technol. 219, 319–329. https://doi.org/10.1016/J.BIORTECH.2016.07.102.
Shete, B.S., Shinkar, N.P., 2013. Dairy industry wastewater sources, characteristics & its effects on environment. Int. J. Curr. Eng. Technol. 3, 1611–1615.
Sikora, A., Błaszczyk, M., Jurkowski, M., Zielenkiewicz, U., 2013. Lactic acid bacteria in hydrogen-producing consortia: on purpose or by coincidence? Lact. Acid Bact. Food, Heal. Livest. Purp. 487–514. https://doi.org/10.5772/50364.
Slavov, A.K., 2017. General characteristics and treatment possibilities of dairy wastewater – a review. Food Technol. Biotechnol. 55, 14–28. https://doi.org/10.17113/ft b.55.01.17.4520.
Stamatelatou, K., Antonopoulou, G., Tremouli, A., Lyberatos, G., 2011. Production of gaseous biofuels and electricity from cheese whey. Ind. Eng. Chem. Res. 50, 639–644. https://doi.org/10.1021/ie1002262.
Staniszewski, M., Kujawski, W., Lewandowska, M., 2007. Ethanol production from whey in bioreactor with co-immobilized enzyme and yeast cells followed by pervaporative recovery of product – kinetic model predictions. J. Food Eng. 82, 618–625. https://doi.org/10.1016/J.JFOODENG.2007.03.031.
Taleghani, H.G., Ghoreyshi, A.A., Najafpour, G.D., 2018. Thin film composite nanofiltration membrane for lactic acid production in membrane bioreactor. Biochem. Eng. J. 132, 152–160. https://doi.org/10.1016/j.bej.2018.01.020.
Traversi, D., Bonetta, S., Degan, R., Villa, S., Porfido, A., Bellero, M., Carraro, E., Gilli, G., 2013. Environmental advances due to the integration of food industries and anaerobic digestion for biogas production: perspectives of the Italian milk and dairy product sector. Bioenerg. Res. 6, 851–863. https://doi.org/10.1007/s12155-013-9341-4.
Tremouli, A., Antonopoulou, G., Bebelis, S., Lyberatos, G., 2013. Operation and characterization of a microbial fuel cell fed with pretreated cheese whey at different organic loads. Bioresour. Technol. 131, 380–389. https://doi.org/10.1016/j.biortech.2012.12.173.
Tribst, A.A.L., Falcade, L.T.P., de Oliveira, M.M., 2019. Strategies for raw sheep milk storage in smallholdings: effect of freezing or long-term refrigerated storage on microbial growth. J. Dairy Sci. 102, 4960–4971. https://doi.org/10.3168/jds.2018-15715.
Ubando, A.T., Felix, C.B., Chen, W.-H., 2020. Biorefineries in circular bioeconomy: a comprehensive review. Bioresour. Technol. 299, 122585. https://doi.org/10.1016/j.biortech.2019.122585.
Valentino, F., Karabegovic, L., Majone, M., Morgan-Sagastume, F., Werker, A., 2015. Polyhydroxyalkanoate (PHA) storage within a mixed-culture biomass with simultaneous growth as a function of accumulation substrate nitrogen and phosphorus levels. Water Res. 77, 49–63. https://doi.org/10.1016/j.watres.2015.03.016.
Vassilev, I., Hernandez, P.A., Batlle-Vilanova, P., Freguia, S., Krömer, J.O., Keller, J., Ledezma, P., Virdis, B., 2018. Microbial electrosynthesis of isobutyric, butyric, caproic acids, and corresponding alcohols from carbon dioxide. ACS Sustain. Chem. Eng. 6, 8485–8493. https://doi.org/10.1021/acssuschemeng.8b00739.
Venetsaneas, N., Antonopoulou, G., Stamatelatou, K., Kornaros, M., Lyberatos, G., 2009. Using cheese whey for hydrogen and methane generation in a two-stage continuous process with alternative pH controlling approaches. Bioresour. Technol. 100, 3713–3717. https://doi.org/10.1016/j.biortech.2009.01.025.
Venkata Mohan, S., Mohanakrishna, G., Velvizhi, G., Babu, V.L., Sarma, P.N., 2010. Bio-catalyzed electrochemical treatment of real field dairy wastewater with simultaneous power generation. Biochem. Eng. J. 51, 32–39. https://doi.org/10.1016/j.bej.2010.04.012.
Vivekanand, V., Mulat, D.G., Eijsink, V.G.H., Horn, S.J., 2018. Synergistic effects of anaerobic co-digestion of whey, manure and fish ensilage. Bioresour. Technol. 249, 35–41. https://doi.org/10.1016/J.BIORTECH.2017.09.169.
Wei, P., Cheng, L.H., Zhang, L., Xu, X.H., Chen, H.L., Gao, C.J., 2014. A review of membrane technology for bioethanol production. Renew. Sustain. Energy Rev. 30, 388–400. https://doi.org/10.1016/j.rser.2013.10.017.
Wenzel, J., Fuentes, L., Cabezas, A., Etchebehere, C., 2017. Microbial fuel cell coupled to biohydrogen reactor: a feasible technology to increase energy yield from cheese whey. Bioproc. Biosyst. Eng. 40, 807–819. https://doi.org/10.1007/s00449-017-1746-6.
Xu, Q., Ouyang, J., Liu, P., Liu, J., Qian, Z., Zheng, Z., 2018. Valorization of dairy waste for enhanced D-lactic acid production at low cost. Process Biochem. 71, 18–22. https://doi.org/10.1016/j.procbio.2018.05.014.
Yang, P., Zhang, R., McGarvey, J.A., Benemann, J.R., 2007. Biohydrogen production from cheese processing wastewater by anaerobic fermentation using mixed microbial communities. Int. J. Hydrogen Energy 32, 4761–4771. https://doi.org/10.1016/j.ijhydene.2007.07.038.
Yazar, E., Cirik, K., Ozdemir, S., Akman, D., Cuci, Y., Cinar, O., 2016. Optimization of two-stage and single-stage anaerobic reactors treating cheese whey. J. Eng. Sci. 19, 1. https://doi.org/10.17780/ksujes.18309.
Yilmazer, G., Yenigün, O., 1999. Two-phase anaerobic treatment of cheese whey. Water Sci. Technol. 40, 289–295. https://doi.org/10.1016/S0273-1223(99)00397-2.
Zoppellari, F., Bardi, L., 2013. Production of bioethanol from effluents of the dairy industry by *Kluyveromyces marxianus*. N. Biotech. 30, 607–613. https://doi.org/10.1016/j.nbt.2012.11.017.

Chapter 3

Dark fermentation in waste management

3.1 Introduction

Although mankind has used fermentation for centuries to obtain food products and, more recently, in various productive sectors, its application in the field of waste management is relatively recent.

The traditional goal of limiting environmental impacts has meant that the use of biological processes for the treatment of organic waste has always aimed at achieving complete mineralization to carbon dioxide, water and nitrogen oxides (aerobic metabolism), or in any case to a strong demolition of the complex organic molecules (production of methane and carbon dioxide via anaerobic metabolism). Therefore, dark fermentation (DF) has been for a long time considered a mere intermediate phase of the anaerobic degradation process, whose products were destined for a total conversion, desired for the purpose of maximizing the production of biomethane.

The evolution that in recent years has involved the field of waste management requires instead that the control of environmental impacts takes place in close combination with the recovery of resources characterized by high demand and value on the market: an approach that finds application in the role that waste management is called to assume in the broader context of the circular economy and, from a technical point of view, in the concept of waste biorefinery.

The recovery of valuable products requires a relatively gentle simplification of the organic substance rather than its demolition, a task that fermentation, whose purpose is to guarantee cellular reproduction rather than the development of energy, performs well.

The variety of fermentation processes allows to convert the organic substance into compounds in the gaseous and solubilized phase, attractive in various fields, from the energy one, such as the bio-hydrogen, to the various sectors of the organic chemical industry. Soluble products, in particular, can be directly placed on the market as biochemicals, or used as building blocks, or as highly available substrates for other biological processes, for example, the production of biopolymers, or as feed to Microbial Electrochemical Systems (MESs), the latter subject of this thesis work.

In this section of the thesis, fermentation principles and main metabolic pathways of interest in the field of waste management are briefly described; moreover, some experiences of application to residues and, finally and specifically, to cheese whey are cited.

3.2 Fermentation foundamentals

As mentioned before, fermentation is an intermediate phase, known also as carboxylate platform, of the anaerobic degradation process, which is carried out by fermentative, acetogens, homoacetogens, hydrogenotrophic and acetoclastic methanogens bacteria. The overall process is rather complex as some of these groups cooperate through syntrophic mechanisms, several are the interconnection of different biochemicals phases, and fermentation itself may be divided into a primary and secondary phase (Kleerebezem and van Loosdrecht, 2007; Agler et al., 2011) (Figure 1).

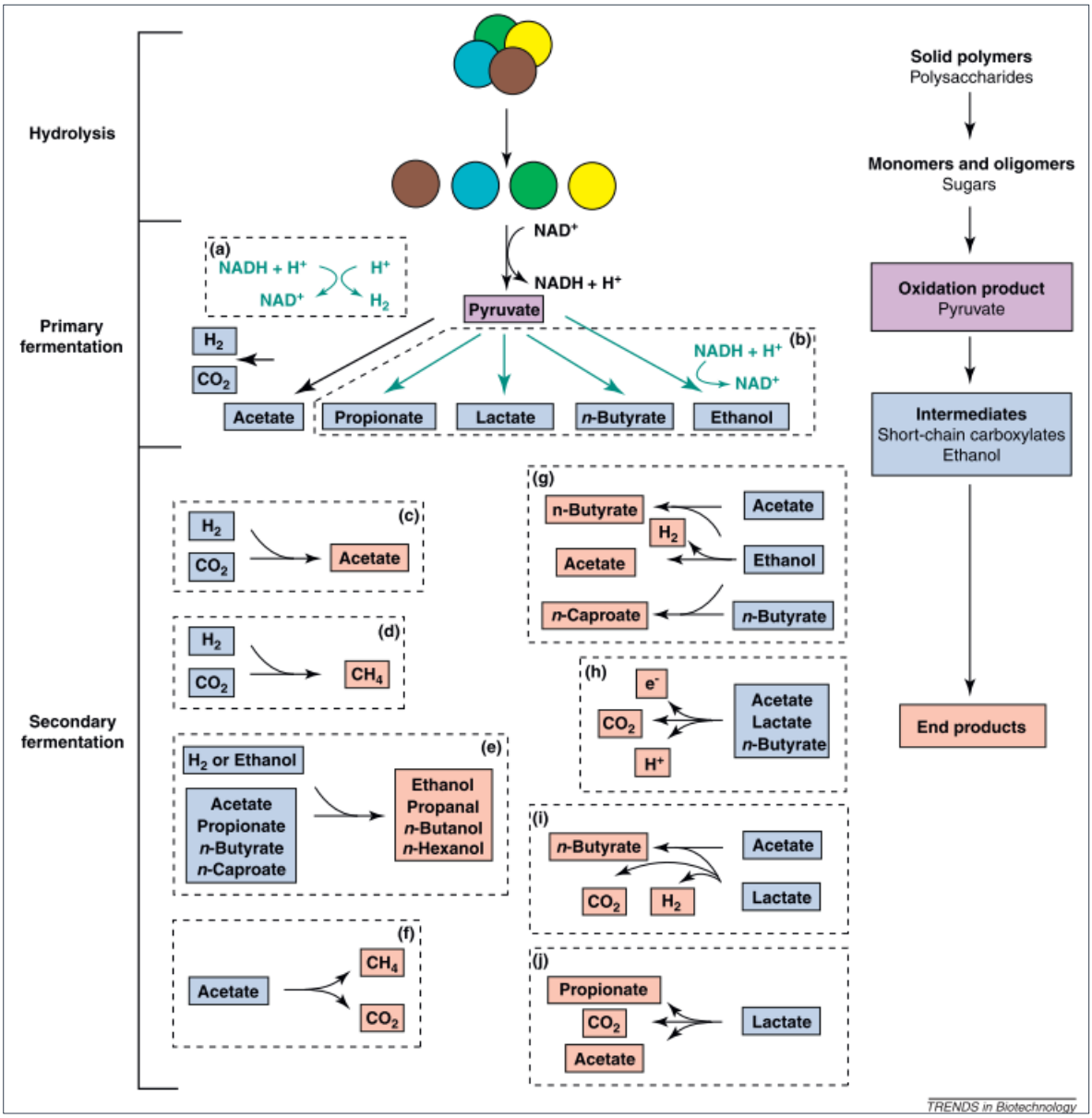

Figure 1 Hydrolysis and subsequent conversion by primary and secondary fermentation reactions carried out by undefined mixed cultures, according to Agler et al. (2011)

Hydrolysis is necessary to broke and eventually solubilise complex polymers. In the case of substrates which contain lactose, only some strains of lactic acid bacteria can hydrolyse it to glucose and galactose. If the specific hydrolytic bacteria, which are present or inoculated, do not produce enzymes of the required type, chemical-physical pretreatments may be necessary in light of the fact that it is the rate-limiting step of the whole degradation process.

Primary fermentation converts sugars to soluble carboxylates, such as acetate, propionate, butyrate, lactate and gaseous by-products (hydrogen and carbon dioxide). Gaseous hydrogen is produced in the framework of the oxidation of glucose to pyruvate and related production of nicotinamide adenine dinucleotide (NADH) and H^+. When the pyruvate oxidation product (acetyl-CoA) is converted to acetate, NADH and a reduced molecule (ferredoxin) are used to convert H^+ to H_2 thanks to an enzyme called hydrogenase, according to a theoretical yield of 4 mol H_2 mol^{-1} glucose. However, if the hydrogen partial pressure increases, the flow of electrons from NADH shifts and is addressed to the production of reduced products, such as butyrate and propionate, and alcohols such as ethanol, and only small shares of NADH and ferredoxin are used for H_2 production.

Butyric fermentation yields 2 mols of hydrogen per mole of glucose and is more favoured in order to avoid the accumulation of inhibitory reducing equivalent when H_2 partial pressure exceeds 60 Pa (Dai et al., 2017). The molar ratio of butyric to acetic acid (HBu/HAc) is a quantitative indicator of the H_2 yield, and if HBu/HAc is higher than 2 means an efficient H_2 production (Ghimire et al., 2015).

However, the actual hydrogen production per mole of glucose is lower than the theoretical yield and usually does not exceed 2 moles since the process may follow other pathways characterised by lower or null hydrogen production, and part of the substrate is utilised for new cells. Propionate fermentation occurs at elevated levels of hydrogen partial pressure and leads to the consumption of hydrogen (Stams et al., 1998). This observation contributes to consider the combination of fermentation with other processes as necessary in order to enhance substrate valorisation (Bastidas-Oyanedel et al., 2015; Bastidas-Oyanedel and Schmidt, 2018; Chandrasekhar et al., 2020; Rajesh Banu et al., 2021)

The products of primary fermentation, such as acetate or lactate, are often substrates for further conversion through secondary fermentation reactions: autotrophic homoacetogenesis; hydrogenotrophic and acetoclastic methanogenesis; carboxylate reduction to alcohols with hydrogen or ethanol; chain elongation of carboxylates with ethanol; bioelectrochemical reactions; lactate oxidation to n-butyrate and lactate reduction to propionate.

Homoacetogenesis is a hydrogen-consuming pathway and it is among the main causes for the decrease of H_2 yields in DF processes. Homoacetogens compete with hydrogenotrophic methanogens at low pH, and are favoured at high H_2 partial pressure (>500 PA) (Saady, 2013).

Methanogenesis represents the last phase of anaerobic digestion. Hydrogenotrophic methanogens produce CH_4 by reducing CO_2 using H_2 as the electron donor (Bundhoo and Mohee, 2016). Acetoclastic methanogens use acetate as both electron donor and acceptor (Karakashev et al., 2006).

The solventogenesis is the biological reduction of carboxylates to alcohols using molecular hydrogen or ethanol. The same bacteria capable of reducing acetate to ethanol can also produce n-butyrate by further reaction of ethanol with acetate.

3.3 Suitable waste feedstocks for fermentation

Over the last decades, fermentation has been extensively studied to produce biofuels from dedicated crops, as a response to environmental issues posed by petrochemical counterparts. However, the exploitation of these crops caused an increase in food prices during the 2010 food crisis, thus leaving room for organic wastes and bio residues to emerge as alternative feedstocks for bio-hydrogen production (Ntaikou et al., 2010). In general carbohydrate-rich wastes are the most suitable for bio-hydrogen recovery (Kapdan and Kargi, 2006): as reported in Lay et al., 2003, a 20 times higher hydrogen production can be achieved using carbohydrate rich wastes compared to protein-rich and fat-rich ones, when fermented with the same inoculum.

Food waste (FW) is indeed one of the most suitable substrates for valorisation through fermentation, in the light of its high energy content and characteristics, e.g. volatile solid content (85-95%) and moisture (75-85%), which favours microbial communities development. (Guo et al., 2010). High variability in FW composition is reflected by a wide range of hydrogen production yields: batch tests conducted with catering residues showed values comprised between 60 and 196 mL H_2 per gram of volatile solids (Kim et al., 2004; Li et al., 2008). Agri-food industry residues have shown promising results in this context: for instance, when digesting cheese whey (CW) and molasses, bio-hydrogen yields closely reached the maximum theoretical values expected from mixed microbial cultures (Aceves-Lara et al., 2008; Venetsaneas et al., 2009). VFAs generated during primary fermentation has been extensively considered as substrate for bio-methane co-generation in two-stages AD reactors (Srisowmeya et al., 2020). Lately, the same approach has been applied for the concomitant recovery of lactic acid and biogas to further increase the economic feasibility of the process (Kim et al., 2016), while the recovery of other carboxylates as

platform for chemicals synthesis is limited by downstream separation technologies costs (Strazzera et al., 2018). DF has been also applied to the valorisation of crop residues like straw, stover, peelings, cobs, stalks, bagasse and lignocellulosic materials (Mtui, 2009). In crop residues, carbohydrates are present in form of lignin, cellulose and hemicellulose (Li and Chen, 2007; Zhang et al., 2007), therefore pre-treatments are necessary to enhance hydrolysis, which would represent the bottleneck stage of the process. For instance, when fermenting wheat straw the hydrogen yield can increase 136 times when pre-treated with acid and microwave heating (Fan et al., 2006). However, it is recognised that pre-treatment methods must be investigated depending on substrate composition and origin (Li et al., 2008; Guo et al., 2010). Another interesting option is the co-digestion of recalcitrant feedstocks with organic wastes, e.g. coffee mucilage amended with wholesale market garbage (Cárdenas et al., 2018). Co-digestion would also positively impact livestock waste valorisation: although it is possible to maximise VFAs (Kuruti et al., 2017) and bio-hydrogen generation (Wang and Zhao, 2009) from raw wastes, the addition of carbohydrates modifies the carbon to nitrogen ratio, thus avoiding ammonia accumulation and consequent inhibition of biochemical reactions.

3.4 Dark fermentation of CW

Lactate fermentation is a common metabolic pathway when the substrate is rich in lactose, a disaccharide composed of one glucose and one galactose molecule. When CW is the substrate, the process develops according to two main stages (Asunis et al., 2019): firstly, carbohydrates are converted to lactate, which represents the substrate for hydrogen and organic acids produced during the second phase.

Lactose fermentative degradation requires hydrolysis in two monosaccharides: glucose and galactose (Eq. 1) following a first-order-type kinetic (Fu and Mathews, 1999).

$$Lactose + H_2O \rightarrow glucose + galactose \quad (1)$$

The reaction kinetics depend chiefly on pH control, though no significant effects have been observed on overall carbohydrates removal (Asunis et al., 2019); indeed, carbohydrates removal is always more than 93% and up to 99%, while the degradation kinetic constant was observed to increase from 0.015 h^{-1} at pH 5 up to 0.176 h^{-1} at pH 7.5. From a practical point of view, this figure reduces the time required for the removal of 95% of carbohydrates from 395 h to 74 h. Effect of pH control can be explained by: 1) increased enzymatic activity at high pH (Tang et al., 2017); 2) inhibition of biomass at low pH, as undissociated acids are able to cross cell membrane causing an excess of metabolic energy need for proton excretion (Rodríguez et al., 2006; Infantes et al., 2011); 3) variation in nutrient transport rate inside the cells. In uncontrolled-pH fermentation tests, carbohydrates final consumption and degradation rate were considerably lower, likely due to

acids accumulation in fermentation broth and consequent pH decrease, which was observed to drop down to 3.78 (Asunis et al., 2019).

The conversion of sugars is carried by lactic acid bacteria (LAB), generally used as starter culture during cheese making and therefore always present in CW (Sikora et al., 2013). LAB are able to catabolise sugars following two main pathways: homolactic fermentation, in which 2 mol of pyruvate are both converted into 2 mol of lactate *via* Embden-Meyerhof-Parna (Eq. 2) (Castillo Martinez et al., 2013; Sikora et al., 2013), and heterolatic fermentation, in which only 1 mol of pyruvate is converted into lactate and the other in either ethanol or acetate and CO_2 *via* phosphoketolase pathway (Eq. 3 and Eq. 4) (Castillo Martinez et al., 2013; Sikora et al., 2013).

$$glucose \rightarrow 2\ lactate \quad (2)$$

$$glucose \rightarrow lactate + ethanol + CO_2 \quad (3)$$

$$glucose \rightarrow lactate + acetate + CO_2 \quad (4)$$

In a lactic acid-oriented fermentation, the onset of heterolactic pathway leads to several downsides. Firstly, lactate production yield is lower than in homolactic, since the theoretical lactate production is 2 and 4 mol of lactate per mol of lactose respectively; in addition, separation from other metabolites and purification of lactate must be provided (Mazzoli et al., 2014). In a test performed with non-pretreated CW and without inoculum addition, no metabolites other than lactate were detected, with a conversion yield of around 4 mol of lactate per mol of lactose (the only exception was the test performed at pH 7, which showed a yield of 3.2 mol of lactate per mol of lactose) (Asunis et al., 2019). This result can be due to the absence of inoculum pretreatment, a stress factor for LAB since it could damage the cell membrane causing inactivation of bacteria (Gomes et al., 2015). An additional explanation may be the antimicrobial activity carried out by LAB , which during the degradation of carbohydrates may have inhibited the activity of other microorganisms (Noike et al., 2002; Jo et al., 2007). Optimal operative conditions for lactate production maximization were found to be pH 6 and fermentation time of 45 h, which allowed recovery of 23 mmol HLa (g TOC)$^{-1}$ (Asunis et al., 2019). Lactic acid can then be oxidised and reduced by secondary fermentation reactions to other carboxylates, such as n-butyrate and propionate. This second stage of DF starts concurrently with lactate production peak. Only short chain fatty acids (acetic, propionic and butyric acids) (SCFA) are detected in the fermentation system, in different proportions depending on pH (Asunis et al., 2019). Conversion of lactate into SCFA have been widely reported in the literature and includes elementary reactions and their combination (Eq. 5-7)

$$lactate + H_2O \rightarrow acetate + CO_2 + 2H_2 \quad (5)$$

$$lactate + H_2O \rightarrow 0.5\ butyrate + CO_2 + H_2 \quad (6)$$

$$lactate + H_2 \rightarrow propionate + H_2O \quad (7)$$

In addition, autotrophic homoacetogenesis (Eq. 8) may occur in fermentation systems (Saady, 2013)

$$4H_2 + 2CO_2 \rightarrow acetate + H_2O \quad (8)$$

Modelling of CW fermentation pathways pointed out that homoacetogenesis contribution to the process is negligible, which is an advantage if H_2 recovery is the main target (Asunis et al., 2019). Values of pH below 6 favour butyrate production, while propionic fermentation slightly overlaps with the former. At higher operational pH, all the metabolites are detected, indicating the overlap of multiple metabolic pathways; propionic fermentation gradually overcame butyric fermentation as main, while acetate production did not vary in the pH range 6.5-7.5 (Asunis et al., 2019). In terms of hydrogen production, a maximum hydrogen production yield (HPY) of 162.7 L H_2 (kg TOC)$^{-1}$ was achieved at pH 6 , while the minimum of 68.1 L H_2 (kg TOC)$^{-1}$ was recorded at pH 7.5 (Asunis et al., 2019). Not surprisingly, HPY decreased at higher pH values because of the major role played by hydrogenotrophic propionate fermentation. Observed results suggest a syntrophic interaction between LAB and hydrogen-producing bacteria (HPB): during the first fermentation step, LAB activity inhibits HPB until hexose concentration becomes a limiting factor and hydrogen production from lactose previously converted can take place (Asunis et al., 2019).

References

Aceves-Lara, C. A., Latrille, E., Bernet, N., Buffière, P., and Steyer, J. P. (2008). A pseudo-stoichiometric dynamic model of anaerobic hydrogen production from molasses. *Water Res.* 42, 2539–2550. doi:10.1016/j.watres.2008.02.018.

Agler, M. T., Wrenn, B. A., Zinder, S. H., and Angenent, L. T. (2011). Waste to bioproduct conversion with undefined mixed cultures: The carboxylate platform. *Trends Biotechnol.* 29, 70–78. doi:10.1016/j.tibtech.2010.11.006.

Asunis, F., De Gioannis, G., Isipato, M., Muntoni, A., Polettini, A., Pomi, R., et al. (2019). Control of fermentation duration and pH to orient biochemicals and biofuels production from cheese whey. *Bioresour. Technol.* 289. doi:10.1016/j.biortech.2019.121722.

Bastidas-Oyanedel, J.-R., and Schmidt, J. (2018). Increasing Profits in Food Waste Biorefinery—A Techno-Economic Analysis. *Energies* 11, 1551. doi:10.3390/en11061551.

Bastidas-Oyanedel, J. R., Bonk, F., Thomsen, M. H., and Schmidt, J. E. (2015). Dark fermentation biorefinery in the present and future (bio)chemical industry. *Rev. Environ. Sci. Biotechnol.* 14, 473–498. doi:10.1007/s11157-015-9369-3.

Bundhoo, M. A. Z. Z., and Mohee, R. (2016). Inhibition of dark fermentative bio-hydrogen production: A review. *Int. J. Hydrogen Energy* 41, 6713–6733. doi:10.1016/j.ijhydene.2016.03.057.

Cárdenas, E., Zapata-Zapata, A., and Kim, D. (2018). Hydrogen Production from Coffee Mucilage in Dark Fermentation with Organic Wastes. *Energies* 12, 71. doi:10.3390/en12010071.

Castillo Martinez, F. A., Balciunas, E. M., Salgado, J. M., Domínguez González, J. M., Converti, A., and Oliveira, R. P. de S. (2013). Lactic acid properties, applications and production: A review. *Trends Food Sci. Technol.* 30, 70–83. doi:10.1016/j.tifs.2012.11.007.

Chandrasekhar, K., Kumar, S., Lee, B. D., and Kim, S. H. (2020). Waste based hydrogen production for circular bioeconomy: Current status and future directions. *Bioresour. Technol.* 302, 122920. doi:10.1016/j.biortech.2020.122920.

Dai, K., Wen, J. L., Zhang, F., and Zeng, R. J. (2017). Valuable biochemical production in mixed culture fermentation: fundamentals and process coupling. *Appl. Microbiol. Biotechnol.* 101, 6575–6586. doi:10.1007/s00253-017-8441-z.

Fan, Y. T., Zhang, Y. H., Zhang, S. F., Hou, H. W., and Ren, B. Z. (2006). Efficient conversion of wheat straw wastes into biohydrogen gas by cow dung compost. *Bioresour. Technol.* 97, 500–505. doi:10.1016/j.biortech.2005.02.049.

Fu, W., and Mathews, A. P. (1999). Lactic acid production from lactose by Lactobacillus plantarum: Kinetic model and effects of pH, substrate, and oxygen. *Biochem. Eng. J.* 3, 163–170. doi:10.1016/S1369-703X(99)00014-5.

Ghimire, A., Frunzo, L., Pirozzi, F., Trably, E., Escudie, R., Lens, P. N. L., et al. (2015). A review on dark fermentative biohydrogen production from organic biomass: Process parameters and use of by-products. *Appl. Energy* 144, 73–95. doi:10.1016/j.apenergy.2015.01.045.

Gomes, B. C., Rosa, P. R. F., Etchebehere, C., Silva, E. L., and AmâncioVaresche, M. B. (2015). Role of homo-and heterofermentative lactic acid bacteria on hydrogen-producing reactors operated with cheese whey wastewater. *Int. J. Hydrogen Energy* 40, 8650–8660. doi:10.1016/j.ijhydene.2015.05.035.

Guo, X. M., Trably, E., Latrille, E., Carrre, H., and Steyer, J. P. (2010). Hydrogen production from agricultural waste by dark fermentation: A review. *Int. J. Hydrogen Energy* 35, 10660–10673. doi:10.1016/j.ijhydene.2010.03.008.

Infantes, D., González Del Campo, A., Villaseñor, J., and Fernández, F. J. (2011). Influence of pH, temperature and volatile fatty acids on hydrogen production by acidogenic fermentation. *Int. J. Hydrogen Energy* 36, 15595–15601. doi:10.1016/j.ijhydene.2011.09.061.

Jo, J. H., Jeon, C. O., Lee, D. S., and Park, J. M. (2007). Process stability and microbial community structure in anaerobic hydrogen-producing microflora from food waste containing kimchi. *J. Biotechnol.* 131, 300–308. doi:10.1016/j.jbiotec.2007.07.492.

Kapdan, I. K., and Kargi, F. (2006). Bio-hydrogen production from waste materials. *Enzyme Microb. Technol.* 38, 569–582. doi:10.1016/j.enzmictec.2005.09.015.

Karakashev, D., Batstone, D. J., Trably, E., and Angelidaki, I. (2006). Acetate oxidation is the dominant methanogenic pathway from acetate in the absence of Methanosaetaceae. *Appl. Environ. Microbiol.* 72, 5138–5141. doi:10.1128/AEM.00489-06.

Kim, M. S., Na, J. G., Lee, M. K., Ryu, H., Chang, Y. K., Triolo, J. M., et al. (2016). More value from food waste: Lactic acid and biogas recovery. *Water Res.* 96, 208–216. doi:10.1016/j.watres.2016.03.064.

Kim, S. H., Han, S. K., and Shin, H. S. (2004). Feasibility of biohydrogen production by anaerobic co-digestion of food waste and sewage sludge. *Int. J. Hydrogen Energy* 29, 1607–1616. doi:10.1016/j.ijhydene.2004.02.018.

Kleerebezem, R., and van Loosdrecht, M. C. (2007). Mixed culture biotechnology for bioenergy production. *Curr. Opin. Biotechnol.* 18, 207–212. doi:10.1016/j.copbio.2007.05.001.

Kuruti, K., Nakkasunchi, S., Begum, S., Juntupally, S., Arelli, V., and Anupoju, G. R. (2017). Rapid generation of volatile fatty acids (VFA) through anaerobic acidification of livestock organic waste at low hydraulic residence time (HRT). *Bioresour. Technol.* 238, 188–193. doi:10.1016/j.biortech.2017.04.005.

Lay, J. J., Fan, K. S., Chang I, J., and Ku, C. H. (2003). Influence of chemical nature of organic wastes on their conversion to hydrogen by heat-shock digested sludge. *Int. J. Hydrogen Energy* 28, 1361–1367. doi:10.1016/S0360-3199(03)00027-2.

Li, D., and Chen, H. (2007). Biological hydrogen production from steam-exploded straw by simultaneous saccharification and fermentation. *Int. J. Hydrogen Energy* 32, 1742–1748. doi:10.1016/j.ijhydene.2006.12.011.

Li, M., Zhao, Y., Guo, Q., Qian, X., and Niu, D. (2008). Bio-hydrogen production from food waste and sewage sludge in the presence of aged refuse excavated from refuse landfill. *Renew. Energy* 33, 2573–2579. doi:10.1016/j.renene.2008.02.018.

Mazzoli, R., Bosco, F., Mizrahi, I., Bayer, E. A., and Pessione, E. (2014). Towards lactic acid bacteria-based biorefineries. *Biotechnol. Adv.* 32, 1216–1236. doi:10.1016/j.biotechadv.2014.07.005.

Mtui, G. Y. S. (2009). Recent advances in pretreatment of lignocellulosic wastes and production of value added products. *African J. Biotechnol.* 8, 1398–1415. doi:10.4314/ajb.v8i8.60134.

Noike, T., Takabatake, H., Mizuno, O., and Ohba, M. (2002). Inhibition of hydrogen fermentation of organic wastes by lactic acid bacteria. in *International Journal of Hydrogen Energy* (Pergamon), 1367–1371. doi:10.1016/S0360-3199(02)00120-9.

Ntaikou, I., Antonopoulou, G., and Lyberatos, G. (2010). Biohydrogen production from biomass and wastes via dark fermentation: A review. *Waste and Biomass Valorization* 1, 21–39. doi:10.1007/s12649-009-9001-2.

Rajesh Banu, J., Ginni, G., Kavitha, S., Yukesh Kannah, R., Adish Kumar, S., Bhatia, S. K., et al. (2021). Integrated biorefinery routes of biohydrogen: Possible utilization of acidogenic fermentative effluent. *Bioresour. Technol.* 319, 124241. doi:10.1016/j.biortech.2020.124241.

Rodríguez, J., Kleerebezem, R., Lema, J. M., and Van Loosdrecht, M. C. M. (2006). Modeling product formation in anaerobic mixed culture fermentations. *Biotechnol. Bioeng.* 93, 592–606. doi:10.1002/bit.20765.

Saady, N. M. C. (2013). Homoacetogenesis during hydrogen production by mixed cultures dark fermentation: Unresolved challenge. *Int. J. Hydrogen Energy* 38, 13172–13191. doi:10.1016/j.ijhydene.2013.07.122.

Sikora, A., Baszczyk, M., Jurkowski, M., and Zielenkiewicz, U. (2013). "Lactic Acid Bacteria in Hydrogen-Producing Consortia: On Purpose or by Coincidence?," in *Lactic Acid Bacteria - R & D for Food, Health and Livestock Purposes* (InTech). doi:10.5772/50364.

Srisowmeya, G., Chakravarthy, M., and Nandhini Devi, G. (2020). Critical considerations in two-

stage anaerobic digestion of food waste – A review. *Renew. Sustain. Energy Rev.* 119, 109587. doi:10.1016/j.rser.2019.109587.

Stams, A. J. M., Dijkema, C., Plugge, C. M., and Lens, P. (1998). Contribution of 13C-NMR spectroscopy to the elucidation of pathways of propionate formation and degradation in methanogenic environments. *Biodegradation* 9, 463–473. doi:10.1023/A:1008342130938.

Strazzera, G., Battista, F., Garcia, N. H., Frison, N., and Bolzonella, D. (2018). Volatile fatty acids production from food wastes for biorefinery platforms: A review. *J. Environ. Manage.* 226, 278–288. doi:10.1016/j.jenvman.2018.08.039.

Tang, J., Wang, X. C., Hu, Y., Zhang, Y., and Li, Y. (2017). Effect of pH on lactic acid production from acidogenic fermentation of food waste with different types of inocula. *Bioresour. Technol.* 224, 544–552. doi:10.1016/j.biortech.2016.11.111.

Venetsaneas, N., Antonopoulou, G., Stamatelatou, K., Kornaros, M., and Lyberatos, G. (2009). Using cheese whey for hydrogen and methane generation in a two-stage continuous process with alternative pH controlling approaches. *Bioresour. Technol.* 100, 3713–3717. doi:10.1016/j.biortech.2009.01.025.

Wang, X., and Zhao, Y. cai (2009). A bench scale study of fermentative hydrogen and methane production from food waste in integrated two-stage process. *Int. J. Hydrogen Energy* 34, 245–254. doi:10.1016/j.ijhydene.2008.09.100.

Zhang, M. L., Fan, Y. T., Xing, Y., Pan, C. M., Zhang, G. S., and Lay, J. J. (2007). Enhanced biohydrogen production from cornstalk wastes with acidification pretreatment by mixed anaerobic cultures. *Biomass and Bioenergy* 31, 250–254. doi:10.1016/j.biombioe.2006.08.004.

Chapter 4

Fundamentals of microbial electrochemistry and applications

4.1 Introduction

In nature, microorganisms are able to gain energy in biological form of ATP (adenosine triphosphate) through a process defined respiration. The energy needed for ATP generation comes from redox potential gradient between two chemical compounds: in general, soluble reduced compounds (e.g., acetate, lactate, sulphides) are used as electron donor, while soluble oxidized forms (e.g. O_2, nitrate, sulphate) act as electron acceptor. However, in the last century it has been observed that certain microorganisms are capable to exchange electrons between insoluble conductive donors and/or acceptors. Such microorganism can be found in all three domains of life (Logan et al., 2019) and are referred to as *electroactive*; more specifically, the term *exoelectrogens* describes the ability to use insoluble donors as electron acceptor, while *electrotrophs* refers to the ones using them as electron acceptor. Biological electro-activity was firstly described by Michael Potter in 1911, when the English researcher observed the generation of an electrical current as consequence of fermentation of glucose from several microorganisms in a galvanic cell equipped with platinum electrodes, including *Saccaromyces* and *Escherichia coli* (Potter and B, 1911). Although later studies demonstrated poor electroactivity from considered species (Qu et al., 2012), Potter's results were later explained considering the composition of medium used during the experiments, which included substances now recognised as mediators for electrons transfer, such as certain B vitamins and flavins, and highly reducing anaerobic condition at the counter electrode(Logan et al., 2019). Later in 1931, Cohen demonstrated how the introduction of proper substances, like potassium ferricyanide and benzoquinone, could allow the maintenance of the reduction-oxidation system in a bacterial electrical half-cell. However, proof of concept current generation from microorganism was given only in the 1960's (Davis, 1963). The enzymatic activity of the microbial cultures used was addressed as main reason of the onset oxidation-reduction potential, defining such system as Microbial Fuel Cell (MFC). At date, the mechanism of electron transfer in not fully understood yet. *Geobactee spp.* and *Shewanella spp*. are used as model microorganisms to explain electron transfer. It is generally accepted that it can occur by two main routes: Direct Extracellular Electron Transfer (DEET) and Mediated Extracellular Electron Transfer (MEET). DEET is achieved when cells are in contact with the electrode, thus usually forming a biofilm on the surface. For cells in the first layer of the biofilm, which are in direct contact with the electrode surface, electron flux involves transmembrane redox proteins like c-type cytochromes (Leang et al., 2003; Schuetz et al., 2009). Cells in further

layers can still perform long distance DEET through conductive pili defined *nanowires*.(Lovley et al., 2011). In MEET, electron transport is achieved through redox-active molecules: in *Shewanella spp.*flavin mononucleotide and riblofavin are naturally excreted by the cell (Lin et al., 2018), while *Geobacter spp.* are able to use externally added mediators (Bond and Lovley, 2003). The interest of scientific community around electroactive bacteria increased and achieved public attention in the end of XX century. The idea of building devices capable to reduce organic content in wastewaters while harvesting energy was appealing, since expensive and energy consuming aerobic treatments were the standard option at the time. First attempts of implementation were based on the use of chemical mediators, which are however toxic and expensive. An example of those mediated MFC is given by Park and Zeikus (2000), which used neutral red for mediating electron transfer. In 1999, Byung Hong Kim, Doo Hyun Park and Kim patented the first mediator-less MFC, and also developed a novel biosensor for lactate detection using a pure culture of *Shewanella putrefaciens* (KIM, 1999; Kim et al., 1999). Even though the activity of electrogenic bacteria have been observed to naturally happen in marine sediments (Reimers et al., 2001), the mechanism of electron transfer in conductive electrodes is still not fully understood. From that point forward, electroactive microorganisms have been exploited in several reactor configurations and operational modes. Nowadays electroactive microorganism find application not only in current generation, but also in hydrogen production, chemicals synthesis from CO_2 reduction and have been successfully implemented in dark fermentation reactors to extend their product output. These systems as a whole are addressed as Microbial Electrochemical Systems (MES). In this chapter, a general overview on current development of Microbial Electrochemical Systems and will be given.

4.2 MESs for electricity production: Microbial Fuel Cells (MFCs)

As reported in the introduction, MFCs were the first type of MES developed. Their operation relies on oxidation of organic and inorganic matter, catalysed by exoelectogen bacteria, for current generation (Logan et al., 2006).In the anodic chamber, organic matter act as electron donor for bacterial metabolism, which results in the generation of CO_2, electrons and protons. Electrons are discharged at the anode though EET and migrate to the cathode *via* an external circuit, equipped with a resistor or operated under load, while protons migrate through the catholyte by concentration gradient. On the surface of abiotic cathodes, protons and electrons are consumed for O_2 reduction to H_2O. The list of possible electron acceptors can be expanded using biocathodes, where electrotrophs can reduce also nitrate and sulphate as final electron acceptor (He and Angenent, 2006). Reactions occurring in MFCs are thermodynamically

favourable, therefore no external energy input is needed (Eq. 3). The theoretical potential difference can be easily calculated from their biological standard potential $E^{0'}$ *vs.* Standard Hydrogen Electrode (SHE) (pH =7, T = 25°C, p= 1 atm, ionic strength 0.25 M), considering NADH as terminal electron donor and oxygen as terminal electron acceptor (Eq. 1 and Eq. 2)

$$NAD^+ + H^+ + 2\,e^- \rightarrow NADH\ (E^{0'}_{anode} = -\,0.320\ V\ vs.SHE) \quad (1)$$

$$O_2 + 2\,H_2O + 4\,e^- \rightarrow 4\,OH^-\ (E^{0'}_{cathode} = 0.820\ V\ vs.SHE) \quad (2)$$

$$E'_{emf} = E^{0'}_{cathode} - E^{0'}_{anode} = 1.14\ V\ vs.SHE \quad (3)$$

However, the electromotive force generally drops down to +0.51 V *vs*. SHE due to ohmic, activation and mass transfer losses (Schröder, 2007). To overcome these limitations, researchers have focused their attention on optimising proton mass transfer, circuit resistance, electrode materials and performance and external operation conditions (Zhou et al., 2011). The most basic MFC design consist of an anodic and cathodic chamber separated by a proton exchange membrane (PEM). Several dual chamber configurations have been reported, and have been deeply analysed by Munoz-Cupa et al. (2021):

- *Cylindrical shape*: also known as up flow MFC, have been mostly applied for wastewater treatment due to their poor electricity production accompanied, however, by high COD removal due to the possibility of recirculation. Main drawbacks are the distance between electrodes and energy requirements for fluid pumping. This configuration have been addressed also for its potential towards system scale up, considering a potential connection in series of multiple devices to enhance both power production and COD removal (He et al., 2005)
- *Rectangular shape*: in this configuration, anodic and cathodic chambers are rectangular vessels. Rectangular MFCs are easy to build and capable of generation of high voltage and power. On the other hand, low coulombic efficiency are achieved and they can be operated only with low loading rates. Janicek et al. (2014) highlighted the possibility of operation in continuous flow and connection through modules.
- *Flat plate:* this design is characterised by a reduced distance between electrodes, being the cathode directly pressed to the cathode in a single assembly (Min and Logan, 2004), thus increasing electron transport and breaking down internal resistance (Janicek et al., 2014). However, membrane permeability to O_2 may reduce

anode performances. In addition, mechanical stress induced during operation could cause membrane damage.

Single chamber MFCs have been object of interest in literature. The configuration is characterised by a direct exposition of the cathode to air, using atmospheric O_2 as electron acceptor (Das and Mangwani, 2010), avoiding the use of aeration systems in cathodic chamber. Power densities could be maximised ensuring close spacing between electrodes and small working volumes (Fornero et al., 2010).

Applicability of MFCs has been studied for several types of wastewaters (Table 1). Compared to other electrochemical technologies, like hydrogen fuel cells, the power output is much lower. In the light of this, it must be considered that treatment in MFCs is potentially suitable for treating a large number of residues, generating clean energy without aid of intermediary processes. In addition, no expensive catalysts are required. Compared to other biological technologies, such as AD, MFCs can operate in mild condition, limiting the energy requirements for the process.

Table 1 Main studies on wastewater treatment using MFCs (adapted from(Munoz-Cupa et al., 2021)))

Anode	Cathode	Type of wastewater	Power output	Ref.
Graphite rod	Graphite rod	Domestic	27 mW/m^3	(Cecconet et al., 2018)
Carbon brush	Carbon powder	Municipal	200 mW	(Ge and He, 2016)
Graphite fiber brush	Carbon cloth + 0.5 mg/cm^2 Pt	Municipal	0.36 kW	(Hiegemann et al., 2016)
Carbon brush + twined titanium	Carbon cloth + Pt crystal	Seafood	340 mW/m^2	(Jamal et al., 2020)
Plain graphite sheet	Plain graphite sheet	Retting	254 mW/m^2	(Jayashree et al., 2015)
Activated carbon fiber felt	Activated carbon fiber felt	Seafood	105 mW/m^2	(Jayashree et al., 2016)
Graphite fiber brush	PDVF + activated carbon	Domestic	1.36 mW	(Kim et al., 2015)
Pt foil	Gas diffusion electrode	Synthetic	0.7 mA/cm^2	(Krieg et al., 2017)
Granular graphite	Carbon fiber + PDVF[a] + C-Mn-Fe-O	Synthetic	1358 W/m^3	(Li et al., 2015)
Granular carbon + stainless steel	Carbon cloth + vulcan carbon	Domestic	135 mW	(Valladares Linares et al., 2019)
Stainless steel	Activated carbon	Yogurt	1043 W/m^2	(Luo et al., 2017)
Carbon brush	Carbon cloth + 0.35 mg/m^2 Pt	Swine	650 mW	(Ma et al., 2016)

Table 1 (continued)

Graphite felt	Carbon cloth + 0.35 mg/m^2 Pt +	Domestic	1.4 mA	(Park et al., 2017)
Carbon felt	Carbon E4 + Mn	Synthetic	10 mW	(Recio-Garrido et al., 2017))
Carbon cloth pre-treated	Carbon cloth + gas diffusion	Synthetic	88 mW/m^2	(Tanikkul and Pisutpaisal, 2018)
Carbon cloth	Cu-B alloy	Municipal	6.1 mW	(Włodarczyk and Włodarczyk, 2019)
Carbon cloth	Platinum bar	Sewage	382.5 W/m^2	(Sevda et al., 2013)
Graphite felt	Carbon cloth + 8 mg/cm^2 MnO2	Swine	225 mW/m^2	(Zhuang et al., 2012)

4.3 MESs for hydrogen production: Microbial Electrolysis Cells (MECs)

Using a completely anaerobic MFC, Liu et al. (2005) achieved hydrogen production in a MES, paving the way towards their implementation for chemicals synthesis. While MFCs and MECs are conceptually similar, hydrogen evolution reaction is not thermodynamically favourable, thus external energy supply is required. Considering acetate as electron donor at the anode, the overall reaction is (Eq. 4-6)

$$CH_3COOH^- + 4H_2O \rightarrow 2\,HCO_3^- + 9\,H^+ + 8\,e^-\ (E^0_{anode} = -0.300\,V\ vs.SHE) \quad (4)$$

$$2\,H^+ + 2\,e^- \rightarrow H_2\ (E^0_{cathode} = -0.414\,V\ vs.SHE) \quad (5)$$

$$E_{cell} = (-0.414\,V) - (-0.300\,V) = -0.114\,V\ vs.SHE \quad (6)$$

Thus, an additional input of 0.114 V should allow to sustain electrochemical reactions in the system. In practice, an additional voltage of ~ 0.25 V is required to overcome reactor limitations, such as internal resistance. Additional voltage can be supplied either with a power source or a potentionstat, through which the potential is set at the working electrode (in this case, anode). Even in the worst-case scenarios, energy requirement is lower than in traditional water electrolysis, typically 1.23-2.00 V (Kadier et al., 2015). In addition, H_2 yield in MECs is higher compared with DF (Kadier et al., 2016). MECs are a great candidate as downstream process for DF reactors effluents (Table 2). As described in chapter 3, the conversion of final soluble metabolites is not thermodynamically feasible in DF, while they represent an optimal substrate for exoelectrogenic bacteria in MEC anodes: the combination of these two technologies may increase the overall hydrogen yield close to the theoretical maximum of 12 mol H_2/mol$_{glucose}$. In addition, while in DF high hydrogen partial pressure affects the thermodynamics of reactions (Khanna and

Das, 2013), this parameter would not significantly affect hydrogen evolution at the cathode. Finally, having the oxidation and reduction reactions in separate chambers would allow to harvest a purer gas, not contaminated by CO_2 and other fermentation gaseous by-products (Sravan et al., 2019). Currently, the main challenge towards a full implementation of a combined treatment resides in DF effluents acidic pH, which is out from anodic biofilms optimal range of 6-9 (Patil et al., 2011). pH adjustment may be therefore required and the use of buffer to sustain values in a neutral range can be challenging in full scale application(Ullery and Logan, 2014).

Table 2 Main studies on DF effluent treatment in MECs (adapted from (Bakonyi et al., 2018)). (N.M: not mentioned, N.D.: not determined, HY: hydrogen yield, HPR: hydrogen production rate)

Major compounds in the DF effluent	**H_2 production**		**CE (%)**	**Reference**
MEC (2nd step)	**HY**	**HPR (L H_2/L-d^{-1})**		
Acetate, ethanol, lactate, formate[a]	0.33 L H_2/g COD	0.12	82	(Ullery and Logan, 2015)
Acetate, butyrate, propionate	0.05 L (STP) H_2/gVFA	0.07	N.M.	(Lenin Babu et al., 2013)
Acetate, ethanol, lactate, formate[a]	N.M.	0.12	70	(Ullery and Logan, 2014)
Acetate, butyrate[c]	0.84 L H_2 (STP)/g COD	0.09	N.M.	(Tommasi et al., 2012)
Acetate, butyrate, ethanol, propionate	0.26 L H_2/g corn stalk	3.43	72	(Li et al., 2014)
Mixture of VFAs, alcohols	1.09 L H_2/g COD	0.49 -d	66	(Kim et al., 2018)
Succinate, acetate, formate	N.D.	N.D.	68	(Mahmoud et al., 2014)
Acetate, propionate, butyrate, valerate	1.2 L H_2/g COD	1.76	92	(Liu et al., 2012)
Acetate, propionate, butyrate (synthetic media)	N.M.	1.42	24.5	(Escapa et al., 2013)
Acetate, butyrate, propionate	0.19 L H_2/g CODadded	N.M.	70	(Dhar et al., 2015)
Acetate, propionate	0.01 L H_2/g COD	0.02	N.M:	(Modestra et al., 2015)
Acetate, propionate, butyrate, valerate	2.78 L H_2/g COD	1.31	N.M.	(Wu et al., 2013)
Ethanol, acetate, propionate, butyrate, valerate	1.15 L H_2/g COD	1.41	87	(Lu et al., 2009)
Butyrate, acetate, valerate, ethanol, propionate	0.74 L (STP) H_2/g COD	0.48	58–175	(Wang et al., 2011)
Acetate, propionate, (synthetic media)	N.M.	0.27	N.M.	(Ruiz et al., 2014)

Table 2 (continued)

Acetate, propionate, valerate, butyrate	0.05 L H2/g COD	0.02	8.4	(Chookaew et al., 2014)
Acetate, butyrate, propionate, ethanol	0.87 L H2/g COD	4.52	76	(Li et al., 2017)
Ethanol, acetate, butyrate	0.65 L H2/g COD	0.011	80	(Marone et al., 2017)
Acetate, butyrate, ethanol, propionate, succinate	0.34 L H2/g COD	0.011	38	
Butyrate, acetate	1.48 L H2/g COD	0.025	76	
Butyrate,1,3 propanediol, acetate, propionate, succinate	1.4 L H2/g COD	0.028	75	
Butyrate, succinate, acetate, ethanol, propionate	0.22 L H2/g COD	0.006	33	

4.4 MESs for chemical synthesis: Electrofermentation (EF) and Bioelectrochemical Synthesis (BES)

The use of MESs for chemical synthesis is probably the most emerging area of the field. Both EF and BES current plays a major role influencing the metabolic activity of bacteria in order to target the production of specific metabolites.

EF can be defined as a system in which current stimulates microbial metabolism and regulates traditional fermentation pathways(Jiang et al., 2019a). In this context, when target products are more oxidised than the substrate the working electrode acts as electron sink for electrons in excess and the process is referred as Anodic EF (AEF); in contrast, more reduced compound can be generated in Cathodic EF (CEF) using the working electrode as electron donor(Moscoviz et al., 2016). An exhaustive model to explain EF was given by Kracke and Krömer (2014) studying the conversion of glucose and glycerol: according to their study, introduction of a cathode in a fermenter would induce an excess of redox cofactors (NADH and NADPH) while the addition of an electron sink increases ATP generation compared to other anaerobic metabolism accompanied by higher biomass yields. In the light of this, both process could improve performances of fermenters, as suggested by a study on lysine production using pure cultures of *Corynebacterium glutamicum* (Xafenias et al., 2017). As emerging technology, the number of studies on EF is, unfortunately, limited. Nikhil et al.(2015) proposed a novel electro fermenter for co-generation of H_2, generated from acidogenic fermentation of sugar, and current, from degradation of VFAs by exoelectrogenic bacteria. Even though their approach is indeed interesting for maximising energy harvesting and waste remediation, performances could be limited due to

H_2 consumption by some electroactive bacteria strains and methanogens (Jiang et al., 2019b). Glycerol AEF to ethanol have been reported using genetically modified bacterial strains (Flynn et al., 2010; Sturm-Richter et al., 2015) and co-coltures of *Geobacter sulfurreducens* and *Clostridium cellobioparum* (Speers et al., 2014). Engineered bacteria were also used to target AEF of acetoin conversion from lactate (Bursac et al., 2017) and glucose (Förster et al., 2017). Finally, the addition of oxidizing power was demonstrated to enhance PHBs accumulation in *Ralstonia eutropha* by Nishio et al. (2013). For what concerns CEF, a significant effort has been put towards exploitation of mixed microbial cultures for production of 1,3-propanediol (1,3-PDO). Using an inoculum from an anaerobic mesophilic digester, Xafenias et al. (2015)showed that operating at -1.1V *vs.* SHE microbial community composition shifted towards typical 1,3-PDO producers like *Clostridiacae* and reduced the population of propionate producers from *Veillonellacae* compered to non-electrochemical controls, increasing production rates up to 6 times. In another study from Zhou et al. (2015), increase in cathodic current was positively correlated to 1,3-PDO yields, accompanied by a decrease of *Citobacter* relative abundance in the biofilm. CEF could also divert microbial metabolism from oxidation of the substrate towards PHA accumulation in microaerofilic environments, as reported by Srikanth et al. (2012).

In BES CO_2 is converted into organic compounds through bio-catalysed reactions, in which microorganism uptake electrons from the cathode *via* DET or MET (Rabaey and Rozendal, 2010). Acetic acid is, at date, the major product obtained in BES (Dessì et al., 2020), and can theoretically be produced posing the cathode at -0.28 V *vs.* SHE (Eq. 7) (Rabaey and Rozendal, 2010)

$$2\,HCO_3^- + 9\,H^+ + 8\,e^- \rightarrow CH_3COO^- + H_2O\ (E_{cat}^0 = -0.28\,vs.SHE) \qquad (7)$$

Also in the case of BES, slightly more negative potential are applied. In Nevin et al. (2011), at an applied potential of -0.4 V *vs.* SHE capability of BES by two *Sporomusa* species, *Clostridium ljungdahlii*, *Clostridium aceticum*, and *Moorella thermoacetica* was demonstrated for the first time with a selectivity higher than 90%, while other side products such as 2-oxobutyrate and formate were identified. Production rates are, however, limited by low current densities which are ten times lower than in electrolysers (Prévoteau et al., 2020). In the last few years, spectrum of organic acids obtainable through BES have been broadened towards more high value products, in particular butyrate (Ganigué et al., 2015) and caproate (Jiang et al., 2020). When operating at acidic pH, organic acids could be converted into corresponding alcohols (Vassilev et al., 2018).

References

Bakonyi, P., Kumar, G., Koók, L., Tóth, G., Rózsenberszki, T., Bélafi-Bakó, K., et al. (2018). Microbial electrohydrogenesis linked to dark fermentation as integrated application for enhanced biohydrogen production: A review on process characteristics, experiences and lessons. *Bioresour. Technol.* 251, 381–389. doi:10.1016/j.biortech.2017.12.064.

Bond, D. R., and Lovley, D. R. (2003). Electricity production by Geobacter sulfurreducens attached to electrodes. *Appl. Environ. Microbiol.* 69, 1548–1555. doi:10.1128/AEM.69.3.1548-1555.2003.

Bursac, T., Gralnick, J. A., and Gescher, J. (2017). Acetoin production via unbalanced fermentation in *Shewanella oneidensis*. *Biotechnol. Bioeng.* 114, 1283–1289. doi:10.1002/bit.26243.

Byung Hong Kim, Doo Hyun Park, P. K. S. and S., and Kim, H. J. (1999). Mediator-less biofuel cell. *U.S. Pat. 5976719*. Available at: https://patentimages.storage.googleapis.com/8e/6b/21/b1e0253beb28ba/US5976719.pdf

Cecconet, D., Molognoni, D., Callegari, A., and Capodaglio, A. G. (2018). Agro-food industry wastewater treatment with microbial fuel cells: Energetic recovery issues. *Int. J. Hydrogen Energy* 43, 500–511. doi:10.1016/j.ijhydene.2017.07.231.

Chookaew, T., Prasertsan, P., and Ren, Z. J. (2014). Two-stage conversion of crude glycerol to energy using dark fermentation linked with microbial fuel cell or microbial electrolysis cell. *N. Biotechnol.* 31, 179–184. doi:10.1016/j.nbt.2013.12.004.

Das, S., and Mangwani, N. (2010). Recent developments in microbial fuel cells: A review. *J. Sci. Ind. Res. (India).* 69, 727–731.

Davis, J. B. (1963). Generation of Electricity by Microbial Action. *Adv. Appl. Microbiol.* 5, 51–64. doi:10.1016/S0065-2164(08)70006-6.

Dessì, P., Rovira-Alsina, L., Sánchez, C., Dinesh, G. K., Tong, W., Chatterjee, P., et al. (2020). Microbial electrosynthesis: Towards sustainable biorefineries for production of green chemicals from CO2 emissions. *Biotechnol. Adv.*, 107675. doi:10.1016/j.biotechadv.2020.107675.

Dhar, B. R., Elbeshbishy, E., Hafez, H., and Lee, H. S. (2015). Hydrogen production from sugar beet juice using an integrated biohydrogen process of dark fermentation and microbial electrolysis cell. *Bioresour. Technol.* 198, 223–230. doi:10.1016/j.biortech.2015.08.048.

Escapa, A., Lobato, A., García, D. M., and Morán, A. (2013). Hydrogen production and COD elimination rate in a continuous microbial electrolysis cell: The influence of hydraulic retention time and applied voltage. *Environ. Prog. Sustain. Energy* 32, 263–268. doi:10.1002/ep.11619.

Flynn, J. M., Ross, D. E., Hunt, K. A., Bond, D. R., and Gralnick, J. A. (2010). Enabling unbalanced fermentations by using engineered electrode- interfaced bacteria. *MBio* 1, 190–200. doi:10.1128/mBio.00190-10.

Fornero, J. J., Rosenbaum, M., and Angenent, L. T. (2010). Electric Power Generation from Municipal, Food, and Animal Wastewaters Using Microbial Fuel Cells. *Electroanalysis* 22, 832–843. doi:10.1002/elan.200980011.

Förster, A. H., Beblawy, S., Golitsch, F., and Gescher, J. (2017). Electrode-assisted acetoin production in a metabolically engineered Escherichia coli strain. *Biotechnol. Biofuels* 10. doi:10.1186/s13068-017-0745-9.

Ganigué, R., Puig, S., Batlle-Vilanova, P., Balaguer, M. D., and Colprim, J. (2015). Microbial electrosynthesis of butyrate from carbon dioxide. *Chem. Commun.* 51, 3235–3238. doi:10.1039/c4cc10121a.

Ge, Z., and He, Z. (2016). Long-term performance of a 200 liter modularized microbial fuel cell system treating municipal wastewater: Treatment, energy, and cost. *Environ. Sci. Water Res. Technol.* 2, 274–281. doi:10.1039/c6ew00020g.

He, Z., and Angenent, L. T. (2006). Application of Bacterial Biocathodes in Microbial Fuel Cells.

Electroanalysis 18, 2009–2015. doi:10.1002/elan.200603628.
He, Z., Minteer, S. D., and Angenent, L. T. (2005). Electricity generation from artificial wastewater using an upflow microbial fuel cell. *Environ. Sci. Technol.* 39, 5262–5267. doi:10.1021/es0502876.
Hiegemann, H., Herzer, D., Nettmann, E., Lübken, M., Schulte, P., Schmelz, K. G., et al. (2016). An integrated 45 L pilot microbial fuel cell system at a full-scale wastewater treatment plant. *Bioresour. Technol.* 218, 115–122. doi:10.1016/j.biortech.2016.06.052.
Jamal, M. T., Pugazhendi, A., and Jeyakumar, R. B. (2020). Application of halophiles in air cathode MFC for seafood industrial wastewater treatment and energy production under high saline condition. *Environ. Technol. Innov.* 20, 101119. doi:10.1016/j.eti.2020.101119.
Janicek, A., Fan, Y., and Liu, H. (2014). Design of microbial fuel cells for practical application: A review and analysis of scale-up studies. *Biofuels* 5, 79–92. doi:10.4155/bfs.13.69.
Jayashree, C., Sweta, S., Arulazhagan, P., Yeom, I. T., Iqbal, M. I. I., and Rajesh Banu, J. (2015). Electricity generation from retting wastewater consisting of recalcitrant compounds using continuous upflow microbial fuel cell. *Biotechnol. Bioprocess Eng.* 20, 753–759. doi:10.1007/s12257-015-0017-0.
Jayashree, C., Tamilarasan, K., Rajkumar, M., Arulazhagan, P., Yogalakshmi, K. N., Srikanth, M., et al. (2016). Treatment of seafood processing wastewater using upflow microbial fuel cell for power generation and identification of bacterial community in anodic biofilm. *J. Environ. Manage.* 180, 351–358. doi:10.1016/j.jenvman.2016.05.050.
Jiang, Y., Chu, N., Qian, D. K., and Jianxiong Zeng, R. (2020). Microbial electrochemical stimulation of caproate production from ethanol and carbon dioxide. *Bioresour. Technol.* 295, 122266. doi:10.1016/j.biortech.2019.122266.
Jiang, Y., May, H. D., Lu, L., Liang, P., Huang, X., and Jason, Z. (2019a). Carbon dioxide and organic waste valorization by microbial electrosynthesis and electro-fermentation. 149, 42–55. doi:10.1016/j.watres.2018.10.092.
Jiang, Y., May, H. D., Lu, L., Liang, P., Huang, X., and Ren, Z. J. (2019b). Carbon dioxide and organic waste valorization by microbial electrosynthesis and electro-fermentation. *Water Res.* 149, 42–55. doi:10.1016/j.watres.2018.10.092.
Kadier, A., Kalil, M. S., Abdeshahian, P., Chandrasekhar, K., Mohamed, A., Azman, N. F., et al. (2016). Recent advances and emerging challenges in microbial electrolysis cells (MECs) for microbial production of hydrogen and value-added chemicals. *Renew. Sustain. Energy Rev.* 61, 501–525. doi:10.1016/j.rser.2016.04.017.
Kadier, A., Simayi, Y., Chandrasekhar, K., Ismail, M., and Kalil, M. S. (2015). Hydrogen gas production with an electroformed Ni mesh cathode catalysts in a single-chamber microbial electrolysis cell (MEC). *Int. J. Hydrogen Energy* 40, 14095–14103. doi:10.1016/j.ijhydene.2015.08.095.
Kim, B. H., Ikeda, T., Park, H. S., Kim, H. J., Hyun, M. S., Kano, K., et al. (1999). Electrochemical activity of an Fe(III)-reducing bacterium, Shewanella putrefaciens IR-1, in the presence of alternative electron acceptors. *Biotechnol. Tech.* 13, 475–478. doi:10.1023/A:1008993029309.
KIM, H. J. S. H. S. C. H. K. (1999). A Microbial Fuel Cell Type Lactate Biosensor Using a Metal-Reducing Bacterium, Shewanella putrefaciens. *J. Microbiol. Biotechnol.* 9, 365–367.
Kim, K. N., Lee, S. H., Kim, H., Park, Y. H., and In, S. Il (2018). Improved microbial electrolysis cell hydrogen production by hybridization with a TiO2 nanotube array photoanode. *Energies* 11. doi:10.3390/en11113184.
Kim, K. Y., Yang, W., and Logan, B. E. (2015). Impact of electrode configurations on retention time and domestic wastewater treatment efficiency using microbial fuel cells. *Water Res.* 80, 41–46. doi:10.1016/j.watres.2015.05.021.
Kracke, F., and Krömer, J. O. (2014). Identifying target processes for microbial electrosynthesis by elementary mode analysis. *BMC Bioinformatics* 15. doi:10.1186/s12859-014-0410-2.

Krieg, T., Enzmann, F., Sell, D., Schrader, J., and Holtmann, D. (2017). Simulation of the current generation of a microbial fuel cell in a laboratory wastewater treatment plant. *Appl. Energy* 195, 942–949. doi:10.1016/j.apenergy.2017.03.101.

Leang, C., Coppi, M. V., and Lovley, D. R. (2003). OmcB, a c-type polyheme cytochrome, involved in Fe(III) reduction in Geobacter sulfurreducens. *J. Bacteriol.* 185, 2096–2103. doi:10.1128/JB.185.7.2096-2103.2003.

Lenin Babu, M., Venkata Subhash, G., Sarma, P. N., and Venkata Mohan, S. (2013). Bio-electrolytic conversion of acidogenic effluents to biohydrogen: An integration strategy for higher substrate conversion and product recovery. *Bioresour. Technol.* 133, 322–331. doi:10.1016/j.biortech.2013.01.029.

Li, X. H., Liang, D. W., Bai, Y. X., Fan, Y. T., and Hou, H. W. (2014). Enhanced H2 production from corn stalk by integrating dark fermentation and single chamber microbial electrolysis cells with double anode arrangement. *Int. J. Hydrogen Energy* 39, 8977–8982. doi:10.1016/j.ijhydene.2014.03.065.

Li, X., Zhang, R., Qian, Y., Angelidaki, I., and Zhang, Y. (2017). The impact of anode acclimation strategy on microbial electrolysis cell treating hydrogen fermentation effluent. *Bioresour. Technol.* doi:10.1016/j.biortech.2017.03.160.

Li, Y., Liu, L., Yang, F., and Ren, N. (2015). Performance of carbon fiber cathode membrane with C-Mn-Fe-O catalyst in MBR-MFC for wastewater treatment. *J. Memb. Sci.* 484, 27–34. doi:10.1016/j.memsci.2015.03.006.

Lin, T., Ding, W., Sun, L., Wang, L., Liu, C. G., and Song, H. (2018). Engineered Shewanella oneidensis-reduced graphene oxide biohybrid with enhanced biosynthesis and transport of flavins enabled a highest bioelectricity output in microbial fuel cells. *Nano Energy* 50, 639–648. doi:10.1016/j.nanoen.2018.05.072.

Liu, H., Grot, S., and Logan, B. E. (2005). Electrochemically assisted microbial production of hydrogen from acetate. *Environ. Sci. Technol.* 39, 4317–4320. doi:10.1021/es050244p.

Liu, W., Huang, S., Zhou, A., Zhou, G., Ren, N., Wang, A., et al. (2012). Hydrogen generation in microbial electrolysis cell feeding with fermentation liquid of waste activated sludge. in *International Journal of Hydrogen Energy* (Pergamon), 13859–13864. doi:10.1016/j.ijhydene.2012.04.090.

Logan, B. E., Hamelers, B., Rozendal, R., Schröder, U., Keller, J., Freguia, S., et al. (2006). Microbial fuel cells: Methodology and technology. *Environ. Sci. Technol.* 40, 5181–5192. doi:10.1021/es0605016.

Logan, B. E., Rossi, R., Ragab, A., and Saikaly, P. E. (2019). Electroactive microorganisms in bioelectrochemical systems. *Nat. Rev. Microbiol.* 17, 307–319. doi:10.1038/s41579-019-0173-x.

Lovley, D. R., Ueki, T., Zhang, T., Malvankar, N. S., Shrestha, P. M., Flanagan, K. A., et al. (2011). "Geobacter. The Microbe Electric's Physiology, Ecology, and Practical Applications," in *Advances in Microbial Physiology* (Academic Press), 1–100. doi:10.1016/B978-0-12-387661-4.00004-5.

Lu, L., Ren, N., Xing, D., and Logan, B. E. (2009). Hydrogen production with effluent from an ethanol-H2-coproducing fermentation reactor using a single-chamber microbial electrolysis cell. *Biosens. Bioelectron.* 24, 3055–3060. doi:10.1016/j.bios.2009.03.024.

Luo, H., Xu, G., Lu, Y., Liu, G., Zhang, R., Li, X., et al. (2017). Electricity generation in a microbial fuel cell using yogurt wastewater under alkaline conditions. *RSC Adv.* 7, 32826–32832. doi:10.1039/c7ra06131e.

Ma, J., Ni, H., Su, D., and Meng, X. (2016). Bioelectricity generation from pig farm wastewater in microbial fuel cell using carbon brush as electrode. *Int. J. Hydrogen Energy* 41, 16191–16195. doi:10.1016/j.ijhydene.2016.05.255.

Mahmoud, M., Parameswaran, P., Torres, C. I., and Rittmann, B. E. (2014). Fermentation pre-treatment of landfill leachate for enhanced electron recovery in a microbial electrolysis

cell. *Bioresour. Technol.* 151, 151–158. doi:10.1016/j.biortech.2013.10.053.
Marone, A., Ayala-Campos, O. R., Trably, E., Carmona-Martínez, A. A., Moscoviz, R., Latrille, E., et al. (2017). Coupling dark fermentation and microbial electrolysis to enhance bio-hydrogen production from agro-industrial wastewaters and by-products in a bio-refinery framework. *Int. J. Hydrogen Energy* 42, 1609–1621. doi:10.1016/j.ijhydene.2016.09.166.
Min, B., and Logan, B. E. (2004). Continuous electricity generation from domestic wastewater and organic substrates in a flat plate microbial fuel cell. *Environ. Sci. Technol.* 38, 5809–5814. doi:10.1021/es0491026.
Modestra, J. A., Babu, M. L., and Mohan, S. V. (2015). Electro-fermentation of real-field acidogenic spent wash effluents for additional biohydrogen production with simultaneous treatment in a microbial electrolysis cell. *Sep. Purif. Technol.* 150, 308–315. doi:10.1016/j.seppur.2015.05.043.
Moscoviz, R., Toledo-Alarcón, J., Trably, E., and Bernet, N. (2016). Electro-Fermentation: How To Drive Fermentation Using Electrochemical Systems. *Trends Biotechnol.* 34, 856–865. doi:10.1016/j.tibtech.2016.04.009.
Munoz-Cupa, C., Hu, Y., Xu, C., and Bassi, A. (2021). An overview of microbial fuel cell usage in wastewater treatment, resource recovery and energy production. *Sci. Total Environ.* 754, 142429. doi:10.1016/j.scitotenv.2020.142429.
Nevin, K. P., Hensley, S. A., Franks, A. E., Summers, Z. M., Ou, J., Woodard, T. L., et al. (2011). Electrosynthesis of organic compounds from carbon dioxide is catalyzed by a diversity of acetogenic microorganisms. *Appl. Environ. Microbiol.* 77, 2882–2886. doi:10.1128/AEM.02642-10.
Nikhil, G. N., Venkata Subhash, G., Yeruva, D. K., and Venkata Mohan, S. (2015). Synergistic yield of dual energy forms through biocatalyzed electrofermentation of waste: Stoichiometric analysis of electron and carbon distribution. *Energy* 88, 281–291. doi:10.1016/j.energy.2015.05.043.
Nishio, K., Kimoto, Y., Song, J., Konno, T., Ishihara, K., Kato, S., et al. (2013). Extracellular Electron Transfer Enhances Polyhydroxybutyrate Productivity in Ralstonia eutropha. *Environ. Sci. Technol. Lett.* 1, 40–43. doi:10.1021/ez400085b.
Park, D. H., and Zeikus, J. G. (2000). Electricity generation in microbial fuel cells using neutral red as an electronophore. *Appl. Environ. Microbiol.* 66, 1292–1297. doi:10.1128/AEM.66.4.1292-1297.2000.
Park, Y., Cho, H., Yu, J., Min, B., Kim, H. S., Kim, B. G., et al. (2017). Response of microbial community structure to pre-acclimation strategies in microbial fuel cells for domestic wastewater treatment. *Bioresour. Technol.* 233, 176–183. doi:10.1016/j.biortech.2017.02.101.
Patil, S. A., Harnisch, F., Koch, C., Hübschmann, T., Fetzer, I., Carmona-Martínez, A. A., et al. (2011). Electroactive mixed culture derived biofilms in microbial bioelectrochemical systems: The role of pH on biofilm formation, performance and composition. *Bioresour. Technol.* 102, 9683–9690. doi:10.1016/j.biortech.2011.07.087.
Potter, M. C., and B, P. R. S. L. (1911). Electrical effects accompanying the decomposition of organic compounds. *Proc. R. Soc. London. Ser. B, Contain. Pap. a Biol. Character* 84, 260–276. doi:10.1098/rspb.1911.0073.
Prévoteau, A., Carvajal-Arroyo, J. M., Ganigué, R., and Rabaey, K. (2020). Microbial electrosynthesis from CO2: forever a promise? *Curr. Opin. Biotechnol.* 62, 48–57. doi:10.1016/j.copbio.2019.08.014.
Qu, Y., Feng, Y., Wang, X., and Logan, B. E. (2012). Use of a coculture to enable current production by Geobacter sulfurreducens. *Appl. Environ. Microbiol.* 78, 3484–3487. doi:10.1128/AEM.00073-12.
Rabaey, K., and Rozendal, R. A. (2010). Microbial electrosynthesis - Revisiting the electrical route for microbial production. *Nat. Rev. Microbiol.* 8, 706–716. doi:10.1038/nrmicro2422.

Recio-Garrido, D., Adekunle, A., Perrier, M., Raghavan, V., and Tartakovsky, B. (2017). Wastewater Treatment and Online Chemical Oxygen Demand Estimation in a Cascade of Microbial Fuel Cells. *Ind. Eng. Chem. Res.* 56, 12471–12478. doi:10.1021/acs.iecr.7b02586.

Reimers, C. E., Tender, L. M., Fertig, S., and Wang, W. (2001). Harvesting energy from the marine sediment - Water interface. *Environ. Sci. Technol.* 35, 192–195. doi:10.1021/es001223s.

Ruiz, V., Ilhan, Z. E., Kang, D.-W., Krajmalnik-Brown, R., and Buitrón, G. (2014). The source of inoculum plays a defining role in the development of MEC microbial consortia fed with acetic and propionic acid mixtures. *J. Biotechnol.* 182–183, 11–18. doi:10.1016/J.JBIOTEC.2014.04.016.

Schröder, U. (2007). Anodic electron transfer mechanisms in microbial fuel cells and their energy efficiency. *Phys. Chem. Chem. Phys.* 9, 2619–2629. doi:10.1039/b703627m.

Schuetz, B., Schicklberger, M., Kuermann, J., Spormann, A. M., and Gescher, J. (2009). Periplasmic electron transfer via the c-type cytochromes Mtra and Fcca of Shewanella oneidensis Mr-1. *Appl. Environ. Microbiol.* 75, 7789–7796. doi:10.1128/AEM.01834-09.

Sevda, S., Dominguez-Benetton, X., Vanbroekhoven, K., De Wever, H., Sreekrishnan, T. R., and Pant, D. (2013). High strength wastewater treatment accompanied by power generation using air cathode microbial fuel cell. *Appl. Energy* 105, 194–206. doi:10.1016/j.apenergy.2012.12.037.

Speers, A. M., Young, J. M., and Reguera, G. (2014). Fermentation of glycerol into ethanol in a microbial electrolysis cell driven by a customized consortium. *Environ. Sci. Technol.* 48, 6350–6358. doi:10.1021/es500690a.

Srikanth, S., Venkateswar Reddy, M., and Venkata Mohan, S. (2012). Microaerophilic microenvironment at biocathode enhances electrogenesis with simultaneous synthesis of polyhydroxyalkanoates (PHA) in bioelectrochemical system (BES). *Bioresour. Technol.* 125, 291–299. doi:10.1016/j.biortech.2012.08.060.

Sturm-Richter, K., Golitsch, F., Sturm, G., Kipf, E., Dittrich, A., Beblawy, S., et al. (2015). Unbalanced fermentation of glycerol in Escherichia coli via heterologous production of an electron transport chain and electrode interaction in microbial electrochemical cells. *Bioresour. Technol.* 186, 89–96. doi:10.1016/j.biortech.2015.02.116.

Tanikkul, P., and Pisutpaisal, N. (2018). Membrane-less MFC based biosensor for monitoring wastewater quality. *Int. J. Hydrogen Energy* 43, 483–489. doi:10.1016/j.ijhydene.2017.10.065.

Tommasi, T., Ruggeri, B., and Sanfilippo, S. (2012). Energy valorisation of residues of dark anaerobic production of Hydrogen. *J. Clean. Prod.* 34, 91–97. doi:10.1016/j.jclepro.2012.01.035.

Ullery, M. L., and Logan, B. E. (2014). Comparison of complex effluent treatability in different bench scale microbial electrolysis cells. *Bioresour. Technol.* 170, 530–537. doi:10.1016/j.biortech.2014.08.028.

Ullery, M. L., and Logan, B. E. (2015). Anode acclimation methods and their impact on microbial electrolysis cells treating fermentation effluent. *Int. J. Hydrogen Energy* 40, 6782–6791. doi:10.1016/j.ijhydene.2015.03.101.

Valladares Linares, R., Domínguez-Maldonado, J., Rodríguez-Leal, E., Patrón, G., Castillo-Hernández, A., Miranda, A., et al. (2019). Scale up of Microbial Fuel Cell Stack System for Residential Wastewater Treatment in Continuous Mode Operation. *Water* 11, 217. doi:10.3390/w11020217.

Vassilev, I., Hernandez, P. A., Batlle-Vilanova, P., Freguia, S., Krömer, J. O., Keller, J., et al. (2018). Microbial Electrosynthesis of Isobutyric, Butyric, Caproic Acids, and Corresponding Alcohols from Carbon Dioxide. *ACS Sustain. Chem. Eng.* 6, 8485–8493. doi:10.1021/acssuschemeng.8b00739.

Wang, A., Sun, D., Cao, G., Wang, H., Ren, N., Wu, W. M., et al. (2011). Integrated hydrogen production process from cellulose by combining dark fermentation, microbial fuel cells, and

a microbial electrolysis cell. *Bioresour. Technol.* 102, 4137–4143. doi:10.1016/j.biortech.2010.10.137.

Włodarczyk, P. P., and Włodarczyk, B. (2019). Wastewater Treatment and Electricity Production in a Microbial Fuel Cell with Cu–B Alloy as the Cathode Catalyst. *Catalysts* 9, 572. doi:10.3390/catal9070572.

Wu, T., Zhu, G., Jha, A. K., Zou, R., Liu, L., Huang, X., et al. (2013). Hydrogen production with effluent from an anaerobic baffled reactor (ABR) using a singlechamber microbial electrolysis cell (MEC). in *International Journal of Hydrogen Energy* (Elsevier Ltd), 11117–11123. doi:10.1016/j.ijhydene.2013.03.029.

Xafenias, N., Anunobi, M. S. O., and Mapelli, V. (2015). Electrochemical startup increases 1,3-propanediol titers in mixed-culture glycerol fermentations. *Process Biochem.* 50, 1499–1508. doi:10.1016/j.procbio.2015.06.020.

Xafenias, N., Kmezik, C., and Mapelli, V. (2017). Enhancement of anaerobic lysine production in Corynebacterium glutamicum electrofermentations. *Bioelectrochemistry* 117, 40–47. doi:10.1016/j.bioelechem.2017.06.001.

Zhou, M., Chi, M., Luo, J., He, H., and Jin, T. (2011). An overview of electrode materials in microbial fuel cells. *J. Power Sources* 196, 4427–4435. doi:10.1016/j.jpowsour.2011.01.012.

Zhou, M., Freguia, S., Dennis, P. G., Keller, J., and Rabaey, K. (2015). Development of bioelectrocatalytic activity stimulates mixed-culture reduction of glycerol in a bioelectrochemical system. *Microb. Biotechnol.* 8, 483–489. doi:10.1111/1751-7915.12240.

Zhuang, L., Zheng, Y., Zhou, S., Yuan, Y., Yuan, H., and Chen, Y. (2012). Scalable microbial fuel cell (MFC) stack for continuous real wastewater treatment. *Bioresour. Technol.* 106, 82–88. doi:10.1016/j.biortech.2011.11.019.

Chapter 5

Propionate production by Bioelectrochemically-Assisted lactate fermentation and simultaneous CO_2 recycling

(Article published in Frontiers in Microbiology)

frontiers in Microbiology

ORIGINAL RESEARCH
published: 15 December 2020
doi: 10.3389/fmicb.2020.599438

Propionate Production by Bioelectrochemically-Assisted Lactate Fermentation and Simultaneous CO_2 Recycling

Marco Isipato[1,2], Paolo Dessì[2], Carlos Sánchez[2], Simon Mills[2], Umer Z. Ijaz[3], Fabiano Asunis[1], Daniela Spiga[1], Giorgia De Gioannis[1,4], Michele Mascia[5], Gavin Collins[2], Aldo Muntoni[1,4] and Piet N. L. Lens[2]*

[1] Department of Civil and Environmental Engineering and Architecture, University of Cagliari, Cagliari, Italy, [2] Microbiology, School of Natural Sciences and Ryan Institute, National University of Ireland Galway, Galway, Ireland, [3] Infrastructure and Environment Research Division, School of Engineering, University of Glasgow, Glasgow, United Kingdom, [4] IGAG-CNR, Environmental Geology and Geoengineering Institute of the National Research Council–Piazza D'Armi 1, Cagliari, Italy, [5] Dipartimento di Ingegneria Meccanica, Chimica, e dei Materiali, Università degli Studi di Cagliari, Cagliari, Italy

OPEN ACCESS

Edited by:
Ludovic Jourdin,
Delft University of Technology,
Netherlands

Reviewed by:
David Strik,
Wageningen University and Research,
Netherlands
Seung Gu Shin,
Pohang University of Science
and Technology, South Korea
Raúl Mateos,
Universidad de León, Spain

***Correspondence:**
Paolo Dessì
paolo.dessi@nuigalway.ie

Specialty section:
This article was submitted to
Microbiotechnology,
a section of the journal
Frontiers in Microbiology

Received: 27 August 2020
Accepted: 23 November 2020
Published: 15 December 2020

Citation:
Isipato M, Dessì P, Sánchez C,
Mills S, Ijaz UZ, Asunis F, Spiga D,
De Gioannis G, Mascia M, Collins G,
Muntoni A and Lens PNL (2020)
Propionate Production by
Bioelectrochemically-Assisted Lactate
Fermentation and Simultaneous CO_2
Recycling.
Front. Microbiol. 11:599438.
doi: 10.3389/fmicb.2020.599438

Production of volatile fatty acids (VFAs), fundamental building blocks for the chemical industry, depends on fossil fuels but organic waste is an emerging alternative substrate. Lactate produced from sugar-containing waste streams can be further processed to VFAs. In this study, electrofermentation (EF) in a two-chamber cell is proposed to enhance propionate production *via* lactate fermentation. At an initial pH of 5, an applied potential of −1 V vs. Ag/AgCl favored propionate production over butyrate from 20 mM lactate (with respect to non-electrochemical control incubations), due to the pH buffering effect of the cathode electrode, with production rates up to 5.9 mM d^{-1} (0.44 g L^{-1} d^{-1}). Microbial community analysis confirmed the enrichment of propionate-producing microorganisms, such as *Tyzzerella* sp. and *Propionibacterium* sp. Organisms commonly found in microbial electrosynthesis reactors, such as *Desulfovibrio* sp. and *Acetobacterium* sp., were also abundant at the cathode, indicating their involvement in recycling CO_2 produced by lactate fermentation into acetate, as confirmed by stoichiometric calculations. Propionate was the main product of lactate fermentation at substrate concentrations up to 150 mM, with a highest production rate of 12.9 mM d^{-1} (0.96 g L^{-1} d^{-1}) and a yield of 0.48 mol mol^{-1} lactate consumed. Furthermore, as high as 81% of the lactate consumed (in terms of carbon) was recovered as soluble product, highlighting the potential for EF application with high-carbon waste streams, such as cheese whey or other food wastes. In summary, EF can be applied to control lactate fermentation toward propionate production and to recycle the resulting CO_2 into acetate, increasing the VFA yield and avoiding carbon emissions and addition of chemicals for pH control.

Keywords: bioelectrochemical systems, cyclic voltammetry, electrofermentation, lactate fermentation, microbial electrosynthesis, miseq sequencing, propionate production

INTRODUCTION

The global chemical industry production capacity nearly doubled from 2000 to 2017, increasing from 1.2 to 2.3 billion tons (UNEP, 2019). Chemical production still largely depends on fossil fuels, consuming about 600 Mt of oil and 105 billion Nm^3 of natural gas as feedstock annually (International Energy and Agency, 2018). Among industries, the chemical sector is the third-largest emitter of greenhouse gases worldwide, releasing about 2 Gt CO_2eq annually (International Energy and Agency, 2018). However, the increasing price of crude oil and stringent legislation regulating waste management and CO_2 emissions are expected to drive a shift toward bio-based chemical production (Alibardi et al., 2020). Several chemicals can be produced biologically from organic substrates, including waste feedstocks. Among biological waste treatment processes, fermentation can link waste treatment and chemicals production, converting organic contaminants to valuable products, such as carboxylic acids for use as building blocks in synthesizing a wide range of other chemicals (Atasoy et al., 2019).

Considering carboxylic acids, propionic acid has a higher market value (1.8–2.3 € kg^{-1}) than butyric (1.4–1.6 € kg^{-1}) and acetic (0.4–0.7 € kg^{-1}) acid (Grand View Research, 2015, 2020; Markets and Markets, 2015; Asunis et al., 2020). Its market is expected to expand at an annual rate of 3.5% up to 2026 (Allied Market Research, 2020) due to its diverse applications, such as in grain and food preservation, herbicide and cellulose acetate propionate (CAP) synthesis, and as intermediate for the pharmaceutical and perfume industries (Liu et al., 2012). Moreover, the use of propionic acid in emerging sectors, e.g., as a precursor for biopolymers production (Larsson et al., 2016; Tebaldi et al., 2019), is a further driver for market expansion. Propionic acid is currently mainly produced by petrochemical processes, whose competitiveness is strictly linked to the price of oil (Ahmadi et al., 2017). Sustainable and low-cost processes, such as fermentation of waste feedstocks, offer interesting alternatives, reducing pressure on non-renewable resources and allowing for de-coupling of propionic acid production from oil market dynamics.

To date, fermentative propionate production has mainly relied on pure *Propionibacterium* cultures (Ahmadi et al., 2017) *via* either direct reduction or the dicarboxylic acid pathway (Murali et al., 2017). Lactose, or its main fermentation product, lactate, are used as carbon source. In direct reduction, also known as the acrylate pathway, lactate is reduced to propionate with acryloyl-CoA as intermediate (Akedo et al., 1983). In the dicarboxylic acid pathway, lactate is first converted to succinate, and then to propionate *via* decarboxylation (Paynter and Elsden, 1970). In both cases, acetate and CO_2 are produced as by-products. Li et al. (2016) showed lactate as a crucial intermediate in fermenting organic waste to propionate, obtaining a maximum concentration of 145 mM (68.3% of total VFAs) with a yield of 0.59 mol mol^{-1} lactate and productivity of 97 mM d^{-1}. However, when organic waste is used as carbon source, a two-stage fermentation process is typically required in which the feedstock is first hydrolysed and fermented into a lactate-rich broth, which is then sterilized and fed to pure cultures of propionate-producing microorganisms (Li et al., 2016). Furthermore, dosing of alkaline chemicals is necessary to increase the pH of fermented organic waste toward neutrality for the propionate-producing bacteria (Liu et al., 2012).

Mixed fermentative cultures are, in general, more resilient to the operational fluctuations typical of waste streams, and easier to handle than pure cultures, not requiring sterilization (Wang and Wan, 2009) and representing a low-cost alternative for one-stage propionate production. However, propionate has seldom been reported as the prevalent organic product in mixed-culture fermentation (Lee et al., 2014; Dionisi and Silva, 2016; Strazzera et al., 2018; Asunis et al., 2020). Rather, acetate and butyrate are the soluble products most commonly obtained, especially at pH < 6 (Asunis et al., 2019). Moreover, due to the fast acidification resulting from organic waste fermentation, a substantial quantity of buffer (e.g., sodium hydroxide) may be required for pH control in large-scale reactors.

Electrofermentation (EF), in which a solid electrode acts as a source of oxidizing (anodic EF) or reducing (cathodic EF) power, is a technology recently proposed to overcome the metabolic limitations of fermentative pathways (Schievano et al., 2016). It is recognized that application of current can affect the extracellular and intracellular oxidation-reduction potential (ORP), and thus the metabolic regulations, in fermentative microorganisms (Moscoviz et al., 2016). The electrode can also act as an additional electron source to obtain otherwise energetically unfavorable reactions, and even promote syntrophic interaction between fermenters and electroactive bacteria (Moscoviz et al., 2018). Thus, anodic EF can be applied to dissipate electrons when the substrate is more reduced than the products, e.g., for the conversion of glycerol to ethanol (Speers et al., 2014) or 3-hydroxypropionic acid (Kim et al., 2017), whereas cathodic EF has been applied to synthesize products not commonly obtained in dark fermentation, such as butanol (Engel et al., 2019) or 1,3-propanediol (Xafenias et al., 2015).

Furthermore, cathodic EF presents two additional advantages over dark fermentation. First, proton consumption/OH^- generation at the cathode (Grim et al., 2020) provides for cost-effective pH buffering. Even when treating acidic substrates, a micro-environment with higher pH is formed on the electrode surface, that could mitigate the inhibitory effects on the microbial community, and shift the metabolic pathways with respect to dark fermentation. Second, when enough negative potential is applied, CO_2 produced from fermentation can potentially be recycled into carboxylic acids *via* microbial electrosynthesis (MES) (Nevin et al., 2010). This could result in higher VFA yields and, theoretically, in full recovery as soluble product of the substrate carbon content. Therefore, in this study, cathodic EF was applied to synthetic wastewaters containing lactate, alone or in combination with butyrate to simulate conditions typically achieved in fermented cheese whey (Asunis et al., 2019), which was selected as a model organic substrate. The metabolic shifts compared to dark fermentation, and the possibility of recycling CO_2 into soluble products *via* MES, were evaluated. The full metabolic pathway was hypothesized based on stoichiometric evaluations, along with the extensive electrochemical and microbiological characterization.

MATERIALS AND METHODS

Microbial Electrochemical Cell Set-Up

The experiments were performed in H-type bioelectrochemical cells (**Figure 1**), each with a working volume of 150 mL. Two chambers were connected through a circular (3 cm diameter) proton exchange membrane (Nafion 117, Fuel Cell Store, United States, or Fumasep FKE-50, Germany). The Nafion membrane was pre-treated according to Modestra and Mohan (2017). The cathode headspace was connected to a gas bag (1 L) for gas monitoring, and sampling ports were incorporated for both catholyte and anolyte. The cathode (3 × 4 × 0.05 cm) was a carbon cloth (Panex 30 Fabric PW06, Fuel Cell Store, United States), whereas the anode (2 × 2 cm) was a platinized titanium mesh (Goodfellow, United Kingdom). Both electrodes were connected to a potentiostat (VMP3, Biologic, France) using Ti-wire, which was connected to the anode and cathode electrodes by direct contact and through a nylon screw, respectively. Both contacts resulted in a resistance < 5 Ω. An Ag/AgCl reference electrode (BASi RE-5B, Alvatek, United Kingdom) was placed in the cathodic chamber, a few centimeters from the cathode electrode and away from the ion migration path (Harnisch and Freguia, 2012). Temperature control (25 ± 3°C) and stirring were achieved using a hot stirring plate (Cole-Parmer, United States).

Inoculum, Anolyte, and Catholyte

The inoculum [66.0 ± 3.0 g L^{-1} total solids (TS), 49.8 ± 2.6 g L^{-1} volatile solids (VS)] was sampled from the anaerobic digester of a dairy processing plant (Dairygold, Ireland). Anolyte composition was as follows, expressed in g L^{-1}: KH_2PO_4 (0.33), K_2HPO_4 (0.45), NH_4Cl (1.0), KCl (0.1), NaCl (0.8), and $MgSO_4 \times 7H_2O$ (0.2). In addition, the catholyte solution contained 1 mL L^{-1} vitamin solution and 10 mL L^{-1} trace metal solution (DSMZ medium 144). D-lactate, butyrate or both were added to the catholyte, as specified in section "MES reactor operation". Methanogenic activity was suppressed by adding 0.5 g L^{-1} bromoethanesulphonic acid (BESA) in the first batch cycle.

MES Reactor Operation

In a first set of experiments, duplicate microbial EF cells (LB1 and LB2) containing both lactate and butyrate (20 mM) were inoculated with 1 g VS L^{-1} digested sludge and operated for four consecutive batch cycles of 5–7 days each. A cathodic potential of −1.2 V vs. Ag/AgCl was imposed on the duplicate cells for the first 24 h of operation, and then reduced to −1

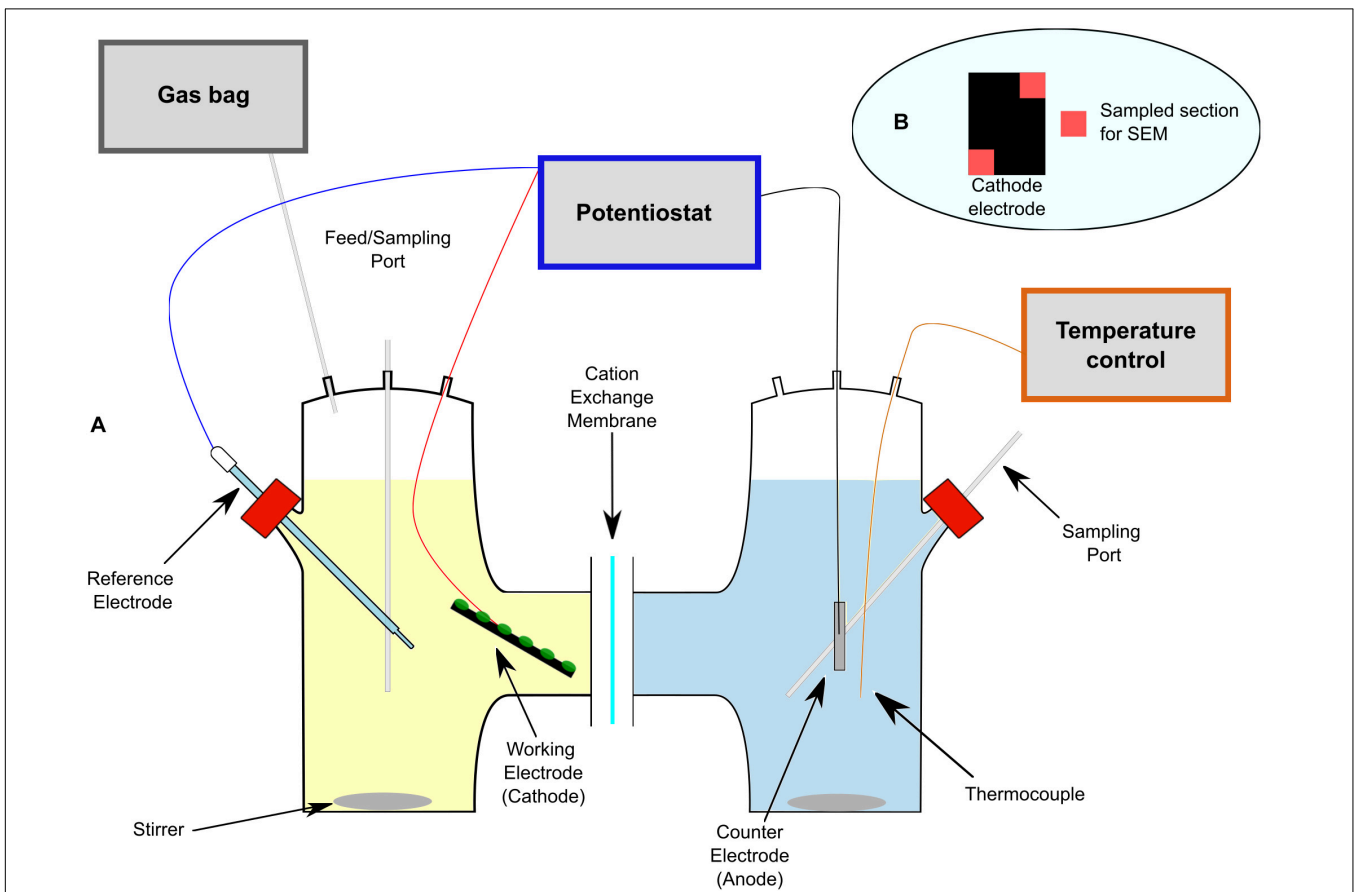

FIGURE 1 | (A) Schematic overview of the electrofermentation cells used in this study. **(B)** Section of the cathode electrode showing the location of samples collected for SEM analysis.

V vs. Ag/AgCl for the remainder of the experiment to prevent an excessive pH increase. Before inoculation, the initial pH of the catholyte was corrected to 5 with 3M NaOH. Catholyte (1 mL) and anolyte (0.5 mL) were sampled each working day for analysis. The decrease in volume of catholyte due to the sample withdrawn for analysis was less than 5% in total. The volume was reintegrated at the beginning of each cycle by addition of fresh medium containing the lactate amount required to restore the initial concentration of 20 mM. Butyrate was only added on the first cycle since it was not consumed by the microbial community. Gas samples were collected from the gas bag for analysis when production was apparent at the end of a batch cycle.

In a second set of experiments, duplicate cells (L1 and L2) were operated with only lactate as the substrate, under the otherwise same operational conditions as in the first set of experiments, for two batch cycles of 8–10 days each. The lactate concentration was 20 mM initially but was increased to 30 mM at the beginning of the second batch cycle to assess the impact of lactate concentration on reactor performance. Finally, a third cell (L3) was operated for one batch cycle with high lactate (150 mM) to simulate concentrations achievable in organic waste fermentation.

Control experiments were included to support the results obtained in the EF studies. A cell with the same characteristics, but without inoculum, served as abiotic control to monitor possible electrochemical reactions, as well as carboxylic acid migration through the membrane. Additionally, non-electrochemical control experiments were performed for one batch cycle to investigate metabolic differences between EF and dark fermentation. Duplicate serum bottles were set up with the same inoculum and solution volume as the EF cells, with lactate and butyrate (C_{LB}), or only lactate (C_L), as substrate. The initial pH of non-electrochemical control incubations was set at 5 or 7 by dosing 2M NaOH, to distinguish between the effects of the applied potential and pH in the EF experiments.

Microbiological Analysis

Cathodic and planktonic community samples were collected from LB1 and LB2 cell at the end of the first set of experiments. Cathodes were removed from the cell, and screws and titanium wire were gently disconnected. Sections of 1 × 1 cm were cut from opposite corners of the electrode (see **Figure 1**) for SEM analysis, under flame, using UV-sterilized instruments and surfaces, and all instruments and surfaces were sterilized with ethanol between two consecutive samples. The remaining part of the electrode was placed in a Falcon tube filled with 5 mL of sterile 0.1 M phosphate-buffered saline (PBS) solution, sonicated at 50–60 Hz and 30% power for 10 min (Bandelin Sonorex Digiplus sonicator), and vigorously vortexed (Fisherbrand ZX3) to detach biofilm. The visible carbon fibers were then removed using sterile tweezers. The cathodic biofilm samples, as well as triplicate sample (5 mL) of catholyte, were then centrifuged at 3,500 rcf for 10 min and resuspended in 3 and 1 mL sterile PBS, respectively. The re-suspended cathodic biofilm was then divided into triplicate 1-mL samples. All samples were snap-frozen in liquid nitrogen and stored at −80°C until further analysis.

DNA was extracted following a chloroform phenol-based extraction method, and 16S rRNA genes were amplified using the primers pair 515F and 806R as previously described (Dessì et al., 2019). The polymerase chain reaction (PCR) protocol included an initial denaturation at 95°C (3 min), followed by 25 cycles of denaturation at 90°C, annealing at 55°C, and extension at 72°C (30 s each). Library preparation and high-throughput sequencing were performed by FISABIO (Valencia, Spain, *fisabio.san.gva.es*) in an Illumina Miseq platform. The sequences generated were deposited in the NCBI Sequence Read Archive (SRA) with accession number PRJNA669689.

Amplicon Sequence Variants (ASVs) were constructed using Qiime2 workflow. In the final analysis, 3,103 clean ASVs were extracted for n = 12 samples on which different multivariate statistical analyses were performed using R software. The details of the bioinformatics steps, along with the procedures on the statistical analyses as well as software and R packages used, are provided in **Supplementary Material.**

SEM Analysis

Cathode electrode samples were stored in Petri dishes, fixed for 2 h using a solution of glutaraldehyde and paraformaldehyde (2% each) in 0.1 sodium cacodylate buffer pH 7.2. Dehydration was done by passing the samples for two times (15 min each) in an ethanol concentration gradient (30, 50, 70, 90, and 100%), and in hexamethyldisilazane (HMDS). After air drying overnight, the samples were mounted into aluminum stubs with double-sided carbon tabs. The samples were coated with gold using an Emitech K550 sputter coater. Imaging was done using a scanning electron microscope (SEM Hitachi S4700) at an acceleration voltage of 15 kV and 50 μA current.

Electrochemical Analyses

Chronoamperometric operation and cyclic voltammetries (CVs) were performed using a multi-channel potentiostat (VMP3, Biologic, France) in three-electrode set-up, where the cathode acted as the working electrode. All potential values were reported against the Ag/AgCl reference electrode. Current and cumulative charge values were extracted from the chronoamperometric data using the EC-Lab software. CVs were executed at the beginning and at the end of LB1, LB2, L1, and L2 experiments (without pH modification) between −1.2 and 0 V for four cycles at a scan rate of 1 mV/s. The results reported refer to the third replicate cycle. First derivative analysis of the CV curve was performed using a personalized code on R studio software (Dessì et al., 2021).

Process Monitoring

Temperature and pH were measured using a thermocouple thermometer (Digi-Sense Temp 10, Cole-Parmer, United Kingdom) and a pH probe (Slimtrode, Hamilton, Switzerland) connected to a controller (Cole Palmer 300, United Kingdom), respectively. Samples from catholyte and anolyte were analysed with a high-performance liquid chromatograph (HPLC) (1260 Infinity II, Agilent, United States) equipped with a Hi-Plex H column held at 60°C and a refractive index detector (RID), using 5 mM H_2SO_4 as the mobile phase

at a flow rate of 0.7 mL min^{-1}. Quantitative analyses were performed to detect carboxylic acids (lactic, acetic, propionic, butyric, valeric, and caproic) and alcohols (ethanol, propanol, and butanol). Only the acids or alcohols concentrations above the detection limit of the instrument were included in the results. Gas composition (H_2, CH_4, O_2, and CO_2) of the cathode headspace was determined using a gas chromatograph (7890B, Agilent, United States) equipped with a Porapak Q column and a thermal conductivity detector (TCD), with the injection port, oven and detector maintained at 250, 60, and 250°C, respectively.

Carbon/Electron Balance, Stoichiometric, and EF Performance Calculations

Carbon balances were calculated based on the total moles of carbon fed as lactate or butyrate at the beginning of each batch cycle, and the moles of carbon present as residual substrates or metabolic products (including carboxylic acids and CO_2) at the end of the experiment. Electron balances (EB) were calculated according to the following equation:

$$EB\,(\%) = \frac{\sum_{i=1}^{n} Q_i^{out}}{\sum_{j=1}^{m} Q_j^{in} + \int_{t0}^{tf} idt} \quad (1)$$

where Q_j^{in} and Q_i^{out} is the charge contained in the carboxylic acids and hydrogen before and after the EF process, respectively, and $\int_{t0}^{tf} idt$ is the charge delivered to the cathode during the experiment.

EF coefficients (η_{EF}) were calculated as follows (Moscoviz et al., 2016), taking into account only soluble fermentation products:

$$\eta_{EF} = \frac{\int_{t0}^{tf} idt}{\sum_{i=1}^{n} Q_i^{out}} \quad (2)$$

Theoretical propionate and acetate production was calculated assuming a metabolic pathway that includes lactate fermentation and acetogenesis from electrochemically-produced H_2 and CO_2, according to the following equations (Saady, 2013):

Lactate fermentation:

$$3C_3H_5O_3^- \rightarrow 2C_3H_5O_2^- + C_2H_3O_2^- + CO_2 + H_2O \quad (3)$$

Acetogenesis:

$$4H_2 + 2HCO_3^- + H^+ \rightarrow C_2H_3O_2^- + 4H_2O (4) \quad (4)$$

Production rates were calculated between two consecutive samples as the increment of carboxylic acid concentration divided by the time interval. Production yields were calculated on the whole batch cycle based on the carbon balances between products and substrate. Analysis of variance (ANOVA) was performed to assess significant differences among production rates and yields in the electrofermentation and fermentation experiments at pH 5 and 7. The output of the analysis is provided in **Supplementary Material.**

Specific energy consumption (E_C) was estimated according to equation (5):

$$E_C = \frac{I_{avg}\ Vt}{\sum_{i=1}^{n} m_i} (5) \quad (5)$$

where m_i represents the produced propionic, acetic or butyric acid (in kg) I_{avg} is the average current during the batch (excluding the start-up with an applied cathodic potential of −1.2 V), V is the cell potential (estimated as 3V from punctual measurements in the L3 cell), and t is the duration of the cycle (in hours). The electric power unit cost was estimated based on the average price for industries in Europe (EUROSTAT, 2020).

RESULTS AND DISCUSSION

Cathodic Electrofermentation of Lactate

Microbial Electrofermentation Cell Performance

Imposing a potential of −1.2 V resulted in a current output of about 10 mA in each of the LB1 and LB2 cells (**Figure 2**). However, the high current caused the pH to increase from an initial value of 5 to 8.6–8.8 in the duplicate cells, and the applied potential was therefore lowered to −1.0 V to avoid further alkalinization of the catholyte. After reducing the potential, the pH returned to 7.7 and 7.1 in LB1 and LB2, respectively, and the current stabilized at around 2.7 and 3.1 mA, compared with currents < 1 mA in the abiotic control (**Supplementary Figure S1**), suggesting the electrocatalytic activity of biofilm. Two days after reducing the potential, the lactate consumption rate was 8.1 and 4.9 mM d^{-1} in LB1 and LB2, respectively, resulting in propionate and acetate production at maximum rates of, respectively, 4.5 and 2.7 mM d^{-1} (0.33 and 0.16 g L^{-1} d^{-1}) in LB1, and 2.0 and 1.4 mM d^{-1} (0.15 and 0.08 g L^{-1} d^{-1}) in LB2 on the first batch cycle (**Table 1**). Such production rates, and yields, are comparable to those obtained in the non-electrochemical control experiment ($C_{LB}1$ and $C_{LB}2$) at an initial pH of 7, whereas significantly lower yields (below 0.1 mM d^{-1}) were obtained in the control incubations at an initial pH of 5 (**Supplementary Figure S2** and **Table 1**). In the three subsequent batch cycles, propionate was produced in both LB1 and LB2 at rates > 1.8 mM d^{-1}, despite the decreasing trend of pH, which approached an average value of 5 in the fourth cycle (**Figure 2**). Since the hydrogen concentration does not affect the propionate-producing lactate fermentation pathway (Seeliger et al., 2002), this suggests that the alkalinization effect of the cathode, rather than the potential applied, triggered lactate conversion into propionate in this study. Cathodic EF can, therefore, be applied to produce propionate from low-pH substrates, mitigating the inhibitory effect of undissociated acids (Van Ginkel and Logan, 2005), with no external addition of bases.

The current increased with subsequent successive cycles, and the highest average currents of 7.68 and 5.43 mA in LB1 and LB2, respectively, were achieved in the fourth batch cycle (**Table 1**). Since a similar average pH of 5.2–5.3 was obtained in the fourth batch cycle, the higher current in LB1 suggests a more effective development of the cathodic microbial community than in LB2.

TABLE 1 | Yields and production rates obtained in each batch experiment.

	Batch	Duration[a] (h)	Average current[a] (mA)	Yield (mol mol^{-1} lactate consumed)			Highest production rate (mM d^{-1})		
				Propionate	Acetate	Butyrate[b]	Propionate	Acetate	Butyrate[b]
LB1	I	158.4	2.19	0.39	0.32	–	4.49	2.67	–
	II	120.0	5.39	0.23	0.31	–	2.2	1.71	–
	III	148.8	6.5	0.28	0.36	–	2.76	2.25	–
	IV	139.2	7.68	0.18	0.23	–	1.87	1.00	–
LB2	I	158.4	2.42	0.17	0.18	–	1.98	1.39	–
	II	120.0	3.62	0.21	0.18	–	4.96	3.91	–
	III	148.8	4.51	0.16	0.35	–	2.12	2.81	–
	IV	139.2	5.43	0.19	0.10	–	3.13	1.27	–
L1	I	146.4	1.28	0.28	0.28	0.00	4.74	2.55	0
	II	244.8	2.03	0.30	0.39	0.02	7.2	5.13	0.14
L2	I	146.4	2.08	0.37	0.34	0.00	5.86	2.83	0
	II	244.8	5.44	0.28	0.30	0.02	6.16	4.44	0.12
L3	I	381.6	2.18	0.48	0.30	0.08	12.88	7.22	1.26
C_{LB}1_pH5	I	285.0	None	0.03	0.10	–	0.04	0.20	–
C_{LB}2_pH5	I	285.0	None	0.02	0.34	–	0.07	0.48	–
C_{LB}1_pH7	I	285.0	None	0.44	0.42	–	2.53	1.53	–
C_{LB}2_pH7	I	285.0	None	0.39	0.42	–	2.40	1.65	–
C_L1_pH5	I	285.0	None	0.25	0.28	0.19	1.67	2.07	0.80
C_L2_pH5	I	285.0	None	0.16	0.37	0.22	0.82	1.15	0.96
C_L1_pH7	I	285.0	None	0.36	0.37	0.00	2.78	1.47	0.09
C_L2_pH7	I	285.0	None	0.45	0.36	0.01	3.94	2.08	0.08

For EF experiments, the data reported include carboxylates detected in the catholyte and anolyte. C_{LB} and C_L refer to the non-electrochemical control experiments with lactate and butyrate, or only lactate, as substrate, respectively.

[a] *The start-up period at −1.2 V applied potential was excluded.*

[b] *Butyrate yield and production rate are not included for LB1, LB2, C_{LB}2, or C_{LB}2 because butyrate was added at the beginning of the experiment.*

Such currents were significantly higher than those obtained in the abiotic control (**Supplementary Figure S1**), further suggesting its biocatalytic origin. Propionate and acetate production *via* lactate fermentation occurred in all the batch cycles (**Figure 2**). In LB1, the highest propionate and acetate production rates were achieved in the first batch cycle, and in the subsequent three cycles propionate was produced at a lower maximum rate of 1.9–2.8 mM d^{-1} (0.14-0.21 g L^{-1} d^{-1}) up to a cumulative concentration of 20.8 mM, whereas acetate was produced at 1.0–2.3 mM d^{-1} (0.06–0.14 g L^{-1} d^{-1}) up to a cumulative concentration of 19.5 mM (**Figure 2** and **Table 1**). The declining trend of production rates observed in the final batch cycle may be attributed to end-product inhibition (Liang et al., 2012) or to biofilm degradation, although the first hypothesis appears more likely, since propionate fermentation is an energetically favorable reaction (Mockaitis et al., 2012) not requiring an electron-donating cathode. This may be mitigated by extracting VFAs before reaching concentrations inhibitive of the microbial community (Jones et al., 2017).

Although the lactate consumption rate was higher in LB2 than in LB1 (11.50 against 7.50 mM d^{-1}), similar propionate and acetate production rates were achieved in both. However, the final concentrations, as well as the yields, were even lower in LB2 than in LB1 (**Figure 2** and **Table 1**). This was possibly attributed to the higher O_2 intrusion from the anodic to the cathodic chamber in LB2, causing a share of carboxylates being consumed by aerobic metabolism. Indeed, at the end of each batch cycle an average of 0.6 mmol O_2 was found in LB2 headspace, against 0.1 in LB1 (**Supplementary Table S1**). Interestingly, in LB1 lactate was not completely consumed, but propionate production ceased when the lactate concentration declined below 6 mM. On the other hand, lactate was further consumed in LB2, likely by aerobic metabolism. In both cells, and particularly in LB1, the acetate concentration continued to increase after lactate concentration stabilized, suggesting that a share of acetate was produced through an alternative acetogenic pathway. Since no CO_2 was detected in the headspace, as would be expected according to Eq. 3, it was likely consumed for the growth of autotrophic organisms at the electrode, and converted into acetate together with (bio)electrochemically-produced H_2 (Eq. 4) (Nevin et al., 2010).

In the first three batch cycles of the first set of experiments, butyrate showed a linear depletion with a rate of 0.45 and 0.67 mM d^{-1} in LB1 and LB2, respectively, until the conclusion of the third batch cycle. The same trend was observed, with a rate of 0.35 mM d^{-1}, in the abiotic control (**Supplementary Figure S1**), suggesting butyrate migration to the anodic chamber through the membrane. A share of butyrate was likely consumed by aerobic metabolism, particularly in LB2 (**Figure 2**). Interestingly, from the beginning of the fourth batch cycle, the butyrate concentration in LB1 increased from 8.5 to 11.7 mM, suggesting the onset of the chain elongation

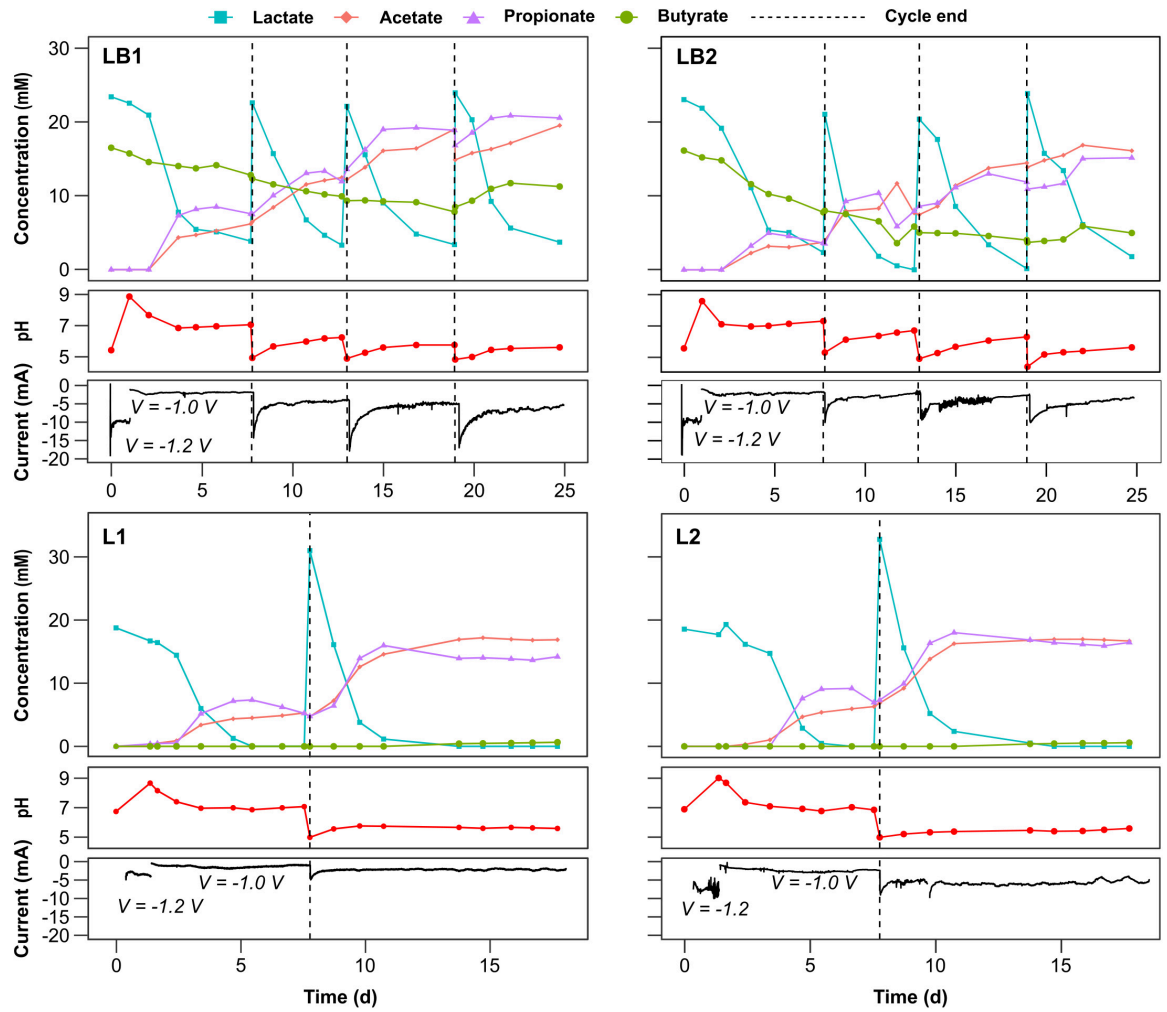

FIGURE 2 | Temporal profiles of carboxylates concentration at the cathode, pH and current profiles for the duplicate cells fed with lactate and butyrate (LB1 and LB2), or in the cells fed with only lactate (L1 and L2). Carboxylates concentration detected at the anode at the end of each batch cycle are reported in **Supplementary Table S2**.

pathway (Wu et al., 2020). The same phenomenon occurred in LB2, but was less evident, likely due to concomitant butyrate production and consumption by aerobic metabolism. Caproate production from lactate and butyrate, reported by previous fermentation studies at butyrate concentrations of 35–50 mM (Nzeteu et al., 2018; Contreras-Dávila et al., 2020), was not achieved in the present study, where the butyrate concentration was only 20 mM.

Effect of Substrate Concentration

In the first batch of the second set of experiments, when only lactate (20 mM) was provided as the carbon source, maximum propionate production rates of 4.7 and 5.9 mM d^{-1} (0.35 and 0.44 g L^{-1} d^{-1}), and acetate production rates of 2.6 and 2.8 mM d^{-1} (0.16 and 0.17 g L^{-1} d^{-1}), were achieved in L1 and L2, respectively (**Table 1**). Such production rates are similar, or slightly higher, than those obtained in LB1, confirming that butyrate was not involved in the fermentation process (**Figure 2**). Notably, increasing the lactate concentration to 30 mM in the second batch cycle positively impacted the fermentation process, resulting in faster lactate consumption (from 5.7 to 13.6 mM d^{-1} in L1, and from 6.0 to 13.7 in L2), and higher rates of both propionate (7.2 and 6.2 mM d^{-1}, or 0.53 and 0.46 g L^{-1} d^{-1}, in L1 and L2, respectively) and acetate production (5.1 and 4.4 mM d^{-1}, or 0.31 and 0.26 g L^{-1} d^{-1}, in L1 and L2, respectively). Butyrate was detected in both cells from day 13 onwards, reaching final concentrations of 0.65 and 0.58 mM in L1 and L2, respectively, suggesting the onset of elongation pathways, as had occurred in the LB1 and LB2 cells. In the non-electrochemical controls, the maximum propionate production rate was 3.9 mM d^{-1} (0.29 g L^{-1} d^{-1}) in C_{L2} at an initial pH of 7 (**Table 1**). However, in the control incubations at pH 5, butyrate was initially produced by lactate fermentation, with the onset of propionate production only 2 days later, when pH rose above 5.5 (**Supplementary Figure S2**). On average, the propionate

TABLE 2 | Carbon and charge balances of the cathodic electrofermentation experiments, considering carboxylates detected in both the cathodic and anodic chamber, and gas products in the cathode headspace.

	Inlet (mmol)					Outlet (mmol)										Balance (%)		η_{EF}
	Lactate		Butyrate		Current	Lactate		Acetate		Propionate		Butyrate		H_2	CO_2			
	C	e^-	C	e^-	e^-	C	e^-	C	e^-	C	e^-	C	e^-	e^-	C	C	e^-	
LB1	36.6	146.5	9.9	49.5	123.8	2.5	9.9	7.9	31.6	12.8	59.6	9.0	45.0	71.0	0.7	70.6	67.9	1.36
LB2	38.6	154.3	9.7	48.4	94.1	2.5	9.9	8.8	35.2	11.5	53.4	5.5	27.7	0.0	0.2	58.9	42.5	1.06
L1	22.3	89.4	0.0	0.0	34.7	0.0	0.0	5.5	22.0	6.8	31.5	0.4	2.0	n.d.[a]	n.d.	56.6	44.7	0.63
L2	23.0	92.2	0.0	0.0	83.9	0.0	0.0	5.6	22.2	8.0	37.1	0.3	1.7	n.d.	n.d.	60.1	34.7	1.38
L3	66.9	267.5	0.0	0.0	36.9	7.6	30.3	12.4	49.7	29.1	135.8	7.3	36.4	n.a.[b]	n.a.	84.3	82.8	0.17
$C_{LB}1$_pH5	9.0	36.0	11.4	57.0	0.0	6.4	25.8	0.2	0.7	0.1	0.3	10.2	51.0	n.d.	n.d.	82.9	83.7	n.a.[b]
$C_{LB}2$_pH5	8.8	35.2	11.0	54.9	0.0	2.9	11.6	1.3	5.4	0.1	0.5	10.7	53.3	n.d.	n.d.	76.0	78.7	n.a.[b]
$C_{LB}1$_pH7	9.0	36.0	12.0	59.8	0.0	0.1	0.2	2.5	10.0	3.9	18.2	11.1	55.4	n.d.	n.d.	83.7	87.5	n.a.[b]
$C_{LB}2$_pH7	9.2	36.7	12.0	59.8	0.0	0.1	0.3	2.5	10.1	3.5	16.5	9.5	47.3	n.d.	n.d.	73.9	77.0	n.a.[b]
C_L1_pH5	9.0	36.0	0.0	0.0	0.0	1.0	3.9	1.5	6.0	2.0	9.4	2.0	10.0	n.d.	n.d.	72.4	81.7	n.a.[b]
C_L2_pH5	8.9	35.5	0.0	0.0	0.0	0.1	0.3	2.2	8.7	1.4	6.6	2.6	13.0	n.d.	n.d.	70.7	80.7	n.a.[b]
C_L1_pH7	8.5	34.2	0.0	0.0	0.0	0.0	0.2	2.1	8.4	3.0	14.2	0.0	0.0	n.d.	n.d.	60.5	66.5	n.a.[b]
C_L2_pH7	9.2	36.9	0.0	0.0	0.0	0.1	0.2	2.2	8.7	4.1	19.3	0.1	0.5	n.d.	n.d.	70.2	77.9	n.a.[b]

Electrofermentation coefficients (η_{EF}) were calculated according to Moscoviz et al. (2016). The lower η_{EF}, the lower is the contribution of microbial electrosynthesis to the electrofermentation process.
[a]*Not detected.*
[b]*Not available.*

production rates in the control incubations at initial pH 5 were significantly lower than those obtained in the EF cells, even after the pH raised above 5.5, whereas no significant differences were obtained between EF cell and control incubations at initial pH 7 (**Supplementary Material 4**). This confirms that cathodic EF can be applied to trigger propionate production at pH values that are typically more favorable for butyric acid production in dark fermentation.

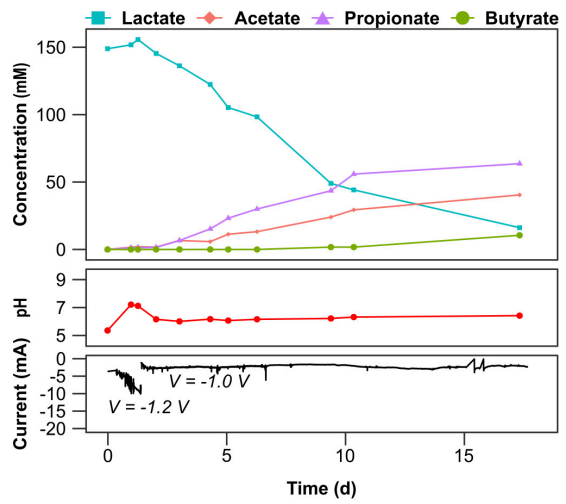

FIGURE 3 | Temporal profiles of carboxylates concentration at the cathode, pH and current profiles for cell L3 fed with 150 mM lactate. Carboxylates concentration detected at the anode at the end of each batch cycle are reported in **Supplementary Table S2**.

Since increasing lactate concentrations positively affected propionate and acetate production, a third cathodic EF cell (L3) was fed with 150 mM lactate, which is a concentration obtained in mixed-culture fermentation of carbohydrate-rich substrates, including cheese whey (Tang et al., 2016; Luongo et al., 2019; Pagliano et al., 2019; Dessì et al., 2020). After 2 days start-up, lactate was converted to propionate and acetate, confirming the reproducibility of the process under different lactate loading. On days 2–9, lactate was consumed at an average rate of 12.9 mM d^{-1}, similar to the rate achieved in L1 and L2 when feeding 30 mM lactate. An average current of 2.2 mA was detected at an applied potential of −1V, which was lower than in the previous experiements and suggested only a minor role for the electrogenic community, possibly inhibited by the high carboxylate concentrations. The high lactate concentration (150 mM) may have inhibited the acetogenic community in L3 although, to the best of our knowledge, no direct studies on the inhibitory effects of lactate on acetogenic communities are available. This is also confirmed by the lower electrofermentation coefficient (η_{EF}) obtained in L3 compared with all experiments with a lower lactate concentration (**Table 2**).

Propionate and acetate were produced in L3 at an average rate of 5.7 and 2.8 mM d^{-1} (0.42 and 0.17 g L^{-1} d^{-1}), with peaks of 12.9 and 7.2 mM d^{-1} (0.96 and 0.43 g L^{-1} d^{-1}), respectively. Butyrate was also produced from day 9 onward, at an average rate of 1.1 mM d^{1} (0.10 g L^{-1} d^{-1}). However, lactate consumption (4 mM d^{-1}), and propionate and acetate production (1.6 and 1.1 mM d^{-1}, respectively), was slower from day 10 (**Figure 3**), as a response to VFA accumulation. Notably, a propionate yield of 0.48 mol mol^{-1} lactate consumed was achieved in L3, substantially higher than the yield achieved at lower lactate

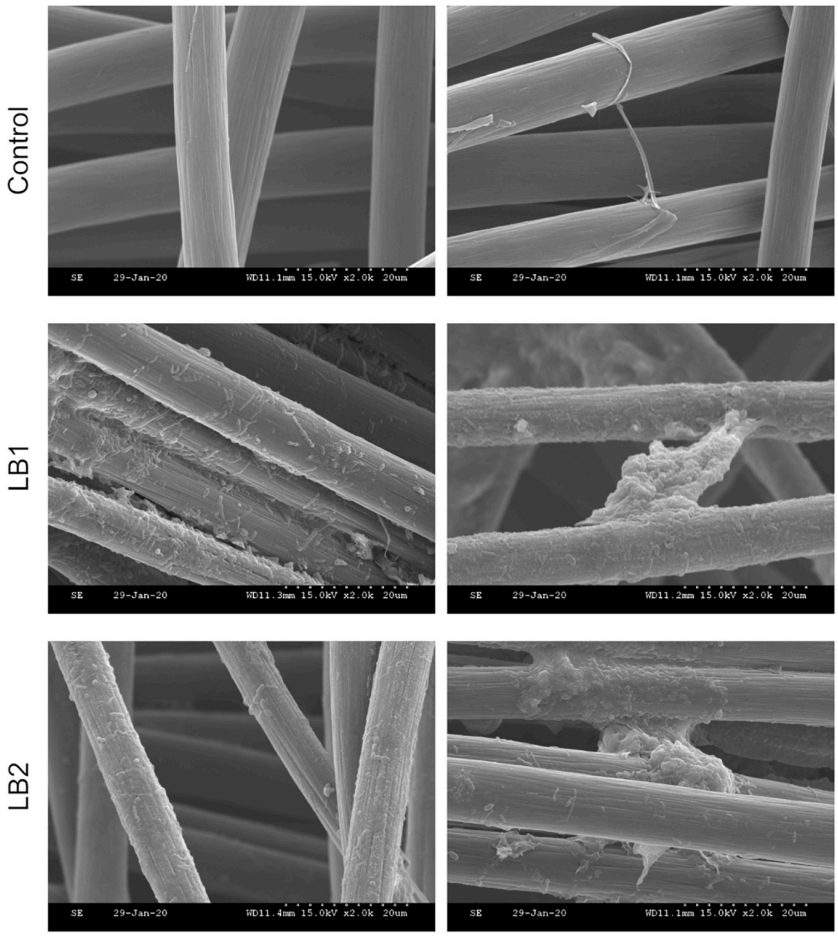

FIGURE 4 | SEM micrographs of the cathodic biofilm from LB1 and LB2 reactors, and in the abiotic control. The magnification is 2,000x.

concentrations (**Table 1**). The energy invested for the EF process was < 1 kWh kg^{-1} $VFA_{produced}$ that, considering the EU-27 average industry price for electricity of 0.1173 € kWh^{-1}, further highlights its potential for industrial applications.

Carbon and Electron Balances

Carbon and electron balances (**Table 2**) showed that, when both lactate and butyrate were supplied as substrates, about 70.6% of the carbon and 67.9% of the electrons supplied both as chemicals or electric current were recovered as soluble products or residual lactate in LB1. The remaining carbon was used for microbial growth or diffused outside the cell as CO_2 from the anodic chamber. Carboxylic acid migrating to the anodic chamber could indeed have been electrochemically oxidized due to the positive potential (around 2 V) at the anode. When Pt-containing electrodes are used, such high potential can result in the formation of PtO_X, which has a high reactivity toward organics (Comninellis and Pulgarin, 1991). A share of electrons was also likely consumed for aerobic metabolism as suggested by the electron balance since only 42.5% of the potential charge was recovered in LB2 compared to 70.6% in LB1. Slightly higher carbon and electron recoveries were achieved in the control incubations (**Table 2**), supporting the conclusion that gas diffusion and oxygen intrusion may have affected the carbon balances of the electrochemical cells. When only lactate was supplied as substrate, 56.6–60.1% of the carbon, and 34.7–44.7% of the electrons, were recovered as products. However, when the lactate concentration was increased to 150 mM, as high as 84.3% of the carbon, and 82.8% of electrons, consumed as lactate were recovered as EF products (acetate, propionate or butyrate) suggesting that, once the microbial community developed, most carbon and electrons were directed toward products, rather than biomass generation. The carbon recovery achieved in L3 is remarkable, being higher than the carbon recoveries of 60–70% typically achieved in traditional dark fermentation (Asunis et al., 2019).

In all EF experiments, regardless of the initial lactate concentration, a total of 7.9–13.7 mmol of carbon were missing in the balance (taking into account carbon removed as samples), likely linked to microbial growth. An exception is LB2, in which the unaccounted carbon was higher (21.8 mmol), likely due to aerobic metabolism. Accumulation of polyhydroxyalkanoates should also be taken into account as a possible explanation for carbon loss, since it was

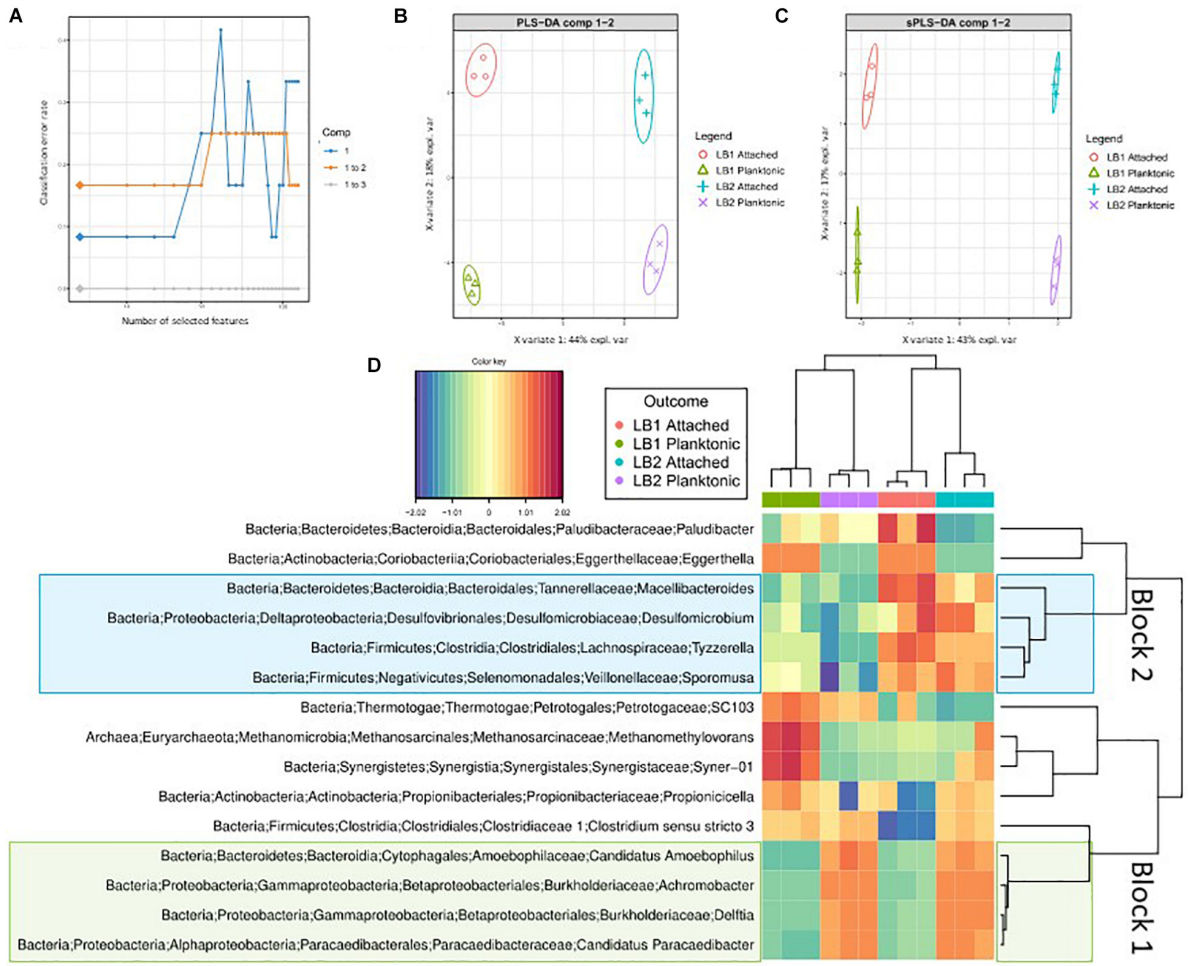

FIGURE 5 | (A) sPLS discriminant analysis of amplicon sequencing data. Classification error rates over the components and the numbers of optimal features (genera) in each component, included in the model, chosen for the lowest error rates and represented by diamonds. **(B)** ordination of samples using all the genera in the first two components (sPLS-DA) where ellipses represent 95% confidence intervals and percentage variations explained by these components are denoted in the axes labels. **(C)** Ordination of discriminant taxa from the two components (sPLS-DA). **(D)** Heatmap showing discriminant genera. Rows and columns are ordered using hierarchical (average linkage) clustering. Heatmap depicts TSS + CLR normalized abundances: higher abundances are red and lower abundances are blue.

already reported in microaerophilic biocathodes (Srikanth et al., 2012). This highlights the fact that, over long-term operation and high substrate concentrations, cathodic EF can result in higher carbon recovery as soluble products than dark fermentation, although oxygen intrusion must be strictly prevented.

Microbial and Metabolic Dynamics

SEM imaging confirmed the microbial attachment on the cathode of both LB1 and LB2 cells (**Figure 4**). Single cells attached to the electrodes were detected, as well as more complicated structures developed on the carbon fibers. Interestingly, bacterial structures connecting different carbon fibers were also detected (**Figure 4**). Alpha diversity analysis (**Supplementary Figure S3**) revealed that evenness, richness and diversity of the cathode-attached microbial community in LB1 were significantly higher than in the equivalent LB2 community. This suggests that a more diverse, and possibly more resilient, cathodic microbiome developed in LB1, likely promoted by the lower oxygen contamination. In LB1, furthermore, the richness and diversity of the planktonic community were substantially higher than in LB2, suggesting the development of a more diverse fermentative community that resulted in a higher propionate production (**Figure 2**). Furthermore, principal component analysis (**Supplementary Figure S3**), using the weighted UniFrac distance metric, along with PERMANOVA, confirmed significant differences in the microbial communities based on cell ($p = 0.001$ ***) and community type ($p = 0.001$ ***) (**Supplementary Figure S3**).

Sparse Projection to Latent Structure discriminant analysis (sPLS-DA) identified 15 discriminant genera, which accounted for variation between groups. As can be seen in the comparison between attached and planktonic communities in LB1 and LB2, the growth of aerobic species such as *Achromobacter* sp.

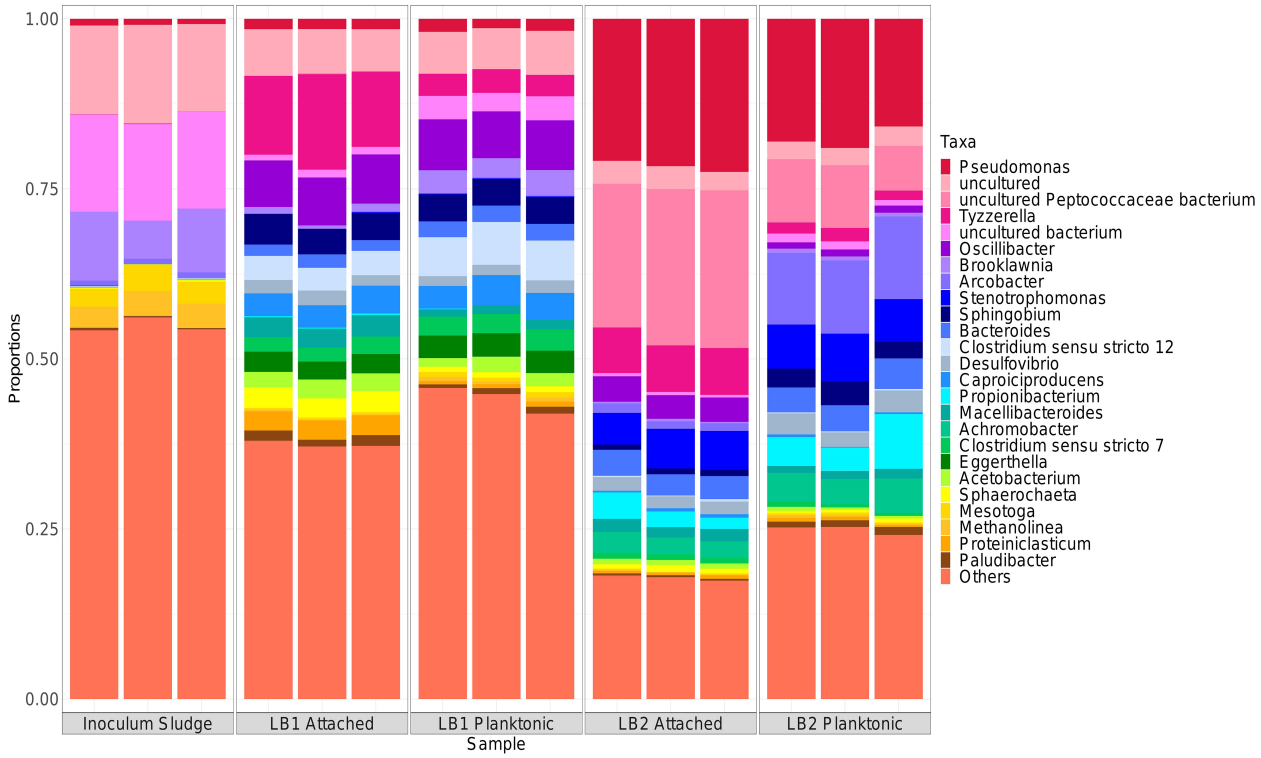

FIGURE 6 | Taxa bars depicting the composition of the cathode-attached and planktonic communities at the conclusion of the experiment with the duplicate cells fed with lactate and butyrate. "Others" represent the sum of the relative abundance of microorganisms outside the top-25.

(Busse and Auling, 2015) and *Delftia* sp. (Sly et al., 2015) in LB2 was the main discriminant between the two cells (**Figure 5**, Block 1), confirming the impact of oxygen in shaping the community structure. sPLS-DA also identified several genera accounting for most of the differences in microbial community between the attached and planktonic biomass of both cells (**Figure 5**, Block 2), including *Paludibacter*, *Eggerthella*, *Macellibacteroides*, *Desulfomicrobium*, *Tyzzerella,* and *Sporomusa*. This difference in community structure between the attached and planktonic communities may have been driven by pH changes caused by the buffering capacity of the cathode electrode. Interestingly, within Block 2 *Paludibacter* and *Eggerthella* were more dominant in the attached community of LB1 than LB2. The relatively higher abundance of *Paludibacter,* which are anaerobic propionate-producing organisms (Ueki et al., 2006), in LB1 was likely due to oxygen intrusion to LB2.

A higher relative abundance of microorganisms belonging to the order *Clostridiales* was found in both LB1 and LB2, with respect to the inoculum, whereas *Gammaproteobacteria* developed only in LB2 (**Supplementary Figure S4**). *Gammaproteobacteria* includes several aerobic microorganisms, such as *Pseudomonas* and *Stenotrophomonas* (Palleroni, 2015), which were more relatively abundant in LB2 (**Figure 6**) and linked to the lower LB2 carboxylate yield compared to LB1. The microbial community in LB1 was indeed composed of anaerobes or facultative anaerobes such as *Clostridium* and *Oscillibacter* (Iino et al., 2007; **Figure 6**), including taxa involved in propionate production, hydrogen evolution, acetogenesis and chain elongation. Based on the chemical, electrochemical and microbiological data, the likely metabolic pathways occurring in the cathodic electrofermentation cells were hypothesized (**Figure 7**). Hydrogen evolution at the cathode electrode was likely catalyzed by *Desulfovibrio*, previously identified as part of the core microbiome in electrosynthesis communities and thought to carry out this function (Marshall et al., 2017).

In MES cells, *Desulfovibrio* are typically found in association with autotrophic acetogenic microorganisms such as *Acetobacterium* and *Clostridium* (Marshall et al., 2017; Mateos et al., 2020), where they syntrophically produce acetate from H_2 and CO_2 through the Wood-Ljungdahl pathway. Both *Acetobacterium* and *Clostridium* were indeed among the 25 most abundant microorganisms of the LB1 and LB2 communities (**Figure 6**). The higher relative abundance of both *Clostridium* and *Acetobacterium* in LB1 than in LB2, linked to the lower oxygen concentration, suggests higher acetogenic activity in LB1, which could be linked to the higher current output (**Figure 2**). Since no CO_2 was supplied to the cells, acetogenic microorganisms were likely growing syntrophically with fermentative microorganisms producing CO_2, along with propionate and acetate, from lactate (**Figure 7**). Interestingly, although a similar lactate fermentation pathway occurred in both cells, the propionate-producing community in LB1 and LB2 was different. *Tyzzerella* sp. were more abundant in LB1 and potentially responsible for most of the propionate production.

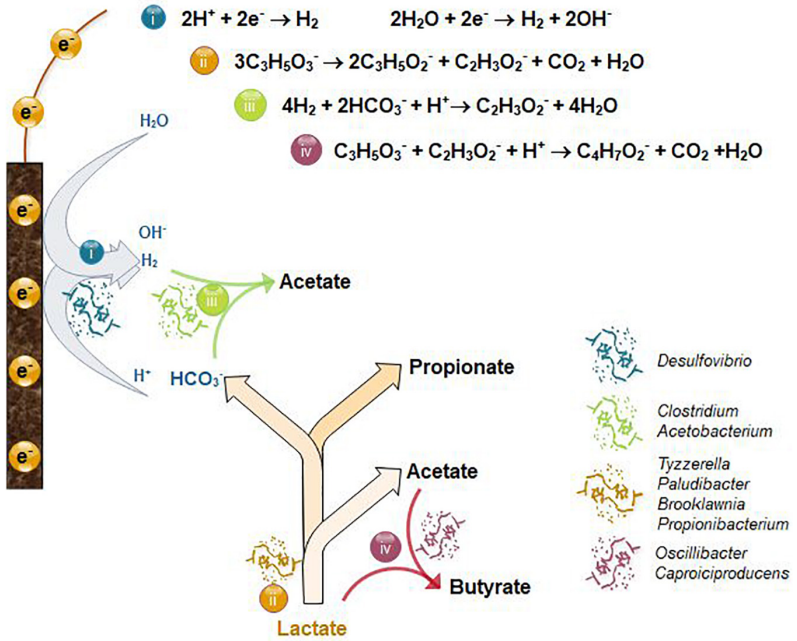

FIGURE 7 | Suggested metabolic pathway for the cathodic electrofermentation of lactate at an applied potential of –1V vs. Ag/AgCl, and the microorganisms involved. The pathway proposed includes (i) (bio)electrochemical hydrogen production, (ii) lactate fermentation, (iii) homoacetogenesis, and (iv) butyrate production by chain elongation.

The *Tyzzerella* genus includes propionate-producing species, such as *T. propionica* (formerly *Clostridium propionicum;* Yutin and Galperin, 2013), and was previously found to be highly abundant in a fermentative reactor converting lactate to propionate and acetate (Xu et al., 2020). Other propionate producers found in LB1 included the facultatively anaerobic *Brooklawnia* (Bae et al., 2006) and *Paludibacter* (discriminant organisms as determined using sPLS-DA). *Propionibacterium* were found in higher relative abundance in LB2 than LB1 in both the cathode-attached and planktonic community. This suggests its role in propionate production in LB2 was facilitated by its optimal growth under microaerophilic conditions. However, in the presence of oxygen, *Propionibacterium* can further oxidize carboxylates to CO_2 (Koussémon et al., 2001), which could explain the lower propionate and acetate concentrations in LB2 than observed in LB1 (**Figure 2**).

In all experiments, butyrate was produced when the acetate concentration exceeded 15–20 mM. Butyrate can be produced: (i) electrochemically from CO_2, H^+ and electrons from the cathode, (ii) *via* the Acetyl-CoA reductive pathway with H_2 as electron donor, and (iii) from acetate and lactate, or ethanol, *via* reverse β oxidation (Raes et al., 2017). The last scenario appears most probable in this study, since butyrate production generally occurs concurrently with lactate consumption (**Figure 2**). In both LB1 and LB2, *Oscillibacter* and *Caproiciproducens* were identified as the butyrate-producing organisms, and their higher abundance in LB1 than LB2 (around 7 and 4%, respectively) (**Figure 6**) correlated with higher butyrate production in LB1 (**Figure 2**). Both *Oscillibacter* (Wu et al., 2020) and *Caproiciproducens* (Contreras-Dávila et al., 2020) were previously associated with chain elongation pathways, indicating that,

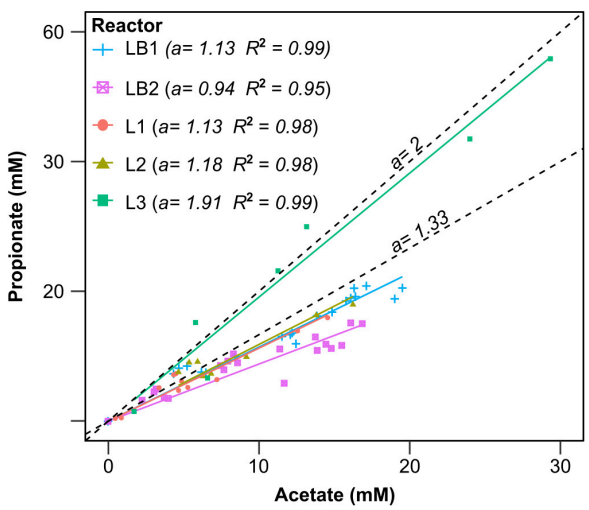

FIGURE 8 | Linear correlation between propionate and acetate concentrations detected in the catholyte of the cells fed with lactate and butyrate (LB1 and LB2), or only lactate (L1, L2, and L3). The data refer to lactate fermentation and acetogenesis only; data collected after the onset of chain elongation pathways, in which butyrate was produced from lactate and acetate, were excluded for simplicity.

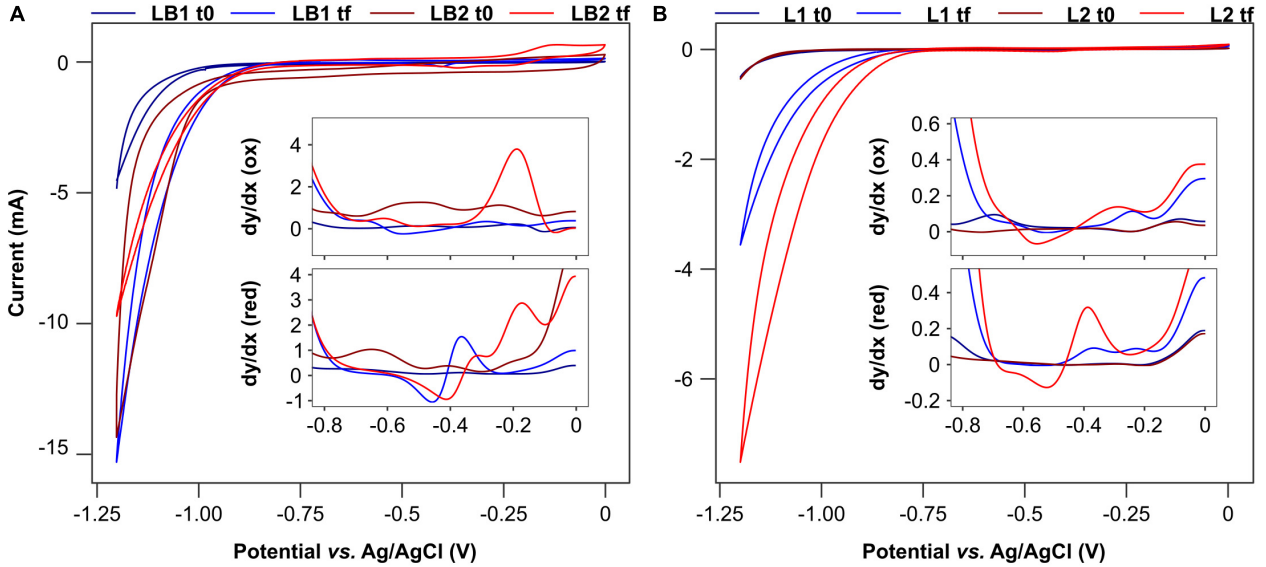

FIGURE 9 | Cyclic voltammetry and first derivative analysis of the cells fed with both lactate and butyrate **(A)**, or only lactate **(B)**.

in this study, lactate was the electron donor for butyrate production (**Figure 7**).

According to **Figure 7**, propionate and acetate are produced from lactate in a molar ratio of 2:1, and an additional mole of acetate is produced from two moles of CO_2. Thus, when the two reactions occur simultaneously, 0.67 mol propionate and 0.50 mol acetate will be produced from 1 mol lactate, with a propionate:acetate ratio of 1.33. When comparing the experimental results with the theoretical estimations, similar propionate:acetate ratios of 1.13–1.18 were achieved in LB1, L1, and L2 (**Figure 8**), within a 15% range of the theoretical yield. This confirms that lactate fermentation and acetogenesis occurred simultaneously, and the slightly lower ratio than theoretically predicted can be explained by propionate consumption *via* microaerobic metabolism (Thierry et al., 2011), or acetogenesis. Indeed, a substantially lower propionate:acetate ratio of 0.94 was achieved in the LB2 cell, where more oxygen intrusion occurred (**Supplementary Table S1**).

Feeding the cell with 150 mM lactate resulted in the highest propionate:acetate ratio of 1.91 (**Figure 7**). Such a ratio is only 5% lower than the ratio theoretically achieved by lactate fermentation to propionate and acetate, suggesting a minor role of acetogenesis. It is indeed plausible that acetogenic microorganisms were inhibited by the high carboxylate concentrations. Despite this, cathodic EF of lactate resulted in propionate and acetate production with remarkable average rates of 5.6 and 4.6 mM d^{-1}, respectively.

Electrochemical Characterization

Cyclic voltammetries (CVs) show a difference of about 0.2–0.3 V between the hydrogen reduction potential at the beginning and at the conclusion of the experiment in LB1, L1 and L2 (**Figure 9**), which suggests the development of an electroactive biofilm (Labelle et al., 2014). This was less evident in LB2, in which the overpotential was reduced by only 0.1 V. Since a similar final pH of 5.6 was measured in LB1 and LB2 at the end of the experiment (when CVs were performed), this confirms the presence of a weaker electroactive community in LB2, explained by the presence of oxygen, as confirmed by the lower current output in LB2 than in LB1 (**Figure 2**).

First derivative analysis confirmed the presence of oxidation and reduction peaks at the conclusion of the experiment, whereas flat curves, or small peaks, were detected at the beginning (**Figure 9**). In LB1, a reversible redox couple was evident, with a reduction peak at −0.24 and the corresponding oxidation peak at −0.29 V, suggesting the presence of reversible redox active molecules at the biofilm-reactor interface (Modestra and Mohan, 2017). A second reduction peak was detected in both LB1 and LB2 at potentials of −0.46 and −0.41 V, respectively. Such a potential is compatible, for example, with cytochromes used by electrogenic bacteria such as *Desulfovibrio* sp. for exchanging electrons with solid electrodes (Yahata et al., 2006). Similar reduction peaks were also detected in L1 and L2, although at lower potential (−0.54 and −0.52 V, respectively), which was attributed to the different biofilm stage than in LB1 and LB2 when the CV analysis was performed (after 2 and 4 batch cycles for L and LB, respectively).

CONCLUSION

In this study, electrofermentation is proposed for the valorization of lactate-rich fermentates. An applied potential of −1.0 V vs. Ag/AgCl favored propionate production with a maximum yield of 0.48 mol mol^{-1} lactate consumed obtained with an initial

lactate concentration of 150 mM. Furthermore, as confirmed by stoichiometric calculations and microbial community analysis, CO_2 produced from lactate fermentation was recycled into acetate *via* microbial electrosynthesis, resulting in higher carbon recovery than in dark fermentation, although this process may be inhibited at high lactate concentrations. At an initial lactate concentration of 150 mM, the energy invested for the EF process was < 1 kWh kg^{-1} VFA produced highlighting its potential for application in industry. Further studies on real fermentates, and under continuous operation, will be required to confirm the results obtained here under batch conditions with synthetic feedstocks.

DATA AVAILABILITY STATEMENT

The datasets presented in this study can be found in online repositories. The names of the repository/repositories and accession number(s) can be found below: NCBI BioProject, accession no: PRJNA669689.

AUTHOR CONTRIBUTIONS

MI and PD conceptualized and designed the experiments, and drafted the manuscript. CS and MI realized the script for CV analysis and assisted in its interpretation. SM and UI performed the bioinformatics work and assisted in interpreting the microbiological results. DS, FA, GDG, MM, and AM assisted in results interpretation and revised the manuscript. GC and PL thoroughly revised the final version for submission. All authors contributed to the article and approved the submitted version.

FUNDING

This work was funded by the Science Foundation of Ireland (SFI) Research Professorship Programme on Innovative Energy Technologies for Bioenergy, Biofuels and a Sustainable Irish Bioeconomy (IETSBIO^3, award 15/RP/2763) and the Research Infrastructure research grant *Platform for Biofuel Analysis* (Grant Number 16/RI/3401). GC and SM were supported by a European Research Council Starting Grant (3C-BIOTECH 261330). GC was supported by an SFI Career Development Award (17/CDA/4658).

ACKNOWLEDGMENTS

We acknowledge the facilities, and scientific and technical assistance, of the Centre for Microscopy and Imaging at the National University of Ireland Galway (www.imaging.nuigalway.ie). MI and FA gratefully acknowledge the Sardinian Regional Government for financial support of their Ph.D. scholarship (P.O.R. Sardegna F.S.E.–Operational Programme of the Autonomous Region of Sardinia, European Social Fund 2014–2020–Axis III Education and Training, Thematic goal 10, Investment Priority 10ii, Specific goal 10.5). We thank Claribel Buenaño (NUIG) for drawing **Figure 7**.

SUPPLEMENTARY MATERIAL

The Supplementary Material for this article can be found online at: https://www.frontiersin.org/articles/10.3389/fmicb.2020.599438/full#supplementary-material

REFERENCES

Ahmadi, N., Khosravi-Darani, K., and Mortazavian, A. M. (2017). An overview of biotechnological production of propionic acid: from upstream to downstream processes. *Electron. J. Biotechnol.* 28, 67–75. doi: 10.1016/j.ejbt.2017.04.004

Akedo, M., Cooney, C. L., and Sinskey, A. J. (1983). Direct demonstration of lactate-acrylate interconversion in clostridium propionicum. *Bio/Technology* 1, 791–794. doi: 10.1038/nbt1183-791

Alibardi, L., Astrup, T. F., Asunis, F., Clarke, W. P., De Gioannis, G., Dessì, P., et al. (2020). Organic waste biorefineries: looking towards implementation. *Waste Manag.* 114, 274–286. doi: 10.1016/j.wasman.2020.07.010

Allied Market Research (2020). *Propionic Acid Market by Application (Herbicides, Rubber Products, Plasticizers, Food Preservative and Others) and End-User Industry (Pharmaceuticals, Personal Care, Food & Beverage, Agriculture, and Others): Global Opportunity Analysis and Industry Forecast, 2019–2026*. Available online at: https://www.alliedmarketresearch.com/propionic-acid-market

Asunis, F., De Gioannis, G., Dessì, P., Isipato, M., Lens, N. L. P., Muntoni, A., et al. (2020). The dairy biorefinery: integrating treatment processes for cheese whey valorisation. *J. Environ. Manag.* 276:111240. doi: 10.1016/j.jenvman.2020.111240

Asunis, F., De Gioannis, G., Isipato, M., Muntoni, A., Polettini, A., Pomi, R., et al. (2019). Control of fermentation duration and pH to orient biochemicals and biofuels production from cheese whey. *Bioresource Technol.* 289, 121722. doi: 10.1016/j.biortech.2019.121722

Atasoy, M., Eyice, O., Schnürer, A., and Cetecioglu, Z. (2019). Volatile fatty acids production via mixed culture fermentation: revealing the link between pH, inoculum type and bacterial composition. *Bioresource Technol.* 292:121889. doi: 10.1016/j.biortech.2019.121889

Bae, H. S., Moe, W. M., Yan, J., Tiago, I., da Costa, M. S., and Rainey, F. A. (2006). Brooklawnia cerclae gen. nov., sp. nov., a propionate-forming bacterium isolated from chlorosolvent-contaminated groundwater. *Int. J. Systematic Evol. Microbiol.* 56, 1977–1983. doi: 10.1099/ijs.0.64317-0

Busse, H.-J., and Auling, G. (2015). "Achromobacter," in *Bergey's Manual of Systematics of Archaea and Bacteria*. eds W. Whitman, M. Goodfellow, P. Kämpfer, H.-J. Busse, M. Trujillo, W. Ludwig (Atlanta, GA: American Cancer Society).

Comninellis, C., and Pulgarin, C. (1991). Anodic oxidation of phenol for waste water treatment. *J. Appl. Electrochem.* 21, 703–708. doi: 10.1007/BF01034049

Contreras-Dávila, C. A., Carrión, V. J., Vonk, V. R., Buisman, C. N. J., and Strik, D. P. B. T. B. (2020). Consecutive lactate formation and chain elongation to reduce exogenous chemicals input in repeated-batch food waste fermentation. *Water Res.* 169:115215. doi: 10.1016/j.watres.2019.115215

Dessì, P., Asunis, F., Ravishankar, H., Cocco, F. G., De Gioannis, G., Muntoni, A., et al. (2020). Fermentative hydrogen production from cheese whey with in-line, concentration gradient-driven butyric acid extraction. *Int. J. Hydrogen Energy* 45, 24453–24466. doi: 10.1016/j.ijhydene.2020.06.081

Dessì, P., Chatterjee, P., Mills, S., Kokko, M., Lakaniemi, A.-M., Collins, G., et al. (2019). Power production and microbial community composition in thermophilic acetate-fed up-flow and flow-through microbial fuel cells. *Bioresource Technol.* 294:122115. doi: 10.1016/j.biortech.2019.122115

Dessì, P., Sánchez, C., Mills, S., Cocco, F. G., Isipato, M., Ijaz, U. Z., et al. (2021). Carboxylic acids production and electrosynthetic microbial community evolution under different CO2 feeding regimens. *Bioelectrochemistry* 137:107686. doi: 10.1016/j.bioelechem.2020.107686

Dionisi, D., and Silva, I. M. O. (2016). Production of ethanol, organic acids and hydrogen: an opportunity for mixed culture biotechnology? *Rev. Environ. Sci. Bio/Technology* 15, 213–242. doi: 10.1007/s11157-016-9393-y

Engel, M., Holtmann, D., Ulber, R., and Tippkötter, N. (2019). Increased biobutanol production by mediator-less electro-fermentation. *Biotechnol. J.* 14:e1800514. doi: 10.1002/biot.201800514

EUROSTAT (2020). *Electricity Price Statistics*. Available online at: https://ec.europa.eu/eurostat. (Accessed 23 October, 2020).

Grand View Research (2015). *Propionic acid market size, share & trends analysis report by application (animal feed & grain preservatives, food preservatives, herbicides, chemicals & pharmaceuticals), and segment forecasts, 2014 – 2025, Industry Report*. Manikchand Galleria: Grand View Research. Report ID: 978-1-68038-294-5.

Grand View Research (2020). *Acetic acid market size, share & trends analysis report by application (vinyl acetate monomer, purified terephthalic acid, acetate esters, ethanol), by region, and segment forecasts, 2020 – 2027, Industry Report*. Manikchand Galleria: Grand View Research. Report ID: 978-1-68038-077-4.

Grim, R. G., Huang, Z., Guarnieri, M. T., Ferrell, J. R. III, Tao, L., and Schaidle, J. A. (2020). Transforming the carbon economy: challenges and opportunities in the convergence of low-cost electricity and reductive CO2 utilization. *Energy Environ. Sci.* 13, 472–494. doi: 10.1039/c9ee02410g

Harnisch, F., and Freguia, S. (2012). A basic tutorial on cyclic voltammetry for the investigation of electroactive microbial biofilms. *Chem. Asian J.* 7, 466–475. doi: 10.1002/ASIA.201100740

Iino, T., Mori, K., Tanaka, K., Suzuki, K., and Harayama, S. (2007). Oscillibacter valericigenes gen. nov., sp. nov., a valerate-producing anaerobic bacterium isolated from the alimentary canal of a Japanese corbicula clam. *Int. J. Systematic Evol. Microbiol.* 57, 1840–1845. doi: 10.1099/ijs.0.64717-0

International Energy and Agency (2018). *The Future of Petrochemicals. Towards more Sustainable Plastics and Fertilisers*. paris: International Energy Agency.

Jones, R. J., Massanet-Nicolau, J., Mulder, M. J. J., Premier, G., Dinsdale, R., and Guwy, A. (2017). Increased biohydrogen yields, volatile fatty acid production and substrate utilisation rates via the electrodialysis of a continually fed sucrose fermenter. *Bioresource Technol.* 229, 46–52. doi: 10.1016/j.biortech.2017.01.015

Kim, C., Kim, M. Y., Michie, I., Jeon, B. H., Premier, G. C., Park, S., et al. (2017). Anodic electro-fermentation of 3-hydroxypropionic acid from glycerol by recombinant *Klebsiella pneumoniae* L17 in a bioelectrochemical system. *Biotechnol. Biofuels* 10:199. doi: 10.1186/s13068-017-0886-x

Koussémon, M., Combet-Blanc, Y., Patel, B. K. C., Cayol, J. L., Thomas, P., Garcia, J. L., et al. (2001). Propionibacterium microaerophilum sp. nov., a microaerophilic bacterium isolated from olive mill wastewater. *Int. J. Systematic Evol. Microbiol.* 51, 1373–1382. doi: 10.1099/00207713-51-4-1373

Labelle, E. V., Marshall, C. W., Gilbert, J. A., and May, H. D. (2014). Influence of acidic pH on hydrogen and acetate production by an electrosynthetic microbiome. *PLoS One* 9:e109935. doi: 10.1371/journal.pone.0109935

Larsson, M., Markbo, O., and Jannasch, P. (2016). Melt processability and thermomechanical properties of blends based on polyhydroxyalkanoates and poly(butylene adipate-co-terephthalate). *RSC Adv.* 6, 44354–44363. doi: 10.1039/c6ra06282b

Lee, W. S., Chua, A. S. M., Yeoh, H. K., and Ngoh, G. C. (2014). A review of the production and applications of waste-derived volatile fatty acids. *Chem. Eng. J.* 235, 83–99. doi: 10.1016/j.cej.2013.09.002

Li, X., Zhang, W., Ma, L., Lai, S., Zhao, S., Chen, Y., et al. (2016). Improved production of propionic acid driven by hydrolyzed liquid containing high concentration of L-lactic acid from co-fermentation of food waste and sludge. *Bioresource Technol.* 220, 523–529. doi: 10.1016/j.biortech.2016.08.066

Liang, Z. X., Li, L., Li, S., Cai, Y. H., Yang, S. T., and Wang, J. F. (2012). Enhanced propionic acid production from jerusalem artichoke hydrolysate by immobilized Propionibacterium acidipropionici in a fibrous-bed bioreactor. *Bioprocess Biosystems Eng.* 35, 915–921. doi: 10.1007/s00449-011-0676-y

Liu, L., Zhu, Y., Li, J., Wang, M., Lee, P., Du, G., et al. (2012). Microbial production of propionic acid from propionibacteria: current state, challenges and perspectives. *Critical Rev. Biotechnol.* 32, 374–381. doi: 10.3109/07388551.2011.651428

Luongo, V., Policastro, G., Ghimire, A., Pirozzi, F., and Fabbricino, M. (2019). Repeated-batch fermentation of cheese whey for semi-continuous lactic acid production using mixed cultures at uncontrolled pH. *Sustainability* 11:3330. doi: 10.3390/su11123330

Markets and Markets (2015). *Butyric acid market by application (animal feed, chemicals intermediate, food & flavors, pharmaceuticals, perfumes, others), by type (synthetic butyric acid, renewable butyric acid) by geography (APAC, North America, Europe, Row) - Global analysis and forecast to 2020*. Rockville, MD: Market research.com.

Marshall, C. W., Ross, D. E., Handley, K. M., Weisenhorn, P. B., Edirisinghe, J. N., Henry, C. S., et al. (2017). Metabolic reconstruction and modeling microbial electrosynthesis. *Sci. Rep.* 7:8391. doi: 10.1038/s41598-017-08877-z

Mateos, R., Escapa, A., San-Martín, M. I., De Wever, H., Sotres, A., and Pant, D. (2020). Long-term open circuit microbial electrosynthesis system promotes methanogenesis. *J. Energy Chem.* 41, 3–6. doi: 10.1016/j.jechem.2019.04.020

Mockaitis, G., Leite, J. A. C., Pasotto, M. B., and Zaiat, M. (2012). Biosynthesis of propionic acid by anaerobic processes. *Adv. Chem. Res.* 16:8. doi: 10.13140/2.1.2530.1763

Modestra, J. A., and Mohan, S. V. (2017). Microbial electrosynthesis of carboxylic acids through CO2 reduction with selectively enriched biocatalyst: microbial dynamics. *J. CO2* Utilization 20, 190–199. doi: 10.1016/j.jcou.2017.05.011

Moscoviz, R., Toledo-Alarcón, J., Trably, E., and Bernet, N. (2016). Electro-fermentation: how to drive fermentation using electrochemical systems. *Trends Biotechnol.* 34, 856–865. doi: 10.1016/j.tibtech.2016.04.009

Moscoviz, R., Trably, E., and Bernet, N. (2018). Electro-fermentation triggering population selection in mixed-culture glycerol fermentation. *Microb. Biotechnol.* 11, 74–83. doi: 10.1111/1751-7915.12747

Murali, N., Srinivas, K., and Ahring, B. K. (2017). Biochemical production and separation of carboxylic acids for biorefinery applications. *Fermentation* 3:22. doi: 10.3390/fermentation3020022

Nevin, K. P., Woodard, T. L., Franks, A. E., Summers, Z. M., and Lovley, D. R. (2010). Microbial electrosynthesis: feeding microbes electricity to convert carbon dioxide and water to multicarbon extracellular organic compounds. *MBio* 1, e103–e110. doi: 10.1128/mBio.00103-10.Editor

Nzeteu, C. O., Trego, A. C., Abram, F., and O'Flaherty, V. (2018). Reproducible, high-yielding, biological caproate production from food waste using a single-phase anaerobic reactor system. *Biotechnol. Biofuels* 11, 1–14. doi: 10.1186/s13068-018-1101-4

Pagliano, G., Ventorino, V., Panico, A., Romano, I., Pirozzi, F., and Pepe, O. (2019). Anaerobic process for bioenergy recovery from dairy waste: meta-analysis and enumeration of microbial community related to intermediates production. *Front. Microbiol.* 9:3229. doi: 10.3389/fmicb.2018.03229

Palleroni, N. J. (2015). *Stenotrophomonas* Bergey's Manual of Systematics of Archaea and Bacteria. Baltimore: Williams & Wilkins.

Paynter, M. J., and Elsden, S. R. (1970). Mechanism of propionate formation by *Selenomonas ruminantium*, a rumen micro-organism. *J. General Microbiol.* 61:1. doi: 10.1099/00221287-61-1-1

Raes, S. M. T., Jourdin, L., Buisman, C. J. N., and Strik, D. P. B. T. B. (2017). Continuous long-term bioelectrochemical chain elongation to butyrate. *Chem. Electro. Chem.* 4, 386–395. doi: 10.1002/celc.201600587

Saady, N. M. C. (2013). Homoacetogenesis during hydrogen production by mixed cultures dark fermentation: unresolved challenge. *Int. J. Hydrogen Energy* 38, 13172–13191. doi: 10.1016/j.ijhydene.2013.07.122

Schievano, A., Pepé Sciarria, T., Vanbroekhoven, K., De Wever, H., Puig, S., Andersen, S. J., et al. (2016). Electro-fermentation – merging electrochemistry with fermentation in industrial applications. *Trends Biotechnol.* 34, 866–878. doi: 10.1016/J.TIBTECH.2016.04.007

Seeliger, S., Janssen, P. H., and Schink, B. (2002). Energetics and kinetics of lactate fermentation to acetate and propionate via methylmalonyl-CoA or acrylyl-CoA. *FEMS Microbiol. Lett.* 211, 65–70. doi: 10.1016/S0378-1097(02)00651-1

Sly, L. I., Wen, A., and Fegan, M. (2015). "Delftia," in *Bergey's Manual of Systematics of Archaea and Bacteria*, ed. W. B. Whitman (Hoboken, NJ: John Wiley & Sons, Inc, Association with Bergey's Manual Trust).

Speers, A. M., Young, J. M., and Reguera, G. (2014). Fermentation of glycerol into ethanol in a microbial electrolysis cell driven by a customized consortium. *Environ. Sci. Technol.* 48, 6350–6358. doi: 10.1021/es500690a

Srikanth, S., Venkateswar Reddy, M., and Venkata Mohan, S. (2012). Microaerophilic microenvironment at biocathode enhances electrogenesis with simultaneous synthesis of polyhydroxyalkanoates (PHA) in bioelectrochemical system (BES). *Bioresource Technol.* 125, 291–299. doi: 10.1016/j.biortech.2012.08.060

Strazzera, G., Battista, F., Garcia, N. H., Frison, N., and Bolzonella, D. (2018). Volatile fatty acids production from food wastes for biorefinery platforms: a review. *J. Environ. Manag.* 226, 278–288. doi: 10.1016/j.jenvman.2018.08.039

Tang, J., Wang, X., Hu, Y., Zhang, Y., and Li, Y. (2016). Lactic acid fermentation from food waste with indigenous microbiota: effects of pH, temperature and high OLR. *Waste Manag.* 52, 278–285. doi: 10.1016/j.wasman.2016.03.034

Tebaldi, M. L., Maia, A. L. C., Poletto, F., de Andrade, F. V., and Soares, D. C. F. (2019). Poly(-3-hydroxybutyrate-co-3-hydroxyvalerate) (PHBV): current advances in synthesis methodologies, antitumor applications and biocompatibility. *J. Drug Delivery Sci. Technol.* 51, 115–126. doi: 10.1016/j.jddst.2019.02.007

Thierry, A., Deutsch, S. M., Falentin, H., Dalmasso, M., Cousin, F. J., and Jan, G. (2011). New insights into physiology and metabolism of *Propionibacterium freudenreichii*. *Int. J. Food Microbiol.* 149, 19–27. doi: 10.1016/j.ijfoodmicro.2011.04.026

Ueki, A., Akasaka, H., Suzuki, D., and Ueki, K. (2006). Paludibacter propionicigenes gen. nov., sp. nov., a novel strictly anaerobic, Gram-negative, propionate-producing bacterium isolated from plant residue in irrigated rice-field soil in Japan. *Int. J. Systematic Evol. Microbiol.* 56, 39–44. doi: 10.1099/ijs.0.63896-0

UNEP (2019). *Global Chemicals Outlook II From legacies to innovative solutions: Implementing the 2030 Agenda for Sustainable Development, United Nations Environment Programme*. Nairobi: UNEP.

Van Ginkel, S., and Logan, B. E. (2005). Inhibition of biohydrogen production by undissociated acetic and butyric acids. *Environ. Sci. Technol.* 39, 9351–9356. doi: 10.1021/es0510515

Wang, J., and Wan, W. (2009). Factors influencing fermentative hydrogen production: a review. *Int. J. Hydrogen Energy* 34, 799–811. doi: 10.1016/j.ijhydene.2008.11.015

Wu, S. L., Sun, J., Chen, X., Wei, W., Song, L., Dai, X., et al. (2020). Unveiling the mechanisms of medium-chain fatty acid production from waste activated sludge alkaline fermentation liquor through physiological, thermodynamic and metagenomic investigations. *Water Res.* 169:115218. doi: 10.1016/j.watres.2019.115218

Xafenias, N., Anunobi, M. S. O., and Mapelli, V. (2015). Electrochemical startup increases 1,3-propanediol titers in mixed-culture glycerol fermentations. *Process Biochem.* 50, 1499–1508. doi: 10.1016/j.procbio.2015.06.020

Xu, X., Zhang, W., Gu, X., Guo, Z., Song, J., Zhu, D., et al. (2020). Stabilizing lactate production through repeated batch fermentation of food waste and waste activated sludge. *Bioresource Technol.* 300:122709. doi: 10.1016/j.biortech.2019.122709

Yahata, N., Saitoh, T., Takayama, Y., Ozawa, K., Ogata, H., Higuchi, Y., et al. (2006). Redox interaction of cytochrome c3 with [NiFe] hydrogenase from *Desulfovibrio vulgaris Miyazaki F*. *Biochemistry* 45, 1653–1662. doi: 10.1021/bi0514360

Yutin, N., and Galperin, M. Y. (2013). A genomic update on clostridial phylogeny: gram-negative spore-formers and other misplaced clostridia. *Environ. Microbiol.* 15, 2631–2641. doi: 10.1038/jid.2014.371

Conflict of Interest: The authors declare that the research was conducted in the absence of any commercial or financial relationships that could be construed as a potential conflict of interest.

Chapter 6

Influence of Hydraulic Retention Time and Organic Load on a continuous flow Microbial Fuel Cell: Experiments and Modelling

Elisa Casula[a], Mirella Di Lorenzo[b], Giorgia De Gioannis[c], Marco Isipato[a,c], Michele Mascia[a], Aldo Muntoni[c], Daniela Spiga[c]

[a] Department of Mechanical, Chemical and Materials Engineering, Via Marengo 2, 09123 Cagliari Italy

[b]Centre for Biosensors, Bioelectronics and Biodevices, University of Bath, Bath, BA2 7AY, United Kingdom

[c]Department of Civil and Environmental Engineering and Architecture, University of Cagliari, Piazza d'Armi, 09123 Cagliari, Italy

Paper under revision by the authors for publication on Journal of Power Sources (ISSN: 0378-7753)

6.1 Introduction

Since few decades, the increasing energy demand and the requirement to limit and control resulting emissions placed major emphasis on providing sustainable energy. Currently, the conventional energy generation approach, based on fossil-fuels, cannot be replaced by any individual renewable energy source (Slate et al., 2019). In the dramatic framework of the COVID-19 pandemic, with industrial shut down, car traffic stopped and flights cancelled to limit virus expansion and preserve people health, an interesting aspect has been the reduction of air pollutants level because of the forced stop of human activities. A decrease of the nitrogen dioxide (NO_2) concentrations, resulting primarily from the burning of fossil fuels has been observed after the corona virus outbreak (Dutheil et al., 2020). To date, in fact, fossil fuels fulfil major fraction of energy requirements (IEA, 2019).

In the contest of the alternative energies, together with the combination of different renewable energy sources such as solar-wind hybrids and/or solar-hydrogen fuel cells, microbial fuel cell technology has captured the attention of the scientific community.

Microbial fuel cells (MFCs) represent the newest approach for generating bioelectricity (Scott and Yu, 2015). The working principle of MFCs is based on the biocatalytic activity of exoelectrogenic microorganisms (Potter and B, 1911). The MFC setup comprises the anode, the cathode, separated or not by an exchange membrane, and the electrolyte as in a classical fuel cell. In the anodic chamber, microbial communities in planktonic state or settled in biofilm oxidize an organic substrate with the result to generate electrons, protons, and other metabolites as end-products. The electrons collected by the anode are transferred to the cathode linked by a conductive material containing a resistor, or operated under a load (Logan et al., 2006). On the other side, the protons move to the cathode passing through the

membrane or by simple diffusion throughout the electrolyte solution to be reduced by the arriving electrons, thus completing the circuit. The flow of electrons through the external load generate electric current that can be utilized for power generation(Roy and Pandit, 2018).

The advantage in using MFCs for electricity production is the substrate which provides nutrients for bacteria, in principle every substrate containing organic matter could be used as refinery wastewater, diary, municipal and swine wastewater (Min et al., 2005; Mahdi Mardanpour et al., 2012; Zhang et al., 2013, 2014). This way, an integration between water remediation and electricity production could be performed.

At the current state, typical MFC systems are known to generate power at milliwatt level preventing the technology to reach the capacity of kilowatt or megawatt level of the conventional power plants (Dong et al., 2015). One of the largest investigated prototype has a capacity of 255 L (Hiegemann et al., 2019) producing 78 mW/m^2. Despite the low power output, the simple technology setup makes it easily scalable up or down volumetrically (Cusick et al., 2011). However, transformation from laboratory scale experiments to large-scale pilot demonstrations are still scarce, mostly empirical and under initial development stages (Babanova et al., 2020).

Among the several biological, operational and design parameters which affect cell performance (Gadkari et al., 2018), the contact time between substrate and microorganism is one of the most critical factors determining the performance in terms of power production and COD removal (Santos et al., 2017; Ye et al., 2020). Contrasting results are reported in literature about the influence of the hydraulic retention time (HRT) on cell performance. Ye *et al*. (2020) found that increasing the HRT determines an improvement of the power output, Santos *et al*. (2017) found an optimum HRT for effective COD removal, as high HRT results in an insufficient organic load limiting bacteria activity and growth, shorter times do not allow to bacteria to efficiently degrade the nutrients. Conversely, Akman *et al*. (2013) found that decreasing the HRT from 1.5 d to 1 d determines an improvement of the power density from 818 mW/m^2 to 909 mW/m^2. Recently, Chen *et al*. (2020) reported an optimal HRT equal to 72 h for voltage outputs when the HRT was raised from 24 to 120 h, while the longer HRTs produced the higher COD removal.

A valid help, in the identification of the most influent parameters for technology scaling up is given by mathematical modelling. A number of studies have been reported in the attempt to mathematically describe the process and evaluate the operational parameters influence (Ortiz-Martínez et al., 2015; Recio-Garrido et al., 2016; Sobieszuk et al., 2017; Gadkari et al., 2018; Xia et al., 2018).

This work aims to provide a 3D mathematical model of a continuous flow air-cathode MFC, integrating equations of charge conservation with mass transport phenomena, hydrodynamics and

kinetics of the involved processes, such as biofilm formation, bioelectrochemical and electrochemical reactions, under transient conditions. Firstly, an estimation of model parameter was performed throughout comparison with experimental runs, then, the variation of operating conditions as residence time and inlet substrate concentration have been simulated in different cell geometries to evaluate how the aspect ratios influence the cell performances.

6.2 Materials and Methods

6.2.1 Experimental set up

3D printed air-cathode single-cell MFCs were produced using a Formlabs Form3 printer with Grey-Pro© resin: an example of cell is shown in figure 1 A. The cells were made by two halves: the anodic half-cell has a rectangular chamber as casing for the anode, and inlet and outlet ports for the electrolyte; the cathodic has rectangular holes to expose the cathode to air. Three anode chambers of different size were used, denoted as S, M, and L with dimensions (T x L x H) of 0.5 cm x 0.5 cm x 3 cm, 0.5 cm x 0.5 cm x 5 cm, and 0.5 cm x 1 cm x 5 cm, respectively. The half-cells were put together through plastic screws, with rubber gaskets.

The cells were inserted in a hydraulic circuit and the electrolyte was pumped from a reservoir to the cells with a peristaltic pump (BVP Ismatec) with eight channels. The system operated either in continuous or in batch recirculated mode, with electrolyte pumped from the reservoir to the cell and back in a closed loop.

Carbon felt (specific surface area 23500 m^{-1} porosity 95%) was used as anode. The material were treated for activation soaking it in pure acetone overnight, then in a solution of ammonium peroxydisulfate (200 g L^{-1}) and HCl 1 M for 15 min, washed in distilled water to remove acid solution then felt in muffle furnace at 450°C for 30 min and rinsed (Feng et al., 2010).

The cathode was made of carbon cloth (thickness of 0.1 cm) activated with a layer of Pt (5 mg cm^{-2}) as described elsewhere (Cheng et al., 2006). It was hot pressed to the Nafion® 115 proton exchange membrane at a temperature of 105°C (Liu and Logan, 2004). Pt or Ti wires were used to connect the cells to the electric circuit.

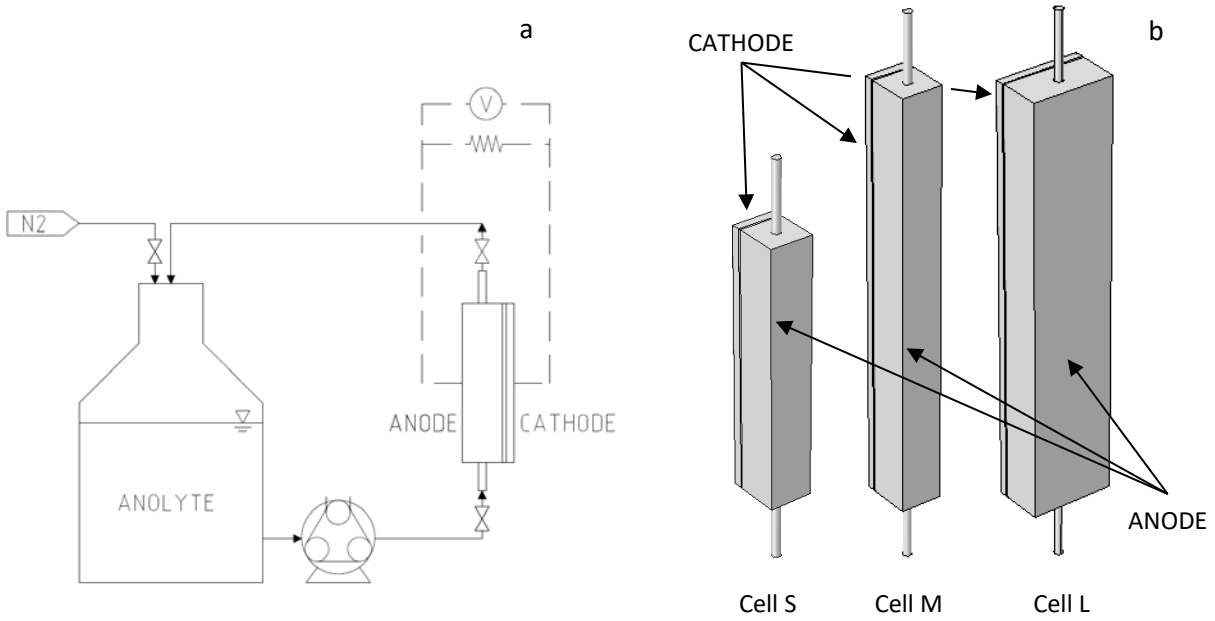

Figure 1: a) Microbial fuel cell and circuit scheme, b) MFCs geometries

MFC Operation The cells were fed with a medium containing $(NH_4)_2SO_2$ (270 mg L^{-1}), $MgSO_4 \cdot 7H_2O$ (60 mg L^{-1}), $MnSO_4 \cdot H_2O$ (6 mg L^{-1}), $NaHCO_3$ (130 mg mg L^{-1}), ($FeCl_3 \cdot 6H_2O$ 3 mg L^{-1}), ($MgCl_2$ 4 mg L^{-1}) and sodium acetate as substrate. The inlet concentration of substrate was in the range 0-2.5 g L^{-1}, depending on the run. Prior the use, solutions were boiled, and nitrogen was fluxed into the reservoir to remove dissolved oxygen. During the runs the reservoir was kept at 30 °C. Flow rates from 0.1 to 1 ml min^{-1} were used. The cells were connected in parallel to electric resistances, and to a multichannel data logger (PicoLog ®) for voltage recording.

Enrichments of biofilm were performed at different flow rates and external resistances feeding the cells with medium (2.5 g $L^{-1}$of substrate) 10% of anaerobic sludge was added to. The sludge was supplied by a local zootechnical waste treatment plant. Once the voltage reached a steady value the cells were fed with medium and substrate.

Polarisation and power density curves were obtained keeping the cells under open circuit and then connecting to external resistances from 10 kΩ to 16 Ω, switching resistors once a steady value of potential was measured. The output current (I) and power (P) were calculated from cell potential (E) and external resistance (R_{ext}) with the Ohm's law ($E = I \times R_{ext}$), and the Joule's law ($P = E^2/R_{ext}$). The internal resistance, R_{int}, was calculated from the slope of ohmic region of each polarisation curve.

Effect of inlet concentration was studied feeding the cells with different substrate concentration, from 2.5 g L^{-1} to 0.01 g L^{-1}).

All the experiments were done at least in triplicate, experimental conditions investigated are resumed in table 1

Table 1: Experimental Runs

Run	Cell Size	Feed	External Resistance (kΩ)	Flow Rate (mL min^{-1})	Acetate Concentration (mg L^{-1})	Type of run
1	S	Sludge + Medium	1	0.15	2.5	Anodic Biofilm Growth
2	M	Sludge + Medium	1	0.15	2.5	Anodic Biofilm Growth
3	M	Sludge + Medium	10	0.15	2.5	Anodic Biofilm Growth
4	M	Sludge + Medium	10	0.6	2.5	Anodic Biofilm Growth
5	M	Sludge + Medium	10	1.2	2.5	Anodic Biofilm Growth
6	S	Medium	2.2 ÷ 10	0.3	2.5	Polarization tests
7	M	Medium	2.2 ÷ 10	0.3	2.5	Polarization tests
8	L	Medium	0.016 ÷ 550	0.3	2.5	Polarization tests
9	S	Medium	5.2	0.15	0.01 ÷ 2.5	Growth Kinetic Study
10	M	Medium	5.2	0.15	0.01 ÷ 2.5	Growth Kinetic Study
11	L	Sludge + Medium	10	0.15	2.5	Anodic Biofilm Growth

6.2.2 Mathematical model

The model was implemented and solved under transient conditions with the COMSOL Multiphysics© software. Three domains of integration have been identified: the inlet and outlet channels, the anodic compartment, and the membrane/cathode assembly (MCA). The domains corresponding to the electrodes and membrane have been modelled as a porous matrix, whilst the channels as a continuous medium in liquid phase.

The model numerically describes the phenomena occurring as MFCs operate, according to the following assumptions.

Biofilm nucleation

The anolyte containing planktonic microorganisms M_S and the substrate Ac^-, enters the inlet channel then flows throughout the porous anode where microorganisms bump into and adhere to the carbon surface or leaves the cell by the exit channel. Once attached onto the carbon surface, adherent

microorganisms M_A start duplicating until the bare surface is covered and then layer by layer until a stable biofilm thickness is reached (Reguera et al., 2006; Marcus et al., 2007). The model only considers adherent microorganisms as electroactive, which oxidise the substrate through the reaction $CH_3COO^- + 4H_2O \rightarrow 2HCO_3^- + 9H^+ + 8e^-$ (Oliveira et al., 2013). Changes in pH in the anolyte due are considered as negligible.

Adhesion of planktonic bacteria is schematised by the reaction: $M_S + Ac^- \overset{k_1}{\rightarrow} M_A + e^-$. Planktonic microorganisms adhere to the anode developing the growth nuclei of the biofilm (adherent microorganisms). The reaction rate of biofilm generation r_1 (mol m^{-3} s^{-1}) has been described using a Nernst-Monod kinetics (Picioreanu et al., 2007):

$$r_1 = k_1 \frac{C_{Ac^-}}{C_{Ac^-} + K_{s,S}} \frac{C_{M_S}}{C_{M_S} + K_{s,M_S}} \left[1 + exp\left(-\frac{F}{RT}\eta_{AN}\right)\right]^{-1} \quad \text{Eq. 1}$$

Where: C_{Ac^-} and C_{M_S} (mol m^{-3}) are the acetate and planktonic microorganisms concentration; k_1 (mol m^{-3} s^{-1}) is the kinetic constant; $K_{s,S}$ and K_{s,M_S} (mol m^{-3}) are the half saturation constants; η_{An} (V) is the anodic overpotential.

Growth of biofilm

The respiration and growth of the biofilm is schematised by the reaction: $M_A + Ac^- \overset{k_2}{\rightarrow} M_A + e^-$. The reaction rate of biofilm production r_2 (mol m^{-3} s^{-1}) has been described by a Nernst-Monod kinetics, which relates the rate of substrate depletion with its concentration and the electrical potential in biofilms (Marcus et al., 2007):

$$r_2 = k_2 \frac{C_{Ac^-}}{C_{Ac^-} + K_{s,A}} \frac{C_{M_A}}{C_{M_A} + K_{s,M_A}} \left[1 + exp\left(-\frac{F}{RT}\eta_{AN}\right)\right]^{-1} \quad \text{Eq. 2}$$

Where: k_2 (mol m^{-3} s^{-1}) is the kinetic constant; $K_{s,A}$ and K_{s,M_A} (mol m^{-3}) are the half saturation constants.

Detachment of biofilm

The reaction rate of detachment r_3 (mol m^{-3} s^{-1}) has been described by a pseudo-first order law depending on the amount of biofilm produced:

$$r_3 = k_d C_{M_A} \quad \text{Eq. 3}$$

Where: C_{M_A} (mol m^{-3}) is the concentration of adherent microorganisms settled in the biofilm; k_d (s^{-1}) is the kinetic constant of detachment.

Cathode

Electrons are transferred to the cathode through the conductive biofilm (Reguera et al., 2006) and the external circuit. Protons H^+ cross the membrane to reach the cathode surface where oxygen is reduced (Rinaldi et al., 2008). Butler-Volmer law has been used to describe the cathodic reaction (Zeng et al., 2010).

Flow

Incompressible Navier-Stokes model was used to obtain velocity profiles.

Mass, charge and momentum conservation equations together with relevant initial and boundary conditions are summarised in Table 2.

Table 2: Model Equations

Momentum Transport

$$\frac{1}{\varepsilon_j}\left[\rho\frac{\partial \boldsymbol{u}}{\partial t}+\frac{1}{\varepsilon_j}\rho\,(\boldsymbol{u}\cdot\nabla)\boldsymbol{u}\right]=\nabla\cdot\left[-p\boldsymbol{I}+\frac{1}{\varepsilon_j}\mu(\nabla\boldsymbol{u}+(\nabla\boldsymbol{u})^T)\right]-\frac{\mu}{k}\,\boldsymbol{u};\;\; \rho\,\nabla(\boldsymbol{u})=0;\;\; j=\begin{cases}channels\rightarrow\;\varepsilon_j=1\\ anode\rightarrow\;\varepsilon_j=\varepsilon_{AN}\end{cases}$$

$$\boldsymbol{u}|_{t=0}=0$$

$$\mathrm{L}_{in}\,\nabla_t\cdot[-p\boldsymbol{I}+\mu(\nabla\boldsymbol{u}+(\nabla\boldsymbol{u})^T)]=-\mathrm{p}_{in}\boldsymbol{n}\quad Inlet\ channel$$

$$[-p\boldsymbol{I}+\mu(\nabla\boldsymbol{u}+(\nabla\boldsymbol{u})^T)]n=-\mathrm{p}_{out}\boldsymbol{n}\qquad Outlet\ channel$$

Eq. 4

Mass Transport

Mass transport for acetate, suspended organisms and hydrogen ions

$$\varepsilon_j\frac{\partial C_i}{\partial t}+\nabla\cdot\left(-\mathcal{D}_{i,j}^{eff}\nabla C_i\right)+\boldsymbol{u}\cdot\nabla C_i=R_{i,j}\;\forall\; i=Ac^-,M_S,H^+;\;\; j=\begin{cases}channels\rightarrow\;\varepsilon_j=1\\ anode\rightarrow\;\varepsilon_j=\varepsilon_{AN}\\ cathode\rightarrow\;\varepsilon_j=\varepsilon_{CAT},\boldsymbol{u}=0\end{cases}$$

$$C_i|_{t=0}=0$$

$$C_i|_{inlet\ channel}=C_i^0\qquad Inlet\ channel$$

$$-\boldsymbol{n}\cdot\left(\mathcal{D}_{i,j}^{eff}\nabla C_i\right)=0\qquad Outlet\ channel$$

Eq. 5

Mass transport for biofilm

$$\varepsilon_{AN}\;\frac{\partial C_{M_A}}{\partial t}=R_{M_A,Anode};\; C_{M_A}\big|_{t=0}=0$$

Eq. 6

$$\mathcal{D}_{i,j}^{eff}=\frac{\varepsilon_j}{\tau_j}\mathcal{D}_i$$

Eq. 7

$$\tau_j=\varepsilon_j{}^{-1/3}$$

Eq. 8

Table 2 (continued)

Reaction Rates	
$R_{Ac^-,Anode} = -\nu_{Ac^-}\,(r_1 + r_2)$	Eq. 9
$R_{Ms,Anode} = -r_1$	Eq. 10
$R_{Ma,Anode} = r_1 + r_2 - r_3$	Eq. 11
$R_{H^+,Anode} = \nu_{H^+}(r_1 + r_2)$	Eq. 12
$R_{H^+,Cathode} = -\frac{I_{CAT}}{F}$	Eq. 13
Electric current	
$I_{CAT} = I^0_{CAT}\, exp\left(-0.5\frac{F}{RT}\eta_{CAT}\right)$	Eq. 14
$I^0_{CAT} = i^0_{CAT}\, a_{CAT}\frac{C_{H^+}}{C^0_{H^+}}$	Eq. 15
$I_{AN} = r_2\, z_{AN} F$	Eq. 16
$\eta_{AN} = V_{AN} - E^0_{AN}$	Eq. 17
$\eta_{CAT} = V_{CAT} - E^0_{CAT}$	Eq. 18
Electric potential	
$\nabla \cdot \left(-\sigma_j \nabla V_j\right) = f;\; j = \begin{cases} anode \rightarrow\; f = I_{AN} \\ P.E.M. \rightarrow\; f = 0 \\ cathode \rightarrow\; f = I_{CAT} \end{cases}$	Eq. 19
$V_j\big\vert_{t=0} = 0$	Eq. 20
$V_j = 0 \qquad Ground - Anode\ interface$	Eq. 21

Eq. 4 represents the momentum transport in free and porous media together with the initial and boundary conditions. $\boldsymbol{u}$ (m s^{-1}) is the velocity field; ρ (kg m^{-3}) and μ (Pa·s) are the fluid density and viscosity, respectively; k (m^2) is the permeability; ε_j (-) is the medium porosity. ε_j is equal 1 in case of free media (inlet and outlet channels), while is equal to ε_{AN} (-) in the anodic compartment. Fluid properties have been considered equal to the water properties. At the starting point, the cell is empty. The inlet velocity of the fluid is equal to u_{in} (m s^{-1}). Normal flow and suppressed backflow conditions are considered in the outlet section.

The mechanisms of mass transport considered are convection and diffusion for anode domain and diffusion only for MCA. Eq. 5 represents the generic transport equation for acetate, suspended organisms and hydrogen ions in free and porous media. C_i (mol m^{-3}) is the concentration of the ith species

(i = Ac^-, M_S, H^+); $\mathcal{D}_{i,j}^{eff}$ ($m^2\ s^{-1}$) is the effective diffusivity of the i^{th} species in the j^{th} domain (i.e. channels, anode, MCA) and $R_{i,j}$ (mol $m^{-3}\ s^{-1}$) is the generation term. Effective diffusivity was determine through Equation 7 starting from diffusivity in free media $\mathcal{D}_i$ ($m^2\ s^{-1}$). Quirk and Millington model was used to relate tortuosity τ_j (-) and porosity ε_j (Eq. 8).

Biofilm variation is affected only by the generation term $R_{M_A,Anode}$ (mol $m^{-3}\ s^{-1}$) (Eq. 6).

The reaction terms $R_{i,j}$ of each species in the different domains are reported from Eq. 9 to Eq. 13 where ν_{Ac^-} (-) and ν_{H^+} (-) are the stoichiometric coefficient for acetate degradation reaction and protons generation, respectively.

The consumption of protons at the cathode (Eq. 13) depends on the cathodic current I_{CAT} (A m^{-3}). The last has been defined with a Butler-Volmer equation (Eq. 14) where I_{CAT}^0 (A m^{-3}) is the exchange current and η_{CAT} (-) is the cathodic overpotential. I_{CAT}^0 depends on the increase in protons concentration $C_{H^+}/C_{H^+}^0$, the exchange current density i_{CAT}^0 (A m^{-2}), and the cathode specific area a_{CAT} ($m^{-2}\ m^{-3}$) as reported in Eq. 15.

The conservation of electric charge has been described using a Poisson's Law (Eq. 19) where σ_j (S m^{-1}) is the electric conductivity of the j^{th} domain and f_j (A m^{-3}) is the current source. In the anodic region, current source I_{AN} (A m^{-3}) is defined through Eq. 16 where z_{AN} is the number of the electrons involved in the degradation of organic matter. Boundary conditions at the interfaces imply an evenness of the voltage; there is not flux charge at external boundaries; the ground is at the anode-case interface. Initial conditions imply a nil electric potential throughout the fuel cell.

6.3 Results and Discussion

6.3.1 Cell characterisation

The three cells were characterised through polarisation experiments, figure 2 shows an example of polarisation and power curves, obtained with cell L. The curves show a general trend reported in the literature and (Logan et al., 2006) and observed with all the 3 cells. An initial non-linear trend of the polarisation curves was always obtained, due to the activation losses at low current densities, followed by a linear dependence of the potential from the current in a wide range of values, indicating that the three cells tested mainly operate at current densities where ohmic losses are dominant (Ortiz-Martínez et al., 2015).

Value of the internal resistance (R_{int}) of the cells were obtained from the slope of the trendline in the linear region of the polarisation curves, activation losses were calculated as the difference between experimental open circuit potentials (OCP) and the intercepts of the linear trendline.

Table 3 reports internal resistance, open circuit potentials and HRT for the three cells: different values of R_{int} can be observed, with an increase of cell volume that leads to a decrease in cell internal resistance.

Table 3: Internal resistance and Open Circuit Potential (OCP) for the three cell S, M, and L.

Cell	R_{int} (kΩ)	OCP (V)	HRT (min)
S	19.60	0.195	2.5
M	9.20	0.202	4.0
L	0.85	0.538	8.5

The total internal resistance R_{int} of a MFC depends on anodic resistance, cathodic resistance, membrane resistance and electrolyte resistances. Anodic and cathodic resistances refer to bioelectrochemical reactions at anode and oxygen reduction at cathode, for anode and cathode resistances, respectively; membrane and electrolyte resistances depend on transport phenomena in liquid and solid phase (Fan et al., 2008). Design factors, such as anode and cathode area, and their ratio may affect R_{int} (Miller et al., 2019). The cells used in this work feature the same ratio cathode/anode area, and the same type of cathode so that the differences observed likely depend on operative parameters and phenomena from the anode side. Operative parameters such as hydraulic residence time (HRT) and hydrodynamics of the electrolyte may affect the overall value of R_{int}: HRT have a direct effect on biofilm formation and performances, in the literature optimal HRT is sometimes referred to the time for generate living microbes (Sharma and Li, 2010), high HRT may decrease the substrate available for microorganisms, thus lowering the power output (Ye et al., 2020). Hydrodynamics has a contrasting effect: high velocity was observed having a positive effect on electricity generation R_{int} (Miller et al., 2019), but it can increases the shear stress, which can reduce biofilm thickness and activity (Yang et al., 2019). High velocity and low HRT may also favour the removal of planktonic microorganisms so reducing their contribute to power generation (Fan et al., 2008). Moreover, space distribution of substrate, electric field and velocity may considerably affect the performance of in-flow MFCs, with local starvation zones that can increase the overall R_{int} (Mateo et al., 2019).

To have an insight into the local phenomena that may affect the performance of the flow MFCs, a mathematical model in 3D was built, calibrated with experimental data and solved.

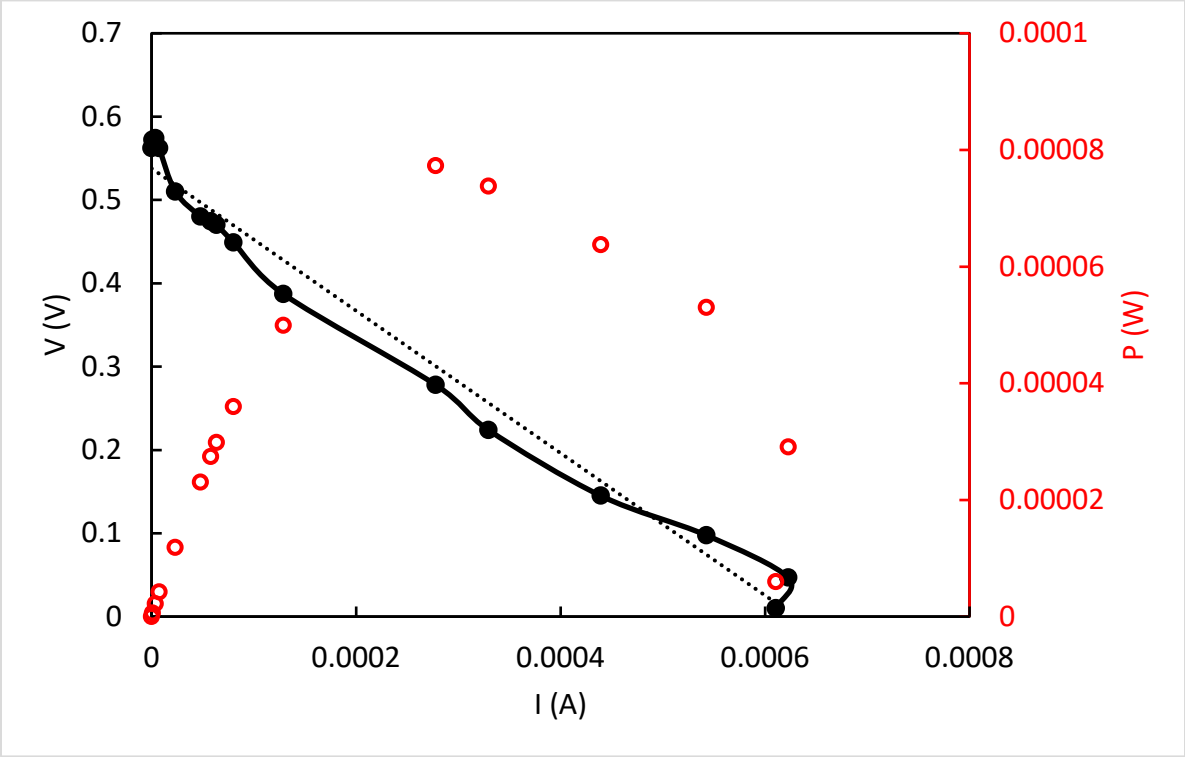

Figure 2: Polarization (black filled circles) and power (red empty circles) curves for the cell L (Run 8)

6.3.2 Parameter estimation and validation

The model parameters were obtained with experimental data, different set of data were used for calibration and validation; literature values were used for general parameters such as viscosity of water or diffusivities of solutes. Model parameter along with the corresponding sources are summarised in Table 4.

Experimental growth curves of cell M (Run 2) were used to calibrate the mathematical model while growth curves in cell S and L, obtained under the same operative conditions were used for parameter validation.

Following the model assumption, an increase of the parameter k1 with the flow rate has been found. Figure 3 shows experimental (symbols) and model predicted data for biofilm growth in the three cells. The typical trend of potential with time can be observed in all the cells: an apparent lag phase of about 40 h is followed by a growth phase and a steady-state phase, which is reached after approximately 120 h of continuous feeding with medium and bacteria. A good agreement between experimental and model predicted data can be observed for all the cells.

Table 4: Model parameters values

Symbol	Value	Unit	Ref.
$\mathcal{D}_{Ac^-}$	$1.1 \cdot 10^{-9}$	$m^2\ s^{-1}$	
$\mathcal{D}_{H^+}$	$9 \cdot 10^{-9}$	$m^2\ s^{-1}$	
$\mathcal{D}_{H^+,m}$	$9 \cdot 10^{-9}$	$m^2\ s^{-1}$	
$\mathcal{D}_{M_S}$	$3 \cdot 10^{-10}$	$m^2\ s^{-1}$	
k_1	$7 \cdot 10^{-8}$	$mol\ m^{-3}\ s^{-1}$	This work
k_2	$8.5 \cdot 10^{-4}$	$mol\ m^{-3}\ s^{-1}$	This work
k_d	3	d^{-1}	This work
$K_{s,A}$	65	$mol\ m^{-3}$	This work
K_{s,M_A}	5	$mol\ m^{-3}$	This work
K_{s,M_S}	10	$mol\ m^{-3}$	This work
$K_{s,S}$	65	$mol\ m^{-3}$	This work

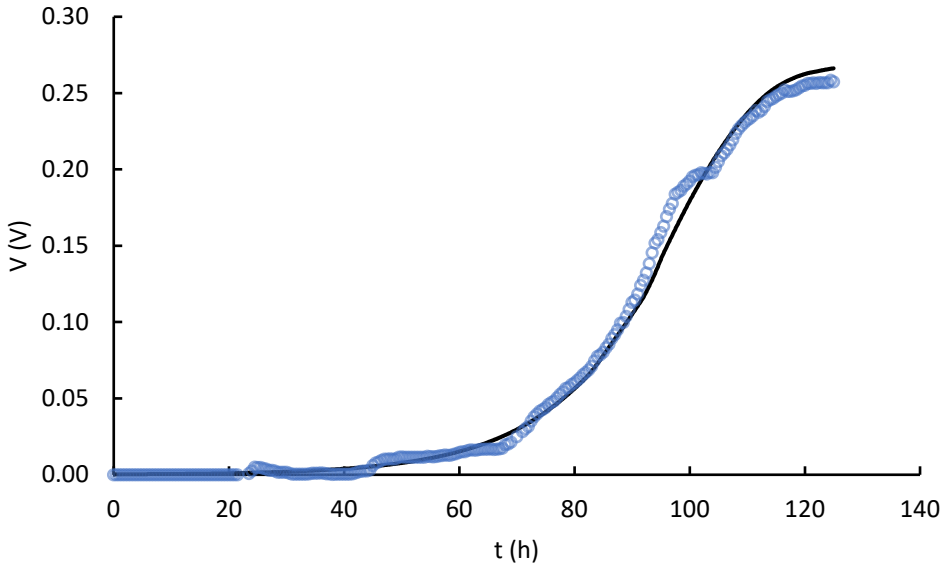

Figure 3: Comparison between experimental data (symbols) and model fitting (lines) of biofilm growth in cells M

The model predictions were also validated though comparison with steady-state responses to increasing substrate concentration in the inlet stream was subsequently tested. With this purpose, the cells were first fed with medium and no substrate until the measured potential was almost null; afterwards were fed with medium and different concentrations of substrate. Figure 4 compares experimental model predicted data in terms of potential vs substrate concentration. A Monod-like trend can be observed, as well as a satisfactory prediction of the model.

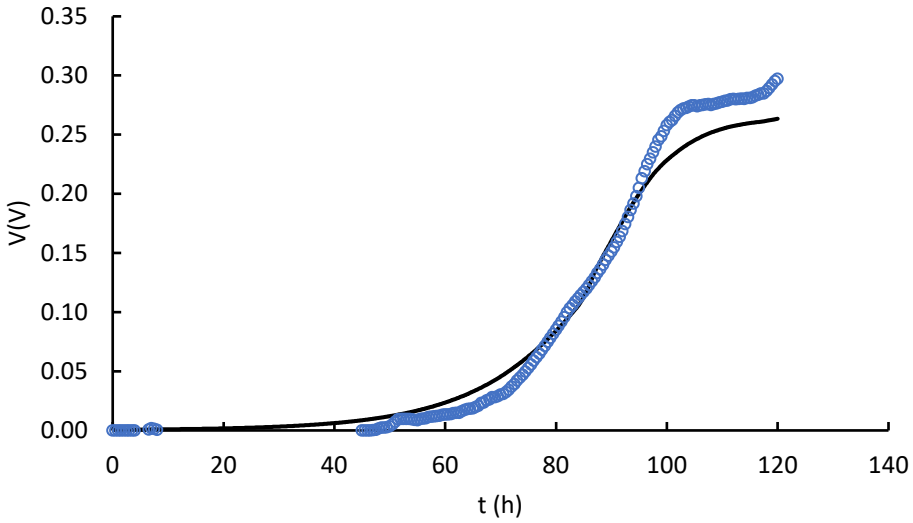

Figure 4: Comparison between experimental data (symbols) and model fitting (lines) of biofilm growth in cells S

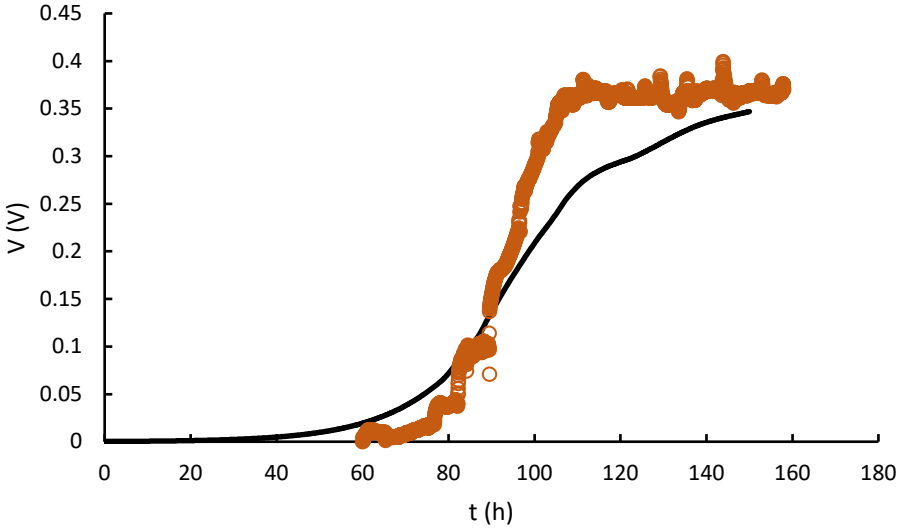

Figure 5: Comparison between experimental data (symbols) and model fitting (lines) of biofilm growth in cells L

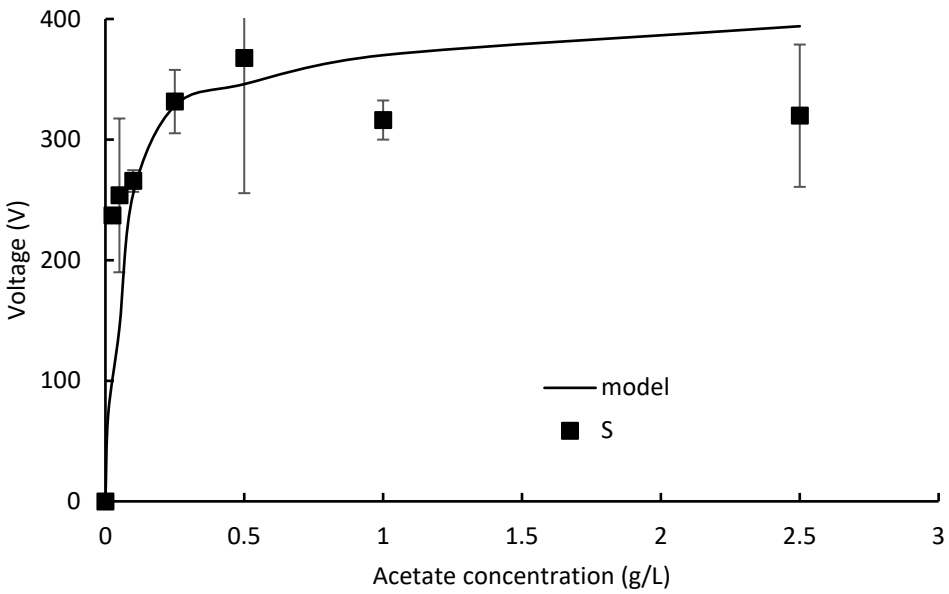

Figure 6: Equilibrium cell voltage at different acetate inlet concentrations. Squares: experimental data, circles: model predictions.

6.3.3 Simulations

Simulations were carried with different inlet flow rates and substrate concentration. Examples of model prediction are reported in the following figures.

Figure 7 shows the influence of inlet substrate concentration on the average current density and substrate degradation in cell M when the flow rate was set equal to 0.05 mL min^{-1} (HRT = 25 min). The increase of substrate availability determines an increase of the current density (Figure 7a) and a faster degradation of substrate (Figure 7b).

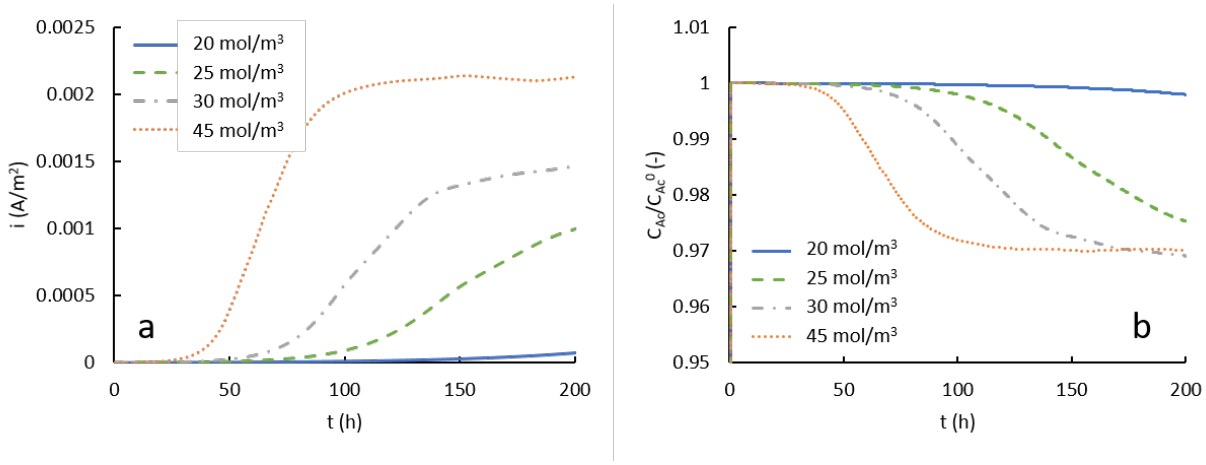

Figure 7: Influence of inlet substrate concentration on cell performance: a) Current density production, b) average outlet concentration normalized with respect to the inlet concentration. Flow rate was set equal to 0.05 mL min^{-1}.

Hydraulic retention time – Figure 8 reports the influence of the flow rate in cell M on the average current density and substrate degradation when the inlet concentration was set equal to 30 mol m^{-3}. Four different flow rate were investigated: 0.01, 0.05, 0.6, and 1.2mL min^{-1}, which correspond to HRT equal to 125, 25, 8.3, and 2.1 min, respectively. The increase of flow rate determines an increase of the current density production (Figure 8a) and a lower degradation of substrate (Figure 8b). At steady-state conditions, the average outlet concentration normalized with respect to the inlet one varies changing accordingly to flow rate.

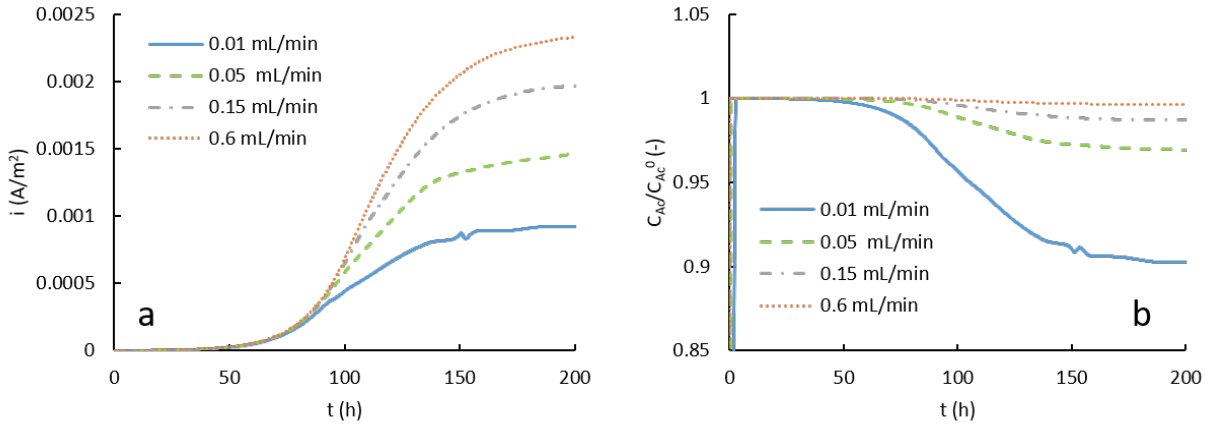

Figure 8: Influence of flow rate on cell performance: a) Current density production, b) average outlet concentration normalized with respect to the inlet concentration. Inlet concentration was set equal to 30 moL m^{-3}.

The influence of HRTs is further investigated in Figure 9. Normalized biofilm with respect to the maximum value, current density, and substrate concentration spatial distributions have been evaluated considering HRT = 125 min (Figures a, c, e, and g) and HRT = 2.1 min (Figures b, d, f, and h). The increase of the flow rate determines a more uniform biofilm production (Figures a and b), which determines a higher current density (Figures c and d). The higher current density is determined by the rapid replenish of the anolyte at higher flow rate. In fact, when low flow rate are used, the substrate is rapidly consumed by the bacteria. Consequently, the concentration is not uniform throughout the cell (Figures e and f) limiting the cell performance. (Santos et al., 2017; Ye et al., 2020).

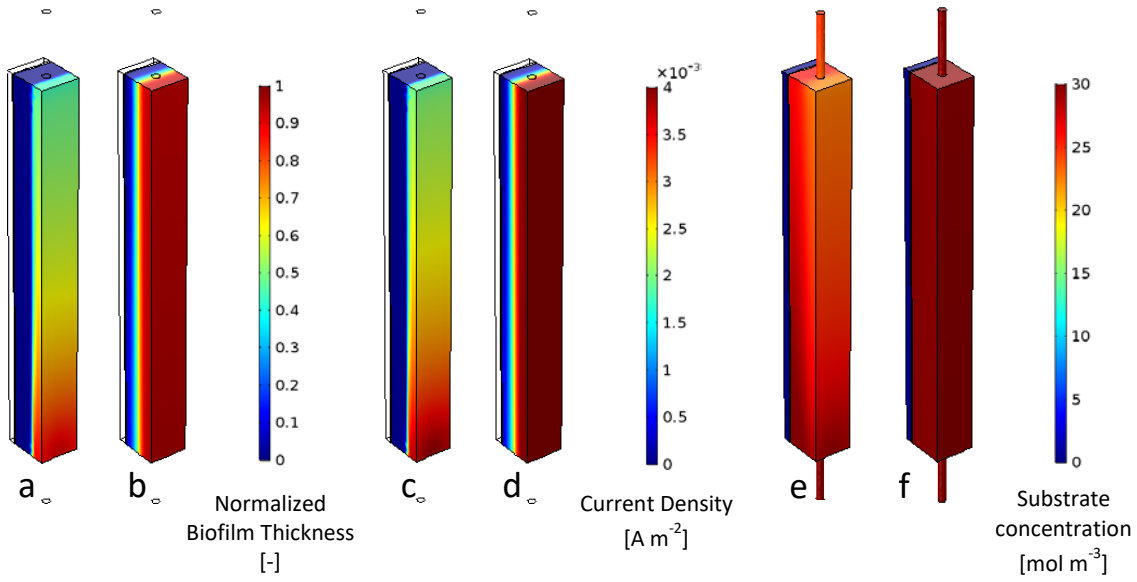

Figure 9: Influence of hydraulic residence time on normalized biofilm a, b), current density c, d), and substrate concentration e, f). a, c, and e) HRT = 125 min; b, d, and f) HRT = 2.1 min.

Figure 10 reports the cell potential in steady state when HRT = 125 min (Figure 10g) and HRT = 2.1 min (Figure 10h).

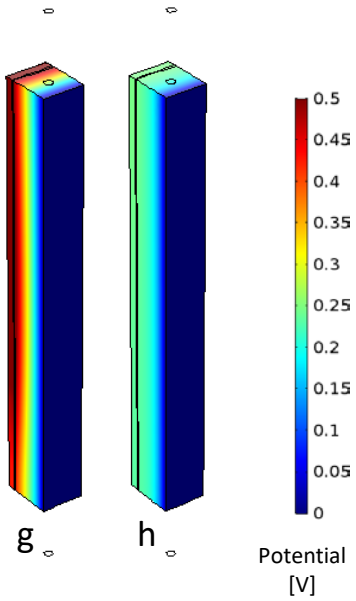

Figure 10: Influence of hydraulic residence time on cell potential: g) HRT = 125 min; h) HRT = 2.1 min.

Cell geometry – Figure 11 compares spatial distributions of biofilm thickness, current density, and potential at fixed inlet substrate concentration and flow rate. The influence of cell geometry is negligible in comparison to the other parameters analysed.

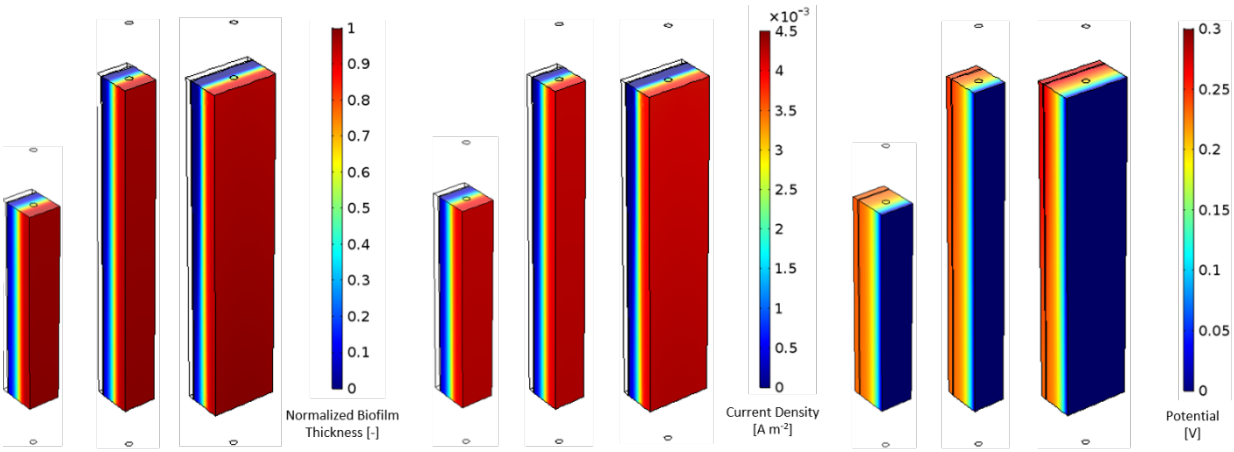

Figure 11: Comparison on a) normalized biofilm thickness, b) current density, and c) cell potential distributions when the flow rate is equal to 0.6 mL min^{-1} and inlet concentration is equal to 30 moL m^{-3} .

6.4 Conclusions

In this work, a 3D mathematical model was implemented and solved to investigate the behaviour of continuous flow air cathode MFC with carbon feltanodes. The model takes into account 1) hydrodynamics, 2) transport of substrate, microorganisms, and protons by diffusion and convection in liquid phase and in porous media, 3) chemical and electrochemical kinetics of substrate consumption and biofilm growth onto the anode surface, 4) charge conservation.

Non-uniform distribution was predicted with simulations under flow conditions, with a further effect of flow rate, where low-velocity zones determine a rapid depletion of acetate available for the biofilms. An increase of the flow rate showed positive effect on electric current generation, with lower conversion of substrate.

Based on the results of the simulation, the system can be optimised for substrate removal or current generation by tuning frequency of refilling when the system operates in fed-batch mode, or flow rate with the system under flow conditions.

The mathematical model presented in this study makes it possible to design modular systems, where in-parallel reactors can be designed from the simulation of one single unit, as simulations of

reactors in-series can be easily implemented. The model will thus provide a versatile tool to design a MFC based process with a novel anode geometry based on carbon felt electrodes.

References

Akman, D., Cirik, K., Ozdemir, S., Ozkaya, B., and Cinar, O. (2013). Bioelectricity generation in continuously-fed microbial fuel cell: Effects of anode electrode material and hydraulic retention time. *Bioresour. Technol.* 149, 459–464. doi:10.1016/j.biortech.2013.09.102.

Babanova, S., Jones, J., Phadke, S., Lu, M., Angulo, C., Garcia, J., et al. (2020). Continuous flow, large-scale, microbial fuel cell system for the sustained treatment of swine waste. *Water Environ. Res.* 92, 60–72. doi:10.1002/wer.1183.

Chen, F., Zeng, S., Luo, Z., Ma, J., Zhu, Q., and Zhang, S. (2020). A novel MBBR–MFC integrated system for high-strength pulp/paper wastewater treatment and bioelectricity generation. *Sep. Sci. Technol.* 55, 2490–2499. doi:10.1080/01496395.2019.1641519.

Cheng, S., Liu, H., and Logan, B. E. (2006). Increased performance of single-chamber microbial fuel cells using an improved cathode structure. *Electrochem. commun.* 8, 489–494. doi:10.1016/j.elecom.2006.01.010.

Cusick, R. D., Bryan, B., Parker, D. S., Merrill, M. D., Mehanna, M., Kiely, P. D., et al. (2011). Performance of a pilot-scale continuous flow microbial electrolysis cell fed winery wastewater. *Appl. Microbiol. Biotechnol.* 89, 2053–2063. doi:10.1007/s00253-011-3130-9.

Dong, Y., Feng, Y., Qu, Y., Du, Y., Zhou, X., and Liu, J. (2015). A combined system of microbial fuel cell and intermittently aerated biological filter for energy self-sufficient wastewater treatment OPEN. *Sci. RepoRts* | 5, 18070. doi:10.1038/srep18070.

Dutheil, F., Baker, J. S., and Navel, V. (2020). COVID-19 as a factor influencing air pollution? *Environ. Pollut.* 263, 114466. doi:10.1016/j.envpol.2020.114466.

Fan, Y., Sharbrough, E., and Liu, H. (2008). Quantification of the internal resistance distribution of microbial fuel cells. *Environ. Sci. Technol.* 42, 8101–8107. doi:10.1021/es801229j.

Feng, Y., Yang, Q., Wang, X., and Logan, B. E. (2010). Treatment of carbon fiber brush anodes for improving power generation in air-cathode microbial fuel cells. *J. Power Sources* 195, 1841–1844. doi:10.1016/j.jpowsour.2009.10.030.

Gadkari, S., Gu, S., and Sadhukhan, J. (2018). Towards automated design of bioelectrochemical systems: A comprehensive review of mathematical models. *Chem. Eng. J.* 343, 303–316. doi:10.1016/j.cej.2018.03.005.

Hiegemann, H., Littfinski, T., Krimmler, S., Lübken, M., Klein, D., Schmelz, K. G., et al. (2019). Performance and inorganic fouling of a submergible 255 L prototype microbial fuel cell module during continuous long-term operation with real municipal wastewater under practical conditions. *Bioresour. Technol.* 294, 122227. doi:10.1016/j.biortech.2019.122227.

Liu, H., and Logan, B. E. (2004). Electricity generation using an air-cathode single chamber microbial fuel cell in the presence and absence of a proton exchange membrane. *Environ. Sci. Technol.* 38, 4040–4046. doi:10.1021/es0499344.

Logan, B. E., Hamelers, B., Rozendal, R., Schröder, U., Keller, J., Freguia, S., et al. (2006). Microbial fuel cells: Methodology and technology. *Environ. Sci. Technol.* 40, 5181–5192. doi:10.1021/es0605016.

Mahdi Mardanpour, M., Nasr Esfahany, M., Behzad, T., and Sedaqatvand, R. (2012). Single chamber microbial fuel cell with spiral anode for dairy wastewater treatment. *Biosens. Bioelectron.* 38, 264–269. doi:10.1016/j.bios.2012.05.046.

Marcus, A. K., Torres, C. I., and Rittmann, B. E. (2007). Conduction-based modeling of the biofilm anode of a microbial fuel cell. *Biotechnol. Bioeng.* 98, 1171–1182. doi:10.1002/bit.21533.

Mateo, S., Mascia, M., Fernandez-Morales, F. J., Rodrigo, M. A., and Di Lorenzo, M. (2019). Assessing the impact of design factors on the performance of two miniature microbial fuel cells. *Electrochim. Acta* 297, 297–306. doi:10.1016/j.electacta.2018.11.193.

Miller, A., Singh, L., Wang, L., and Liu, H. (2019). Linking internal resistance with design and operation

decisions in microbial electrolysis cells. *Environ. Int.* 126, 611–618. doi:10.1016/j.envint.2019.02.056.
Min, B., Kim, J. R., Oh, S. E., Regan, J. M., and Logan, B. E. (2005). Electricity generation from swine wastewater using microbial fuel cells. *Water Res.* 39, 4961–4968. doi:10.1016/j.watres.2005.09.039.
Oliveira, V. B., Simões, M., Melo, L. F., and Pinto, A. M. F. R. (2013). A 1D mathematical model for a microbial fuel cell. *Energy* 61, 463–471. doi:10.1016/j.energy.2013.08.055.
Ortiz-Martínez, V. M., Salar-García, M. J., de los Ríos, A. P., Hernández-Fernández, F. J., Egea, J. A., and Lozano, L. J. (2015). Developments in microbial fuel cell modeling. *Chem. Eng. J.* 271, 50–60. doi:10.1016/j.cej.2015.02.076.
Picioreanu, C., Head, I. M., Katuri, K. P., van Loosdrecht, M. C. M., and Scott, K. (2007). A computational model for biofilm-based microbial fuel cells. *Water Res.* 41, 2921–2940. doi:10.1016/j.watres.2007.04.009.
Potter, M. C., and B, P. R. S. L. (1911). Electrical effects accompanying the decomposition of organic compounds. *Proc. R. Soc. London. Ser. B, Contain. Pap. a Biol. Character* 84, 260–276. doi:10.1098/rspb.1911.0073.
Recio-Garrido, D., Perrier, M., and Tartakovsky, B. (2016). Modeling, optimization and control of bioelectrochemical systems. *Chem. Eng. J.* 289, 180–190. doi:10.1016/j.cej.2015.11.112.
Reguera, G., Nevin, K. P., Nicoll, J. S., Covalla, S. F., Woodard, T. L., and Lovley, D. R. (2006). Biofilm and nanowire production leads to increased current in Geobacter sulfurreducens fuel cells. *Appl. Environ. Microbiol.* 72, 7345–7348. doi:10.1128/AEM.01444-06.
Rinaldi, A., Mecheri, B., Garavaglia, V., Licoccia, S., Di Nardo, P., and Traversa, E. (2008). Engineering materials and biology to boost performance of microbial fuel cells: A critical review. *Energy Environ. Sci.* 1, 417–429. doi:10.1039/b806498a.
Roy, S., and Pandit, S. (2018). "Microbial electrochemical system: Principles and application," in *Biomass, Biofuels, Biochemicals: Microbial Electrochemical Technology: Sustainable Platform for Fuels, Chemicals and Remediation* (Elsevier), 19–48. doi:10.1016/B978-0-444-64052-9.00002-9.
Santos, J. B. C., de Barros, V. V. S., and Linares, J. J. (2017). The Hydraulic Retention Time as a Key Parameter for the Performance of a Cyclically Fed Glycerol-Based Microbial Fuel Cell from Biodiesel. *J. Electrochem. Soc.* 164, H3001–H3006. doi:10.1149/2.0011703jes.
Scott, K., and Yu, E. H. (2015). *Microbial Electrochemical and Fuel Cells: Fundamentals and Applications*. Elsevier Inc. doi:10.1016/C2014-0-01767-4.
Sharma, Y., and Li, B. (2010). Optimizing energy harvest in wastewater treatment by combining anaerobic hydrogen producing biofermentor (HPB) and microbial fuel cell (MFC). *Int. J. Hydrogen Energy* 35, 3789–3797. doi:10.1016/j.ijhydene.2010.01.042.
Slate, A. J., Whitehead, K. A., Brownson, D. A. C., and Banks, C. E. (2019). Microbial fuel cells: An overview of current technology. *Renew. Sustain. Energy Rev.* 101, 60–81. doi:10.1016/j.rser.2018.09.044.
Sobieszuk, P., Zamojska-Jaroszewicz, A., and Makowski, Ł. (2017). Influence of the operational parameters on bioelectricity generation in continuous microbial fuel cell, experimental and computational fluid dynamics modelling. *J. Power Sources* 371, 178–187. doi:10.1016/j.jpowsour.2017.10.032.
World Energy Outlook 2019 – Analysis - IEA Available at: https://www.iea.org/reports/world-energy-outlook-2019 [Accessed March 30, 2021].
Xia, C., Zhang, D., Pedrycz, W., Zhu, Y., and Guo, Y. (2018). Models for Microbial Fuel Cells: A critical review. *J. Power Sources* 373, 119–131. doi:10.1016/j.jpowsour.2017.11.001.
Yang, J., Cheng, S., Li, C., Sun, Y., and Huang, H. (2019). Shear Stress Affects Biofilm Structure and Consequently Current Generation of Bioanode in Microbial Electrochemical Systems (MESs). *Front.*

Microbiol. 10, 398. doi:10.3389/fmicb.2019.00398.
Ye, Y., Ngo, H. H., Guo, W., Chang, S. W., Nguyen, D. D., Zhang, X., et al. (2020). Impacts of hydraulic retention time on a continuous flow mode dual-chamber microbial fuel cell for recovering nutrients from municipal wastewater. *Sci. Total Environ.* 734, 139220. doi:10.1016/j.scitotenv.2020.139220.
Zeng, Y., Choo, Y. F., Kim, B. H., and Wu, P. (2010). Modelling and simulation of two-chamber microbial fuel cell. *J. Power Sources* 195, 79–89. doi:10.1016/j.jpowsour.2009.06.101.
Zhang, F., Ahn, Y., and Logan, B. E. (2014). Treating refinery wastewaters in microbial fuel cells using separator electrode assembly or spaced electrode configurations. *Bioresour. Technol.* 152, 46–52. doi:10.1016/j.biortech.2013.10.103.
Zhang, F., Ge, Z., Grimaud, J., Hurst, J., and He, Z. (2013). Long-term performance of liter-scale microbial fuel cells treating primary effluent installed in a municipal wastewater treatment facility. *Environ. Sci. Technol.* 47, 4941–4948. doi:10.1021/es400631r.

Chapter 7

Integrated biohydrogen production from cheese whey by combination of dark fermentation and microbial electrolysis cells

7.1 Introduction

Nowadays, the decarbonisation of the energy sector is crucial to reach climate neutrality by 2050. With the European Green Deal, H_2 has been addressed as a key component to deliver carbon-neutral energy wherever the use of renewable electricity is challenged by storage, heavy duty transport and energy-intensive industries (European Commission, 2019). In fact, H_2 has the highest energy content per unit of weight (142 kJ g^{-1}) among all known fuels, and can be transported by conventional means (Benemann, 1996). Currently, H_2 usage in Europe accounts for 9.7 Mt (Fuel Cells and Hydrogen Joint Undertaking, 2019), which is however mainly generated by steam methane reforming (European Commission, 2020) causing the release of huge amounts of carbon dioxide. The two major alternatives for the generation of green H_2 are water electrolysis based on renewable resources and exploitation of biomasses in biorefinery networks. Amidst the available technologies for bio-based H_2 production, DF has gained interest due to high production rates and low costs for the degradation of complex and unsterilised substrates (Guo et al., 2010). In particular, wastewaters and industrial by products represent an optimal substrate for H_2 oriented DF, considered their wide availability and cheap price (Kapdan and Kargi, 2006). In addition, reactors can be operated using high organic loading rates, low nutrient addition requirements and net energy gain (Lin et al., 2012). In this context, Sheep Cheese Whey (SCW) is a promising by-product, which has been demonstrated to be exploitable for the production of either H_2 in energy-driven biorefineries or platforms in material-driven biorefineries (Asunis et al., 2019). However, in the first scenario only 30-40% of the substrate is used for bio- H_2 production due to thermodynamic limitations, while the remaining quota is converted into soluble metabolites depending on the main metabolic pathway (Sarma et al., 2015). Therefore, a full-scale implementation can be achieved only by integrating DF within technologies capable of further convert these metabolites into H_2. Microbial Electrochemical Cells (MECs) have been proposed as a downstream process for DF effluents (Rozendal et al., 2006). In MECs, organic substrates are microbially oxidised at the anode providing the required energy for H_2 evolution from water at the cathode (see Chapter 4). A relatively small external energy input is required to make H_2 production thermodynamically favourable (Escapa et al., 2016). Therefore, the combination of DF and MEC in a two-step process allows a more optimal conversion of the biodegradable by-products into energy, while increasing the quality of the final effluent (Rozendal et al., 2006). To date, only a

few studies have systematically investigated the organic wastes and by-products valorisation using a cascade DF-MEC process, and focused on: corn stalk (Li et al., 2014), crude glycerol (Chookaew et al., 2014), cheese whey (Moreno et al., 2015; Marone et al., 2017), waste activated sludge (Liu et al., 2012; Lu et al., 2012), fruit processing wastewater, sugar production wastewater, residues from spirit distillation and paper mill wastewater (Marone et al., 2017). All the mentioned studies reported higher H_2 yields and energy efficiency when compared to a standalone treatment through DF. Although performed at a bench scale, the suitability of fermentation dead-end products as the carbon source in MEC was demonstrated.

The aim of this study is to evaluate biohydrogen production from cheese whey in a fermentation-centred biorefinery approach, comparing H_2 production and final carbon content in the effluent when DF was a standalone process and when was coupled with MEC.

7.2 Materials and Methods

7.2.1 Microbial electrolysis cell set-up and operation

A two-chamber MEC (MEC-Q) was constructed from a polycarbonate cube. The anodic chamber had 25 mL working volume (3 cm diameter by 4 cm length, 28.3 mL empty volume), while the cathodic compartment (3 cm diameter by 6 cm length) had a working volume of 42.4 mL. A polycarbonate gas collection tube (1.6 cm diameter by 7 cm height) was glued to the top of the cathodic chamber to provide headspace. A butyl rubber stopper and aluminium crimp cap assured the sealing of the compartment. Chambers were separated by a proton exchange membrane (Nafion 117, Fuel Cell Store, Boulder, CO, U.S.A.), and gas tightness was provided by rubber gaskets.

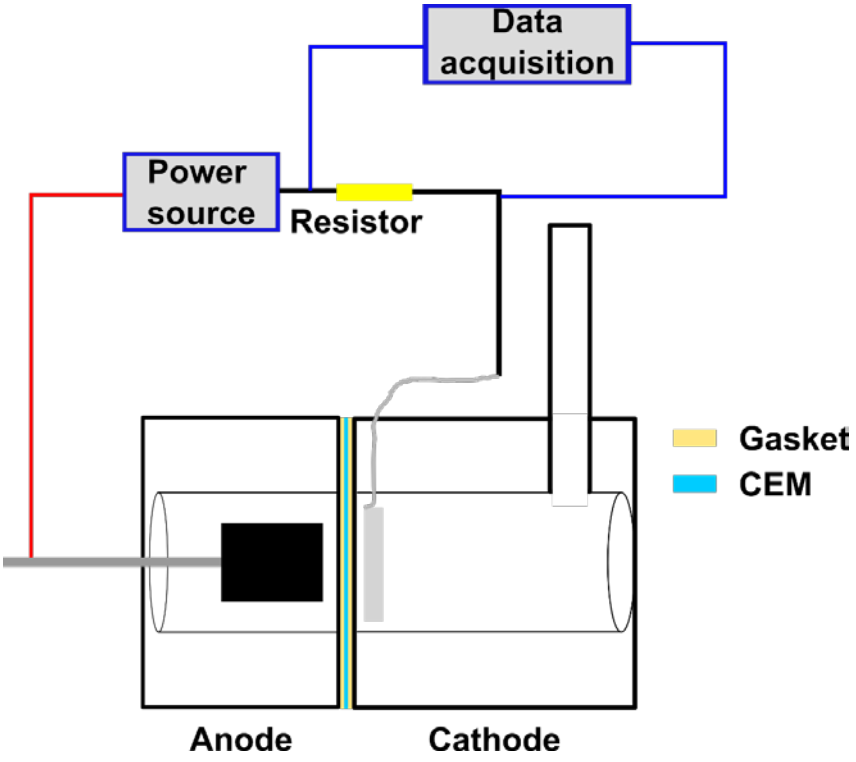

Figure 1Schematic representation of MEC-Q

A carbon fibre brush electrode was used as anode (2.5 cm diameter by 2.5 cm length; Panex 35 polyacrylonitrile fibre, Zoltek, St. Louis, MO, USA), pretreated at 450 °C for 1 h before use to remove eventual contamination and modify the surface condition to favour biofilm formation (LaBarge et al., 2017). Based on the mass of fibres used in a single brush and an average fibre diameter of 7.2 µm, a surface area of 0.22 m^2 or 18,200 m^2/m^3 (95% porosity) was estimated (Logan et al., 2007). The brush electrode was positioned in the middle of the anodic chamber. The metal end of the brush protruded through a hole drilled in the reactor and was fixed in the chamber so that the other end was around 0.5 cm from the cathode. The cathode was a platinum coated titanium mesh (0.5 mg cm^{-2}) with a surface area equal to 4.9 cm^2. Electrodes were connected to the external circuit through titanium wire, and an additional voltage of 0.8 V was provided to the system by a power supply (GPS-3030D, Good Will DC, CA, USA). Voltage variation was measured across a 10 Ω external resistor placed in series between the positive terminal of the power supply (Call and Logan, 2008) and anode of MEC-Q. Voltage variation was recorded using a data acquisition system (PicoLog 1012, Pico Technology, Cambridgeshire, UK) connected to a personal computer, with sampling frequency of 1 minute.

Before experiments, MEC-Q was inoculated with a mixed bacterial culture that was originally enriched from a local domestic wastewater treatment plant using 1 g L^{-1} sodium acetate (NaAc) as a carbon source with a medium solution containing in 1 L: KH_2PO_4·6.8 g; K_2HPO_4·8.7 g; NH_4Cl 0.8 g; NaCl 0.58 g; KCl 0.74 g; $MgSO_4$ x $7H_2O$ 0.1 g; $CaCl_2x2H_2O$ 0.1 g; mineral solution 12.5

mL; vitamin solution 12.5 mL; conductivity 25.0 mS cm^{-1}. (Omidi and Sathasivan, 2013). Catholyte had the same composition, even though mineral and vitamin solution were not included to avoid microbial contamination in the chamber. MEC-Q was operated at room temperature (25 °C).

After acclimation, MEC-Q was fed for 26 days with SCW fermented at pH 6 for 168 h (Table 1) (Asunis et al., 2019), with a step increase concentration from 150 to 450 mgTOC L^{-1} of organic acids to favour biomass adaptation to the new substrate and inlet carbon load . Initial pH was set at 7 using 5M NaOH. Prior to dilution, fermented SCW was centrifuged for 20 min at 10000 rpm and filtered at 0.45 µm in order to remove indigenous biomass. Substrate was replaced when current decreases below 0.2 mA (Ullery and Logan, 2014).

Table 1 FCW characteristics

Parameter	
Acetate (g L^{-1})	1.14
Propionate (g L^{-1})	6.38
Butyrate (g L^{-1})	13.45
Valerate (g L^{-1})	0.32
Caproate (g L^{-1})	0.22
Lactate (g L^{-1})	2.95
Soluble Carbohydrates (g L^{-1})	0.3
Soluble Proteins	6
TOC (g L^{-1})	24.8
Theoretical VFAs COD (g L^{-1})	35.4
C/N	25
TS (%)	7.4
VS (%)	6.8
Conductivity (mS cm^{-1})	25.3

7.2.2 Analytical Methods

The concentration of H_2, N_2, O_2, CO_2 and CH_4 were determined by gas chromatography. The gas was sampled periodically from the Q-MEC headspace with a 1-mL gastight syringe and injected through a valve in a gas chromatograph (Model 7890B, Agilent Technology) equipped with a thermal conductivity detector (TCD) and two stainless columns packed with HayeSep N (80/100 mesh) and Shincarbon ST (50/80 mesh) connected in series. The operating temperatures of the valve and the TCD were 90 and 200 °C, respectively, and He was the carrier gas at a constant pressure of 8 psi in the HayeSep N column and 25 psi in the Shincarbon ST column (at 70°C). The oven temperature was set initially to 70°C (3-min holding time), followed by a ramp up in 10°C/min increments up to 160°C (3-min holding time).

7.2.3 Calculations

Current density (I) (Eq. 1) was normalised to the anode surface and calculated according to Ohm's law:

$$I = \frac{V}{R_{ext}\, A_{an}} \quad (1)$$

where V is the voltage measured across the resistor, R_{ext} is the external resistance and A_{an} is the anode surface area.

Coulombic efficiency (CE) (Eq.2), which represent the share of electrons generated by substrate degradation converted into electrical current, was calculated according to (Logan et al., 2006) (Eq.2)

$$CE = \frac{M \int_0^{t_f} I\, dt}{F\, b\, v_{an}\, \Delta COD} \quad (2)$$

where M = 32 g mol^{-1} is the molecular weight of oxygen, F is the Faraday constant, b = 4 is the number of electrons exchanged per mole of oxygen, v_{an} is the working volume of the anode and ΔCOD is the variation of COD concentration during each batch cycle.

H_2 yield was calculated on the basis of TOC removal (Eq.3)

$$Y_{MEC} = \frac{v_{H_2}}{\Delta TOC\, v_{an}} \quad (3)$$

where v_{H_2} is the volume produced during the batch cycle and ΔTOC is carbon *TOC* removal.

Hydrogen production rate was calculated according to (Eq.4)

$$HPR = \frac{v_{H_2}}{v_{react}\, t} \quad (4)$$

where v_{react} is MEC-Q total volume and t is the batch cycle duration.

Energy recovered from H_2 was calculated on the base of its heat combustion energy, -285.8 kJ mol^{-1}.

Finally, the overall hydrogen yield (Y_{all}) was calculated considering Y_{MEC} + Y_{ferm}, with a yield from dark fermentation Y_{ferm}= 5.2 LH_2 L^{-1} (Asunis et al., 2020).

7.3. Results and discussion

7.3.1 Biohydrogen production by dark fermentation

Dark fermentation (DF) of CW was performed for 168 h at 39 ± 1 °C, and pH was automatically fixed at 6 by addion of 5M NaOH. The main metabolites detected in the fermentation broth were butyrate and propionate, in concentration of 13.45 and 6.38 g L^{-1} respectively. Only a small fraction of lactate, generated during the first 45 h of the experiment up to a concentration of 65 g L^{-1}, was not converted into final bioproducts. The experimental condition guaranteed an H_2 production of 162.1 LH_2 $(kgTOC_{in})^{-1}$, equivalent to 5.2 LH_2 $(L_{CW})^{-1}$. Results suggest the onset of butyrate metabolical pathway, which is optimal for hydrogen production (see Chapter 3).

7.3.2 Coulombic efficiency and current generation

In this work, a real cheese whey effluent was tested in a two-chambered MEC to determine how the MEC perform with respect to an increased carbon load (to 150 up to 400 mgTOC L^{-1}) in terms of biohydrogen production, electrical generation current and TOC removal.

MEC results showed satisfactory performances in terms of electrical current. Four operational stage can be identified: (I) acclimation to new substrate (FCW instead of acetate) fed in concentration of 150-205 mgTOC L^{-1} (batch 1-5, phase I), when current ranged between 3.3 and 8.0 mA m^{-2} ; (II) stable operation (batch 6-11, phase II) for inlet substrate concentration of 210-250 mgTOC L^{-1}, during which maximum achieved current density was stable at values of 10 mA m^{-2} and never below 8.3 mA m^{-2}; (III) system failure due to incresed concentration of substrate (410-420 mgTOC L^{-1}), which took place during batch 12-15 (phase III) and maximum current density ranged between 3.3-6.7 mA m^{-2}; (IV) stable operation at high concentration of substrate (315-450 mgTOC L^{-1}) until batch 20 (phase IV), when the system recovery lead to a current density of 20.0 mA m^{-2}, the maximum achieved during the experiment (Figure 1).

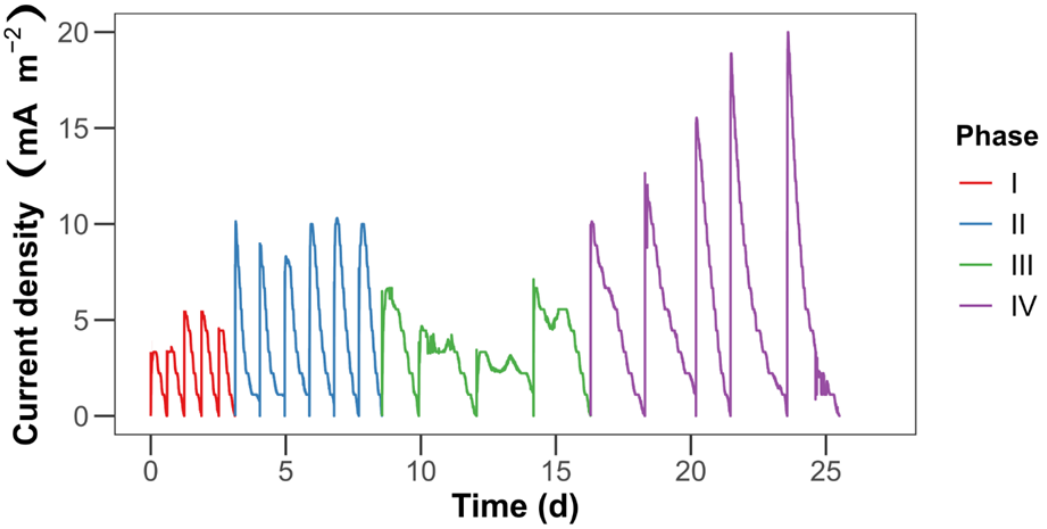

Figure 2 MEC-Q current density profile

The low currents observed during the phase I were linked to CE of 31.1 ± 5.8% The more complex carbon source (with respect to only acetate, acclimation phase) may have caused a shift in metabolic pathways followed by bacteria, reducing the overall ability of the biofilm to transfer electrons to the anode (Teng et al., 2010). Further increase in inlet substrate concentration at the beginning of phase II positively affected CE, which increased to 41.3 ± 6.6 % (Table 1).

Performance of MEC-Q was negatively impacted at the beginning of phase III, when inlet concentration was increased by 40%. At the end of the first batch of the phase, pH dramatically dropped to 4.17. Such acidic pH, out of the optimal range of 6-9 according to (Patil et al., 2011),

caused a deterioration of exoelectrogenic bacteria activity. Profiles of subsequent cycles support this hypothesis: current densities peaks were larger and less defined, stabilising around their maximum, while CE was comparable to phase I (Table 1). To avoid further biofilm damage, initial pH was increased to 7.4 by adding 5 M NaOH from second last batch of phase III, and a positive effect was recorded at the beginning of phase IV. From that point on, increased substrate concentration positively affected current generation (up to 20.0 mA m^{-2}) and CE stabilised at 55.2 ± 2.2 %.

Table 2 Main results of MEC-Q opearation

Phase	Batch	Duration (d)	TOC in (mg L^{-1})	TOC removal (%)	pH out	HPR (L H_2 L^{-1} d^{-1})	CE (%)	Max current density (mA m^{-2})
I	1	0.60	153.2	43.3	6	0.014	35.1	3.3
	2	0.64	162.7	46.2	6.08	0.012	34.6	3.6
	3	0.64	197.5	54.3	5.94	0.011	32.5	6.8
	4	0.64	202.1	65.9	5.97	0.039	21.1	8.0
	5	0.61	202.4	57.0	5.91	0.034	32.3	4.4
II	6	0.92	212.1	62.8	5.43	0.051	44.8	10.1
	7	0.92	191.1	82.9	5.08	0.056	36.5	8.9
	8	0.92	250.5	86.9	5.25	0.057	31.7	8.3
	9	0.92	211.2	81.5	5.01	0.074	46.5	10.0
	10	0.92	199.2	86.6	4.96	0.085	48.9	10.3
	11	0.86	252.7	89.1	5.22	0.059	39.1	10.0
III	12	1.36	418.0	66.1	4.17	0.054	36.5	6.7
	13	2.14	410.4	70.4	4.26	0.039	39.4	4.7
	14	2.11	422.0	61.5	5.41	0.026	36.1	3.3
	15	2.12	413.6	63.6	5.79	0.068	63.5	6.7
IV	16	2.01	425.7	81.2	5.56	0.082	51.9	10.1
	17	1.89	433.6	74.9	5.86	0.107	57.6	12.0
	18	1.28	316.1	89.0	5.85	0.127	56.3	15.5
	19	2.10	451.8	91.5	5.4	0.118	55.8	18.9
	20	1.94	421.7	89.7	5.83	0.125	54.3	20.0

7.3.3 Biohydrogen production and TOC removal in MEC

Performances in terms of TOC removal followed the same pattern as electrical ones through the four phases of the experiment (Figure 3A). During phase 1, a gradual rise was observed and an average value of 53 % ± 9% was recorded. Biomass acclimatation favoured further TOC removal in phase 2: an overall average of 82% ± 10% was achieved, but after the first cycle of the phase the value stabilised at of 85% ± 3%, comparable to the ones reported by Moreno et al. (2015) in similar when operating a MEC with diluited FCW. However, authors amended diluted FCW with acetate, alterating the initial composition of DF effluent. On the other hand, Marone et al.(2017) reported a carbon removal equal to 63% when treating raw FCW. Indeed, the diluition of FCW in PBS has to be deeper investigated in future studies. Biomass degradation during phase III heavily affected TOC removal, which dropped to 65% ± 4%, but rapidly recovered in phase IV (85% ± 7%).For what concerns HPR, higher substrates availability lead to higher production rates. In addition, methane was never detected in cathode headspace, indicating a suppression of methanogens activity without need of biomass pretreatment or inhbiotrs addition. HPR during phase I was 0.022 ± 0.013 LH_2 L^{-1} d^{-1} and is comparable to results reported by Marone et al. (2017), which operated a dual chamber MEC in mesophilic conditions. Results of phase II,

0.063 ± 0.013 LH_2 L^{-1} d^{-1},are in line with Rivera et al. (2017), where headspace was however highly contamined by methane (43%) due also to the single chamber configuration used. Finally highest HPR were achieved during Phase IV (0.112 ± 0.018 LH_2 L^{-1} d^{-1}), when the maximum of 0.127 LH_2 L^{-1} d^{-1} was recorded. Such values are lower than the maximum reported by Moreno et al.(2015), but a comparison is difficult because of different operational conditions and reactor configuration.

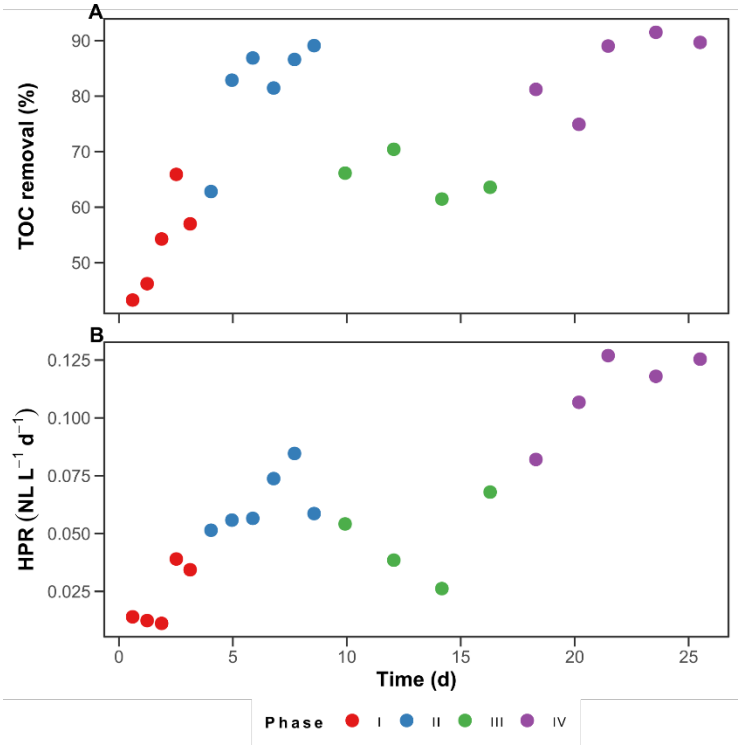

Figure 3 TOC removal (A) and H_2 production rates (B) during experimental phases

7.3.4 Prospects of DF and MEC integration

The use of MECs as downstream had a positive impact on H_2 generation from CW (Table 3). The highest Y_{MEC}, recorded was equal to 1.61 NL $gTOC^{-1}$ (Table 3), similar to what reported by Marone et al. (2017) when treating effluents from DF of vinasse, while in the same study, Y_{MEC} was only 0.71 NL $gTOC^{-1}$ when treating CW fermentate. An explanation to such difference may reside in fermentate composition, since in the latter case the main metabolite found in the broath was ethanol instead of butyrate, which was the main component of vinasse fermentate. Therefore, a proper management of DF operational condition is crucial towards the optimisation of integrated processes.

Table 3 Hydrogen production yields in MEC and in combined processes

Phase	Batch	Y_{MEC} (NL gTOC^{-1})	Y_{MEC} (NL H_2 L^{-1})	Y_{All} (NL H_2 L^{-1})
I	1	0.32	3.4	8.6
	2	0.26	3.0	8.2
	3	0.17	2.2	7.4
	4	0.47	7.7	12.9
	5	0.45	6.4	11.6
II	6	0.88	13.8	19.0
	7	0.81	16.6	21.8
	8	0.59	12.8	18.0
	9	0.98	19.8	25.0
	10	1.12	24.1	29.3
	11	0.56	12.3	17.5
III	12	0.67	10.9	16.1
	13	0.71	12.4	17.6
	14	0.53	8.1	13.3
	15	1.37	21.5	26.7
IV	16	1.19	24.0	29.2
	17	1.55	28.8	34.0
	18	1.44	31.8	37.0
	19	1.49	33.9	39.1
	20	1.61	35.7	40.9

In terms of energy, up to 522 kJ L^{-1} could be obtained from H_2. Part of this energy could be spent to run microbial electrolysis, eventually accompanied by green energy from other renewable resources. In this regard, MFCs appear feasible in improving overall treatment performances. Event hough the experiment was carried using a single reactor and diluited FCW, equivalent carbon loads could be fed to stacked MECs connected in parallel and/or in series. In fact, the use of stacked MEC have been proposed for the treatment of brewery wastewater (Dong et al., 2015), swine manure (Vilajeliu-Pons et al., 2017) and municipal wastewaters (Feng et al., 2014) and is currently considered a more promising strategy towards full scale application rather than using of single stage reactors.

7.4 Conclusions

This chapter provides new insights into the treatment of DF reactors effluents for the maximisation of hydrogen production and carbon removal from SCW. The approach is based on the integration of DF with MECs, which would allow further energy recovery from the substrate, the simultaneous reduction of final TOC and cutting the energy requirements of the process.

In order to evaluate a possible upscale of the MEC for the treatment of FCW, the inlet carbon concentration was taken into account as pivot parameter to optimise the process. With this work a proof of concept towards a more sustainable waste management of dairy residues have been achieved and it opens new interesting scenarios for future research. The achievement of carbon removal from FCW up to 91.5% accompanied by hydrogen yields up to 1.61 NL $gTOC^{-1}$ is indeed promising, even for experiments conducted at bench scale. In optimal operational conditions an overall H_2 yield would be 40.9 LH_2 per litre of raw CW, equivalent to 522 kJ L^{-1} of energy. The resilience of MEC bio-catalyst, which was able to recover after strong pH shocks, must not be overlooked when considering scalability of the system.

References

Asunis, F., De Gioannis, G., Dessì, P., Isipato, M., Lens, P. N. L., Muntoni, A., et al. (2020). The dairy biorefinery: Integrating treatment processes for cheese whey valorisation. *J. Environ. Manage.* 276. doi:10.1016/j.jenvman.2020.111240.

Asunis, F., De Gioannis, G., Isipato, M., Muntoni, A., Polettini, A., Pomi, R., et al. (2019). Control of fermentation duration and pH to orient biochemicals and biofuels production from cheese whey. *Bioresour. Technol.* 289. doi:10.1016/j.biortech.2019.121722.

Benemann, J. (1996). Hydrogen biotechnology: Progress and prospects. *Nat. Biotechnol.* 14, 1101–1103. doi:10.1038/nbt0996-1101.

Chookaew, T., Prasertsan, P., and Ren, Z. J. (2014). Two-stage conversion of crude glycerol to energy using dark fermentation linked with microbial fuel cell or microbial electrolysis cell. *N. Biotechnol.* 31, 179–184. doi:10.1016/j.nbt.2013.12.004.

Dong, Y., Qu, Y., He, W., Du, Y., Liu, J., Han, X., et al. (2015). A 90-liter stackable baffled microbial fuel cell for brewery wastewater treatment based on energy self-sufficient mode. *Bioresour. Technol.* 195, 66–72. doi:10.1016/j.biortech.2015.06.026.

Escapa, A., Mateos, R., Martínez, E. J., and Blanes, J. (2016). Microbial electrolysis cells: An emerging technology for wastewater treatment and energy recovery. from laboratory to pilot plant and beyond. *Renew. Sustain. Energy Rev.* doi:10.1016/j.rser.2015.11.029.

European Commission (2019). A European Green Deal. *Eur. Comm.*, 24. Available at: https://ec.europa.eu/info/strategy/priorities-2019-2024/european-green-deal_en.

European Commission (2020). Hydrogen generation in Europe. doi:10.2833/122757.

Feng, Y., He, W., Liu, J., Wang, X., Qu, Y., and Ren, N. (2014). A horizontal plug flow and stackable pilot microbial fuel cell for municipal wastewater treatment. *Bioresour. Technol.* 156, 132–138. doi:10.1016/j.biortech.2013.12.104.

Fuel Cells and Hydrogen Joint Undertaking (FCH) (2019). A SUSTAINABLE PATHWAY FOR THE EUROPEAN ENERGY TRANSITION HYDROGEN ROADMAP EUROPE. Brussels, Belgium doi:10.2843/249013.

Guo, X. M., Trably, E., Latrille, E., Carrre, H., and Steyer, J. P. (2010). Hydrogen production from agricultural waste by dark fermentation: A review. *Int. J. Hydrogen Energy* 35, 10660–10673. doi:10.1016/j.ijhydene.2010.03.008.

Kapdan, I. K., and Kargi, F. (2006). Bio-hydrogen production from waste materials. *Enzyme Microb. Technol.* 38, 569–582. doi:10.1016/j.enzmictec.2005.09.015.

LaBarge, N., Yilmazel, Y. D., Hong, P. Y., and Logan, B. E. (2017). Effect of pre-acclimation of granular activated carbon on microbial electrolysis cell startup and performance. *Bioelectrochemistry* 113, 20–25. doi:10.1016/j.bioelechem.2016.08.003.

Li, X. H., Liang, D. W., Bai, Y. X., Fan, Y. T., and Hou, H. W. (2014). Enhanced H2 production from corn stalk by integrating dark fermentation and single chamber microbial electrolysis cells with double anode arrangement. *Int. J. Hydrogen Energy* 39, 8977–8982. doi:10.1016/j.ijhydene.2014.03.065.

Lin, C. Y., Lay, C. H., Sen, B., Chu, C. Y., Kumar, G., Chen, C. C., et al. (2012). Fermentative hydrogen production from wastewaters: A review and prognosis. in *International Journal of Hydrogen Energy* (Pergamon), 15632–15642. doi:10.1016/j.ijhydene.2012.02.072.

Liu, W., Huang, S., Zhou, A., Zhou, G., Ren, N., Wang, A., et al. (2012). Hydrogen generation in microbial electrolysis cell feeding with fermentation liquid of waste activated sludge. in *International Journal of Hydrogen Energy* (Pergamon), 13859–13864. doi:10.1016/j.ijhydene.2012.04.090.

Logan, B., Cheng, S., Watson, V., and Estadt, G. (2007). Graphite fiber brush anodes for increased power production in air-cathode microbial fuel cells. *Environ. Sci. Technol.* 41, 3341–3346. doi:10.1021/es062644y.

Logan, B. E., Hamelers, B., Rozendal, R., Schröder, U., Keller, J., Freguia, S., et al. (2006). Microbial fuel cells: Methodology and technology. *Environ. Sci. Technol.* 40, 5181–5192.

doi:10.1021/es0605016.
Lu, L., Xing, D., Liu, B., and Ren, N. (2012). Enhanced hydrogen production from waste activated sludge by cascade utilization of organic matter in microbial electrolysis cells. *Water Res.* 46, 1015–1026. doi:10.1016/j.watres.2011.11.073.
Marone, A., Ayala-Campos, O. R., Trably, E., Carmona-Martínez, A. A., Moscoviz, R., Latrille, E., et al. (2017). Coupling dark fermentation and microbial electrolysis to enhance bio-hydrogen production from agro-industrial wastewaters and by-products in a bio-refinery framework. *Int. J. Hydrogen Energy* 42, 1609–1621. doi:10.1016/j.ijhydene.2016.09.166.
Moreno, R., Escapa, A., Cara, J., Carracedo, B., and Gómez, X. (2015). A two-stage process for hydrogen production from cheese whey: Integration of dark fermentation and biocatalyzed electrolysis. *Int. J. Hydrogen Energy* 40, 168–175. doi:10.1016/j.ijhydene.2014.10.120.
Omidi, H., and Sathasivan, A. (2013). Optimal temperature for microbes in an acetate fed microbial electrolysis cell (MEC). *Int. Biodeterior. Biodegrad.* 85, 688–692. doi:10.1016/j.ibiod.2013.05.026.
Patil, S. A., Harnisch, F., Koch, C., Hübschmann, T., Fetzer, I., Carmona-Martínez, A. A., et al. (2011). Electroactive mixed culture derived biofilms in microbial bioelectrochemical systems: The role of pH on biofilm formation, performance and composition. *Bioresour. Technol.* 102, 9683–9690. doi:10.1016/j.biortech.2011.07.087.
Rivera, I., Bakonyi, P., Cuautle-Marín, M. A., and Buitrón, G. (2017). Evaluation of various cheese whey treatment scenarios in single-chamber microbial electrolysis cells for improved biohydrogen production. *Chemosphere*. doi:10.1016/j.chemosphere.2017.01.128.
Rozendal, R. A., Hamelers, H. V. M., Euverink, G. J. W., Metz, S. J., and Buisman, C. J. N. (2006). Principle and perspectives of hydrogen production through biocatalyzed electrolysis. *Int. J. Hydrogen Energy* 31, 1632–1640. doi:10.1016/j.ijhydene.2005.12.006.
Sarma, S. J., Pachapur, V., Brar, S. K., Le Bihan, Y., and Buelna, G. (2015). Hydrogen biorefinery: Potential utilization of the liquid waste from fermentative hydrogen production. *Renew. Sustain. Energy Rev.* 50, 942–951. doi:10.1016/j.rser.2015.04.191.
Teng, S. X., Tong, Z. H., Li, W. W., Wang, S. G., Sheng, G. P., Shi, X. Y., et al. (2010). Electricity generation from mixed volatile fatty acids using microbial fuel cells. *Appl. Microbiol. Biotechnol.* 87, 2365–2372. doi:10.1007/s00253-010-2746-5.
Ullery, M. L., and Logan, B. E. (2014). Comparison of complex effluent treatability in different bench scale microbial electrolysis cells. *Bioresour. Technol.* 170, 530–537. doi:10.1016/j.biortech.2014.08.028.
Vilajeliu-Pons, A., Puig, S., Salcedo-Dávila, I., Balaguer, M. D., and Colprim, J. (2017). Long-term assessment of six-stacked scaled-up MFCs treating swine manure with different electrode materials. *Environ. Sci. Water Res. Technol.* 3, 947–959. doi:10.1039/c7ew00079k.

Chapter 8

Considerations on the application of the MESs

8.1 Introduction

From an engineering point of view, it is necessary to frame the studied processes in an application context. In doing this, the two application extremes of the biorefinery concept were taken into consideration, that is a process scheme oriented only to ***energy*** recovery and, on the contrary, one oriented only to ***bioproducts*** recovery. We proceeded in this way despite the awareness that the perspectives for implementing the concept of biorefinery, and therefore also of waste biorefinery, are instead linked to a balanced combination of energy/biofuel and bioproduct production, to combine large market shares with high specific value. This combination is considered necessary in order to make biofuels competitive with fossil fuels.

In both cases considered, the use of MESs supports dark fermentation; in the case of the energy recovery scheme, the MESs complete the energy enhancement in light of the limits that characterize the use of DF for bio-hydrogen recovery; in the case of recovery of bioproducts, on the other hand, the performance in terms of conversion of the organic load that would be obtained with the DF alone is improved and some operational aspects, such as the process temperature and pH control, are improved.

Both the considered approaches are summarized below underlining the yields obtainable for the main products and the final fate of the organic carbon.

Finally, they are compared by calculating the respective Biorefinery Complexity Index and Profile (BCI and BCP).

8.2 Calculations

8.2.1 Carbon recovery and residual organic load

The fate of the carbon was calculated as a percentage of the initial carbon content in the raw sheep cheese whey (SCW), i.e. about 32 g L^{-1}. Prior to MESs feeding, centrifugation of SCW was considered as pretreatment to avoid reactors failure. The residual organic load removed from supernatant accounted for the 10% of initial CW volume.

8.2.2 BCI and BCP calculation

Calculation of BCI and BCP is based on the Technology Readiness Level (TRL) (Jungmeier, 2014). The TRL is assessed for each of the four main features of a biorefinery according to the definitions provided by IEA: feedstocks, platforms, processes and products. The TRL value spans between 1

(basic principles of technology observed and reported) to 9 (technology already applied at the full scale). The so-called Feature Complexity (FC, Eq. 1) is calculated for all the sub-features included in the main four, e.g. for DF and EF which are included in processes; finally, the Feature Complexity Index (FCI, Eq. 2) is calculated as the sum of FCs of feedstocks, platforms, processes and products. BCI is than defined as sum of FCIs (Cherubini and Jungmeier, 2009; Jungmeier, 2014) (Eq. 3)

$$FC_i = 10 - TRL_i \quad (1)$$

$$FCI_i = \sum_{j=1}^{m} NF_j \quad (2)$$

$$BCI = NF_{platforms} \cdot FC_{platforms} + NF_{feedstocks} \cdot FC_{feedstocks} + NF_{products} \cdot FC_{products} + NF_{processes} \cdot FC_{processes} \quad (3)$$

where NF_j represents the feature complexity of each sub-feature present in the considered biorefinery scheme.

BCP was firstly introduced by IEA as a compact form to express the complexity of a biorefinery, given the BCI and FCIs, and it is reported according to (Eq. 4).

$$BCP = BCI\ (FCI_{platforms}/\ FCI_{feedstocks}/\ FCI_{products}/\ FCI_{processes}\ ) \quad (4)$$

A BCP of 8 (1/1/3/3) refers to a biorefinery producing biodiesel from vegetable oil, and it is generally considered as a benchmark value associated with a fully developed biorefinery. A high BCI corresponds to a biorefinery scheme ready to be implemented at the full scale, and low values of FCI are associated with processes easy to be applied.

8.3 Integration of an MFC in an energy-driven biorefinery scheme

The proposed scheme is based on the integration of DF, MFC and MEC discussed in chapter 7, using real fermented SCW as the substrate. In the proposed scheme (Figure 1), the MFC would be preceded by a fermentation conducted at an operating pH of 6, which according to previously conducted studies was found to be optimal for H_2 production at a yield of 5.2 L per litre of SCW (Asunis et al., 2019). Electrical energy generated by MFC would be then used as external input for further H_2 generation through MECs, operated in stacks, fed with an equivalent carbon load of 421.7 $mg_{TOC}\ L^{-1}$ (see chapter 7 for further details)

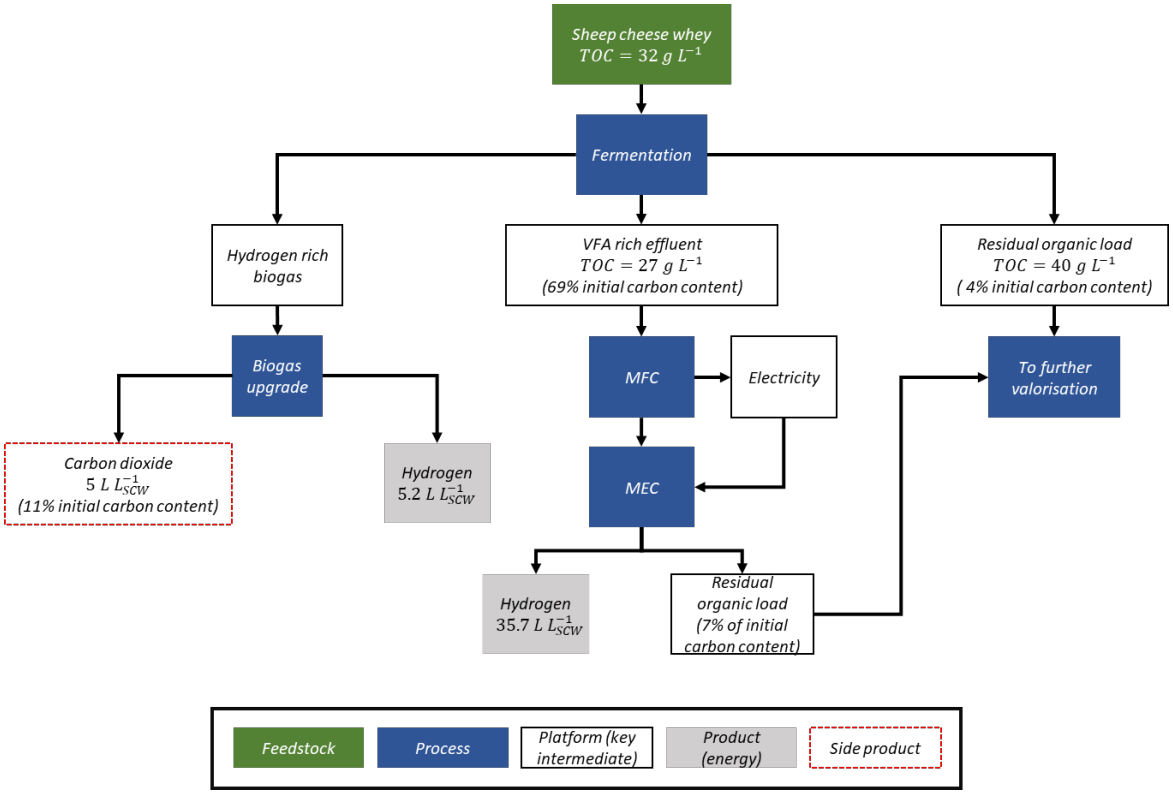

Figure 1 Schematization of the integration between dark fermentation and MFC processes for energy recovery from SCW

During the fermentation treatment, the carbon loss due to CO_2 production accounted for 11% of the TOC in the raw SCW, while 45% was mainly converted into short chain fatty acids (C2-C4). The remaining part of initial TOC was composed of proteins, fats and residual lactate. Feeding centrifuged fermentation effluent to MECs would further reduce TOC to only 7% of raw SCW initial value, and would permit an overall H_2 recovery of 40.9 L per litre of SCW.

8.4 Integration of EF in a material-driven biorefinery scheme

The integration of fermentation and electro-fermentation processes is the second proposed scheme (Figure 2). As already illustrated, the organic load of the SCW is converted by DF into lactic acid (see Chapter 3) which in turn is converted by electro-fermentation into a mixture of propionic and acetic acid (see Chapter 5).

With reference to the conversion of the SCW lactose into lactic acid, our previous study has shown that the metabolic pathway is the homolactic one, when DF is conducted at pH 6 (reaction time 45 h), with the production of 65 g L^{-1} of lactic acid (Asunis et al., 2019).

In terms of fate of the organic carbon contained in the raw SCW, DF leads to the conversion of 81% of the initial carbon into lactic acid.

Although the production of propionic acid is achievable by prolonging the DF phase under suitable conditions, in our studies (Isipato et al., 2020) the use of electro-fermentation has shown

considerable advantages, in terms of carbon conversion efficiency, in light of the possibility of carrying out the EF process under room temperature conditions instead of mesophilic ones, of controlling the pH through the cathodic reactions, of valorising also the CO_2 produced during lactate conversion. A carbon recovery into final products of 50% would be expected, when operating DF at pH 6.

The separation of propionic acid, or of the mix of propionic acid and acetic acid, from the electro-fermentation broth can be obtained more or less effectively depending on the use of the products to be separated. Diluted downstream from separation can be treated by recirculating it at the anode of the EF system and obtaining the oxidative removal of the residual TOC.

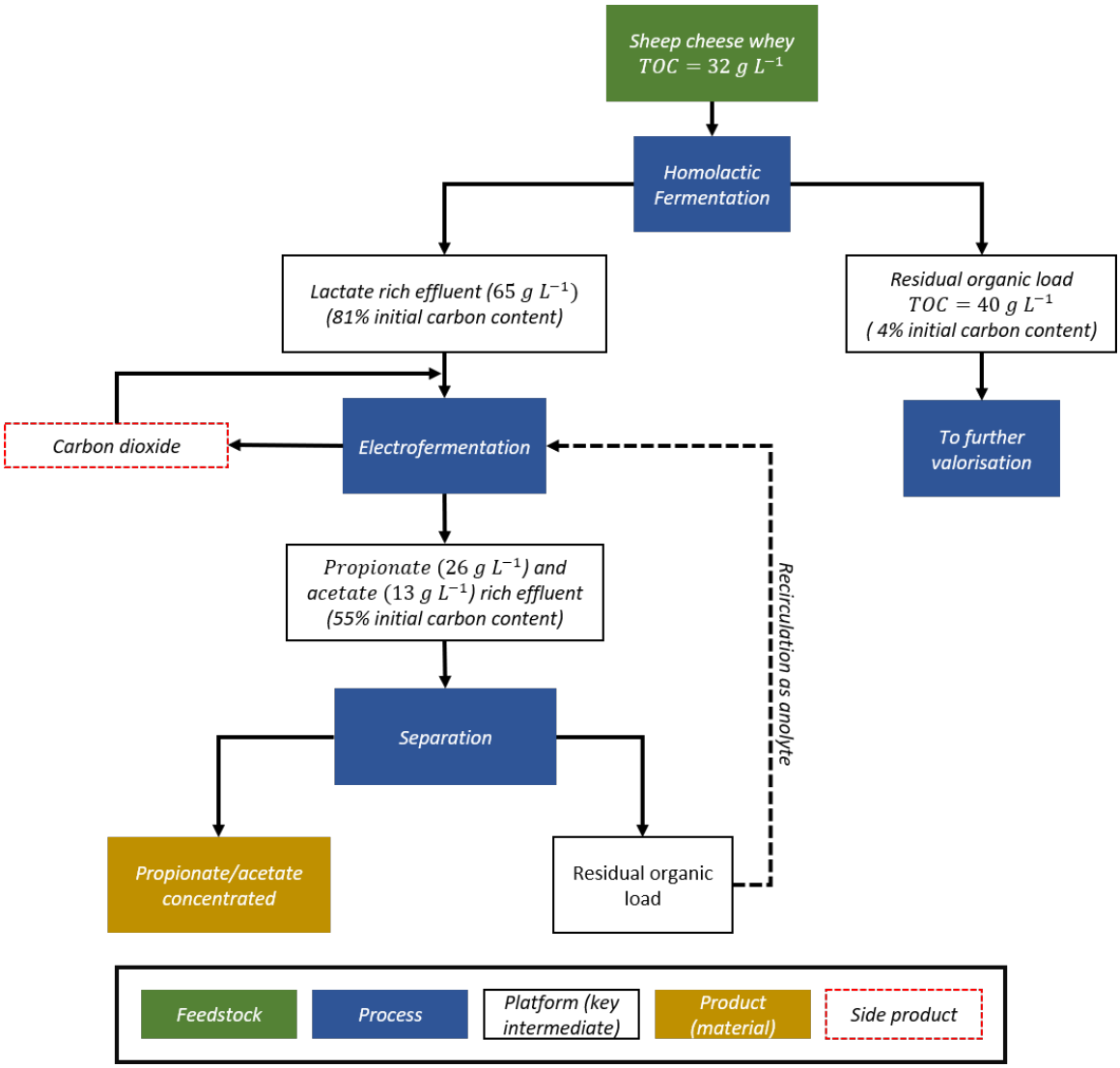

Figure 2 Schematization of the integration between DF, conducted at pH 6, and electro-fermentation processes for propionate and acetate production from SCW

8.5 Application perspectives

The synthetic Schemes of the combined application of DF and MES processes have further highlighted the potential and theoretically achievable advantages.

Microbial Electrochemical Systems are an appealing alternative to traditional processes because of their versatility. MESs are capable of reducing COD concentration while harvesting energy instead of consuming it; cathodic processes may synthesise chemicals, use of concentrated bases/acids may be avoided thanks to the buffering effect of cathodic OH^- generation, metabolic pathways can be better addressed than in DF and, in turn, generation of specific products is enhanced; finally, CO_2 generated during lactate conversion is further converted into volatile fatty acids through microbial electrosynthesis, increasing the carbon recovery from biological platforms.

However, it is worth mentioning that relatively few studies on the pilot scale application of MES are available and even less data is available on the application of electro-fermentation.

This finding is confirmed by the assessment of BCI and BCP for the previously proposed Schemes (Table 1). The BCI values confirm the novelty of the proposed schemes, but processes TRL ranges between 3-4, except for separation. Complexity may increase considering the valorisation of the residual organic load in the effluent of the MEC reactor, and by hydrogen storage (technology that still shows inefficiencies) in the proposed Scheme 1. On the other hand, the waste biorefinery concept more and more requires that waste treatment is designed and operated industrially, with a high degree of technological development (Alibardi et al., 2020) Therefore, pre-treatments, bioreactors and downstream separation processes require development to produce bioproducts with consistent physical–chemical characteristics at feasible costs.

Table 1 BCI and BCP assessment for the two proposed SCW biorefinery schemes. NF = number of features

Feature	Energy driven biorefinery (Scheme 1)	Material driven biorefinery (Scheme 2)
Platforms	Carboxylate (TRL 5) Biogas (TRL 9) Electricity (TRL 9) *NF =3*	Sugars (TRL 5) Lactate (TRL 9) *NF =2*
Feedstock	SCW (TRL8) *NF = 1*	SCW (TRL8) *NF = 1*
Processes	DF (TRL 4) MFC (TRL 4) MEC (TRL 4) *NF = 3*	DF (TRL 4) EF (TRL 4) Separation (TRL 8) *NF = 3*
Products	Biohydrogen (TRL 5) *NF =2*	Propionate (TRL 5) Acetate (TRL 5) *NF= 2*
BCI	37	28
BCP	37 (7/2/10/18)	28(6/2/5/15)

That said, it is interesting to propose a hypothetical full-scale application for the proposed schemes to an average Sardinian production plant of the dairy sector, with an estimation of the potential products generation (Table 2).

SCW specific production was assumed to be 0.9 L_{SCW} $L_{sheep\ milk}^{-1}$ (Carvalho et al., 2013). Considering Scheme 1, hydrogen would be the main energetical output, with a production of 227 x 10^6 L_{H2} per year, corresponding to 758 MJ of energy. This energy recovery would exceed energy needs of the dairy plant However, the energy consumption of the associated biorefinery for SCW should also be considered. It would therefore become interesting to consider the production of biogas through anaerobic digestion of the residual organic load in process effluents. The upgrade of biogas to biomethane would allow access to important incentives, especially in the case of the use of biomethane for transport, a concrete hypothesis in the case of the dairy sector.

When considering Scheme 2, propionate and acetate production would account for 109 and 56 t per year respectively. Given a market price of 1.8-2.3 € kg^{-1} for propionate and of 0.4-0.7 € kg^{-1} for acetate (see Chapter 5), the potential revenue from pure compounds sell may vary between 196,200-250,700 € $year^{-1}$ and 22,400-39,200 € $year^{-1}$ respectively. The biological production of these molecules will indirectly reduce GHG emissions from the petrochemical industry, since they are currently produced by oxidation or carboxylation of petroleum processed precursors, like aldehydes and alkenes (Riemenschneider, 2000). Propionate finds application in

several areas, i.e. herbicide and cellulose propionate synthesis, grain and food preservation and as intermediate in pharmaceutical and perfume industries (Liu et al., 2012). In the emerging sector of bioplastics biosynthesis, it is an important precursor of the biopolymer 3-hydroxybutyrate-co-3-hydroxyvalerate (PHBV) (Larsson et al., 2016; Tebaldi et al., 2019). On the other hand, acetate is used as well as food preservative, solvent or intermediate ingredient in the synthesis of commercial-grade chemicals (Pal and Nayak, 2017).

These are general considerations, which do not include for example an estimate of the costs and energy consumption associated with the proposed SCW treatment. One aspect that should certainly be considered is that of the minimum size of the biorefinery. The minimum economically viable size of complex biorefinery installations is still subject of debate. It is acknowledged that traditional biorefineries are large plants with a minimum size in the range of about 500,000–700,000 tons/year to ensure economic sustainability (Kuchta, K.,2016). However, using a residue as feedstock would presumably reduce the minimum size required, because of the expected income from waste treatment fees on top of the revenues from the obtained products (Alibardi et al., 2020).

Table 2 Relevant data for SCW biorefinery based on feedstock generated in a middle-sized dairy plant (elaborated from (Vagnoni et al., 2017))

Parameter	Value
Milk processed ($L\ y^{-1}$)	6,000,000
Sheep cheese whey produced ($L\ y^{-1}$)	5,400,000
Energy consumption, dairy plant ($kW\ y^{-1}$)	600,000
Energy recovery through H_2 production ($kW\ y^{-1}$)	758,500
Propionate, total ($t\ y^{-1}$)	109
Acetate, total ($t\ y^{-1}$)	56

References

Alibardi, L., Astrup, T. F., Asunis, F., Clarke, W. P., De Gioannis, G., Dessì, P., et al. (2020). Organic waste biorefineries: Looking towards implementation. *Waste Manag.* 114, 274–286. doi:10.1016/j.wasman.2020.07.010.

Asunis, F., De Gioannis, G., Isipato, M., Muntoni, A., Polettini, A., Pomi, R., et al. (2019). Control of fermentation duration and pH to orient biochemicals and biofuels production from cheese whey. *Bioresour. Technol.* 289. doi:10.1016/j.biortech.2019.121722.

Carvalho, F., Prazeres, A. R., and Rivas, J. (2013). Cheese whey wastewater: Characterization and treatment. *Sci. Total Environ.* 445–446, 385–396. doi:10.1016/j.scitotenv.2012.12.038.

Cherubini, F., and Jungmeier, G. (2009). Toward a common classification approach for biorefinery systems. *Biofuels, Bioprod. Biorefining*. doi:10.1002/bbb.

Isipato, M., Dessì, P., Sánchez, C., Mills, S., Ijaz, U. Z., Asunis, F., et al. (2020). Propionate Production by Bioelectrochemically-Assisted Lactate Fermentation and Simultaneous CO2 Recycling. *Front. Microbiol.* 11. doi:10.3389/fmicb.2020.599438.

Jungmeier, G. (2014). The Biorefinery Complexity Index. *IEA-Bioenergy Task 42*, 36.

Larsson, M., Markbo, O., and Jannasch, P. (2016). Melt processability and thermomechanical properties of blends based on polyhydroxyalkanoates and poly(butylene adipate-: Co - terephthalate). *RSC Adv.* 6, 44354–44363. doi:10.1039/c6ra06282b.

Liu, L., Zhu, Y., Li, J., Wang, M., Lee, P., Du, G., et al. (2012). Microbial production of propionic acid from propionibacteria: Current state, challenges and perspectives. *Crit. Rev. Biotechnol.* 32, 374–381. doi:10.3109/07388551.2011.651428.

Pal, P., and Nayak, J. (2017). Acetic Acid Production and Purification: Critical Review Towards Process Intensification. *Sep. Purif. Rev.* 46, 44–61. doi:10.1080/15422119.2016.1185017.

Riemenschneider, W. (2000). "Carboxylic Acids, Aliphatic," in *Ullmann's Encyclopedia of Industrial Chemistry* (Weinheim, Germany: Wiley-VCH Verlag GmbH & Co. KGaA). doi:10.1002/14356007.a05_235.

Tebaldi, M. L., Maia, A. L. C., Poletto, F., de Andrade, F. V., and Soares, D. C. F. (2019). Poly(-3-hydroxybutyrate-co-3-hydroxyvalerate) (PHBV): Current advances in synthesis methodologies, antitumor applications and biocompatibility. *J. Drug Deliv. Sci. Technol.* 51, 115–126. doi:10.1016/j.jddst.2019.02.007.

Chapter 9

Conclusions

The research conducted during the three years of Ph.D., and presented in this manuscript, was aimed to investigate the role of MES in a fermentation-pivoted sheep cheese whey biorefinery.

Cheese whey (CW) represents the most important residue of the dairy industry (0.8-0.9 L produced per L of processed milk) and is considered of great concern due to the produced amounts, high organic load, presence of salts and low alkalinity. The volumes of production entail significant treatment costs. Improper management results in dissolved oxygen depletion, toxicity for aquatic animals, groundwater contamination, impairment of soil characteristics; even CW discharge to sewer may affect the wastewater treatment plants, and the high contents of lactose and minerals can cause issues when it is used as animal feed. Therefore, proper CW management is mandatory, and traditional approaches have included so far physio-chemical and biological treatments, mainly aimed at removing the polluting organic load. In this respect, an innovation of the sector is strongly needed, particularly in smaller regions like Sardinia, which are more exposed to dairy market fluctuations and thus cyclically experience structural crisis which is made worse by environmental issue and eventual inappropriate solutions.

The sustainability and circular economy principles require a step forward in waste management, aimed at combining the prevention of impacts with the recovery of high value resources. Cheese whey is potentially eligible for valorisation though multi-step treatments which possibly lead to the recovery of high-quality products, consistently with an integrated approach known as waste biorefinery. The implementation of biorefinery, and waste biorefineries in particular, is also recognized as a key factor to contrast global warming, since bio-products can substitute fossil fuels in energy generation and chemicals synthesis, tackling CO_2 emissions from these sectors.

In this context, MES could play a crucial role in output diversification and/or recovery extent, widening the range of opportunities and linking biorefineries design to local necessities and requirements.

During the three years of activity, an overview of the available biotechnologies for CW valorisation was firstly developed and published (Asunis et al., 2020). From such analysis, DF emerged as the pivotal process in CW biorefineries: proper changes of operational conditions, such as pH or HRT, allow to address the process towards the production of soluble carboxylates that may serve as industrial platforms, eventually accompanied by hydrogen generation and recovery.

The present thesis work investigated the use of MESs in CW biorefineries. Through the analysis of the current state of the art and available literature, published in Asunis et al. (2020) highlighted their potential as a downstream process for DF reactors effluent. In addition, lack of studies on hydrodynamic characterization of microbial electrochemical reactors was pointed out as a crucial factor towards full-scale implementation. In this context, experimental activity focused on:

- Electrofermentation of lactate to propionate and acetate, with focus on metabolic pathways shift in comparison to standard DF, microbial community dynamics and product yields. Results were published in Frontiers of Microbiology (Isipato et al., 2020);
- Development of a novel MFC configuration, whose performance in terms of energy output and organics removal was characterised through mathematical modeling. The results are currently being submitted to Journal of Power Sources (ISSN: 0378-7753);
- DF effluents treatment in MECs for enhanced hydrogen production and organics removal. The study focused on the effect of the influent carbon content on hydrogen yields and carbon removal.

Finally, in view of a practical application, two alternative scenarios of integration between DF and MES were taken into account, one fully oriented towards energy recovery, the second mainly aimed at matter recovery.

The first focused on hydrogen production maximisation through the integration of DF and MEC, which would allow further conversion of VFAs obtained by cheese whey dark fermentation into the desired product, in an energy-driven CW biorefinery scheme.

The second scenario proposed is based on DF of CW lactose into lactate followed by the conversion of the latter into propionate and acetate through EF in the framework of a material-driven biorefinery. It is worth reminding that no biohydrogen is produced during propionic fermentation.

The main experimental evidences and results of the research activity can be summarised as follows:

- Dark fermentation confirms to be a process suitable for the simplification of complex organic substrates and preparation for further treatments, as well as being itself suitable for the recovery of high value products (hydrogen, lactic acid, etc.).

- Implementation of MFCs and MECs in waste biorefineries is appealing for productive sectors, like the dairy one, characterised by significant and constant waste production and remarkable energy needs. In this respect, the energy driven scenario can be a more feasible alternative as compared to the matter-oriented option, in particular where the dairy activity is characterised by small plants.
- Hydrodynamic and electrochemical modelling in MFC are important instruments for system scale-up. A characterisation in that sense can guide new configuration developments from early lab experiments, highlighting the weakness of all factors enhancing or affecting the process. That is particularly true for MFC, for which the basic microbial reactions have been already deeply investigated, thus more effort should be put into the reactors design.
- EF is a valid support to DF, giving the possibility to convert lactate into more selected products at room temperature. The energy needs can be potentially met by renewable resources, and even buying it from the network may be convenient.
- Selective propionate production in EF can be achieved using mixed bacterial cultures contained in CW, simplifying the process. The achieved conversion yields were comparable to those observed using pure culture fermentation which should be used under sterile conditions.
- The EF process is resilient to oxygen intrusion, which would eventually favour facultative anaerobes bacteria over obligate ones. From an applicative point of view, that may prevent sudden fails of the reactions.

I am confident that the results produced in the three years of activity represent contributions, albeit technically very specific in some cases, to an interesting but very complex topic such as the implementation of MES systems in the field of waste management and in integrated contexts such as waste-type bio-refinery approaches.

The results obtained do not represent absolute and univocal answers to the many technical aspects that need to be investigated.

Among these, I consider the following as appropriate to be pointed out:

- MFC reactors scale up should consider the use of stacked devices, connected either in series or in parallel, in order to enhance voltage and current output respectively. Model data would help in optimizing the design of each stack, maximizing power output depending on influent TOC.

- Membranes are a key point in EF development. In fact, the types used in the experiments caused product loss and oxygen intrusion, that could be avoided by installing less permeable materials. On the other hand, less permeable materials could affect other aspects, like the process energy needs, therefore more studies are necessary.
- Effects of circulating currents on metabolic pathways should be further investigated since significant variations may lead to different end products.
- As demonstrated during my collaboration with HyBiosol Project at National University of Galway, CO_2 generated in dairy plants or in other facilities located in proximity represents an important resource to produce high-value products. Preliminary results, reported in Dessì et al. (2021), strongly sustain the opportunity lying on broader biorefinery networks.
- Although the results obtained are encouraging, they need to be confirmed and deepened with further tests to be carried out on real substrates, an aspect to which much less time has been spent in these three years compared to what was done with synthetic substrates.

References

Asunis, F., De Gioannis, G., Dessì, P., Isipato, M., Lens, P. N. L., Muntoni, A., et al. (2020). The dairy biorefinery: Integrating treatment processes for cheese whey valorisation. *J. Environ. Manage.* 276. doi:10.1016/j.jenvman.2020.111240.

Dessì, P., Sánchez, C., Mills, S., Cocco, F. G., Isipato, M., Ijaz, U. Z., et al. (2021). Carboxylic acids production and electrosynthetic microbial community evolution under different CO2 feeding regimens. *Bioelectrochemistry* 137, 107686. doi:10.1016/j.bioelechem.2020.107686.

Isipato, M., Dessì, P., Sánchez, C., Mills, S., Ijaz, U. Z., Asunis, F., et al. (2020). Propionate Production by Bioelectrochemically-Assisted Lactate Fermentation and Simultaneous CO2 Recycling. *Front. Microbiol.* 11. doi:10.3389/fmicb.2020.599438.